University of Verona

Department of Diagnostics and Public Health

Section of Physiology and Psychology

Graduate School of Sciences, Engineering and Medicine

PhD Program in Psychological and Psychiatric Sciences

Psychological curriculum

Cycle XXVIII

THE NEURAL BASIS OF RESIDUAL VISION AND ATTENTION IN THE BLIND FIELD OF HEMIANOPIC PATIENTS: BEHAVIOURAL, ELECTROPHYSIOLOGICAL AND NEUROIMAGING EVIDENCE.

S.S.D. M-PSI/01

Coordinator: Prof.ssa Mirella Ruggeri

Tutor: Prof. Carlo Alberto Marzi

Doctoral Student: Dott./ssa Pedersini Caterina Annalaura

The Neural Basis of residual vision and attention in the blind field of hemianopic patients: Behavioural, electrophysiological and neuroimaging evidence.

Caterina Annalaura Pedersini
Tesi di Dottorato
Verona, 21 Novembre 2016
ISBN 9788869250378

Sommario

L'emianopsia è un disturbo visivo caratterizzato da cecità in una porzione del campo, controlaterale alla sede di lesione che coinvolge il circuito visivo. Nonostante tale difficoltà, alcune abilità visive residue ("blindsight") possono essere mantenute nel campo cieco; la probabilità di riscontrare tale fenomeno risulta incrementata dalla presentazione di stimoli in movimento che possono attivare l'area visiva motoria (hMT) senza passare dall'area visiva primaria (V1). Di conseguenza, un comportamento guidato dalla visione risulta possibile nel campo cieco, in assenza di consapevolezza percettiva. Questo progetto di ricerca è costituito da tre sessioni sperimentali svolte con sei pazienti emianoptici e partecipanti sani, allo scopo di esplorare le basi neurali del "blindsight" o della visione residua, valutare la risposta neurale determinata da stimoli presentati nel campo cieco e valutare se lo spostamento dell'attenzione spaziale verso il campo cieco incrementi la risposta sia neurale che comportamentale. Durante la prima sessione è stata valutata la presenza di "blindsight" o di visione residua esaminando la presenza di un punteggio superiore al caso durante lo svolgimento di compiti di discriminazione di movimento e orientamento di stimoli presentati nel campo cieco. In un paziente su quattro (L.F.) si è ottenuto un punteggio superiore al caso in assenza di consapevolezza percettiva nel compito di discriminazione del movimento. In questo caso il punteggio era associato alla sensazione di presentazione dello stimolo riportata dal paziente, che può rimandare al Blindsight di secondo tipo. Nella seconda parte è stata svolta una sessione di neuroimaging (fMRI) utilizzando uno scanner a 3Tesla, allo scopo di i) valutare la presenza di anormalità nella rappresentazione corticale del campo cieco, all'interno della corteccia visiva (Retinotopic Mapping), ii) valutare la posizione e l'attivazione dell'area hMT (hMT Localizer) e iii) valutare la connettività strutturale e l'integrità delle fibre di sostanza bianca nello stesso paziente (Imaging con Tensore di Diffusione, DTI). Nel paziente A.G. abbiamo riscontrato un' organizzazione retinotopica delle aree visive di basso livello in entrambi gli emisferi, nonostante la lesione interessasse prevalentemente la porzione dorsale della corteccia visiva primaria di sinistra (Retinotopic Mapping);

abbiamo osservato l'attivazione dell'area hMT nell'emisfero leso (hMT Localizer) e l'integrità delle vie visive ad eccezione delle radiazioni ottiche nell' area lesa (DTI). Durante la terza sessione è stato utilizzato un approccio elettrofisiologico. Per ottenere una risposta affidabile presentando stimoli nel campo cieco, è stata utilizzata la tecnica dei potenziali evocati Steady-state (SSVEP) che ha dimostrato essere più informativa rispetto ai potenziali evocati transienti in questo tipo di pazienti. La sessione includeva una stimolazione passiva e un compito di attenzione. L'obiettivo della prima era di valutare la risposta a stimoli che "sfarfallavano" (flickering) ad una frequenza specifica all'interno dei quattro quadranti; è stato osservato che in tutti i pazienti la presentazione dello stimolo nel quadrante cieco produceva una modulazione della risposta neurale che coinvolgeva entrambi gli emisferi. Nel compito di attenzione l'orientamento di quest'ultima verso il campo cieco determinava un incremento della risposta evocata rispetto alla condizione di non attenzione, anche quando quest'ultima veniva rivolta verso il campo cieco, seppur in assenza di consapevolezza percettiva. E' stata confermata quindi l'utilità degli SSVEP nella valutazione della risposta neurale in seguito alla presentazione di stimoli nel campo cieco. Questi risultati rappresentano un punto chiave interessante per lo studio delle basi neurali della visione inconsapevole in quanto dimostrano come stimoli presentati nel campo cieco possano determinare un' attività neurale attendibile in varie aree corticali.

Abstract

Hemianopia is a visual field defect characterized by blindness in the hemifield contralateral to the side of a lesion of the central visual pathways. Typically both eyes are affected. Despite loss of vision, it has been shown that some unconscious visual abilities ("blindsight") might be present in the blind field. It has been repeatedly shown that the probability of finding this phenomenon can be increased by presenting moving stimuli in the blind field which activate the motion visual area hMT, bypassing the damaged primary visual area V1. As a

consequence visually guided behaviour is made possible but perceptual awareness is lacking.

The present research project consists of three experimental sessions carried out with six hemianopic patients and healthy participants, in order to explore the neural basis of blindsight or residual vision. In particular, the project is focused on finding out whether unseen visual stimuli presented to the blind field can evoke neural responses in the lesioned or intact hemisphere and whether shifts of spatial attention to the blind field can enhance these response as well as the behavioural performance.

In the first session we assessed the presence of blindsight or conscious residual vision by carrying out a visual field mapping in binocular vision and by testing for the presence of unconscious above chance performance in motion and orientation discrimination tasks with stimuli presented to the blind area. We found evidence of unconscious above chance performance in one patient (L.F.) in the Motion Discrimination Task. In this case the above chance performance was associated with a feeling of something occurring on the screen, reported by the patient that resembles the so-called Blindsight Type II.

In the second session we used a neuroimaging technique with the purpose of: i) assess the presence of abnormalities in the cortical representation of the blind visual field in the visual cortex of one hemianopic patient (A.G.), ii) evaluate position and activation of area hMT and iii) assess the structural connectivity and the integrity of white matter fibers in the same patient. To do that, by using a 3 Tesla Scanner, we carried out a fMRI session with Retinotopic Mapping, hMT Localizer and Diffusion Tensor Imaging procedures. In patient A.G. we found a retinotopic organization of low-level visual areas in the blind as well as in the intact hemisphere, despite the lesion involving mainly the dorsal portion of the left primary visual cortex. Importantly, we documented an activation of area hMT in the damaged hemisphere and the integrity of the entire visual pathways except for the optic radiations in the area of the lesion.

In the third session we used an electrophysiological approach to study the neural basis of attention in the blind field of hemianopics. In order to obtain a reliable response with stimuli presented to the blind field, we used the Steady-State

Evoked-Potentials (SSVEP) technique that is likely to be more informative than transient Visual Evoked Potentials in these kind of patients. This session included a passive stimulation and an attentional task. The former was performed to assess the response to stimuli flickering at a specific frequency in four visual field quadrants, two in the left and two in the right hemifield. In this session, we found in all hemianopic patients that visual stimuli presented to the blind hemifield produced a modulation of the neural response involving the damaged as well as the intact hemisphere. In the attentional task we found that orienting attention toward the blind field yielded an enhanced evoked response with respect to the non-orienting condition. Thus, SSVEP confirmed to be a useful means to assess a neural response following stimulus presentation in a blind field. Importantly, this response was enhanced by focusing of attention despite lack of stimulus perceptual awareness. In a broader perspective these results represent novel interesting evidence on the neural bases of unconscious vision in that they show that despite being unseen visual stimuli presented to the blind field elicit reliable neural activity in various cortical areas. In some patients these areas are located in occipital lobe while in others they are located in frontal parietal areas depending on the site and extent of the lesion causing hemianopia.

Index

CHAPTER ONE

CHAPTER TWO

CHAPTER THREE

GENERAL INTRODUCTION

Hemianopia: a visual field defect

The visual system has a complex neural circuitry characterized by the transmission of visual information from the retina to the visual cortex. The first structure that records visual information from the environment is the retina, divided in nasal and temporal hemi-retina, composed by receptors that, via the retinal ganglion cells, translate visual information in electrical signals that are transmitted to the brain. Most projections from the retina (90%) go through the lateral geniculate nucleus (LGN) to primary visual cortex V1 (retinogenicolostriate pathway; Felleman & Van Essen, 1991; fig. 1). The remaining 10% of retinal fibers project to various subcortical structures and include a pathway going through the superior colliculus (SC) to the pulvinar and to extrastriate visual areas in the occipital and temporal lobes (retinotectal pathway; Cowey & Stoerig, 1991; fig. 1).

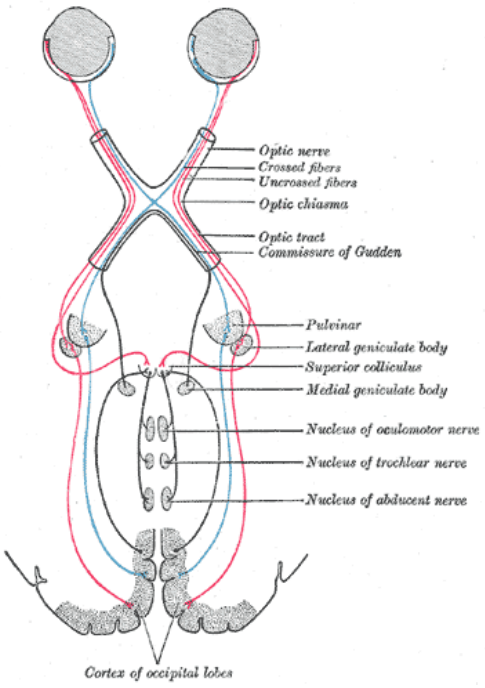

Fig 1. The Visual Pathway: retinogenicolostriate and retinotectal pathways

The primary visual cortex (striate cortex or area 17 or V1) is located in the occipital lobe within and surrounding the calcarine fissure. This area is retinotopically organized; it means that moving from the lower to the upper lip of the calcarine fissure, the representation of the visual field shifts from the upper to the lower field crossing the horizontal meridian, while moving from posterior to anterior cortex shifts from the center to the periphery (Engel, Glover & Wandell, 1997).

This retinotopic organization is maintained in several visual association areas (Felleman & Van Essen, 1991). From V1, visual information is sent to different extrastriate visual areas in the occipital and temporal lobes for further analysis (V2, V3, V4, hMT or MT) (Cowey & Stoerig, 1991; Felleman & Van Essen, 1991; Salin & Bullier, 1995). V1 has direct reciprocal connections with these areas (fig. 2).

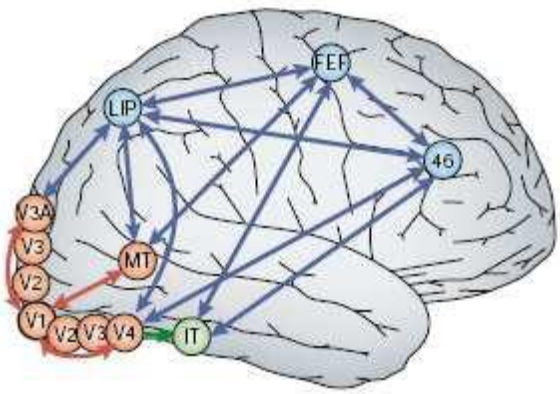

Fig.2. Connections between a subset of cortical visual areas (see Tong, 2003).

Along the visual pathways, different lesions can cause a specific defect of visual perception called **Hemianopia** that is characterized by decreased vision or blindness in half of the contralesional visual field of both eyes. In most cases the visual field loss does not extend beyond the vertical midline sometimes sparing the representation of the fovea (see below, fig. 3). The orderly anatomical connection of the visual pathways enables to localize the anatomical site of the lesion from clinical assessment of the visual field. The most common kind of Hemianopia is called **Lateral Homonymous Hemianopia (LHH)**, caused by a

retrochiasmatic damage involving either the two right or left halves of the visual field of both eyes.

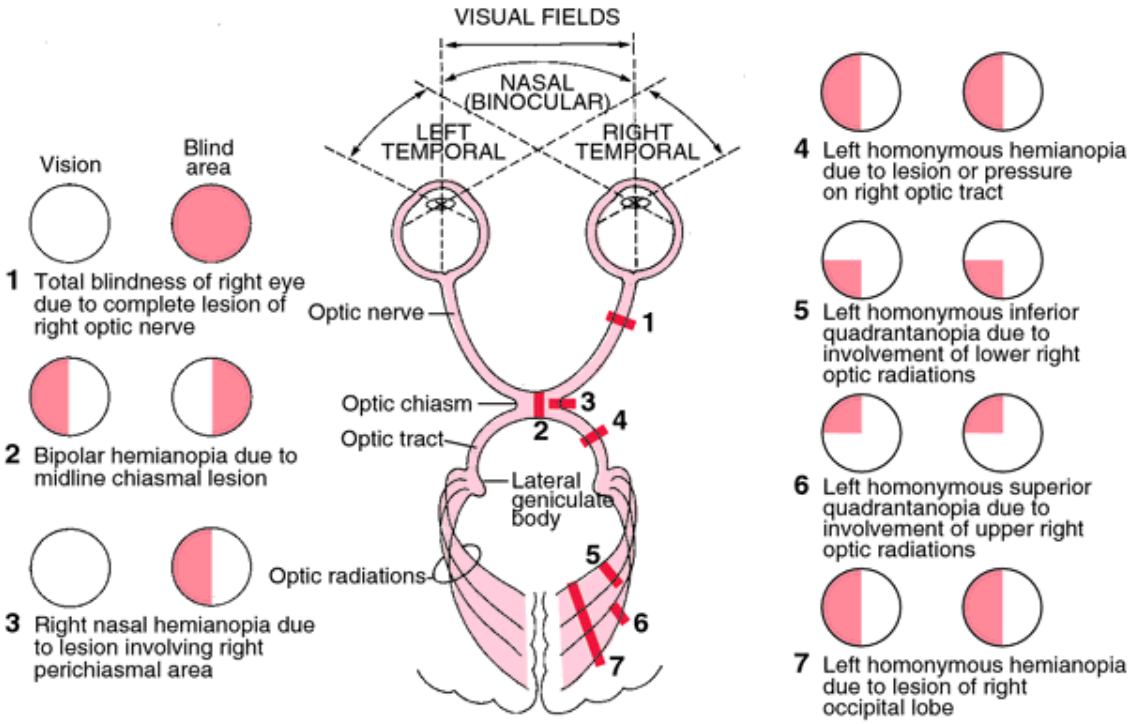

Fig 3. Visual Field Defects (from Polaski & Tatro, 1996)

- A lesion of the **Optic Nerve** causes a total blindness of the specific eye;
- A midline lesion of the **Optic Chiasm** causes a loss of vision in the temporal halves of both visual fields. This kind of deficit is referred to as Bitemporal Heteronymous Hemianopia (i.e., a deficit in two different halves of the visual field).
- A lesion interrupting the **Optic Tract** (OT) causes a complete loss of vision in the opposite half of the visual field of the two eyes. This kind of deficit is referred to as Contralateral Hemianopia.
- A lesion along the **Optic Radiation Fibers** (OR: bundle of axons from relay neurons in the LGN carrying visual information to V1 and other cortical visual areas) causes a loss of vision within a specific quadrant of the opposite half of the visual field of both eyes. In this case it is possible to find a superior or an inferior contralateral quadrantanopia depending on

the lesion site (for example an upper quadrantanopia caused by a lesion in the lower part of the radiation).

- A lesion of the **Striate Cortex (Area 17)** may cause a partial field deficit on the opposite site, depending on the specific bank of the calcarine fissure affected by the lesion.

  A lesion in the upper bank of area 17 causes a deficit in the inferior quadrant of the visual field in the opposite side; a lesion in the lower bank causes a deficit in the superior quadrant of the visual field on the opposite side. A lesion that involves both banks causes a complete deficit in the visual field in the opposite side.

Even if a widespread lesion of the visual cortex causes a more extensive loss of vision in the contralateral visual field, usually the central area of the visual field (fovea) is unaffected by cortical lesions. This phenomenon, known as macular sparing, can be explained by two main reasons: the former refers to the fact that the cortical representation of the foveal region is so extensive (the so called cortical magnification factor) that a single lesion is unlikely to destroy the entire visual representation; the latter refers to an overlap of ipsi- and contra-lateral projections of the ganglion cells in the foveal retinal area (Chelazzi et al., 1988; Marzi & Di Stefano, 1981; Slotnick et al., 2001).

Primary Visual Cortex and Visual Awareness

Visual awareness represents the ability to consciously perceive an event or an object present in the environment. The role that V1 and extrastriate areas play in visual awareness is still debated: the dominant point of view is that V1 is necessary for conscious but not for unconscious vision (for a review: Silvanto, 2014). Two main kinds of models have been proposed: a hierarchical feedforward model and a recursive model. According to the former, visual information processing giving rise to conscious perception is hierarchical in nature (Crick & Koch, 1995; Felleman & Van Essen, 1991): lower-level visual areas such as V1 have the role to provide input to regions at the top of the hierarchy where high-

level visual perception and awareness arise. Recursive models, instead, propose that all visual areas along the visual ventral stream, from V1 to inferotemporal cortex, serve as a substrate for different aspects of phenomenal visual experience. In this way, V1 would participate to visual awareness by forming dynamic recurrent circuits together with extrastriate areas (Pollen et al., 1999; Bullier, 2001; Lamme & Roefsema, 2000).

To clarify the role of V1 and other cortical and subcortical areas in visual awareness the aim of this project is to study visual perceptual awareness in hemianopic patients with lesion at different levels of the central visual system. Healthy and hemianopic participants have been tested in behavioural, electrophysiological and functional imaging sessions while performing various visual tasks. Importantly, in hemianopic patients the visual stimuli were presented not only to the sighted but also to the affected hemifield. This enables to compare visual performance with and without perceptual awareness and to assess the neural structures selectively activated during unconscious and conscious vision.

Research Project: Patients recruitment

Three different experiments were carried out with healthy control participants and hemianopic patients with lesion at different levels of the visual pathway. To be included in this study, the latter participants were required to fill in an informed consent form, accepting to take part in the project, to be previously diagnosed with a lateral homonymous hemianopia as a consequence of a retrochiasmatic lesion occurred at least three months before, to have performed a campimetry and a structural MRI in order to evaluate position and extent of the lesion. Exclusion criteria were the following: 1) other pre-existing neurologic or psychiatric disorders 2) drugs or alcohol addiction; 3) presence of some medical-surgical implant that could prevent the execution of EEG, fMRI or MEG (such as Pacemaker); 4) presence of a general cognitive impairment as revealed by a score equal or less than 24 at the Mini Mental State Examination (MMSE, Folstein et al., 1975); 5) presence of Spatial Attention impairment (such as Neglect). In order to carefully investigate the presence of a general cognitive impairment or a

visuospatial disorder, patients and healthy participants were administered with a neuropsychological battery including:

- Specific tests in order to evaluate visuospatial impairments:
    - Line Bisection Task (Schenkenberg et al., 1980)
    - Diller letter H cancellation test (Diller et al., 1977)
    - Bell Cancellation Test (Gauthier et al., 1989) .
- The Mini Mental State Examination, as a screening test for cognitive loss;
- Only with patients, we performed a standardized Questionnaire; the Visual Function Questionnaire (VFQ25), in order to assess their subjective impressions on their visual abilities in everyday life (Mangione et al., 2001).

  This test includes 12 subscales concerning different aspects of vision: general health, general vision, ocular pain, near activities, distance activities, social functioning, mental health, role difficulties, dependency, driving, color vision and peripheral vision.

On the basis of these criteria, we selected 6 patients; some of whom performed the entire series of behavioural, electrophysiological and neuroimaging experiments while others performed only some of the tests.

First experiment:

Evaluation of "Blindsight" in Hemianopics

Introduction

In the last 50 years, it has been established that unperceived stimuli can influence behaviour in both healthy participants and hemianopic patients. As to the latter, it has been found that some patients with damage along the visual pathway show a peculiar form of unconscious vision called blindsight: i.e. the ability to respond to visual stimuli presented in their visual field even if they cannot consciously perceive them. Importantly, blindsight should not be confused with residual vision that defines conscious visually guided behaviour spared or restored following a visual cortical lesion. Hemianopic patients with blindsight can localize an unseen stimulus presented in the blind hemifield with above chance accuracy either by moving their eyes or by pointing toward the site of the visual target (Poeppel et al., 1973; Weiskrantz et al., 1974, 1996). Those patients are characterized by the dissociation between functional visual processing and subjective visual experience. For this reason, blindsight can play a role in the study of the neural bases of visual awareness especially as far as assessing which alternative visual pathways can subserve unconscious vision. Weiskrantz, in 1998, proposed the existence of two different types of blindsight: type I and type II (Kentrige, 2014). The former refers to the ability to guess, at levels significantly above chance, various features of a visual stimulus, like location or motion, without any acknowledged awareness of the stimulus; the latter refers to the feeling that a change within the blind field has occurred, even without any perceptual awareness of the visual stimulus presented.

Blindsight can be studied through two different approaches: one is the direct method that includes forced-choice guessing in which participants have to detect or discriminate some feature of a stimulus shown in the blind visual field, that they cannot consciously perceive; the other is an indirect method, where the influence of the unseen stimulus on the response to stimuli presented in the sighted hemifield is evaluated (i.e., speeding of RT in the intact field for stimuli simultaneously presented in the blind field in a Redundant Target Effect

paradigm; Miller, 1982; Raab, 1962) (Marzi et al., 1986; Rafal et al., 1990; Tomaiuolo et al., 1997).

According to a growing number of behavioural and neuroimaging studies, Blindsight could be mediated by subcortical visual centers, such as the Superior Colliculus (**SC**), **LGN** and Pulvinar, that receives direct projections from the retina and sends connections to the cortex, the collicular-extrastriate pathway (Tamietto et al, 2009, Morris et a., 1999, 2000), the direct route that links LGN to the middle temporal cortex, bypassing the striate cortex (Ptito et al., 1999; Leh et al., 2010; Tamietto et al., 2010; Gaglianese et al., 2012) or some spared "islands" of cortex within the lesion in V1 (Wessinger, Fendrich & Gazzaniga, 1997, 1999).

The possibility that SC could be involved in blindsight has been raised originally from a study in monkeys, which demonstrated that they lost their ability to foveate visual stimuli presented in the scotoma as a consequence of a lesion n SC (Mohler & Wurtz, 1977). Studies of macaques showed that SC is anatomically and functionally divided into superficial and deep layers. Neurons in the deep layers are involved in orienting movements of the head and eyes in response to sensory stimuli. Neurons in the superficial layers, respond to stationary and moving visual stimuli not considering stimulus orientation, size, shape, or velocity (Cynader & Berman, 1972; Goldberg & Wurtz, 1972; Marrocco & Li, 1977) and contain a map of the contralateral visual field (Cynader & Berman, 1972). Their main input is coming from the retinotectal pathway (Schiller & Malpeli, 1977), but their response properties may also be influenced by feedback projections from striate (Wilson & Toyne, 1970) and extrastriate cortex (Fries, 1984). In humans, the SC shows responses to contralateral visual field stimulation and has a retinotopic organization (Schneider & Kastner, 2005). The SC is more sensitive to the temporal periphery of visual field and this is reflected by RT to peripheral stimuli.

The SC hypothesis has received further support by performing neuroimaging studies with hemispherectomized patients. Leh et al. (2006a) found that two hemispherectomized patients with blindsight had connections from ipsilateral and contralateral SC to intact hemisphere and to the spared frontal cortex of the other hemisphere. Another neuroimaging study (Leh et al., 2010) showed, in a hemispherectomized patient (temporo-parieto-occipital removal), activation of

MT and frontal eye fields (but not of V1 and V2) when achromatic stimuli were presented in the blind field, while no activation was evident when purple-blue stimuli invisible to SC were displayed in the blind field. Furthermore, Tamietto et al. (2010) found that a grey stimulus presented in the blind field of blindsight patient GY although not consciously seen, could influence his visuo-motor and pupillary responses to consciously perceived stimuli in the intact field (implicit redundant signal effect). Importantly, this was accompanied by selective fMRI activations in the SC and in visual extrastriate areas. However, when purple stimuli, which are invisible to the SC, were presented, no evidence of implicit visuomotor integration remained and SC activation dropped significantly. For what concerns the role of **spared "island" of V1** in Blindsight, Fendrich and collaborators (1992) described a patient who showed blindsight in a small area of the visual field (1°) and a small corresponding activation in V1. This kind of small activation, probably, is not always detectable but might be responsible of some cases of blindsight. For what concerns extrastriate areas, data from monkeys show that after lesion in V1 and a degeneration of projection cells in the dorsal LGN and in the retina (Cowey, Stoering, & Perry, 1989; Van Buren, 1963), some subcortical nuclei still receive input from parts of the retina and project directly to extrastriate visual cortex. Furthermore a part of LGN cells are spared after V1 ablation (koniocellular system; Cowey & Stoering, 1989). These cells project from the interlaminar layers of the LGN directly to the extrastriate cortex. Interlaminar layers, interestingly receive input also from the SCs (Harting, Huerta, Hashikawa, & van Lieshout, 1991).

Moving stimuli and Blindsight

The primary visual cortex V1 and other extrastriate visual areas are part of the two main visual pathways: the ventral or "what" system, specialized in fine-grained analysis of the visual scene and the dorsal or "where" system, specialized in spatial and motion analysis.

The two visual pathways originate in V1 and go to the temporal (ventral stream) and parietal lobe (dorsal stream) respectively. The former is also thought to mediate "vision for perception" and is typical of perceptual awareness, while the

second sub-serves “vision for action” (Milner & Goodale, 1995; Mishkin, Ungerleider & Macko, 1983; fig. 4) and can be involved in unconscious behaviour.

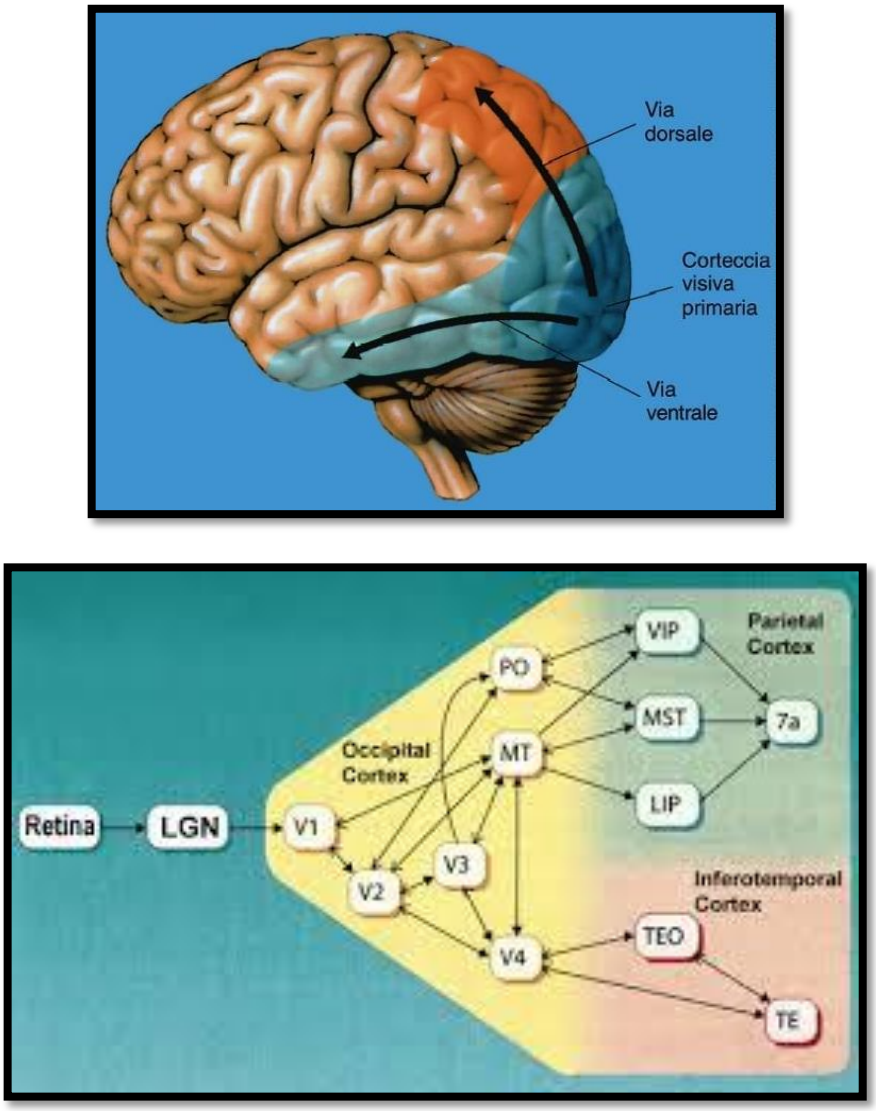

Fig.4. Ventral and Dorsal Pathways

Numerous imaging studies performed with healthy participants have demonstrated that in area hMT (human middle temporal/V5) along the dorsal stream, neural activity increases more in response to moving compared to stationary stimuli, indicating preferential involvement in the processing of motion information (Goebel et al., 1998; Tootell et al., 1995; Watson et al., 1993). A dynamic parallelism has been found by neuroimaging studies with healthy participants

showing that motion perception is mediated by two dissociable pathways: a route going from the retina to area hMT via subcortical nuclei bypassing V1 (Barleben et al., 2014), that is involved in visual perception of fast moving stimuli (speed > 6°/sec) and an indirect cortical route via striate cortex, which is involved in processing slow motion (< 6°7sec). In hemianopic patients with blindsight, it has been observed that area hMT could be activated by presenting moving stimuli in the blind visual field (real or apparent motion) indicating that responsiveness to moving stimuli could be maintained despite the V1 lesion (Ajina et al., 2014). Thus, the persistence of this unconscious motion detection in patients with destruction of primary visual cortex could be explained by the existence of a connection between LGN and cortical area hMT (Gaglianese et al., 2012). Azzopardi and Cowey, 2001, tested three hemianopic patients in a forced choice task, asking them to discriminate moving vs static stimuli. They showed different kinds of stimuli (single bars, random dots, gratings, plaids defined by either luminance contrast, first-order movement, or dynamic texture contrast without a luminance cue, second order movement) at four different speeds (4/20/32/64 °/sec). They found that all patients could discriminate moving vs static stimuli at fast speed, low spatial frequency and high temporal frequency (objectless motion energy; Azzopardi & Hock, 2011). When they asked patients to discriminate motion direction, they found that they could always discriminate it using bars while using gratings or dots they could perform the task correctly only when lateral occipital visual areas were preserved by the lesion. According to different papers reported in the literature, blindsight could be elicited most reliably by large square-ware gratings with sharp border (Alexander & Cowey, 2010; > 4° in diameter) and that it can be tuned in the spatiotemporal domain, with best performance between 0,5 and 2 cycle/° (Barbur et al., 1994; Morland et al., 1999) and temporal frequencies between 5 and 20 Hz that represent only a portion of the spatiotemporal range exhibited by normal vision (Das et al., 2014).

Behavioural Experiments

Main purposes of this behavioural session were two: first of all, to verify patient's campimetry by performing a visual mapping using a visual stimulus similar to the

one we would use in the following sessions, and then to evaluate the presence of blindsight in hemianopics, by using apparent motion (Pavan et al., 2011) and bars orientation.

Materials and Method:

Participants:

In this experiment we tested one age-matched healthy participant and four hemianopic patients. All participants had normal or corrected-to-normal visual acuity and no history of psychiatric disorders. All gave their written informed consent to participate in the experiment that was carried out according to the principles laid down in the 1964 Declaration of Helsinki and approved by the Verona AOUI and by the ERC Ethics Committee.

Healthy Participant:

P.G, a 49 years old female, right handed and without any neurological impairment. In neuropsychological tests performed to evaluate cognitive impairment and visuo-spatial attention deficit, P.G. scores were in the range of normality.

Hemianopic Patients:

L.F., F.B., S.L. and A.M. who participated in this study, had long-standing post-chiasmatic lesions.

L.F. is a 50 years old female, right-handed, with an upper left quadrantanopia (fig.5) as a consequence of an ischemic stroke occurred in 2012, affecting a small portion of the right primary visual cortex, along the calcarine fissure. The lesion caused also a fiber reduction of the optic radiation. During the MRI session performed 3 years ago, it was observed a significant activation (75%) of visual areas in the damaged right hemisphere) during the presentation of visual stimuli on the whole screen and a normal activation within the intact left hemisphere.

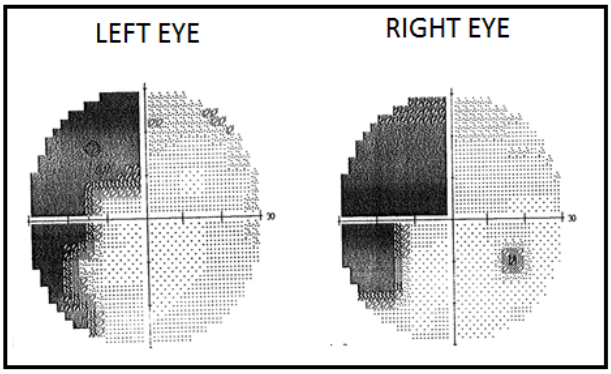

Fig. 5. L. F. Visual Field Map: upper left quadrantanopia; some blind area involved also the lower left quadrant.

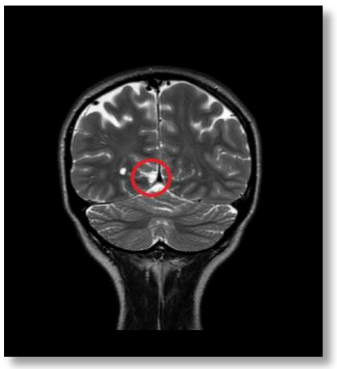

Fig.6. MRI (T2) coronal section of patient L.F. with the localization of the lesion (left side of the image).

L.F. lesion is small and located only along the calcarine fissure; for this reason it is impossible to visualize it on the surface. Fig. 7 represents a reconstruction of the lesion on coronal slices of a T1-weighted image.

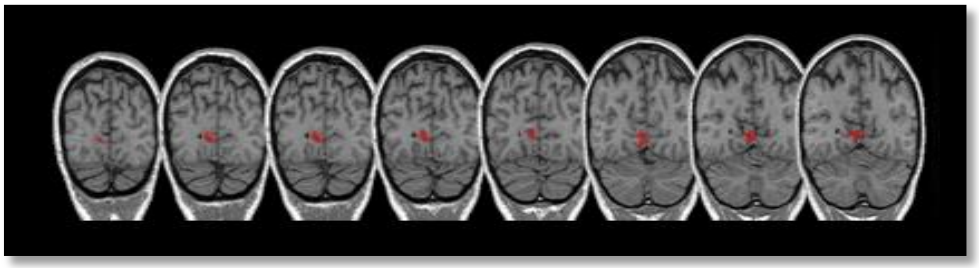

Fig. 7

L.F. performed neuro-psychological tests without showing any kind of cognitive and visuo-spatial impairment (MMSE = 28.89/30; LINE BISECTION TASK = -0.56cm; DILLER H CANCELLATION TEST = 106/106; BELL CANCELLATION TEST = 35/35).

In VFQ25 Questionnaire, she obtained a high score: 90.71.

F.B. is a 49 years old female, right handed, with a Left Lateral Homonymous Hemianopia (fig. 8) as a consequence of a right temporal-parietal-occipital head trauma occurred one year ago, that affected that area as well as the right optic radiations.

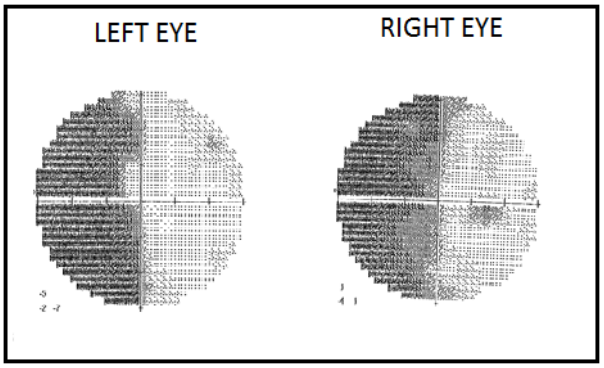

Fig. 8. F.B. Visual Field Map: left homonymous hemianopia without foveal sparing and with some areas with survived sensitivity in the left eye, along the vertical midline.

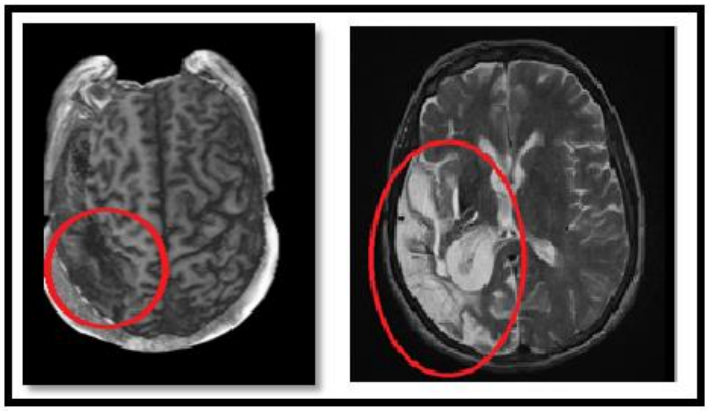

Fig. 9. Surface and T2-weighted axial section of patient F.B. with the localization of the lesion (left side of the image).

Fig. 10 represents the reconstruction of the lesion on axial slices of a T1-weighted image:

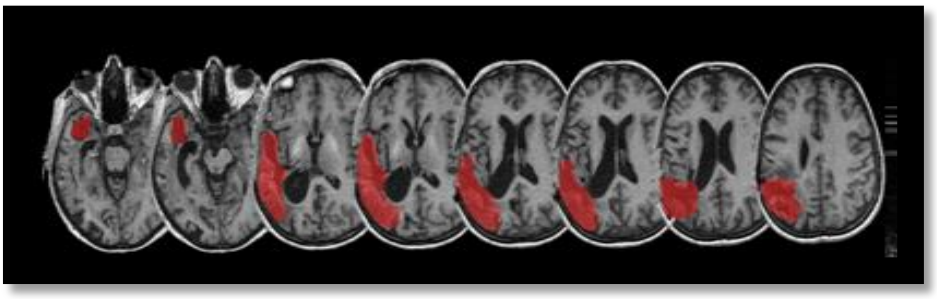

Fig. 10

F.B. performed neuropsychological tests without showing any kind of cognitive impairment (MMSE = 29.62/30). In the visual-spatial evaluation, the performance was affected by her motion and postural difficulties: during the Diller H Cancellation Test, she could not keep the head still in a central position but she needed always to move it toward the left side (94/106) and during the Bell Cancellation Test she had some difficulties in recognizing bells in the center of the paper (24/35). In contrast, her performance was completely in the normal range in the Line Bisection Test (LINE BISECTION TASK = -0.34). At the end of the evaluation she was very tired as those tests were quite demanding for her.
In VFQ25 Questionnaire, she obtained a high score: 82.38. Therefore she reported that the quality of her life was significantly affected by some problems not directly related to the visual impairment. Thus, she has to move using the wheelchair and is unable to meet her physiological needs on her own, thus requiring always the presence of her husband or someone else who can help her.

S.L. is a 50 years old female, with a right Lateral Homonymous Hemianopia (fig. 11) as a consequence of an ischemic stroke with a hemorrhagic development, occurred in 2009; the lesion involves the medial part of the left occipital lobe.

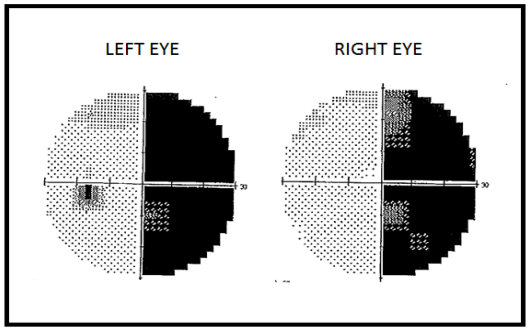

Fig. 11. S.L. Visual Field Map (23/02/2015): right homonymous hemianopia without foveal spearing and with some areas with survived sensitivity, mainly in the right eye.

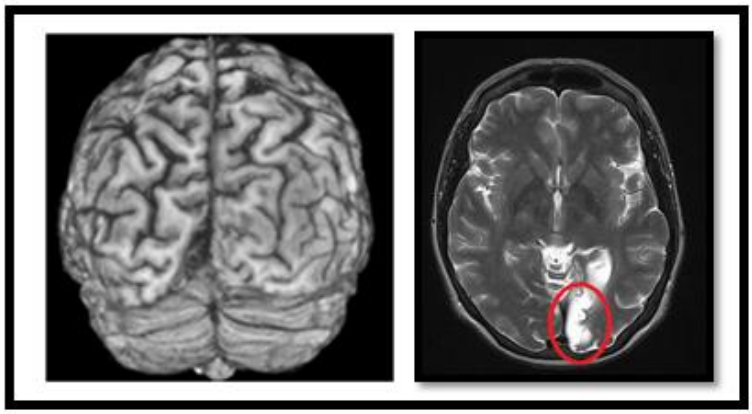

Fig. 12. Surface and T2-weighted axial section of patient S.L. with the localization of the lesion (right side of the image).

Fig. 13 represents a reconstruction of the lesion on axial slices of a T1-weighted image:

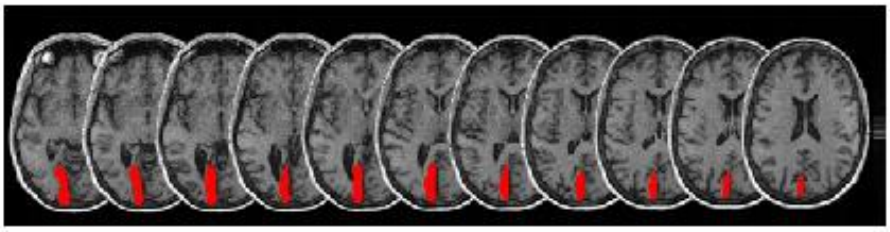

Fig. 13

S.L. performed the neuropsychological tests without showing any kind of cognitive and visuo-spatial impairment (MMSE = 29/30; LINE BISECTION TASK = +0.08; DILLER H CANCELLATION TEST = 106/106; BELL CANCELLATION TEST =

35/35). In VFQ25 Questionnaire, she obtained a total score within the normal range: 78.42.

A.M. is a 65 years old man, right-handed, with an Altitudinal Bilateral Hemianopia (fig. 14) as a consequence of an ischemic stroke caused by a dissection of the vertebral artery, which caused a damage involving the whole area of the Willis' Circle. In details, the stoke compromised the activation of some cortical and subcortical districts: bilaterally sotto-cortical white matter fibers, in correspondence of occipital lobe, close to the calcarine fissure, the right thalamus and the pulvinar. He performed a visual compensatory training (Nova Vision) that increased his skills in moving attention toward the blind hemifield.

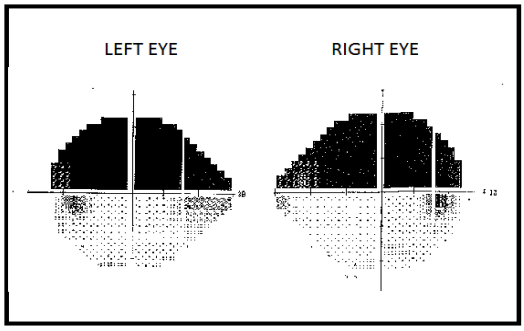

Fig. 14. A.M. Visual Field Map (15/12/2014): Altitudinal Bilateral Hemianopia without foveal spearing and with some areas with survived sensitivity.

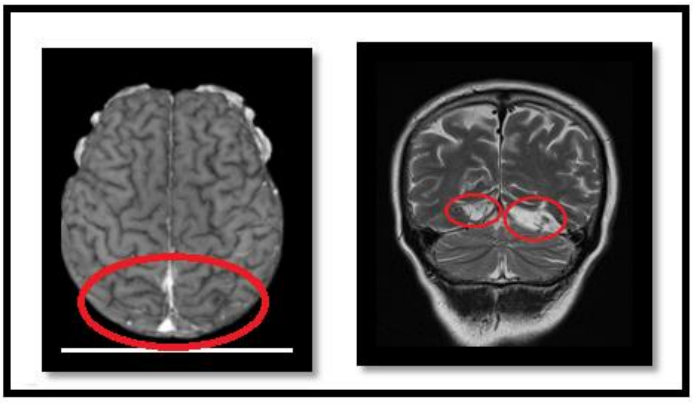

Fig. 15. Surface and T2-weighted coronal section of patient A.M. showing the lesion in the whole area of the Willis' Circle.

Fig. 16 represents a reconstruction of the lesion on coronal slices of a T1-weighted image:

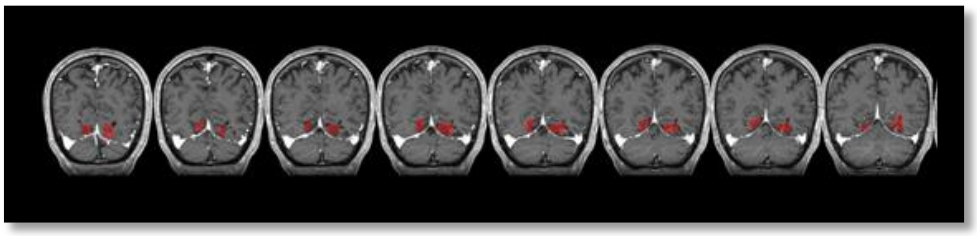

Fig. 16

A.M. performed the neuropsychological tests without showing any kind of cognitive and visuo-spatial impairment (MMSE = 28.46/30; LINE BISECTION TASK = +0.2; DILLER H CANCELLATION TEST = 106/106; BELL CANCELLATION TEST = 34/35). In VFQ25 Questionnaire, A.M. obtained a total score within the normal range: 74.25. He reported that his daily life was significantly affected by both the visual defect and the permanent pain that affects the whole left side of his body.

Apparatus, Stimuli and Procedure:

Background and stimuli were presented on a LCD (100Hz/ 1920x1080 pixels) monitor and were generated by E-Prime software version 2. Monitor luminance was measured with a Minolta CL-200 Chroma Meter (Minolta Co., Japan). Participants were seated 57 cm from the monitor, in a dark room where the light source was represented by the monitor screen.

We asked participants to keep their head still but we decided not to use the chin rest as it could be uncomfortable for some of them; their gaze was controlled by the use of a closed-circuit TV camera. We used also an Eye Tracker (EyeTribe, software OGAMA) to control that participants were fixating a central point on the screen without saccading to the stimulus.

At the beginning of the session we performed a visual mapping in order to assess with precision the location of the blind area. For **visual mapping**, we used sqare-wave gratings (fig. 17; Michelson contrast = 1; size = 2°; 7 bars; stimulus duration = 150ms) presented in a random order at different positions in the blind field.

Fig.17. Stimulus used for visual mapping

We presented some stimuli also in the sighted visual field to maintain attention focused on both hemifields. Patients were to signal stimulus detection by pressing a PC key. Considering different lesions and visual defects, we prepared different kinds of visual mapping each one specific for a particular visual defect. With patients with a full hemianopic loss, we presented visual stimuli in 195 positions, moving them in step of 2° of visual angle, each presentation repeated three times. We alternated these positions with 20 presentations in the sighted visual field, each repeated three times. In patients with quadrantanopia, we presented visual stimuli in 91 positions, moving them in step of 2° of visual angle, each presentation repeated three times. We alternated these positions with 10 presentations in the corresponding sighted quadrant of the visual field, each one repeated three times.

In the following session, participants performed two different tasks with the same instructions but with two different stimulus features, motion and orientation. In the **Motion Task**, stimuli were represented by horizontally oriented sqare-wave gratings (Michelson contrast = 1; size = 4°; 7 bars, stimulus duration = 250ms; temporal frequency = 8.33deg/sec) lateralized to the right or the left hemifield, either static or moving. The speed of downward movement was 8.33 °/sec. In the **Orientation Task**, the same stimuli were static with horizontal or vertical orientation (Fig. 18).

Fig.18. Stimuli used in the Orientation Task

On each trial, participants were asked to discriminate either stimulus motion or orientation in different blocks (forced-choice paradigm). The response key was represented by button “z” and “x” of the spacing bar of the PC. After each presentation to the blind field, patients were asked to respond according to an awareness scale similar to the perceptual awareness scale (PAS) of Ramsoy et al., 2004. There were three possible choices:

1- I saw nothing
2- I had the feeling of something appearing on the screen but I could not see it.
3- I saw the stimulus.

In the presence of above-chance discrimination performance, response 1 was likely to indicate Blindsight Type I while response 2 might indicate Blindsight Type II. Finally, response 3 would indicate normal or degraded conscious vision.

Both tasks included 6 blocks repeated in a sequential order. Each block included 96 trials, 80 experimental and 16 catch trials where the fixation dot appeared without the visual stimulus. In those trials we asked participants to respond by pressing one or the other response key, in order to evaluate the presence of response bias.

Design of the experiment:

The various phases of the discrimination experiments are schematized in Fig.19.

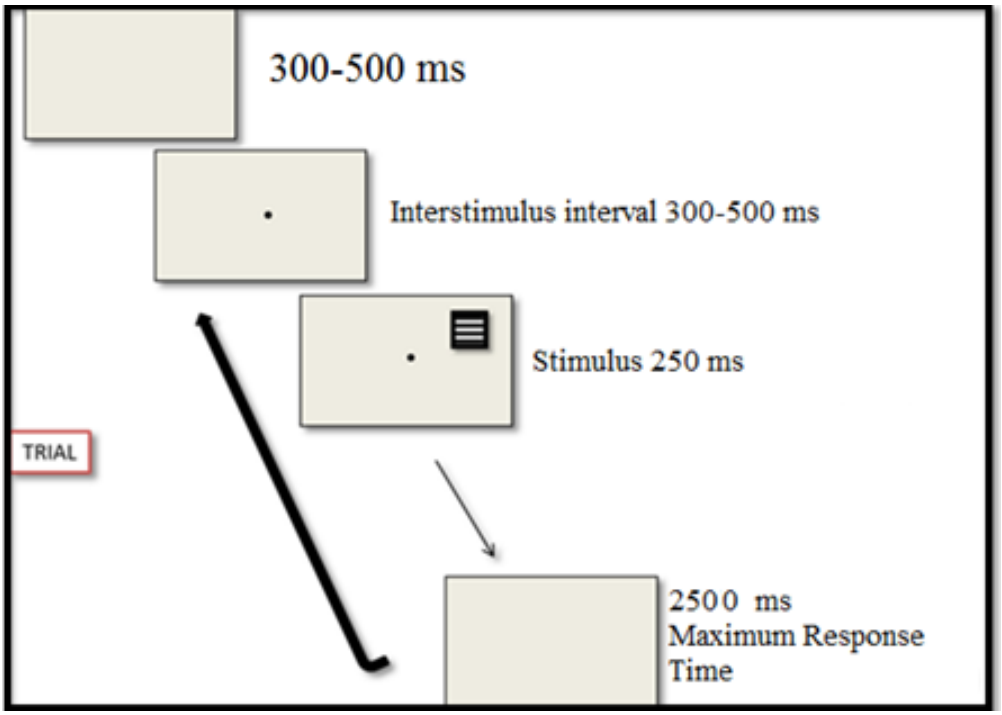

Fig.19. Structure of the behavioural experiment.

Results: Healthy Participant P.G.

Stimulus Position: x axes = 12°; y axes = 4°

Only reaction times between 140ms and 650ms were considered.

Motion Discrimination Experiment

Behavioural results of P.G. for left and right upper visual quadrants (table 1).

MOTION	HEMIFIELD	INCORRECT RESP	CORRECT RESP
STATIC	LEFT	4,17%	95,83%
MOTION	LEFT	1,67%	98,33%
STATIC	RIGHT	2,50%	97,50%
MOTION	RIGHT	0,83%	99,17%

Table 1

The percentage of errors was very low in both conditions. Reaction Times were similar considering correct responses for both moving and static gratings; they

were around 560ms as the task was difficult. In catch trials we observed the predominant presence of static response in both hemifields; those results indicated the presence of a response bias toward that condition.

Orientation Discrimination Experiment

Behavioural results of P.G. for left and right upper visual quadrants (table 2).

ORIENTATION	HEMIFIELD	INCORRECT RESP	CORRECT RESP
VERTICAL	LEFT	4.17%	95.83%
HORIZONTAL	LEFT	1.67%	98.33%
VERTICAL	RIGHT	0.83%	99.17%
HORIZONTAL	RIGHT	1.67%	98.33%

Table 2

The percentage of errors was very low considering both conditions. Reaction Times were around 580ms considering both orientations. In catch trials we observed the absence of a response bias.

Results: Hemianopic Patients

PATIENT L.F.

Stimulus Position: x axes = 12°; y axes = 4°, in the upper hemifield

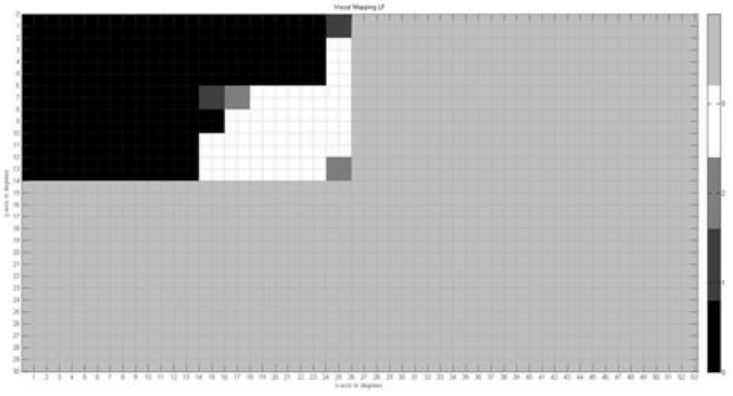

Fig. 20. L.F. Visual Mapping: Black squares indicate absence of response (0 over 3); dark grey indicates the presence of 1 response over 3; light grey the presence of 2 responses over 3 while white squares the presence of 3 correct responses over 3.

Motion Discrimination Experiment:

Behavioural results of L.F. for blind and sighted upper visual quadrants

(graph 1 and table 3)

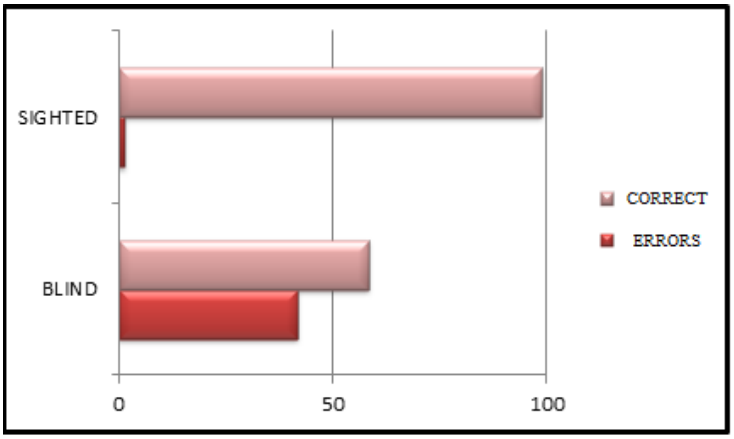

Graph 1

HEMIFIELD	INCORRECT RESP	CORRECT RESP
BLIND (MOTION and STATIC)	**41,67%**	**58,33%**
SIGHTED (MOTION and STATIC)	1,25%	98,75%

Table 3

In the sighted quadrant the performance was almost faultless, see Graph 1, while in the blind visual quadrant L.F. gave 58.33% correct responses and 41.67% incorrect responses. To verify if this difference was significant we performed the **Binomial Test** (table 4).

		Category	N	Observed Prop.	Test Prop.	Asymp. Sig. (2-tailed)
BLIND	CORRECT	1,00	140	,58	,50	**,012**[a]
	INCORRECT	,00	100	,42		
SIGHTED	CORRECT	1,00	237	,99	,50	**,000**[a]
	INCORRECT	,00	3	,01		

Table 4

As shown in Table 4 this difference was significant considering both visual quadrants. We also analyzed results separately for moving and static condition (Table 5).

MOTION	HEMIFIELD	INCORRECT RESP	CORRECT RESP
STATIC	BLIND	**52,50 %**	**47,50 %**
MOTION	BLIND	**30,83 %**	**69,17 %**
STATIC	SIGHTED	1,67 %	98,33 %
MOTION	SIGHTED	0,83 %	99,17 %

Table 5

With the **Binomial Test** (table 6) we found that L.F. performance was significantly above chance only for detecting moving gratings.

		Category	N	Observed Prop.	Test Prop.	Asymp. Sig. (2-tailed)
STATIC	CORRECT	,00	63	,53	,50	,648[a]
	INCORRECT	1,00	57	,48		
MOTION	CORRECT	1,00	83	,69	,50	**,000**[a]
	INCORRECT	,00	37	,31		

Table 6

On the basis of these results, we checked the correspondence between behavioural results and responses given in the **Awareness Scale** at the end of each trial, in the blind visual field, considering both conditions.

Static condition (table 7):

AWARENESS SCALE	PERCENTAGE of TOTAL RESP	PERCENTAGE of CORRECT RESP
1	67%	**61,25%**
2	33%	**20%**

Table 7. Awareness Scale. Response 1: I did not see anything;
Response 2: I had the feeling of something on the screen but I could not see it.

M**otion condition**: (table 8):

AWARENESS SCALE	PERCENTAGE of TOTAL RESP	PERCENTAGE of CORRECT RESP
1	57%	**50 %**
2	43%	**94,23 %**

Table 8.

With static gratings, in almost 67% of trials she chose level 1 of the awareness scale while in 33% of trials she chose level 2. Nevertheless, responses were almost always incorrect (80%) in the latter case. It means that she had a feeling of something presented in the blind visual quadrant but it was not enough to give the correct response. With moving gratings, in almost 57% of trials L.F. chose level 1 of the awareness scale, while in 43% of trials she chose level 2, indicating that she perceived something in the blind field. These results were interesting as she used to give correct responses (94% of correct responses) while choosing level 2 in the awareness scale; it means that she could perceive something in the blind visual field and that this unconscious perception was sufficient to give the correct response. Considering both conditions, she has never chosen level 3 of the awareness scale as she could not consciously see and discriminate features of stimuli shown in the blind quadrant. Reaction times were always slower with moving gratings in both sighted and blind visual quadrants.

In catch trials presented in the blind visual field, L.F. chose the static condition in 71% of cases while only in 29% of cases she chose the moving condition. This result indicated that the increased performance observed with moving gratings was not related to the presence of a response bias but to a **better performance in the moving condition**.

Orientation Discrimination Experiment

Behavioural results of L.F. for left and right upper visual quadrants

(graph 2 and table 9)

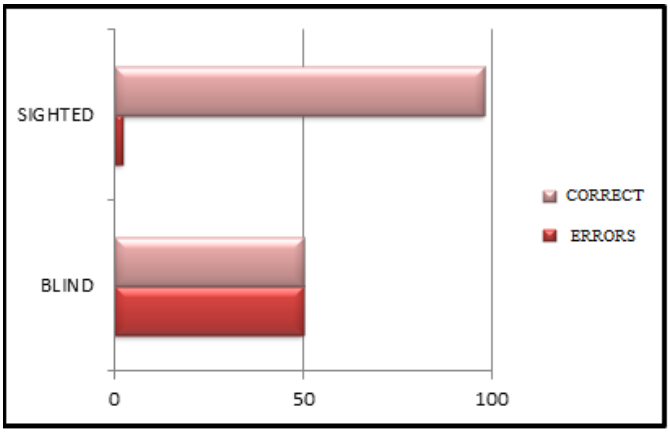

Graph 2

HEMIFIELD	INCORRECT RESP	CORRECT RESP
BLIND (VERTICAL + HORIZONTAL)	**50%**	**50%**
SIGHTED (VERTICAL + HORIZONTAL)	2,08%	97,92%

Table 9

In the blind visual quadrant her performance was exactly at the chance level combining both vertical and horizontal orientations; for this reason we decided not to perform the Binomial Test. Even analyzing results for vertical and horizontal orientations separately, we did not find any relevant difference. We decided to verify the correspondence between behavioural results and responses given in the **Awareness Scale** at the end of each trial, in the blind visual field.

Concerning the **vertical orientation** we observed these results (table 10):

AWARENESS SCALE	PERCENTAGE TOTAL RESPONSE	PERCENTAGE CORRECT RESP
1	97.5%	**52.14 %**
2	2.5%	**100 %**

Table 10. Awareness Scale. Response 1: I did not see anything;
Response 2: I had the feeling of something on the screen but I could not see it.

Concerning the **horizontal orientation,** we observed these results (table 11):

AWARENESS SCALE	PERCENTAGE TOTAL RESPONSE	PERCENTAGE CORRECT RESP
1	97.5%	**47.01%**
2	2.5%	**33.33 %**

Table 11

Presenting both horizontal and vertical gratings, in 97.5% of trials she chose level 1 of the awareness scale, while in 2.5% of trials she chose level 2, indicating that in almost all trials she could not perceive anything in the blind visual field. With vertical gratings, the performance was at the chance level when she chose level 1 of the awareness scale, while it was always correct when she chose level 2 (only in 2,5% of cases). With horizontal gratings, the performance was at the chance level when she chose level 1 of the awareness scale, while it was worse than the chance level when choosing level 2 (33.33% of correct responses), indicating her inability to discriminate stimulus features even if she reported a feeling. Considering both conditions, she has never chosen level 3 of the awareness scale as she could not consciously see and discriminate features of stimuli shown in the blind quadrant. Reaction Times were slower for errors in the sighted visual field; in other conditions they were similar. In catch trials in the blind visual field, L.F. chose the vertical condition in 48% of cases while in 52% of cases she chose the

horizontal one. This result indicated that there was no response bias toward a specific condition.

CONCLUSION:

In conclusion we observed that the motion feature could increase the probability of finding a performance above chance with an unconscious perception of the stimulus, creating a feeling of something on the screen; instead the modulation of bars orientations could not produce any behavioural difference in a discrimination task. These results confirmed the idea that motion is a feature that hemianopic patients could discriminate better and easier than others in the blind hemifield, since with moving gratings, in 43% of trials, she chose level 2 of the awareness scale indicating her ability to feel the presence of something in the blind field and this sensation corresponded to a good performance.

PATIENT F.B.

Stimulus position: x axes = 10°; y axes = 6°, in the lower hemifield.

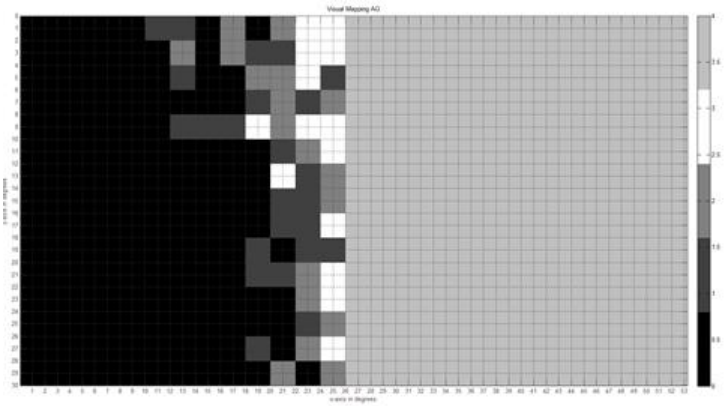

Fig. 21. F.B. Visual Mapping: Black squares indicate absence of response (0 over 3); dark grey indicates the presence of 1 response over 3; light grey the presence of 2 responses over 3 while white squares the presence of 3 correct responses over 3.

Motion Discrimination Experiment

Behavioural results of F.B. for left and right lower visual quadrants

(graph 3 and table 12)

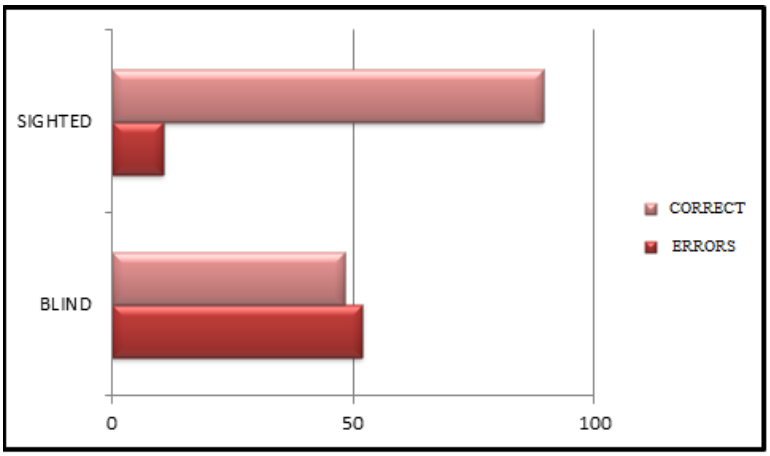

Graph 3

HEMIFIELD	INCORRECT RESP	CORRECT RESP
BLIND (MOTION + STATIC)	**51,87%**	**48,13%**
SIGHTED (MOTION + STATIC)	10,62%	89,38%

Table 12

In this case we observed that in the blind visual field, F.B. gave 48.13% of correct responses (at the chance level) and almost 52% of incorrect responses. The Binomial Test demonstrated that the performance was not significantly different from chance level. The analysis performed considering the two features separately did not show the presence of any relevant difference.

In the awareness scale, F.B. chose always level 1, indicating her inability to feel something occurring in the blind visual hemifield. Reaction Times were slower for correct responses in the sighted visual field, instead in other conditions they were similar for moving and static gratings. Considering catch trials in the blind visual field, F.B. chose almost always the static condition (91%), indicating the presence of a response bias.

Orientation Discrimination Experiment

Behavioural results of F.B. for left and right lower visual quadrants

(graph 4 and table 13)

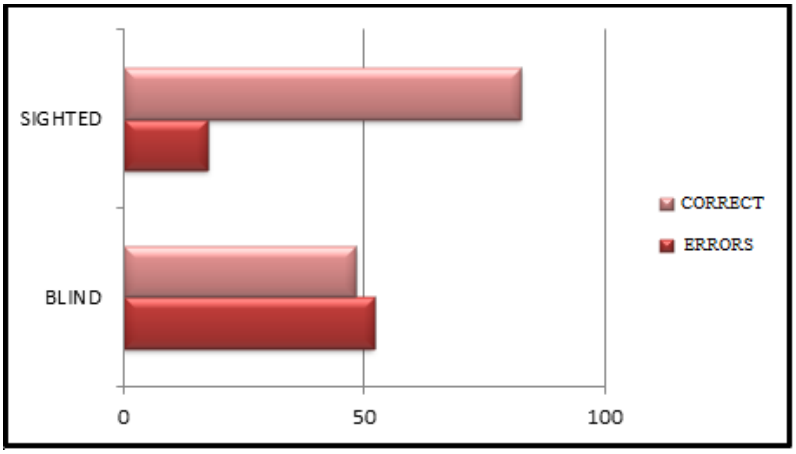

Graph 4

HEMIFIELD	INCORRECT RESP	CORRECT RESP
BLIND (VERTICAL + HORIZONTAL)	**51,87%**	**48,12%**
SIGHTED (VERTICAL + HORIZONTAL)	17,5%	82,5%

Table 13

Also in this case we found that in the blind visual quadrant the performance was at the chance level combining both vertical and horizontal orientations. The Binomial Test demonstrated that the performance was not significantly different from chance level and the analysis performed considering the two features separately did not show the presence of any relevant difference. Also in this experiment she chose always level 1 of the awareness scale indicating her inability to perceive something in the blind visual hemifield.

Considering reaction times, they were slower in the blind visual hemifield, above all in giving correct responses. Considering catch trials in the blind visual field, F.B. chose almost always the vertical condition (78%), indicating the presence of a response bias toward that condition.

CONCLUSION:

This patient did not show any sign of correct stimulus discrimination and her performance relied entirely on a response bias. It means that, even changing orientation and motion stimulus features, the behavioural performance could not improve .

PATIENT S.L.

Stimulus position: x axes = 18°; y axes = 7°, in the upper hemifield

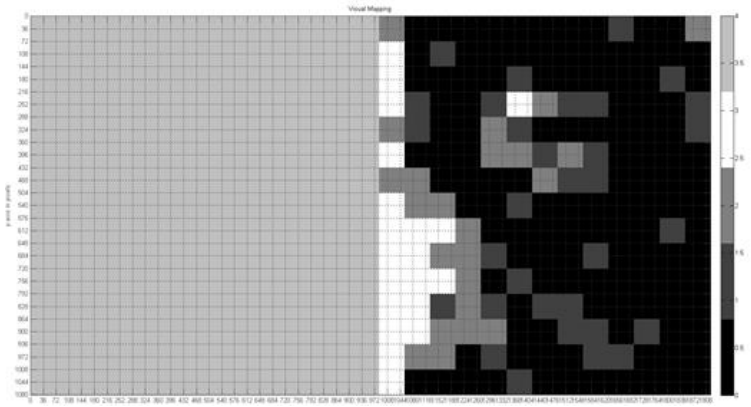

Fig. 22. S.L. Visual Mapping: Black squares indicate absence of response (0 over 3); dark grey indicates the presence of 1 response over 3; light grey the presence of 2 responses over 3 while white squares the presence of 3 correct responses over 3.

Motion Discrimination Experiment

Behavioural results of S.L. for left and right upper visual quadrants

(graph 5 and table 14)

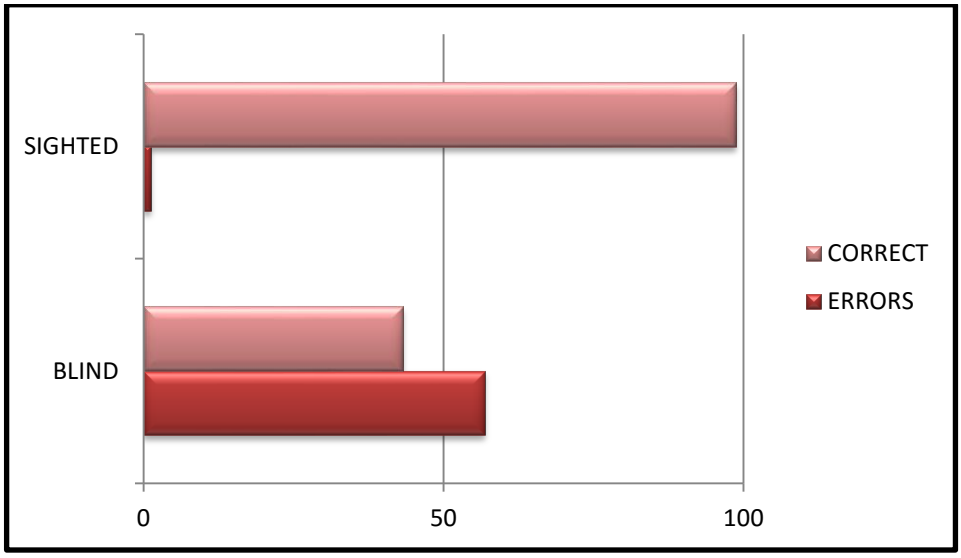

Graph 5

HEMIFIELD	INCORRECT RESP	CORRECT RESP
BLIND (MOTION + STATIC)	**56,88%**	**43,13%**
SIGHTED (MOTION + STATIC)	1,25%	98,75%

Table 14

In the blind visual field S.L. gave 43.13% of correct responses and almost 57% of incorrect responses. This result indicated that her performance was at the chance level, at the Binomial Test. Even the analysis performed considering the two features separately did not show the presence of any relevant difference. Instead, in the sighted visual field, her performance was comparable to healthy participants for both stimuli.

Considering this result, we checked the responses given in the **Awareness Scale** at the end of each trial, in the blind visual field.

S**tatic condition** (table 15):

AWARENESS SCALE	PERCENTAGE TOTAL RESPONSE	PERCENTAGE CORRECT RESP
1	39%	**45.16%**
2	62%	**55.10 %**

Table 15. Awareness Scale. Response 1: I did not see anything;
Response 2: I had the feeling of something on the screen but I could not see it.

M**oving condition** (table 16):

AWARENESS SCALE	PERCENTAGE TOTAL RESPONSE	PERCENTAGE CORRECT RESP
1	11%	**22.22%**
2	89%	**36.62 %**

Table 16

With static gratings, in 39% of trials S.L. chose level 1 while in about 62% of trials she chose level 2 of the awareness scale indicating that she perceived something in the blind field. In this case her performance was above chance giving 55.1% of correct responses and confirming her feeling of the occurrence of a stimulus even in absence of a conscious visual perception. In contrast, the performance was at the chance level while choosing level 1 of the awareness scale. With moving gratings, in almost 89% of trials S.L. chose level 2 of the awareness scale indicating that she perceived something in the blind field, while in 11% of trials she chose level 1 (absence of any feeling about the visual stimulus). However, regardless of the level of the awareness scale she chose, she could not correctly discriminate the stimulus as the percentage of correct responses in both cases was lower than the chance level. Reaction times were similar considering correct responses in both the blind and sighted visual fields being faster with moving than static gratings.

Considering catch trials in the blind visual field, in half of trials she chose the static condition and in the other half the motion condition, indicating the absence of a response bias toward a condition.

Orientation Discrimination Experiment

Behavioural results of S.L. for left and right upper visual quadrants

(graph 6 and table 17)

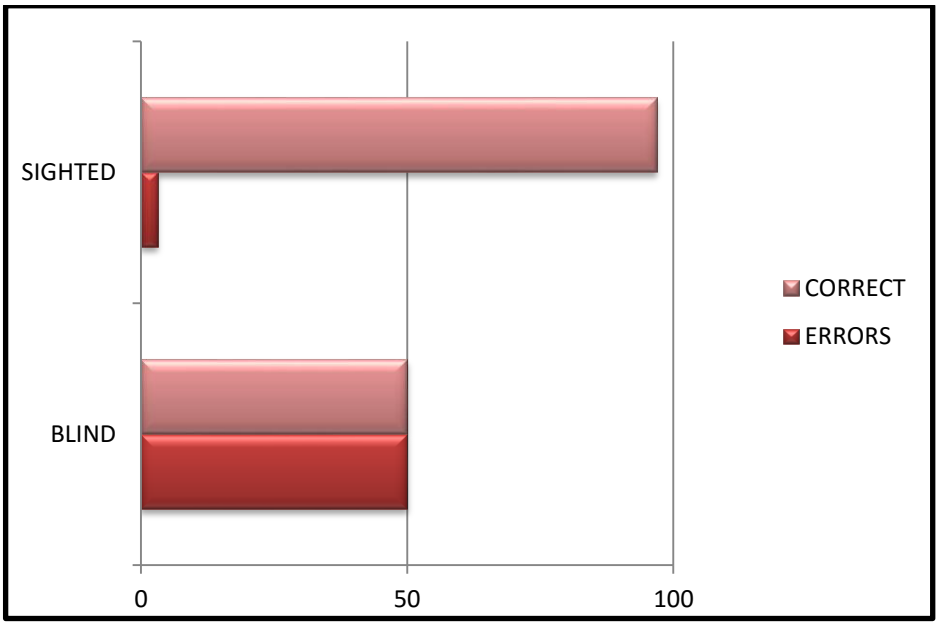

Graph 6

HEMIFIELD	INCORRECT RESP	CORRECT RESP
BLIND (VERTICAL + HORIZONTAL)	**50,00%**	**50,00%**
SIGHTED (VERTICAL + HORIZONTAL)	3,13%	96,88%

Table 17

In the blind visual field the performance was exactly at the chance level; for this reason we decided not to perform the Binomial Test. In the sighted visual field her performance was comparable to healthy participants. Considering this result, we checked responses given to the **Awareness Scale** at the end of each trial, in the blind visual field.

Vertical orientation we observed these results (table 18):

AWARENESS SCALE	PERCENTAGE TOTAL RESPONSE	PERCENTAGE CORRECT RESP
1	44%	**45.71%**
2	56%	**57.78 %**

Table 18. Awareness Scale. Response 1: I did not see anything;
Response 2: I had the feeling of something on the screen but I could not see it.

H**orizontal orientation,** we observed these results (table 19):

AWARENESS SCALE	PERCENTAGE TOTAL RESPONSE	PERCENTAGE CORRECT RESP
1	31%	**56%**
2	69%	**43.64 %**

Table 19

With vertical gratings, in almost 44% of trials S.L. chose level 1 while in almost 56% of trials she chose level 2 of the awareness scale indicating that she perceived something in the blind field. In this case the performance was above chance confirming her feeling of the occurrence of a stimulus; instead, it was at the chance level while choosing level 1 of the awareness scale.

With horizontally oriented gratings, in almost 69% of trials S.L. chose level 2 of the awareness scale indicating that she perceived something in the blind field, while in 31% of trials she chose level 1. However, the number of correct responses was higher while choosing level 1 of the awareness scale indicating the absence of an unconscious perception of visual stimuli. Reaction times in the blind hemifield were slower considering correct responses while in the sighted hemifield they were slower considering incorrect responses.

In catch trials presented in the blind visual field, S.L. chose the vertical condition in 59% of cases and in 41% of cases she chose the horizontal condition demonstrating the absence of a response bias.

CONCLUSION:

Her performance was below (motion experiment) or around (orientation experiment) the chance level indicating her inability to unconsciously (or consciously) perceive and discriminate a visual stimulus feature in the blind field.

PATIENT A.M.

Stimulus position: x axes = 12°; y axes = 4°

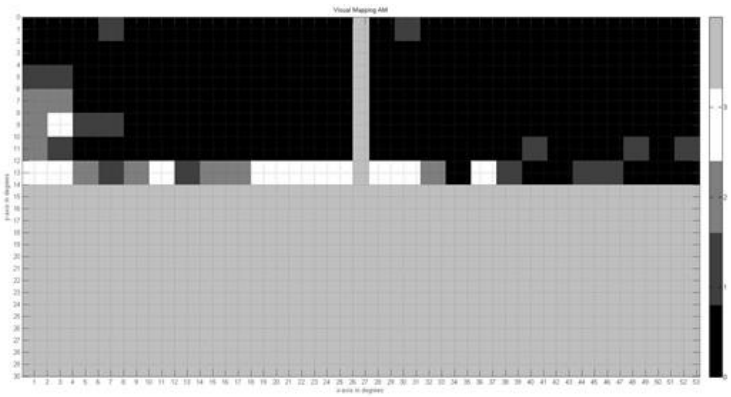

Fig. 23. A.M. Visual mapping: Black squares indicate absence of response (0 over 3); dark grey indicates the presence of 1 response over 3; light grey the presence of 2 responses over 3 while white squares the presence of 3 correct responses over 3.

With A.M. we decided to double the experiment as the hemianopia was represented by a bilateral visual defect. For this reason we performed two sessions: in the first we presented stimuli in upper and lower right visual quadrants while in the second we presented stimuli in upper and lower left visual quadrants.

Motion Discrimination Experiment in the RIGHT visual field

Behavioural results of A.M. for upper and lower right visual quadrants

(graph 7 and table 20)

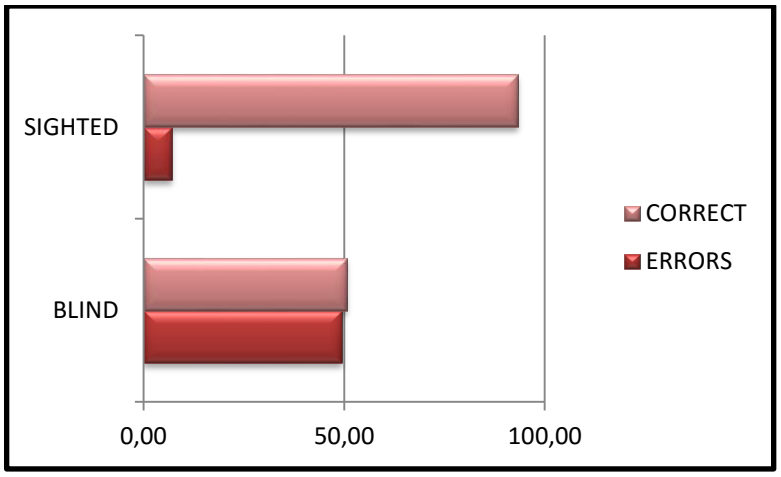

Graph. 7

HEMIFIELD	INCORRECT RESP	CORRECT RESP
BLIND (MOTION + STATIC)	**49,38%**	**50,63%**
SIGHTED (MOTION + STATIC)	6,88%	93,13%

Table 20

Clearly, the performance in the blind visual hemifield was at the chance level. The Binomial Test confirmed the absence of a significant difference; even analyzing results for moving and static gratings separately, we could not find any significant difference. In the sighted visual field the performance was comparable to healthy participants. Considering these results, we checked the responses given in the **Awareness Scale** at the end of each trial, in the blind visual field.

S**tatic condition** (table 21):

AWARENESS SCALE	PERCENTAGE TOTAL RESPONSE	PERCENTAGE CORRECT RESP
1	80%	**95.31%**
2	20%	**12.50 %**

Table 21. Awareness Scale. Response 1: I did not see anything;
Response 2: I had the feeling of something on the screen but I could not see it.

M**oving condition** (table 22):

AWARENESS SCALE	PERCENTAGE TOTAL RESPONSE	PERCENTAGE CORRECT RESP
1	80%	**9.23%**
2	20%	**80 %**

Table 22

In both conditions A.M. chose in almost 80% of cases the level 1 of the awareness scale indicating his inability to perceive something in the blind visual area. With static gratings, the performance was higher than the chance level while choosing level 1 of the awareness scale and lower while choosing level 2 of the awareness scale, indicating that the feeling reported in the latter case was not sufficient to correctly discriminate the stimulus. With moving gratings, the performance was higher than the chance level while choosing the level 2 of the awareness scale indicating that this feeling was sufficient to correctly discriminate the stimulus, instead it was lower choosing level 1 of the awareness scale.

Reaction times were similar considering both correct and incorrect responses in both blind and sighted visual fields. Considering catch trials in the blind visual field, results indicated the presence of a response bias toward the static condition.

Orientation Discrimination Experiment in the RIGHT visual field

Behavioural results of A.M. for upper and lower right visual quadrants

(graph 8 and table 23)

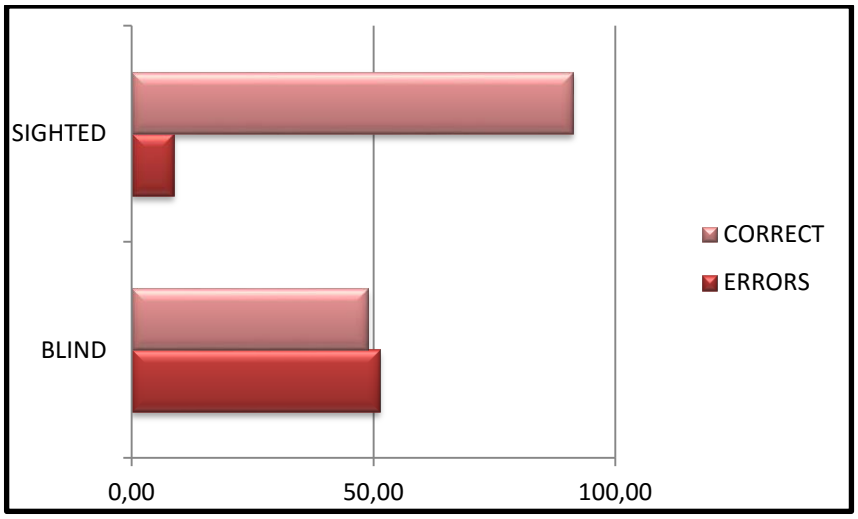

Graph. 8

HEMIFIELD	INCORRECT RESP	CORRECT RESP
BLIND (VERTICAL + HORIZONTAL)	**51,25%**	**48,75%**
SIGHTED (VERTICAL + HORIZONTAL)	8,75%	91,25%

Table 23

In this case we observed that the performance in the blind visual hemifield was at the chance level; even analyzing vertical and horizontal orientations separately, we could not find any significant difference. In the sighted visual field the performance was comparable to healthy participants considering both conditions. Considering these results, we checked the responses given in the **Awareness Scale** at the end of each trial, in the blind visual field.

V**ertical orientation** (table 24):

AWARENESS SCALE	PERCENTAGE TOTAL RESPONSE	PERCENTAGE CORRECT RESP
1	60%	**93.62%**
2	40%	**6.06 %**

Table 24. Awareness Scale. Response 1: I did not see anything;
Response 2: I had the feeling of something on the screen but I could not see it.

H**orizontal orientation** (table 25):

AWARENESS SCALE	PERCENTAGE TOTAL RESPONSE	PERCENTAGE CORRECT RESP
1	60%	**7.84%**
2	40%	**96.55 %**

Table 25

These results confirmed findings observed during the previous experiment. Therefore, in both conditions A.M. chose in almost 60% of cases the level 1 of the awareness scale indicating his inability to perceive something in the blind visual area. With vertical gratings, the performance was higher than the chance level while choosing the level 1 of the awareness scale and lower while choosing level 2 of the awareness scale, indicating that the feeling reported in the latter case was not sufficient to correctly discriminate the stimulus.

With horizontal gratings, the performance was higher than the chance level while choosing level 2 of the awareness scale indicating that this feeling was sufficient to correctly discriminate the stimulus while it was lower while choosing level 1 of the awareness scale. Reaction times were similar considering both correct and incorrect responses in both blind and sighted visual fields, except for incorrect responses with horizontal orientation in the sighted visual hemifield. Considering catch trials in the blind visual field, results confirmed the absence of a response bias toward the vertical condition as A.M. chose in 56% of cases the horizontal

condition. Indeed, in the sighted visual quadrant we observed the presence of a response bias toward the vertical condition.

Motion Discrimination Experiment in the LEFT visual field

Behavioural results of A.M. for upper and lower left visual quadrants

(graph 9 and table 26)

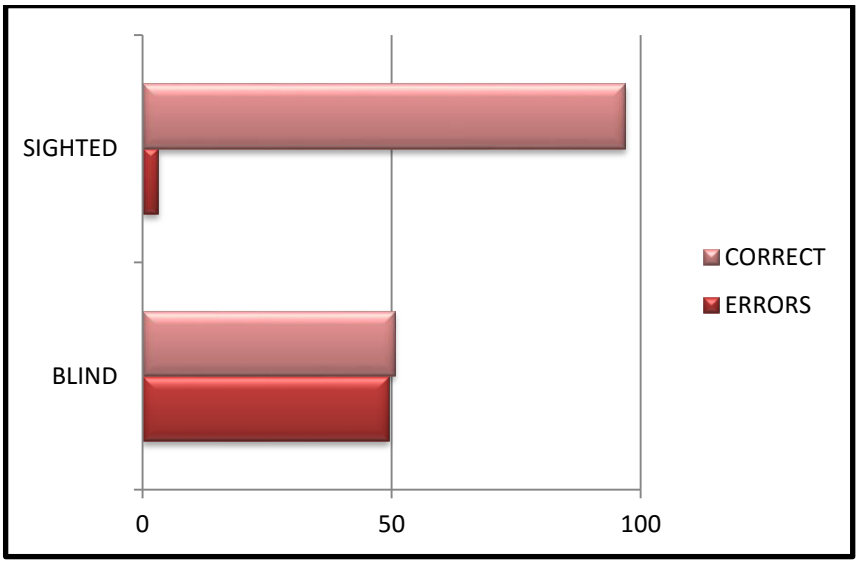

Graph 9

HEMIFIELD	INCORRECT RESP	CORRECT RESP
BLIND (MOTION + STATIC)	**49,38%**	**50,63%**
SIGHTED (MOTION + STATIC)	3,13%	96,88%

Table 26

In this case we observed that the performance in the blind visual quadrant was at the chance level; performing the Binomial Test we assessed that the difference between performance and chance level was not significant, even considering motion and static gratings separately. In the sighted visual field it was comparable to healthy participants considering both conditions.

Considering these results, we checked the responses given in the **Awareness Scale** at the end of each trial, in the blind visual field.

Concerning the **static condition** we observed these results (table 27):

AWARENESS SCALE	PERCENTAGE TOTAL RESPONSE	PERCENTAGE CORRECT RESP
1	42.50%	**97.06%**
2	57.50%	**2.17 %**

Table 27. Awareness Scale. Response 1: I did not see anything;
Response 2: I had the feeling of something on the screen but I could not see it.

Concerning the **motion condition,** we observed these results (table 28):

AWARENESS SCALE	PERCENTAGE TOTAL RESPONSE	PERCENTAGE CORRECT RESP
1	37.5%	**3.33%**
2	62.5%	**92 %**

Table 28

With static gratings, the performance was higher than the chance level while choosing level 1 of the awareness scale (42.5% of cases) while it was almost totally incorrect while choosing level 2 (57.5% of cases) indicating his inability to correctly discriminate the unconscious feeling of visual stimulus. Indeed, with moving gratings, the performance was higher than the chance level while choosing the level 2 of the awareness scale (62.5%) indicating that this feeling was sufficient to correctly discriminate the stimulus, instead it was lower while choosing level 1 of the awareness scale (37.5% of cases). Reaction times were similar considering both correct and incorrect responses in both blind and sighted visual fields, except for correct responses in the sighted visual quadrant whose reaction times were slower. Considering catch trials in the blind visual field, results indicated the preference in responding choosing the static condition. This trend indicated the presence of a response bias in catch trials that was not replicated in real experimental trials where we observed a better performance with moving than static gratings.

Orientation Discrimination Experiment in the LEFT visual field

Behavioural results of A.M. for upper and lower right visual quadrants

(graph 10 and table 29)

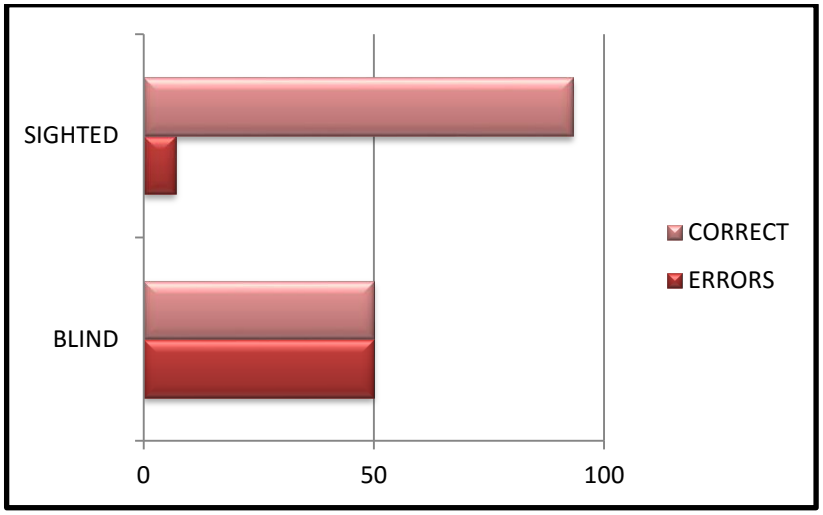

Graph 10

HEMIFIELD	INCORRECT RESP	CORRECT RESP
BLIND (VERTICAL + HORIZONTAL)	50,00%	50,00%
SIGHTED (VERTICAL + HORIZONTAL)	6,88%	93,13%

Table 29

In this case the performance was exactly at the chance level; obviously we decided not to perform the Binomial Test being the performance exactly at the chance level. Even analyzing results for vertical and horizontal orientations separately, we could not find any relevant difference. In the sighted visual field the performance was comparable to healthy participant's one.

Considering these results, we checked responses given to the **Awareness Scale** at the end of each trial, in the blind visual field.

Concerning the **vertical orientation** we observed these results (Table 30):

AWARENESS SCALE	PERCENTAGE TOTAL RESPONSE	PERCENTAGE CORRECT RESP
1	47%	**100%**
2	53%	**0 %**

Table 30. Awareness Scale. Response 1: I did not see anything;
Response 2: I had the feeling of something on the screen but I could not see it.

Concerning the **horizontal orientation,** we observed these results (Table 31):

AWARENESS SCALE	PERCENTAGE TOTAL RESPONSE	PERCENTAGE CORRECT RESP
1	46,25%	**0%**
2	53,73%	**97,27%**

Table 31

In both conditions A.M. chose in almost 53% of cases the level 2 of the awareness scale indicating his feeling of something happening in the blind visual area. With vertically oriented gratings the performance was always correct while choosing the level 1 of the awareness scale and always incorrect while choosing level 2, indicating his inability to correctly discriminate the unconscious feeling of visual stimulus.

With horizontally oriented gratings, the performance was higher than the chance level while choosing the level 2 of the awareness scale indicating that this feeling was sufficient to correctly discriminate the stimulus while it was always incorrect while choosing level 1 of the awareness scale. Reaction times were similar considering both correct and incorrect responses in both blind and sighted visual hemifields.

Considering catch trials in the blind visual field, results confirmed the absence of a response bias toward a condition as A.M. chose horizontal and vertical orientations exactly in the same number of cases.

CONCLUSION:

In conclusion we observed that even changing orientation and motion stimulus features, the behavioural performance could not improve as it could not produce any behavioural difference in a discrimination task.

DISCUSSION:

During this session we tested the discrimination of motion and orientation features of gratings shown in sighted and blind visual hemifield alternatively, to assess the presence of blindsight, knowing from previous studies (see “Moving stimuli and Blindsight” in the introduction) that motion feature can increase the probability of finding blindsight in hemianopic patients. Out of four patients we found an unconscious above chance performance in one patient (L.F.), in the motion discrimination task. In this case the above chance performance was associated with a feeling reported by the patient of something appearing on the screen during stimulus presentation. In contrast, in the orientation discrimination task, we could not find any evidence of blindsight. One straightforward consideration is that patient L.F. had a small lesion restricted to the striate cortex and this may justify the difference of performance with respect to the other patients even though in all patients the stimuli were presented to the blind portion of the visual field.

Second study:

fMRI Activation In Sighted and Blind Visual HemiField

Introduction:

Magnetic Resonance Imaging (MRI) and Functional MRI (fMRI)

MRI is an extremely versatile imaging method based on a set of physical principles that can be used to study both brain structure and function. The MRI signal is based on physical properties of hydrogen atoms consisting of a single proton; these nuclei can be considered as positively charged spheres which are always spinning thus giving rise to a net magnetic moment along the axis of the spins. During MRI it is possible to measure the net magnetization of all nuclei within a specific volume. The net magnetization is a vector composed by two components: longitudinal and transverse. The former is parallel to the magnetic field and is created as the consequence of placing protons within a strong magnetic field; the latter is perpendicular to the field and is caused by a radio frequency (RF) pulse used to align the phase of nuclei perpendicularly to the magnetic field, see Fig.24.

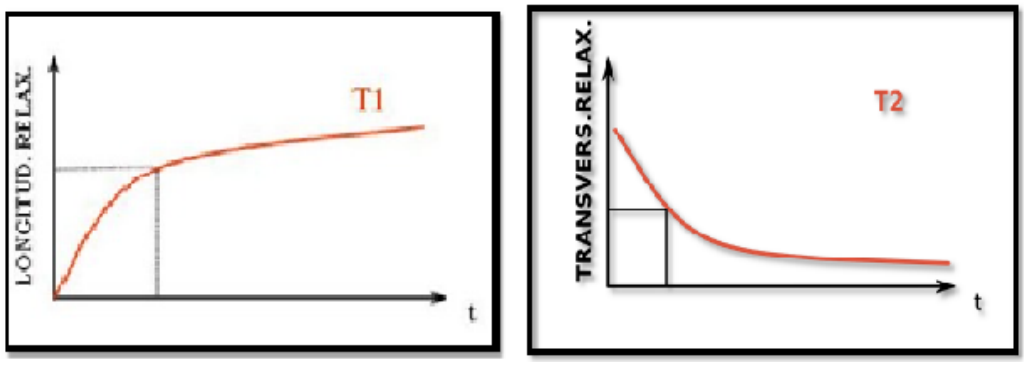

Figure 24. Representation of Longitudinal and Transversal Relaxation Time.

After the RF pulse is removed the system seeks to return to equilibrium: the transverse magnetization starts disappearing (transverse relaxation: loss of net magnetization due to loss of phase coherence) and the longitudinal magnetization grows back to its original size (longitudinal relaxation: restoration of net magnetization as spins return to their parallel state). The restoration of longitudinal magnetization is described by a time constant T1 while the decay of magnetization due to the interaction between nuclei is described as time constant T2. T2* is the combined effect of T2 and local inhomogeneity in the magnetic field; this type of procedure represents the basis of **Blood Oxygenation Level Dependent (BOLD) fMRI**, which is sensitive to flow and oxygenation.

Functional magnetic resonance imaging (fMRI) is a non-invasive technique used to study brain activity by detecting associated changes in blood flow (**Bold Effect**) in order to make inferences regarding stimulus or task-related activations in the brain. Therefore, fMRI does not measure neuronal activity directly, instead it measures the metabolic demands of active neurons by evaluating the ratio of oxygenated (diamagnetic) to deoxygenated (paramagnetic) hemoglobin in the blood. The change in the MRI signal triggered by instantaneous neuronal activity is known as the hemodynamic response function (**HRF**; Fig. 25).The rationale for analyzing HRF stems from the fact that as neuronal activity increases, so does metabolic demand for oxygen. During the execution of a task within a specific area of the brain, the oxygen demand increases and there is an over-compensation of oxygen in blood flow causing a decrease of deoxyhemoglobin that leads to a peak in BOLD signal about 4-8 seconds after the activation. After reaching this peak the oxygen is extracted from the blood, the hemoglobin becomes paramagnetic, the blood volume increases and, as a result, the BOLD signal decreases to an amplitude below the baseline level (negative overshoot).

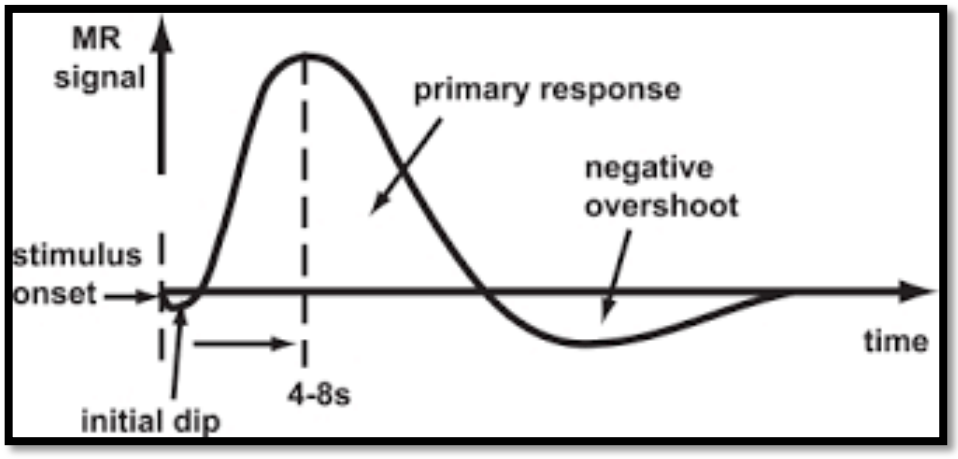

Figure 25. Representation of the Hemodynamic Response Function.

The **initial dip** represents the initial signal decrease caused by an increase of deoxygenate hemoglobin, immediately after stimulus onset. The **peak of the hemodynamic response** arises 4-8seconds after stimulus onset and is caused by an increase of oxygenate and a decrease of deoxygenate hemoglobin during the execution of the task. The post-stimulus **negative overshoot** is a decrease in signal below the baseline due to a combination of reduced blood flow and increased blood volume.

These changes create distortions in the magnetic field that cause a T2* decrease. fMRI is characterized by a good spatial resolution, while temporal resolution is not optimal being related to blood flow changes.

In explaining MRI data acquisition it is important to define the chosen values of specific parameters that are fundamental in order for others to be able to reproduce the results obtained. The **Echo Time (TE)** is the waiting time before receiving the return signal; **Repetition Time (TR)** is the time between consecutive radio frequency pulses and the **Flip Angle (FA)** is the rotation angle considering the direction of the static magnetic field caused by the magnetization vector with a specific radio frequency pulse (Huettel, S.A., Song, A.W. & McCarthy G., 2009. Functional Magnetic Resonance Imaging, second edition; Wandell et a.., 2011)

Retinotopic Mapping, hMT Localizer, Diffusion Tensor Imaging

In humans, the visual cortex is organized in different functional areas where adjacent neurons have receptive fields sensitive to adjacent positions in the visual

field providing a continuous mapping of the entire visual scene (Bordier et al., 2015) (fig. 26).

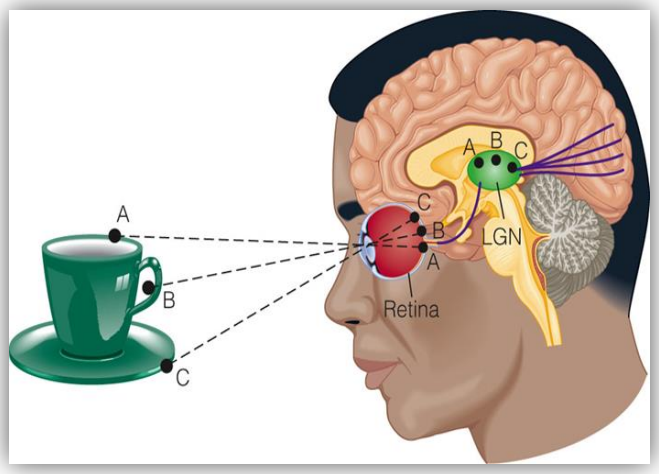

Fig.26. Retinotopic Organization of Visual Areas

In hemianopic patients it is important to individuate borders of low-level visual areas in order to evaluate their integrity and to identify abnormalities in the cortical representation of the visual field. Therefore, we decided to perform a session in the MRI scanner, to define low-level visual areas by using the **Retinotopic Mapping Procedure**. Based on seminal papers (Engel et al., 1994; Sereno et al., 1995; DeYoe et al., 1996) different methodological techniques have been proposed (Slotnick and Yantis, 2003; Kraft et al., 2005; Vanni et al., 2005; Henriksson et al., 2012) for the delineation of low-level visual areas in individual subject: in this study we decided to perform a Polar Angle Tecnique to reach that purpose.

During the previous behavioural session (chapter 1) we decided to use moving visual stimuli in order to increase the probability of finding blindsight. For this reason, another important issue for this project, was the assessment of activation and localization of area hMT, that is an area located in the occipital-temporal pit, specialized for detecting and discriminating visual motion. To do that, we used a **hMT Localizer procedure.**

Finally, with hemianopic patients it is important to evaluate the integrity of white matter fibers that convey visual information to the visual cortex (structural connectivity) as different kinds of hemianopia could be determined by a lesion at

different levels along the post-chiasmatic visual pathways and as hemianopia could cause different changes in connectivity (Bridge et al., 2008). To do that we used the **diffusion MRI techniques** that allow the mapping of the diffusion process of molecules, mainly water, in biological tissue non-invasively. The rationale of the technique is that molecular diffusion in tissues is not free but reflects interactions with many obstacles, such as macromolecules, fibers and membranes. Water molecule diffusion patterns can therefore reveal microscopic details about tissue architecture, either normal or in a diseased state.

The **Diffusion Weighted Imaging (DWI)** can be used when the diffusion is isotropic within the specific tissue. In this case the intensity of each voxel reflects the best estimate of the rate of water diffusion at that specific location; therefore its contrast is based on the rate of water diffusion in the tissue described by a parameter called apparent diffusion constant (ADC). It is used for evaluation of the consequences of stroke and many other diseases. DWI is more applicable when the tissue of interest is dominated by isotropic water movement (e.g. grey matter in the cerebral cortex, because the diffusion rate appears to be the same when measured along any axis). Alternatively, the **Diffusion Tensor Imaging (DTI)** can be used when the diffusion is anisotropic within the tissue (Fig. 27).

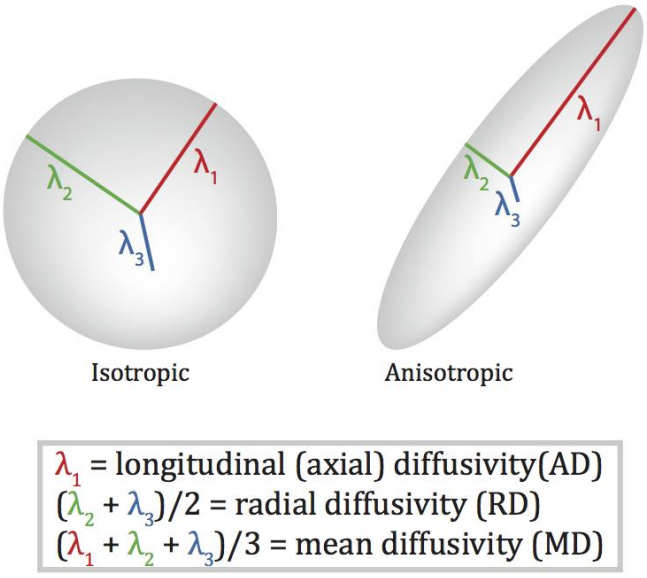

Fig.27 Representation of diffusivity axes in an isotropic and anisotropic manner (http://www.diffusion-imaging.com/2012/10/voxel-based-versus-track-based.html)

In this case a diffusion tensor is created as a matrix that summarizes the diffusion pattern in each voxel (symmetric matrix 3x3 composed by independent values); therefore, this technique is used to map the anisotropy of the water diffusion in the tissues. DTI is important when a tissue - such as the **white matter fibers** in the brain (Fig.28) - has an internal fibrous structure analogous to the anisotropy of some crystals.

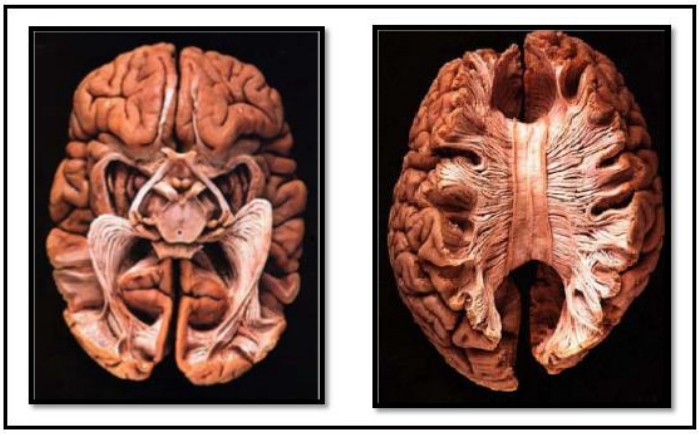

Fig. 28 Representation of white matter fibers in the brain (The Virtual Hospital (www.vh.org); TH Williams, N Gluhbegovic, JY Jew).

In the white matter, water molecules will diffuse more rapidly in the direction aligned with the internal structure, and more slowly as it moves perpendicular to the preferred direction. Applying some diffusion gradients (i.e. changes in the magnetic field) that could create at least 3 directional vectors (6 gradients represent the minimum to create directional vectors) it would be possible to evaluate a diffusion tensor for each single voxel that could describe the 3D diffusion of water molecules (Fig. 29). Fibers direction is indicated by the basic eigenvalue of the tensor (diagonal value).This value could be represented by using different colors letting possible to create the image of direction and position of fibers tracts.

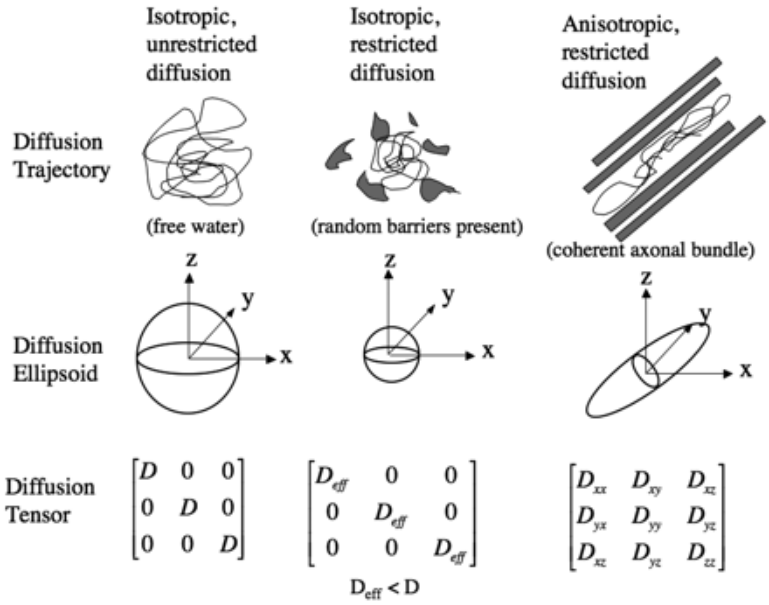

Fig. 29 Representation of the diffusion tensor (P. Mukherjee et al. AJNR Am J Neuroradiol 2008;29:632-641).

Diffusion tensor data can be analyzed in three ways to provide information on tissue microstructure and architecture for each voxel. The **Mean Diffusivity** allows obtaining an overall evaluation of the diffusion in a voxel or region avoiding anisotropic diffusion effects; it characterizes the overall mean-squared displacement of molecules (average ellipsoid size) and the overall presence of obstacles to diffusion.

The main direction of diffusivities (main ellipsoid axes) or **Fibers Orientation Mapping** relate to the mapping of the orientation in space of tissue structure. The assumption is that the direction of the fibers is colinear with the direction of the eigen-vector (in the diffusion tensor) associated with the largest eigen diffusivity. Direction orientation can be derived from DTI directly from diffusion/orientation-weighted images or through the calculation of the diffusion tensor.

The **Degree of Anisotropy** allows describing how much molecular displacements vary in space (ellipsoid eccentricity) and is related to the presence of oriented structures. Several indices have been proposed in order to evaluate diffusion anisotropy. The degree of anisotropy would vary according to the respective orientation of the gradient hardware and the tissue frames of reference and would generally be underestimated. For this reason invariant indices made of combinations of the terms of the diagonalized diffusion tensor (eigen-values) were

developed: the **Fractional Anisotropy (Fig.30)**, the **Relative Anisotropy** and **the Volume Ratio**. The first is a scalar quantity computed for each voxel to express the preference of water to diffuse in an isotropic (diffusion similar in all directions) or anisotropic (diffusion along a specific preferred axis) manner. FA values approaching the maximum of 1 indicates that nearly all of the water molecules in the voxel are diffusing along the same preferred axis (anisotropic manner), while FA values approaching the minimum of 0 indicate that the water molecules are equally likely to diffuse in any direction (isotropic manner).

Fig.30 Example of FA image

The second index is the ratio of the anisotropic part of the diffusion tensor to its isotropic part while the latter is the ratio of the ellipsoid volume to the volume of a sphere of radius. These three DTI meta-parameters can all be derived from the whole knowledge of the diffusion tensor (Bridge et al., 2008; Alexander et al. 2007; Le Bihan et al.).

Method:

Participants:

In this experiment we tested one healthy participant and one hemianopic patient. Both had normal or corrected-to-normal visual acuity and gave their written informed consent to participate in the experiment that was carried out according to the principles laid down in the 1964 Declaration of Helsinki and approved by the Verona AOUI Ethics Committee and by the ERC Ethics Committee..

Healthy Participant:

S.M (male, right handed, 41 years old) with no history of neurological disease.

Hemianopic Patient:

A.G. (male, right handed, 61 years old) with a lower right quadrantanopia (fig.31) as a consequence of an ischemic stroke occurred 25 months ago, that involved the basal ganglia and the dorsal portion of the left visual primary cortex.

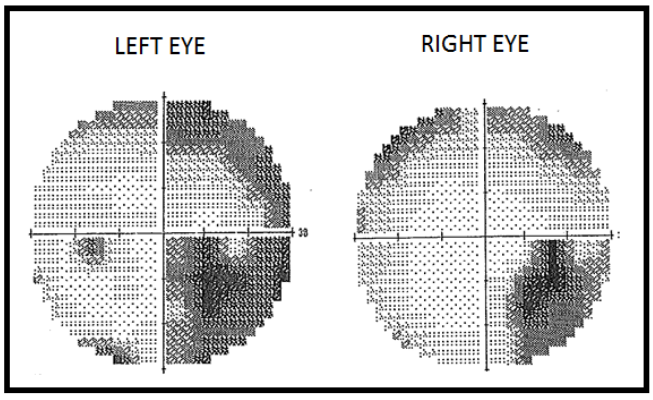

Fig. 31. A.G. Visual Field Map (19/09/2014): lower right quadrantanopia with foveal sparing and some areas with survived sensitivity in the blind quadrnat and with some blind areas in the upper right and left visual quadrant.

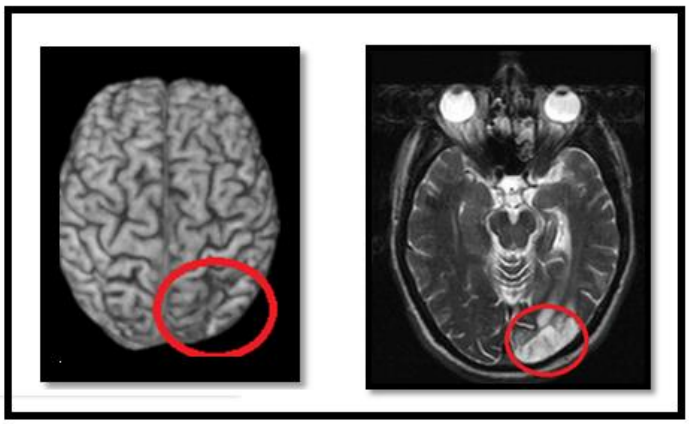

Fig.32. Surface and T2-weighted axial section of patient A.G. with the localization of the lesion (right side of the image).

Fig. 33 represents the reconstruction of the lesion on axial slices of a T1-weighted image:

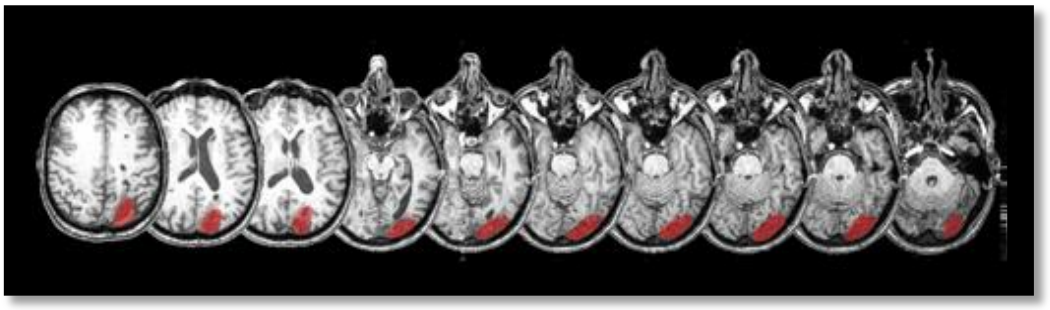

Fig. 33

A.G. performed the neuropsychological tests without showing any kind of cognitive and visuo-spatial impairment (MMSE = 29.49/30; LINE BISECTION TASK = +0.98; DILLER H CANCELLATION TEST = 106/106; BELL CANCELLATION TEST = 33/35). In VFQ25 Questionnaire, A.G. obtained a total score included in the normal range: 89.13. Responding to the questionnaire, he explained that the most impairing consequence of the ischemic stroke was represented by the difficulty in reading and recognizing letters of the alphabet.

A.G. performed the Visual Mapping (see Study One) in binocular vision (fig.34).

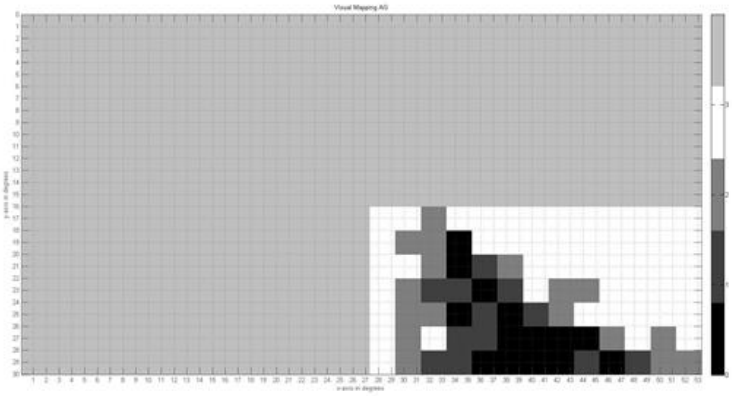

Fig. 34. A.G. Visual Mapping. Black squares represent the absence of response (0 over 3); dark grey indicates the presence of 1 response over 3; light grey the presence of 2 responses over 3 while white squares the presence of 3 correct responses over 3.

Apparatus, Stimuli and Procedure:

Retinotopic Mapping

The responsiveness and organization of early visual areas were investigated using the retinotopic mapping. Visual stimulus was generated using the VismapDX_Donders software. A **Polar angle** mapping experiment was performed (Goebel et al., 2001); the stimulus was shown on a grey background and was represented by a red and green wedge shaped checkerboard, with the tip at the fixation point, turning clockwise around it (fig.35). The wedge started at the right horizontal meridian and slowly rotated clockwise for a full cycle of 360° within 64 s. Each mapping consisted of 9 repetitions of a full rotation. During this session, participants were asked to fixate the central point, without executing any task.

Fig.35. Stimulus presented on the screen during the retinotopic mapping, rotating clockwise as indicated by black arrows.

hMT Localizer: Mapping of the human motion complex

Motion-selective areas were identified by comparing the hemodynamic response during the presentation of moving random dots with that during presentation of stationary dots. Therefore, a **blocked-design** experiment was carried out by alternating blocks with black dots moving in a random order in the whole screen, blocks with static dots and resting blocks with only the fixation point presented (fig. 36). During this session, participants were asked to fixate the central point, without executing any task.

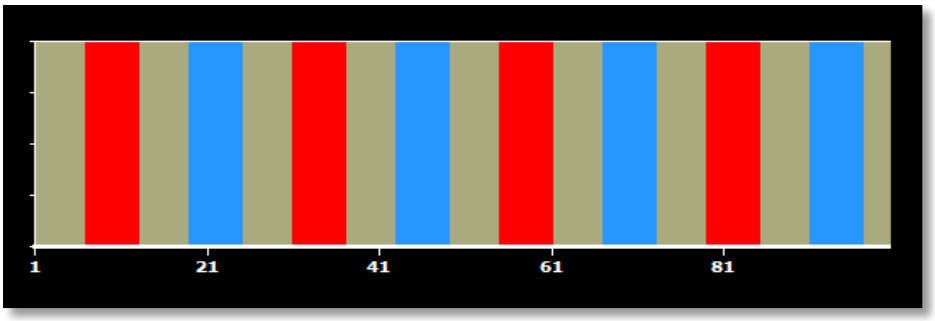

Fig. 36. Blocked design experiment;
Grey Blocks = REST; Red Blocks = MOTION; Blue Blocks = STATIC.

DTI

Fractional anisotropy was performed to evaluate the level of anisotropy in water molecules diffusion and Mean Diffusivity was executed to visualize the integrity of white matter fibers (Fig. 37) focusing our attention on the optic radiations.

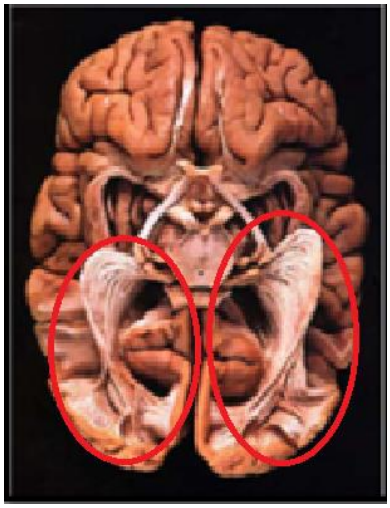

Fig 37. Representation of white matter fibers. Red circles indicate optic radiations.

MRI Acquisition:

Functional magnetic resonance imaging was performed with a 3 Tesla scanner using an Echo Planar sequence.

At the beginning of the session we performed a whole brain T1-weighted structural iso-volumetric sequence (TE = 2,83ms; TR= 1840ms; matrix 256x256; slices = 160; slice thickness = 1x1x1 mm). During both retinotopic mapping and hMT Localizer we recorded functional images by using a similar sequence: TE = 31msec, TR = 2000msec, FA = 90°, FOV = 192 x 192 mm2, matrix size = 64 x 64, voxel size = 3x3x3 mm3, slice thickness = 3mm, number of volumes = 262 and number of slices in each volume = 34 (retinotopic mapping) 33 (hMT Localizer). Slices were positioned parallel and centered on the calcarine fissure. Visual stimuli were generated using the software E-Prime 1 and projected on a mirror located in front of the participant as the computer was located behind him, inside the scanner. At the end of the session a DTI recording was performed to evaluate the integrity of white matter fibers. TE/TR were set to 87ms/9000msec, Matrix Size = 128x128, Voxel Size = 1.9x1.9x1.9 mm, number of slices in each

volume = 60 and 30 diffusion sensitizing directions were collected at B = 1000 s/mm^2, along with a single T2-weighted (b=0 s/mm^2) image.

Data Analysis

Preprocessing of Functional Images:

fMRI data analysis was performed by using BrainVoyager QX 2.8.4 (Brain Innovation, Maastricht, The Netherlands, www.BrainVoyager.com). During the preprocessing of functional images of both retinotopic mapping and hMT Localizer, we carried out some procedures in order to improve the quality and reliability of functional images. We performed the **Slice Time Correction** interpolating data from each slice (within each volume) as if they were acquired at the same time. We executed a SINC interpolation, considering the order of slice acquisition (ascending order). We performed the M**otion Correction** to re-align all images from a given subject by generating parameters that could be used to correct for head motion and to create a mean functional image. In this session, each volume was aligned to the first one and 100 iterations were performed to correct the image. We carried out **Temporal Filtering** to eliminate changes in signal due to temporal components as noise and drifts that can modulate the signal. In this session we executed a High-Pass Filtering = 3 Cycles per Run and a temporal smoothing of 20 sec. Finally, we accomplished a **Spatial Smoothing** that is a Gaussian filter used to spread intensity at each voxel to neighboring voxels, to increase SNR and to reduce intra-subject variability. In this session we chose 6 mm as the maximal distance to smooth the signal.

Once obtained preprocessed images, we carried out the **Co-Registration** of functional data with anatomical T1-weighted image, corrected by using the spatial transformation (iso-voxeling) and the inhomogeneity correction. We chose the rigid-body transformation to perform the co-registration, as it does not change the structure of the image and then we checked the outcome to make some manual transformations if they were necessary. Then we performed the **Spatial Normalization** of T1-weighted data to a reference space based on the Talairach Atlas. At the end of this normalization, we created the **Volume Time Course (VTC)** file starting from the slice time course data set (storing format of original

voxel data) to perform a whole-brain single-case analysis. This conversion process from slice time course to volume time course file is performed by using several spatial transformation files that are obtained during the FMR-VMR co-registration step and the anatomical brain normalization step (Warnking et al., 2002; Bordier et al., 2015).

Single-Case Analysis

Once carried out all these steps, we loaded the VTC file on the structural image normalized in a Talairach space, put the stimulation protocol on the VTC and performed the statistical analysis. In the retinotopic mapping we executed the **Linear Correlation**, while in the hMT Localizer the **General Linear Model**.

For the Linear Correlation we evaluated the Correlation Coefficient that illustrated a quantitative measure of statistical relationships between two or more variables. Therefore, here we evaluated brain activation in terms of correlation with the specific position of the stimulus on the screen. It means that each color of activation in the brain corresponded to a specific position of the wedge rotating around the fixation point. We used 16 lag values, as the wedge was rotating for 32 sec (16 scans) in each visual hemifield (64sec = 32 scans in the entire visual field); in this way the predictor indicated the beginning of visual stimulation in one visual hemifield and 16 lags were then calculated to indicate the level of correlation with that specific predictor considering the whole brain. In order to detect weak activity within and surrounding the lesioned or denervated regions, the retinotopic mapping data were analyzed with a low correlation threshold.

For the hMT Localizer, we executed the General Linear Model (GLM) aimed to explain or to predict the dependent variable (Hemodynamic Response) in terms of a linear combination of some predictors (motion, static, rest: the design matrix) which are combined in order to minimize residuals. The GLM returns the estimation of B(eta) that represents a measure of the strength of each predictor's influence on the voxel signal. In the GLM the predictor time course is obtained by convoluting a condition time course with a standard hemodynamic response function (two-gamma HRF). In this way we obtained the percentage of variation of the Hemodynamic Response considering each predictor: MOTION, STATIC

and REST conditions. Once obtained these values we contrasted the activation found during the moving stimulation with the activation found during the static presentation of dots, to obtain the activation purely related to the motion condition. In both cases, we decided to clean the image by deleting the activation outside the brain, as a consequence of the noise recorded during the registration. To do that, we created two different brain masks: the first represented by the VTC volume, used to select the brain area where to perform the statistical analysis and the second including all the activation found on the brain.

After performing both statistical analyses on a 2D surface (T1-weighted image), we loaded the **smoothed, inflated and flattened surface** (Dumoulin et al., 2003) of both hemispheres of a template represented in a Talairach Space, to visualize linear correlation or GLM maps there. We decided to use a template surface as the segmentation of damaged brain was difficult to be performed and it was meaningless because of the presence of the lesion, which appeared as a hole in the segmented brain. For this reason it was better to visualize the inactivated area on a template surface to visualize borders of the missing area.

In the retinotopic mapping we visualized the activation within the occipital lobe, reducing the correlation level to better visualize the exact extent of the lesion in terms of lack of activation. In the hMT Localizer we visualized the activation within Brodmann Area 19 as hMT is a part of it; then we visualized Area hMT on the surface considering the Talairach Coordinates and finally we drew borders of the specific area activated on that surface. In this way we could evaluate position and cortical activation of this area even in a damaged hemisphere, contrasting moving and static condition.

Results:

Results in healthy participant: S.M.

RIGHT VISUAL HEMIFIELD

CORTICAL ACTIVATION ON A 2D MODEL

(TALAIRACH SPACE; Fig. 38):

Linear correlation between cortical activation and the specific position of the stimulus on the screen, in the right hemifield.

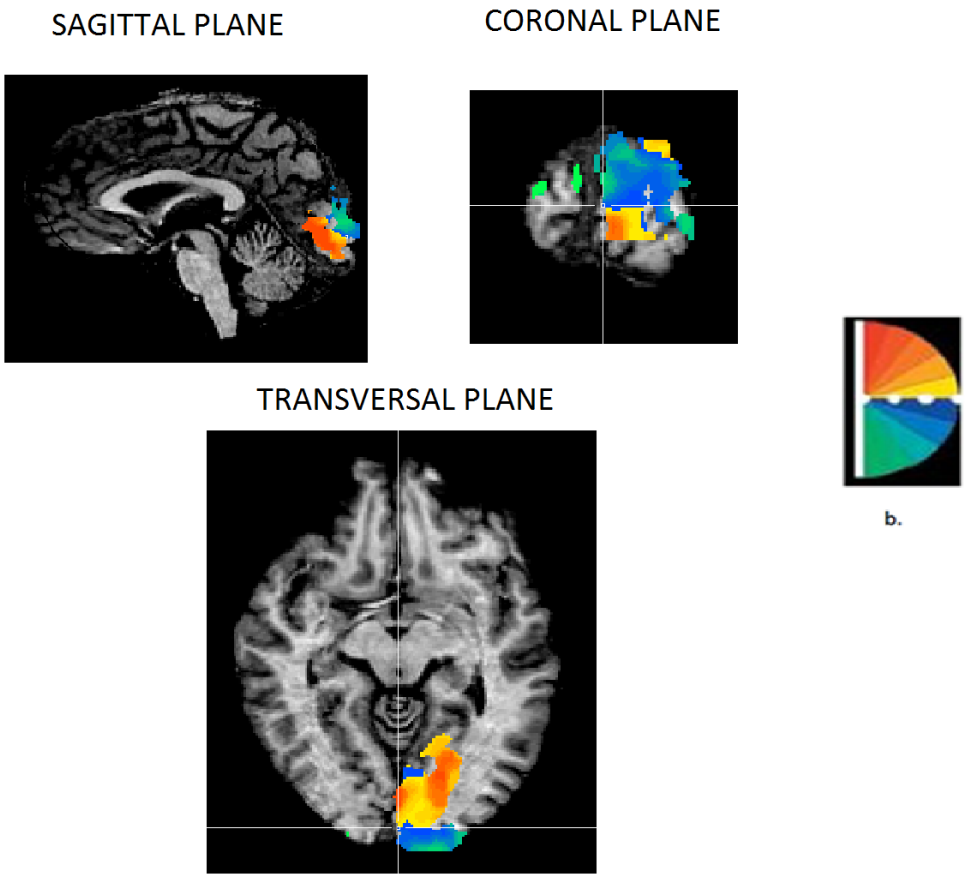

Fig. 38. Cortical activation on a 2D Model within the occipital lobe (r > 0.30). b). Representation of the colors indicating different positions of the stimulus on the screen.
Red and yellow = upper right quadrant; blue and green = lower right quadrant.

We found a normal retinotopic organization of low-level visual areas within the occipital lobe. Therefore, the upper right visual quadrant was represented below

the calcarine sulcus in the left hemisphere while the lower right visual quadrant was represented above the calcarine sulcus in the left hemisphere.

CORTICAL ACTIVATION ON SMOOTHED, INFLATED and FLATTENED TEMPLATE SURFACES (Fig. 39):

Retinotopic Organization of low-level visual areas within the occipital lobe.

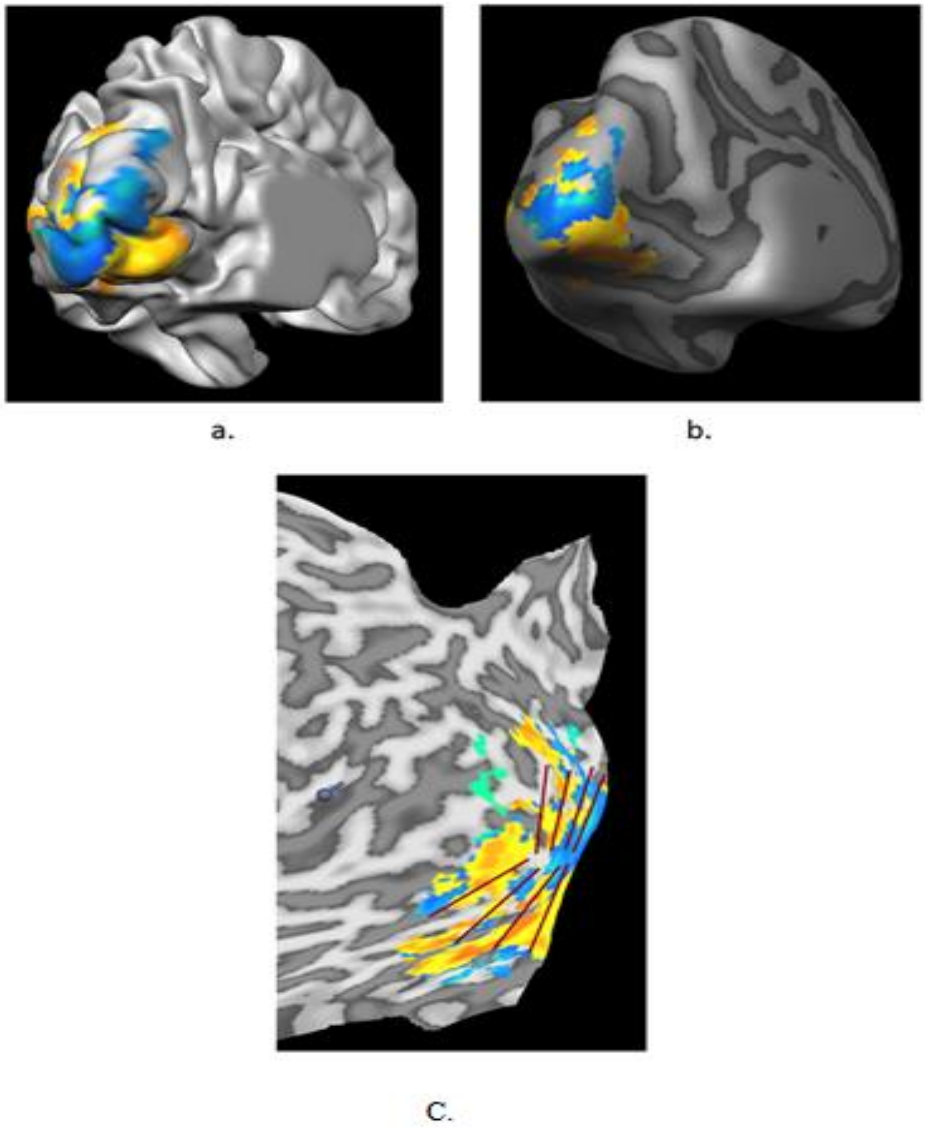

Fig.39. a). Smoothed Surface (r > 0.30); b). Inflated Surface (r > 0.30);
c). Occipital Lobe represented on a Flattened Surface (r > 0.21). Representation of the activation within the occipital lobe; visualization of borders of low level visual areas (red lines): V1-V2d-V3d-V3A/V3B in the dorsal portion; V1-V2v-V3v-V4v in the vental portion.

The results confirmed the presence of a retinotopic activation within the occipital lobe.

LEFT VISUAL HEMIFIELD
CORTICAL ACTIVATION ON A 2D MODEL
(TALAIRACH SPACE, Fig. 40):
Linear correlation between cortical activation and the specific position of the stimulus on the screen, in the left hemifield.

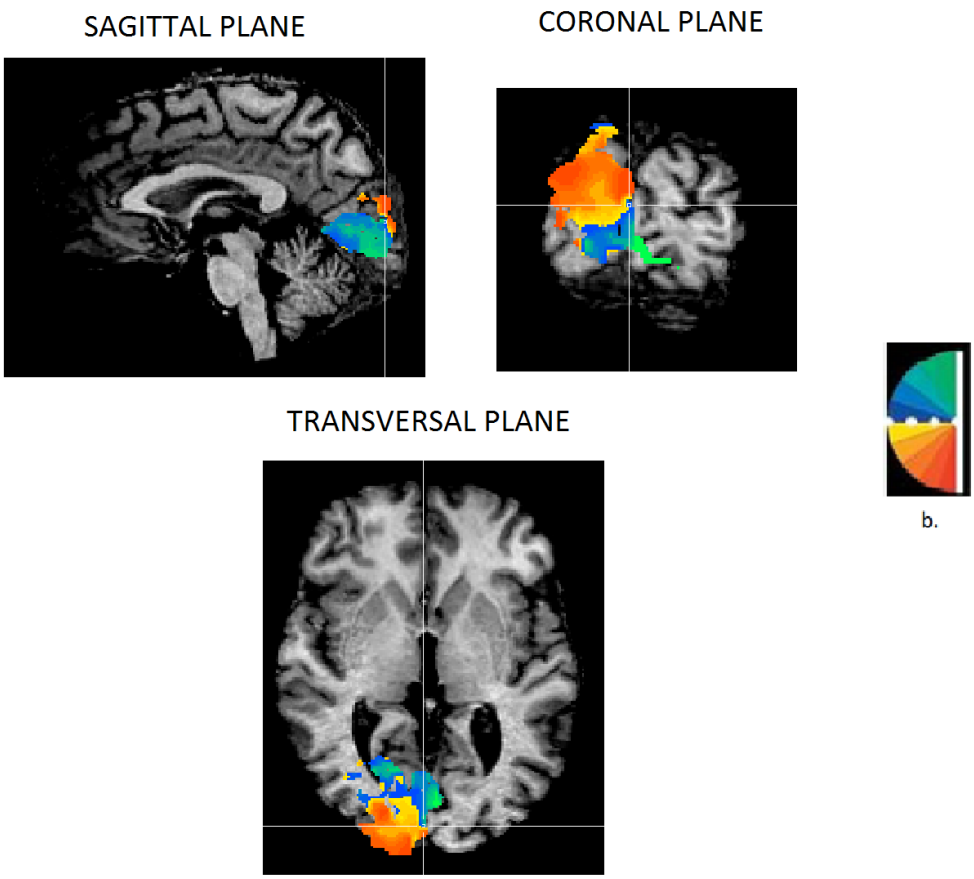

Fig. 40. Cortical activation on a 2D Model within the occipital lobe ($r > 0.29$). b). Representation of colors indicating different positions of the stimulus on the screen.
Green and blue = upper left quadrant; red and yellow = lower left quadrant.

We found a normal retinotopic organization of low-level visual areas within the occipital lobe. The upper left visual quadrant was represented below the calcarine

sulcus in the right hemisphere while the lower left visual quadrant was represented above the calcarine sulcus in the right hemisphere.

.

CORTICAL ACTIVATION ON SMOOTHED, INFLATED and FLATTENED TEMPLATE SURFACES (Fig. 41):

Retinotopic Organization of low-level visual areas within the occipital lobe

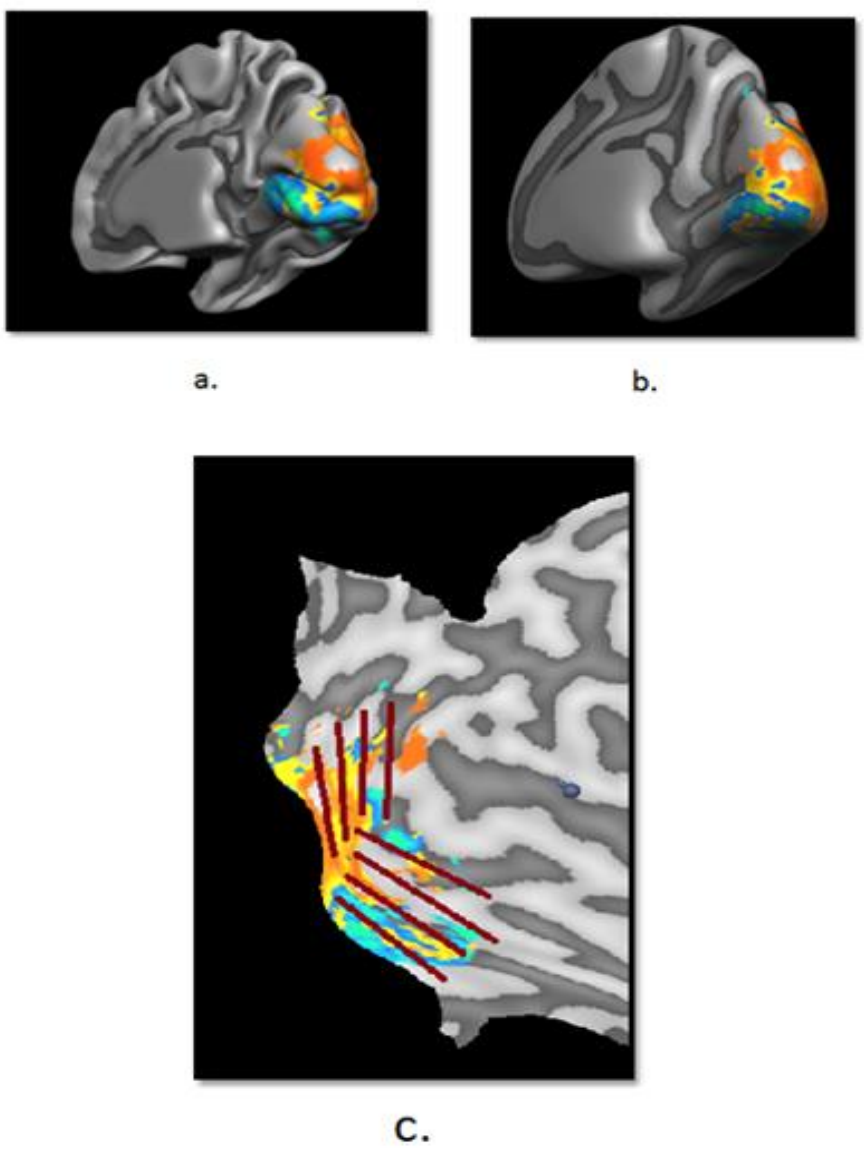

Fig. 41. a). Smoothed Surface (r > 0.20); b). Inflated Surface (r > 0.20);
c). Occipital Lobe represented on a Flattened Surface (r > 0.18). Representation of the activation within the occipital lobe; visualization of borders of low level visual areas (red lines): V1-V2d-V3d-V3A/V3B in the dorsal portion; V1-V2v-V3v-V4v in the ventral portion.

Again the results confirmed the presence of a retinotopic activation within the occipital lobe.

In conclusion, in the healthy participant, we found a retinotopic organization of low-level visual areas in both hemispheres. This technique appeared to be powerful and useful to investigate cortical organization of visual areas in the healthy participant and confirmed its utility also with hemianopic patients.

Results in hemianopic Patient:

A.G.

Lesion involving basal ganglia and
the dorsal portion of the left visual primary cortex.

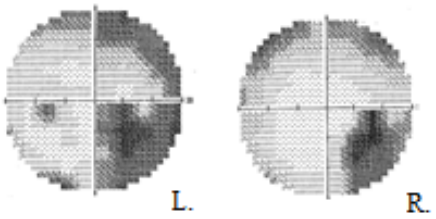

Fig. 42. Campimetry of patient A.G.

BLIND RIGHT VISUAL HEMIFIELD
CORTICAL ACTIVATION ON A 2D MODEL
(TALAIRACH SPACE; Fig. 43):
Linear correlation between cortical activation and the specific position of the stimulus on the screen, in the right hemifield.

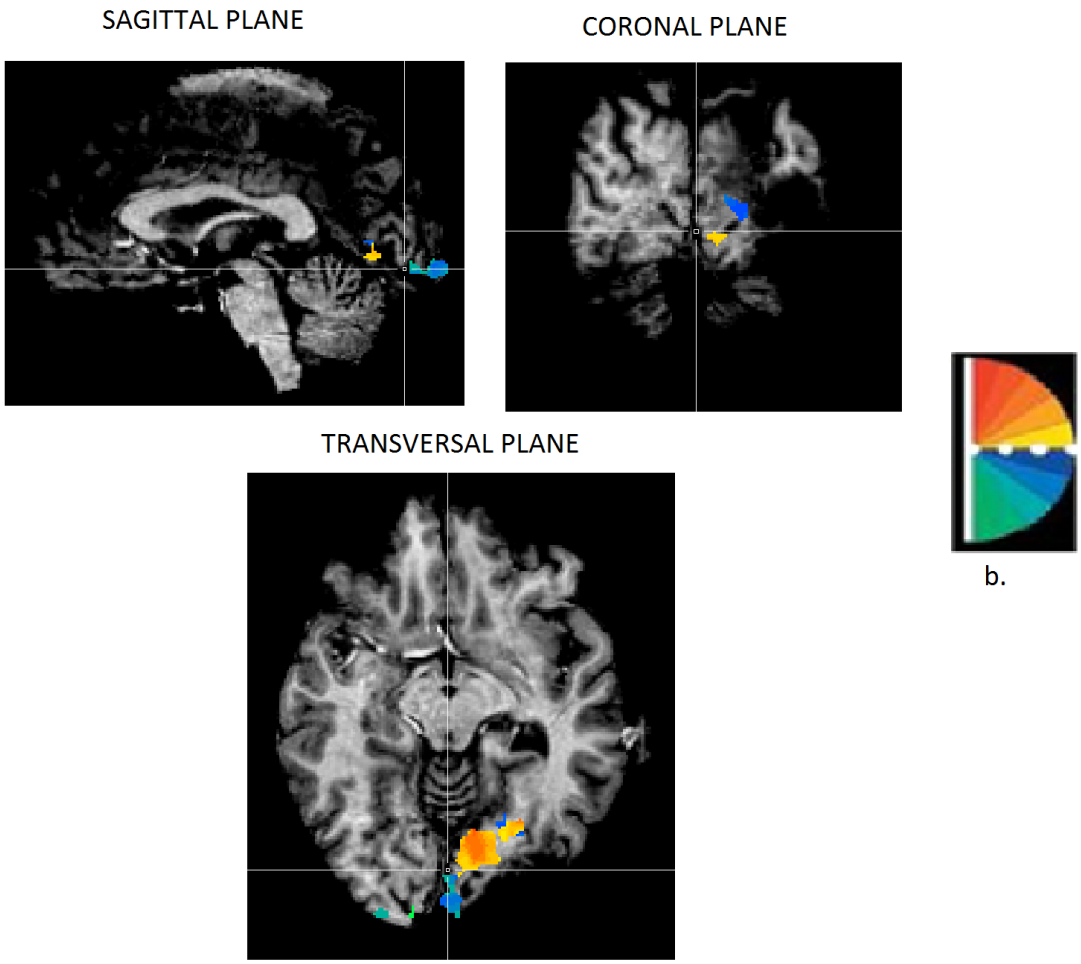

Fig. 43. Cortical activation on a 2D Model in a Talairach Space within the occipital lobe (r > 0.30). b). Representation of the colors indicating different positions of the stimulus on the screen. Red and yellow = upper right quadrant; blue and green = lower right quadrant.

We found a normal retinotopic organization within visual areas apart from the missing activation in the lesioned area of dorsal striate cortex. To visualize the activation in the occipital lobe in both inflated and flattened surface we decided to visualize it on a template, in order to avoid problems related to the segmentation process of a damaged brain, and only within the occipital lobe.

CORTICAL ACTIVATION ON SMOOTHED, INFLATED and FLATTENED TEMPLATE SURFACES (Fig. 44):

Retinotopic Organization of low-level visual areas within the occipital lobe.

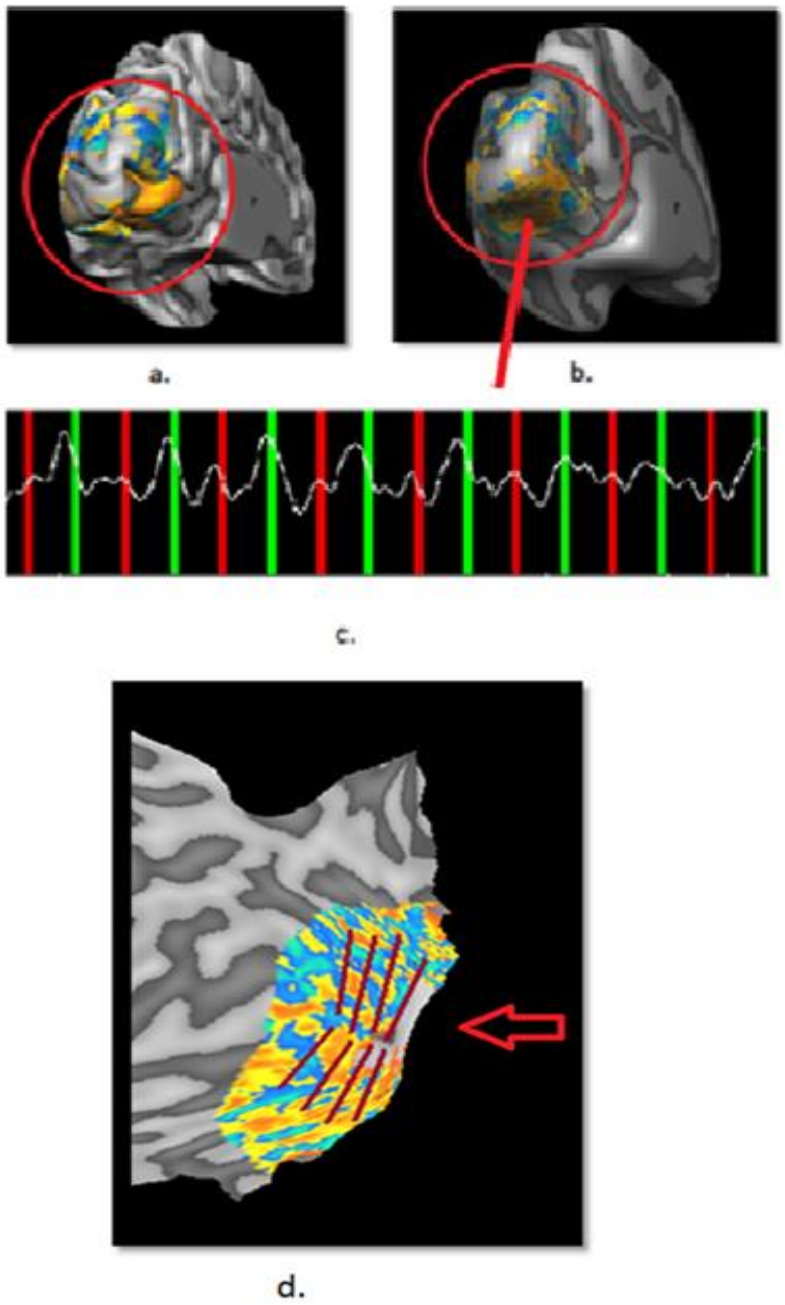

Fig. 44. a). Smoothed Surface (r > 0.14) b). Inflated Surface (r > 0.14) c). Linear correlation during the retinotopic mapping. The green line indicated the beginning of the stimulus rotating in the right hemifield; the peak of activation found in the red correlation was observed over the green line indicating that the correlation was higher when the stimulus started rotating within the right visual hemifield. d). Flattened Surface (r > 0.08). Visualization of borders of low level visual areas (red lines): V1-V2d-V3d-V3A/V3B in the dorsal portion; V1-V2v-V3v-V4v in the vental portion.

To describe the activation on the flattened surface we decided to use a low level of correlation in order to draw borders of visual area directly damaged by the lesion, starting from V1 close to the calcarine sulcus, until V4, close to temporal and parietal lobes. In all different surfaces, the activation found in the occipital lobe was retinotopically organized even if the signal was noisier than in healthy participants and we found a lack of activation in the lesioned area represented mainly by the dorsal portion of V1 corresponding to the specific site of the quadrantanopia.

SIGHTED LEFT VISUAL HEMIFIELD

CORTICAL ACTIVATION ON A 2D MODEL

(TALAIRACH SPACE; Fig. 45):

Linear correlation between cortical activation and the specific position of the stimulus on the screen, in the left hemifield.

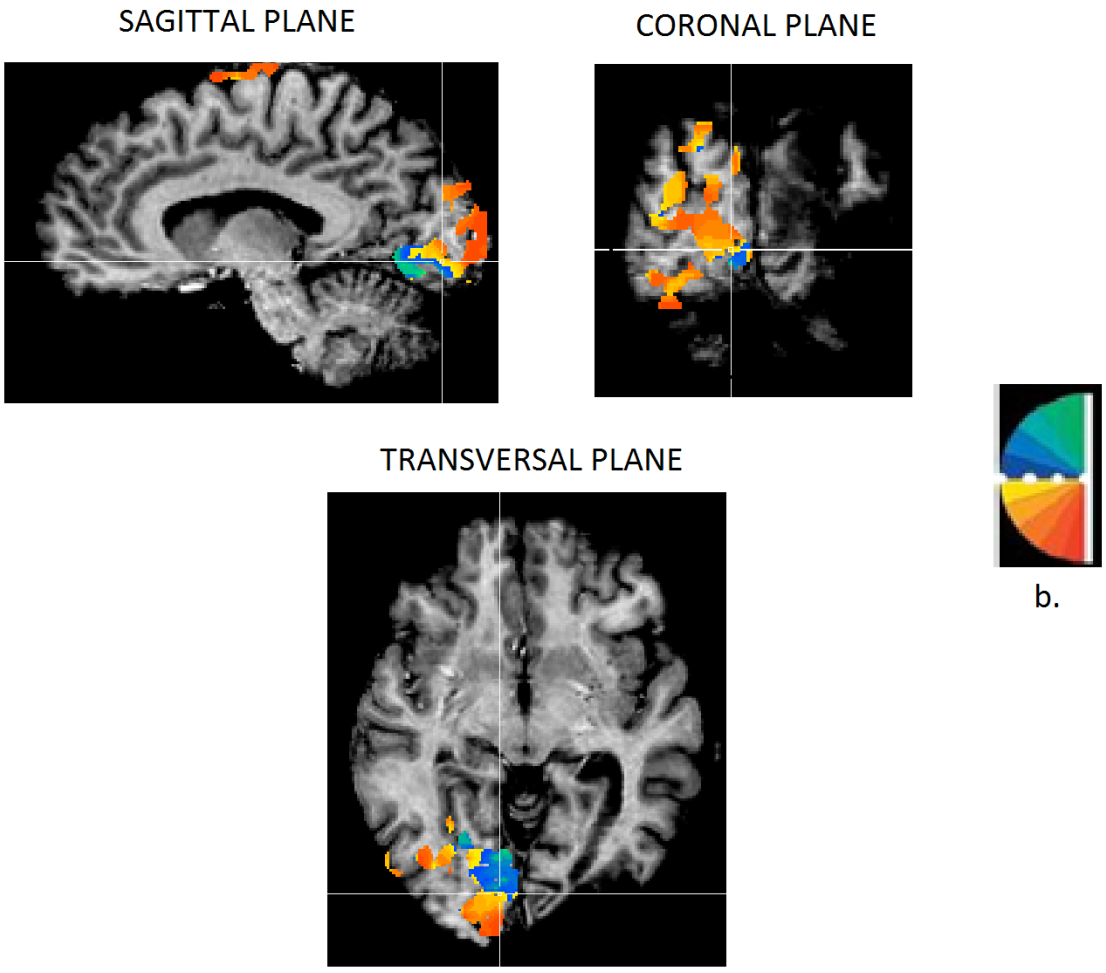

Fig. 45. Cortical activation on a 2D Model in a Talairach Space within the occipital lobe (r > 0.30).
b). Representation of colors indicating different positions of the stimulus on the screen.
Red and yellow = lower left quadrant; blue and green = upper left quadrant.

We found a normal retinotopic organization within the occipital lobe, in the intact right hemisphere.

CORTICAL ACTIVATION ON SMOOTHED, INFLATED and FLATTENED TEMPLATE SURFACES (Fig. 46):

Retinotopic Organization of low-level visual areas within the occipital lobe.

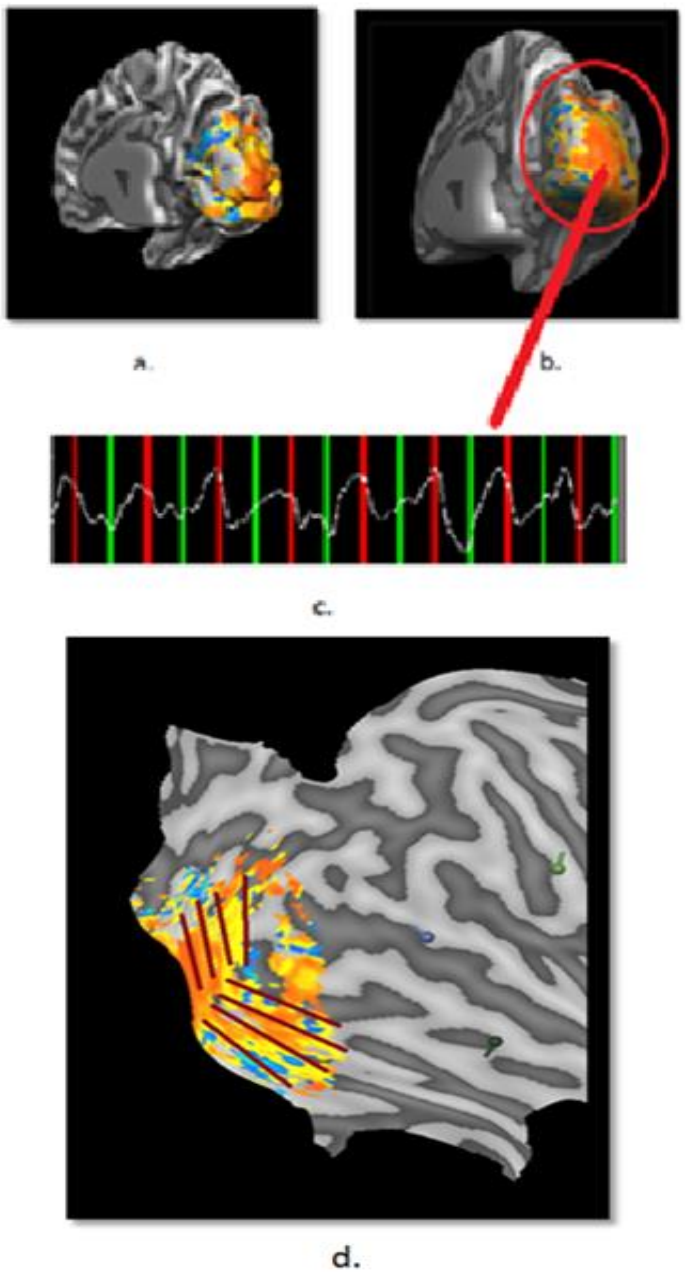

Fig. 46. a). Smoothed Surface (r > 0.14) b). Inflated Surface (r > 0.14) c). Linear correlation during the retinotopic mapping. The green line indicated the beginning of the stimulus rotating within the right hemifield; the peak of activation found within the red correlation was observed over the red line indicating that the correlation was higher when the stimulus started rotating within the left visual hemifield. d). Flattened Surface (r > 0.08). Visualization of borders of low level visual areas (red lines): V1-V2d-V3d-V3A/V3B in the dorsal portion; V1-V2v-V3v-V4v in the vental portion.

Looking at all different surfaces, the activation found in the occipital lobe was basically retinotopically organized even if the signal was noisier than in healthy participants. On the flattened surface we visualized the activation and drew borders of low-level visual areas, starting from V1 close to the calcarine sulcus, until V4, close to borders with temporal and parietal lobes.

CONCLUSION:

In conclusion, in A.G. we observed a retinotopic organization of both intact and damaged low level visual areas despite of a complete lack of activation involving mainly the dorsal portion of the left primary visual cortex.

hMT Localizer (Fig. 47):

GENERAL LINEAR MODEL (contrast applied: motion – static)

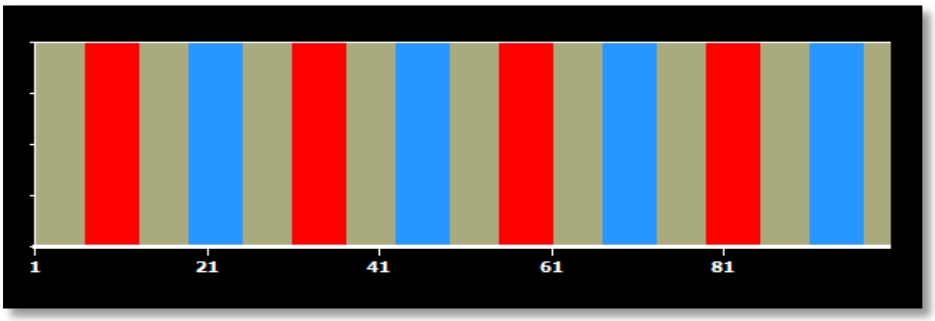

Fig. 47. Grey Blocks: REST; Red Blocks: MOTION; Blue Blocks: STATIC

Results in healthy participant:

S.M.

LEFT HEMISPHERE: activation within Brodmann area 19 (Fig. 48)

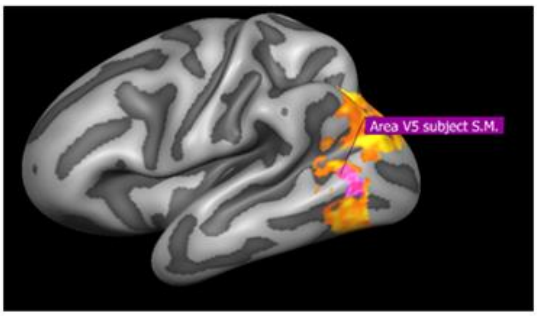

a.

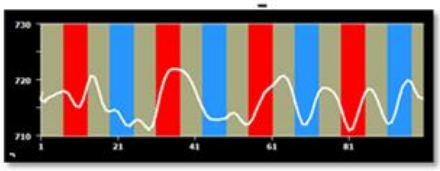

b.

Fig. 48. a). Activation on a left inflated surface within Brodmann Area 19. The pink area represents area hMT. b). Activation within area hMT during the entire run. Talairach Coordinates fall within the average coordinates indicated by BrainVoyager Brain Tutor application (Left Area hMT = -50, -62, 9) and by Dumoulin et al., 2000.

Event-Related Averaging (graph. 11):

Averaged cortical activation in moving (red) and static (blue) blocks

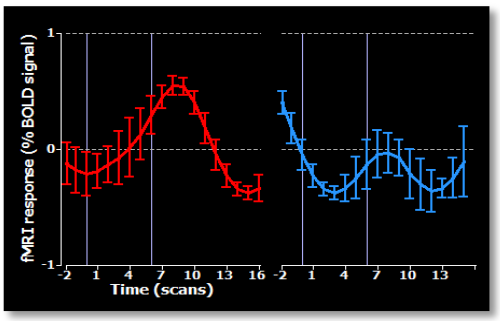

Graph. 11 Averaged cortical activation comparing moving and static blocks.

In the left hemisphere we found an activation within area hMT directly related to the presentation of moving in comparison to static random dots. Looking at the Event-Related Averaging we found that the mean activation was greater in the motion compared with the static condition.

RIGHT HEMISPHERE: activation within Brodmann area 19 (Fig. 49)

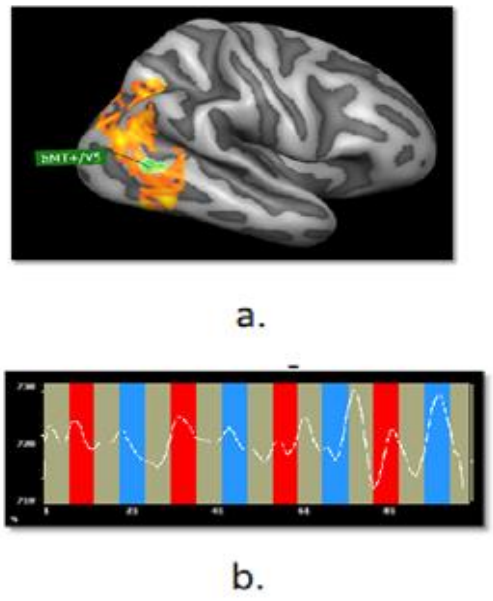

Fig. 49. a). Activation on a right inflated surface within Brodmann Area 19. The green area represents area hMT. b). Activation within area hMT during the entire run. Talairach Coordinated fall within the average coordinates indicated by BrainVoyager Brain Tutor application (Right Area hMT = 48, -61, 9) and by Dumoulin et al., 2000.

Event-Related Averaging (graph. 12):

Averaged cortical activation in moving (red) and static (blue) blocks.

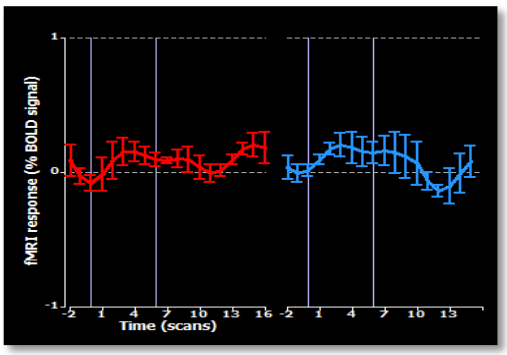

Graph. 12 Averaged cortical activation comparing moving and static blocks.

In the right hemisphere we found a weak, partial activation within area hMT directly related to the presentation of moving versus static random dots. Furthermore, looking at the Event-Related Averaging, we observed that the mean activation was similar in both conditions.

Results in the hemianopic patient:

A.G.

DAMAGED LEFT HEMISPHERE:

activation within Brodmann area 19 (Fig.50)

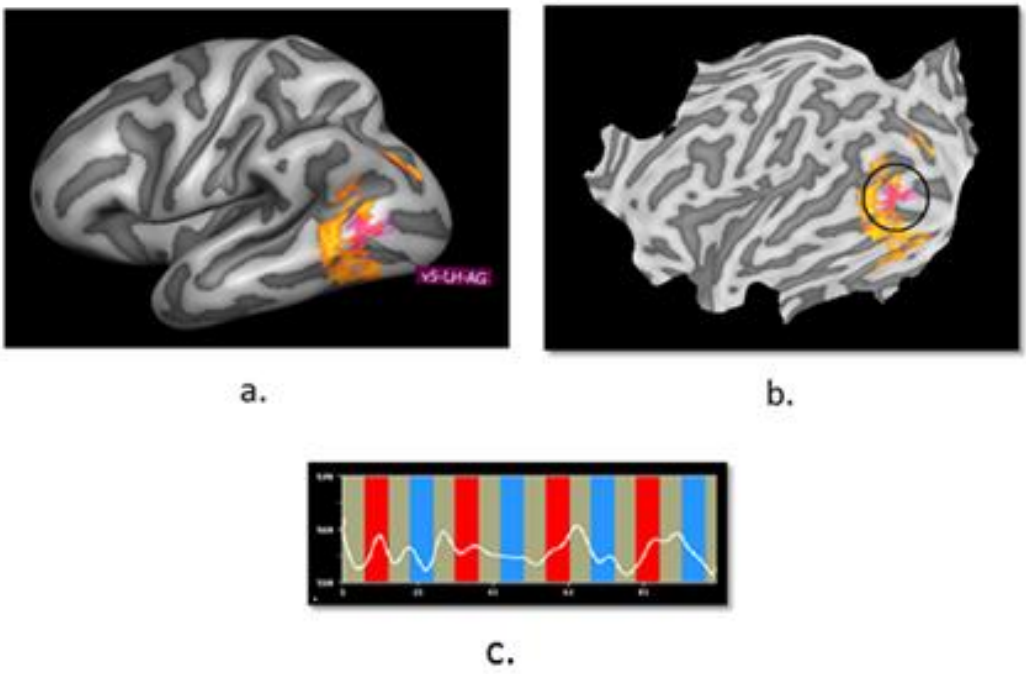

Fig. 50. a). Activation on a left inflated surface within Brodmann Area 19. The pink area represents area hMT b). Activation within area hMT in. during the entire run. Talairach Coordinated fall within the average coordinates indicated by BrainVoyager Brain Tutor application (Left Area hMT = -50, -62, 9) and by Dumoulin et al., 2000.

Event-Related Averaging (Graph.13):

Averaged cortical activation in moving (red) and static (blue) blocks

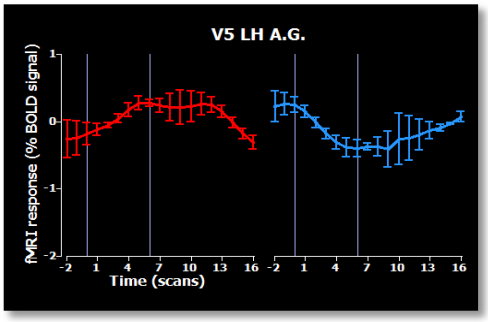

Graph.13. Averaged cortical activation comparing moving and static blocks.

In the damaged hemisphere we found an activation within area hMT despite the lesion in V1. The graph.13 confirmed that the area identified as hMT in patient A.G. was more activated during moving compared with static blocks.

INTACT RIGHT HEMISPHERE: activation within Brodmann area 19

(Fig. 51)

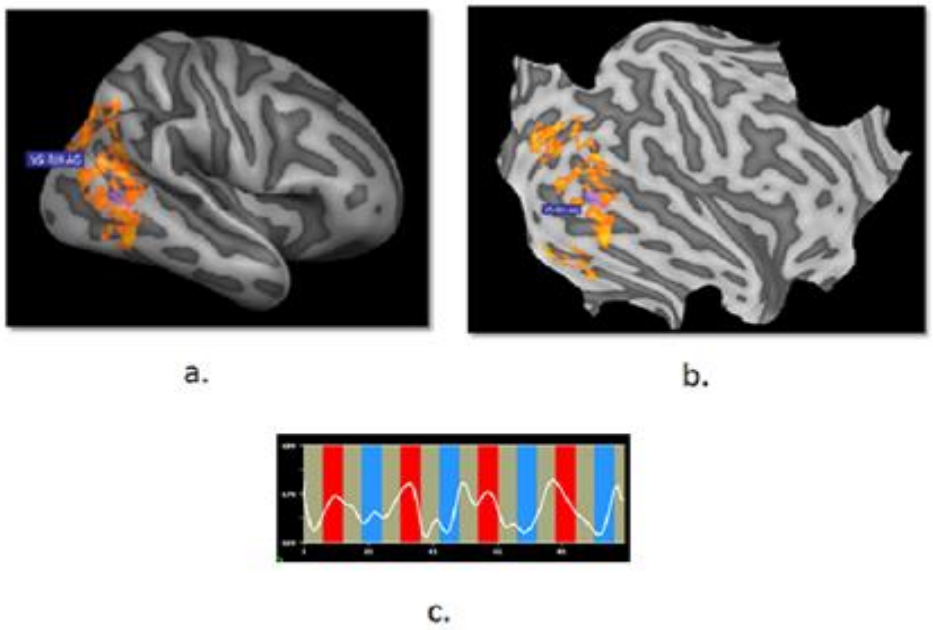

Fig. 51. a). Activation on a right inflated surface within Brodmann Area 19. The pink area represents area hMT. b). Activation within area hMT during the entire run. Talairach Coordinated fall within the average coordinates indicated by BrainVoyager Brain Tutor application (Right Area hMT = 48, -61, 9) and by Dumoulin et al., 2000.

Event-Related Averaging (Graph. 14):

Averaged cortical activation in moving (red) and static (blue) blocks.

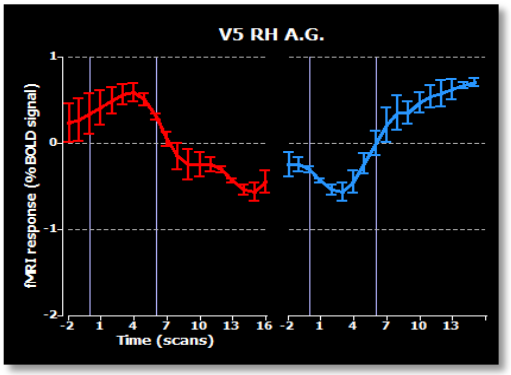

Graph. 14 Averaged cortical activation comparing moving and static blocks.

In the intact hemisphere we found an activation within area hMT. The graph 14 confirmed that the area identified as hMT in Patient A.G. was more activated during moving compared with static blocks in the first 7 scans while in the following scans the activation was higher in static compared with moving blocks. Furthermore, the mean difference observed between moving and static condition conditions was greater in the damaged than in the intact hemisphere.

CONCLUSION:

In conclusion, the hMT Localizer session demonstrated the presence of an activation in A.G. in area hMT during the moving condition, considering both hemispheres, despite of the lesion involving mainly the dorsal portion of left area V1.

DIFFUSION TENSOR IMAGING in A.G.:

The DTI image is flipped in such a way that the damaged left hemisphere is represented on the left side (Fig. 52).

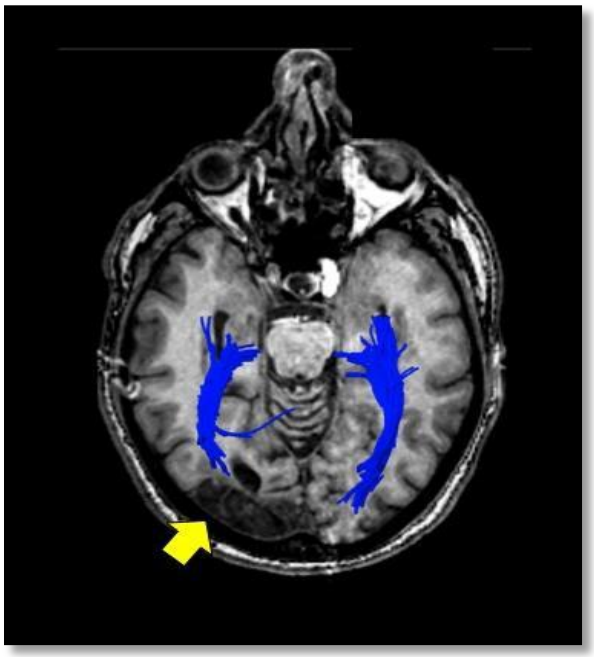

Fig. 52. Mean Diffusivity DTI executed to evaluate the integrity of white matter fibers, mainly of optic radiations.

By performing the DTI we could observe that optic radiations were lesioned within the area of the lesion while the rest of the visual pathways was intact.

DISCUSSION:

In conclusion the fMRI Localizer Session has been useful working with both the healthy participant and the patient, to visualize cortical activation and the organization of low-level visual areas, to analyze the activation of area hMT within both the intact and the injured hemisphere and to evaluate the structural connectivity within the damaged brain.

Spatiotemporal Analysis of the Cortical Response during Passive Visual Stimulation and Orienting of Visual Attention

General Introduction: Transient and Steady-state visual evoked Potentials

Visual Evoked Potentials (VEPs) are electrical voltage potentials elicited by brief visual stimuli and recorded from the central nervous system of humans and animals. There are two basic kinds of VEP: **Transient** and **Steady-State Visual Evoked Potentials (SSVEP)**. The former are useful for clinical applications and for carrying out a chronometric analysis of the brain activity evoked in different cortical areas by visual stimuli. The latter is a technique where a repetitive or flickering visual stimulus is presented at a rate of around 4Hz or higher eliciting a continuous sequence of oscillatory amplitude changes mainly in the visual cortex but also in other cortical areas. The SSVEP generally appears in scalp recordings as a near-sinusoidal waveform at the frequency of the driving stimulus or its harmonics (Regan, 1989): therefore the waveforms are typically modulated at the fundamental stimulus frequency in the case of an unstructured stimulus (e.g. flash) or at the pattern reversal rate (that is the double of the fundamental frequency) if the stimulus is a contrast-reversing pattern (e.g. checkerboard or sinusoidal grating). Thus, a flickering or moving visual stimulus at a constant frequency elicits a response in the brain at the same frequency and its even harmonics (SSVEP frequency = stimulus frequency plus its even harmonics) (Vialatte et al., 2010). SSVEP can be measured in both time and frequency domain in terms of **amplitude** (average of the voltage stimulus-locked in time) and **power** (result of the Fast Fourier Transformation, on the waveform), see Fig.53 that are conceptually equivalent with the difference that the first is in the time and the second in the frequency domain. Moreover, they can be measured in terms of **phase**, that is, the amplitude of the activation during the presentation of half cycle of a pattern reversal (one pattern of the pattern reversal), see Fig. 53. The amplitude and phase of SSVEP could vary as a function of stimulus parameters as luminance, temporal and spatial frequency, contrast and hue of the

visual stimulus (Di Russo et al., 2001, 2002). The Amplitude analysis would be useful in order to evaluate the distribution of cortical activity in the time domain while the Power analysis would be useful to evaluate the resonance of the cortical activity at the specific frequency of visual stimulation.

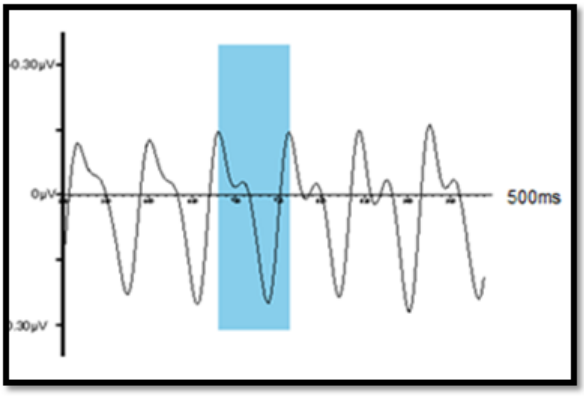

a.

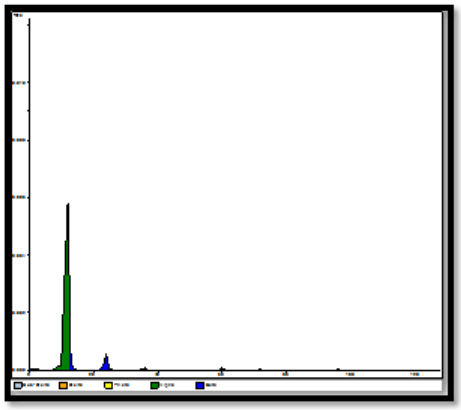

b.

Fig. 53. a). Representation of the amplitude of waveforms in the time window of a phase (83ms; blue box), starting with a negative peak of amplitude and following a sinusoidal trend synchronized with the visual stimulation. b). Representation of the absolute power at the second harmonic of 12 Hz.

This technique has shown to be useful for many paradigms in cognitive and clinical neurosciences such as perception, visual attention, binocular rivalry, working memory, aging, neurodegenerative disorders, etc. Previous findings suggested the utility of using a flickering stimulation to evaluate the visual processing in patients with visual disorders (Di Russo et al, 2007; Di Russo et al,

2012); however its use for studying hemianopic patients has not been reported previously. A major advantage of the this technique is that the signal is easily quantified in the frequency domain and can be rapidly extracted from background noise (Regan, 1989); this makes the SSVEP an advantageous method under conditions of limited recording time and can be recorded under conditions that have certain ecological validity. In contrast, an intrinsic disadvantage of SSVEP is that the rapid visual stimulation does not allow brain activity to return to a baseline before the following stimulus appears, so that the contribution of several visual areas might overlap in the averaged waveform.

Previous SSVEP studies, combined with fMRI, have found that repetitive 6 Hz pattern-reversal stimulation produces the activation of primary visual cortex (V1), of motion sensitive areas (MT/HMT) and minor contributions of mid-occipital (V3A) and ventral occipital (V4/V8) areas (Di Russo et al., 2012).

In the light of these findings we decided to conduct a passive SSVEP stimulation with healthy participants and hemianopic patients by using a pattern-reversal stimulation with a fundamental frequency of 6Hz in order to evaluate the brain electrical response produced in intact and damaged hemispheres. In addition we decided to record the SSVEP during a visual-spatial attention task using a fundamental frequency of 5.5 and 6.5 Hz pattern-reversal simultaneous stimulations, in the same patients and healthy controls. The aim was to investigate the difference in the behavioural performance and SSVEP response when patients attending to either the intact or the hemianopic field.

In sum, with the passive SSVEP experiment we wanted to find out whether a behaviourally blind hemisphere can still respond neuro-physiologically to repeated visual stimulation. Moreover, with the attention task we wanted to find out behaviourally and neuro-physiologically whether it is possible to increase performance and SSVEP response by focusing spatial attention on the blind hemifield. A positive answer to this question would be important for understanding the neural bases of unconscious vision and for devising new methods for rehabilitation of cortical blindness.

Passive Stimulation

Method:

Apparatus, Stimuli, Procedure

During the experiment participants were comfortably seated in a dimly lit room while visual stimuli were presented on a LCD video monitor with a resolution of 1920x1080 and a refresh rate of 144Hz, at a viewing distance of 57cm. They viewed the stimuli binocularly and were trained to maintain stable fixation on a central point throughout stimulus presentation. Steadiness of fixation was monitored by a closed-circuit video camera. After applying the cap with 64 electrodes for EEG recording, we controlled asking patients if they could perceive the stimulus in the blind area chosen for stimulus presentation. The same area was chosen for stimulus presentation in the intact hemifield.

With patients, we always started with the passive session followed by the attentional task because the former was less demanding and therefore more suitable for the initial session. With healthy participants we decided to counterbalance the order of the sessions so as to check for learning and habituation processes. Given the small number of patients we preferred not to do the counterbalancing. However, the data gathered in the healthy group might help explaining possible problematic results in patients.

The visual stimulus consisted of a circular sinusoidal black and white Gabor grating horizontally oriented; the stimulus diameter was 2° of visual angle with a spatial frequency of 4 c/°. The background luminance (22cd/m ^{2} of luminance) was the same as the mean luminance of the Gabor grating pattern which was contrast modulated at 32%. In healthy participants the stimulus was located 4° from the fixation point at polar angles of 25° above and 45° below while with patients the position of stimuli varied according to the position of the patient's blind area.

In the **Passive Session**, four sinusoidal Gabor gratings were presented on the screen in four different positions: right-up, left-up, right-down and left down (see fig. 54). During a block each Gabor grating started flickering one at a time; the

contrast reversed every 83.3ms (one phase; fundamental frequency of 6Hz; reversed rate of 12Hz) producing a complete cycle every 166.7ms.

During the entire experiment, participants were asked to fixate the central point while stimuli were flickering in a random order. Testing included 48 blocks each of them lasting for 20s during which every Gabor grating flickered for 5s with a inter-stimulation interval of 400ms.

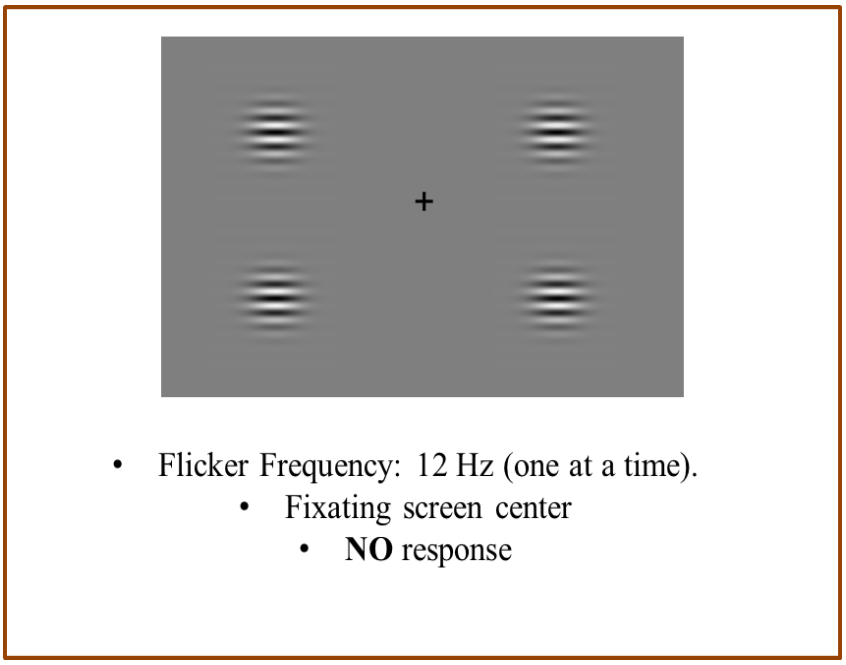

Fig.54. Stimuli used in the Passive Stimulation experiment

Participants

In this experiment we tested 19 healthy participants (right-handed; Mean Age = 25) and 6 hemianopic patients (right-handed); 5 of them were tested during the previous sessions: L.F., F.B., A.M., S.L., A.G. while a new hemianopic patient, L.C., was included. All gave their written informed consent and the experiment was carried out according to the principles laid down in the 1964 Declaration of Helsinki and approved by the AOUI Verona Ethics Committee and by the ERC Ethics Committee.

L.C. is a 65 years old man, right handed hemianopic patient with a Left Lateral Homonymous Hemianopia as a consequence of a hemorrhagic stroke that involved the right parietal-temporal-occipital lobe. One year ago a right parietal-

temporal-occipital craniotomy was performed to absorb the bleeding. He performed a visual compensatory training (Nova Vision) that increased his skills in moving attention toward the blind hemifield.

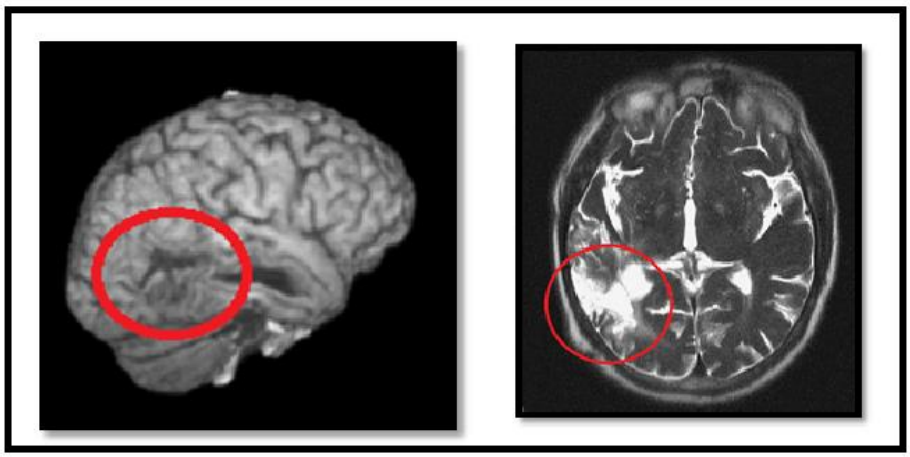

Fig. 55. Surface and MRI (T2) axial section of patient L.C. with the localization of the lesion (left side of the image).

Fig. 56. represented a reconstruction of the lesion on axial slices of a T1-weighted image.

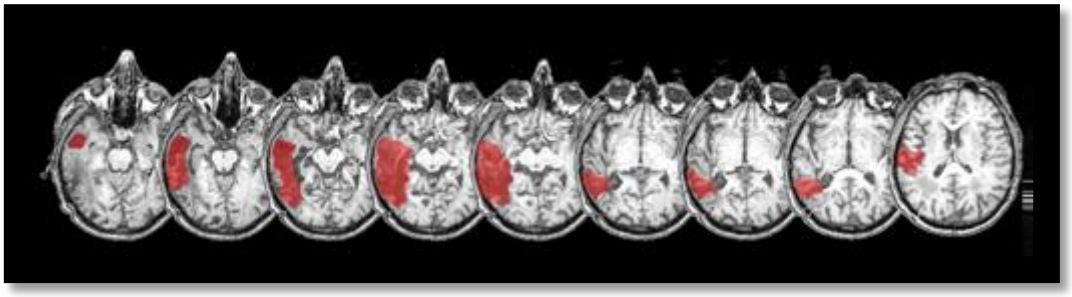

Fig. 56

L.C. performed the neuropsychological tests without showing any kind of cognitive and visuo-spatial impairment (MMSE = 26/30; DILLER H CANCELLATION TEST = 103/106; BELL CANCELLATION TEST = 32/35). In VFQ25 Questionnaire, L.C. obtained a total score included in the normal range: 73. L.C. performed the Visual Mapping (see Study One) in binocular vision (fig. 57).

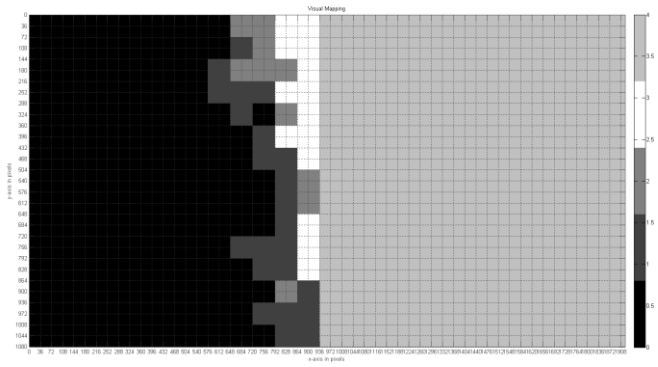

Fig. 57.L.C. Visual Mapping. Black squares represent the absence of response (0 over 3); dark grey indicates the presence of 1 response over 3; light grey the presence of 2 responses over 3 while white squares the presence of 3 correct responses over 3.

Electrophysiological recordings

The Electroencephalogram (EEG) was recorded by means of acti-CAP with 64 electrodes mounted on an elastic cap (fig. 58). Electrodes were positioned at frontal, central, parietal, temporal and occipital areas of the scalp, according to the International 10-20 System.

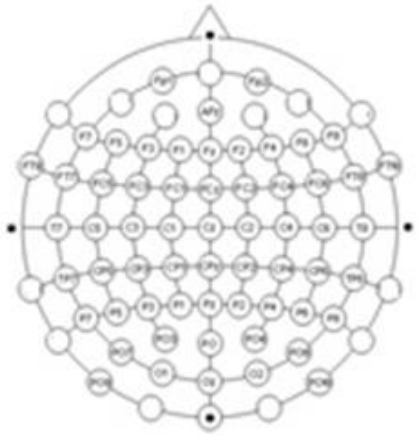

Fig. 58. Localization of 64 active recording electrodes while using an easy-cap.

The left mastoid electrode (LRM) served as on-line reference; additionally, the right mastoid electrode (RRM) was used. EEG data were re-referenced offline to the average of the right and left mastoid electrodes. The ground electrode was placed in AFz. Horizontal and vertical eye movements were monitored with electrodes placed at the left and right canthi (HEOG) and up and below the right eye (VEOG) respectively. The impedance of all electrodes was kept below 5KΩ.

The EEG was recorded at 1000 Hz sampling rate with a time constant of 10Hz as low cut-off and a high cut-off of 1000 Hz. The EEG signal was processed offline using Brain Vision Analyser 2.0.

SSVEP Analysis in Passive Stimulation: Time and Frequency domain

Time Domain:

In a preliminary analysis we performed a visual inspection of the **amplitude of waveforms** elicited at selected electrode sites by stimuli flickering in each of the four quadrants. The waveforms were sinusoidal in form and modulated at 12Hz with maximal amplitude over midline parieto-occipital electrodes. Therefore, we decided to assess and describe activation over electrodes POz, along the vertical midline, PO4 within the right and PO3 within the left hemisphere.

To visualize the voltage topography of SSVEP during one **phase range** (360° = 83ms), **topographic maps** were constructed for the dominant frequency response (second harmonic 12 Hz), separately for visual stimulation in each quadrant. We chose a specific phase represented by a time window of 83 ms (360° of the phase) and divided it into 9 time ranges each one representing 9 ms / 40° of the phase, to visualize the activation in time during the presentation of one pattern, see fig. 59.

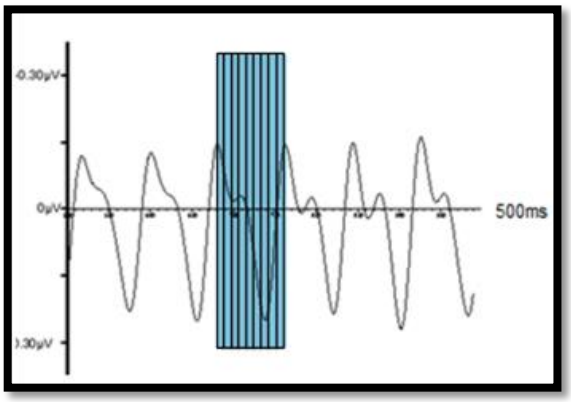

Fig.59 . Representation of one phase of the pattern reversal (blue box), divided into 9 time windows of 9ms / 40° of the phase.

Frequency Domain:

The 12Hz waveform was extracted at each recording site by performing the Fast Fourier Transformation of the SSVEP over the 2,000-ms epoch. We evaluated the position of the peak of absolute power of activation to check if it was related to

the specific frequency of visual stimulation (Second Harmonic of 12 Hz). To perform this single-case analysis we assessed the absolute power of activation of 48 blocks, each one including 60 trials per condition and we calculated the difference at 12Hz between the real and simulated frequency (performed at 6.58Hz). The difference in absolute power for the two conditions was analyzed by means of a non-parametric **Monte Carlo Percentile Bootstrap Simulation** (Efron and Tibshirani, 1993; Oruc et al., 2011; Bagattini et al., 2015) . This procedure creates a simulated data by re-sampling the raw data with replacement. We created 50000 re-samples of 48 blocks for real minus simulated power values. The lower 5^{th} percentile of the re-sampled data distribution served as the critical values for the one-tailed 0.05 significance level on the basis of the strong hypothesis that the power in the real frequency would be higher than in the simulated one. If the 5^{th} percentile was above the zero level (real frequency > simulated frequency), then the real frequency condition would yield a significantly larger power than the simulated frequency.

Then, to represent the **topographic distribution of absolute power of activation** we created topographic maps separately for stimulation in each quadrant showing the distribution of absolute power in the whole recorded brain. We decided to focus our attention on posterior electrodes as flickering visual stimuli should produce a continuous sequence of oscillatory amplitude changes mainly within visual areas. Therefore, we compared the absolute power in the blind field of each patient with the mean absolute power of healthy participants in the same field, for each posterior electrode, in order to locate the main difference in absolute power.

Results in healthy participants
Passive stimulation in the TIME DOMAIN:
1. Amplitude of Waveforms

The grand-average SSVEP waveforms elicited at selected electrode sites by pattern reversal stimuli in each of the four quadrants are shown in Fig.60.

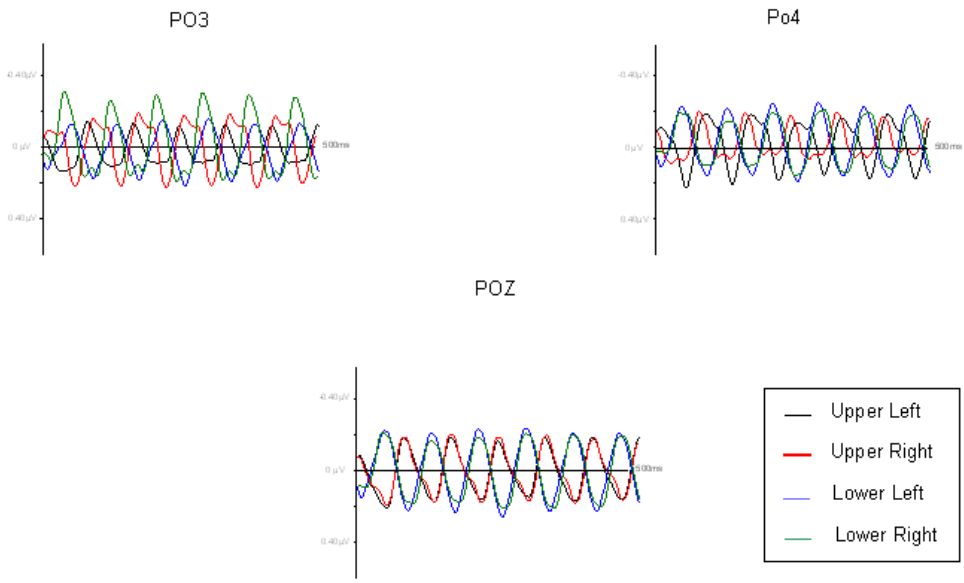

Fig.60. Grand-average SSVEP waveforms elicited at electrodes PO3, POz and PO4.

In all electrodes we found a difference in phase of activation between upper and lower visual quadrants and left and right visual hemifields. At the midline site (POz) the SSVEP phase was similar for left and right stimuli in both upper and lower visual quadrants. At the lateral recording sites (PO3 and PO4) the amplitudes were generally larger over the contralateral than the ipsilateral hemisphere as expected given the pattern of lateralization of the visual pathways.

2. Topography of phase range

The scalp topography of SSVEP phase range varied systematically as a function of response phase, which indicated that more than a generator was contributing to the waveform. In the following Fig.61 nine maps are represented, indicating the

sequential scalp voltage topography within a phase range, considering single quadrants of visual stimulation, at the second harmonic of 12 Hz (group-averaged data). Each single map represents a range of response phase equivalent to 40° (9ms).

For stimulus presentation to the upper visual quadrants, both left and right, the response started with a negative peak.

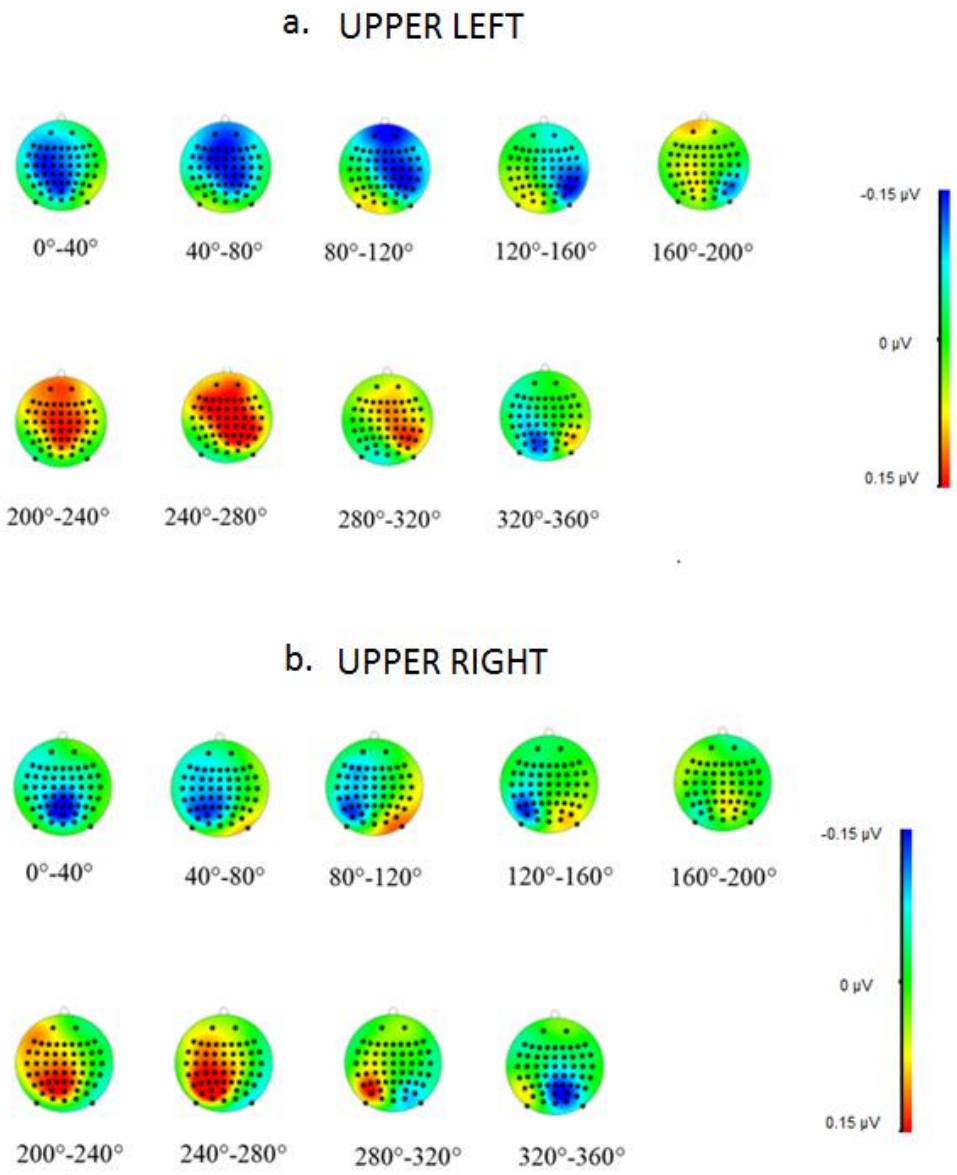

Fig.61. Topography of the phase range. Blue = negative amplitude; red = positive amplitude. a). Upper left visual quadrant; b). Upper right visual quadrant.

Upper left visual quadrant:

- Phase range 0°-80°: unitary negative focus over parietal-central and frontal electrodes bilaterally distributed;
- Phase range 80°-200°: negative focus over parietal-occipital electrodes in the contralateral right hemisphere, positive focus in the left hemisphere, over occipital-parietal electrodes.
- Phase range 200°-280°: strong positive focus mainly in the right hemisphere.
- Phase range 280°-320°: positive focus over frontal, central and posterior electrodes in the right hemisphere.
- Phase range 320°-360°: negative focus over occipital-parietal electrodes in the left hemisphere, weak positive focus over posterior electrodes in the right hemisphere

Upper right visual quadrant:

- Phase range 0°-40°: unitary negative focus over occipital-parietal electrodes bilaterally distributed;
- Phase range 40°-200°: negative focus over parietal-occipital electrodes in the contralateral left hemisphere and a positive focus over occipital-parietal electrodes in the right hemisphere.
- Phase range 200°-280°: strong positive focus mainly in the left hemisphere, involving posterior, frontal and central electrodes.
- Phase range 280°-320°: positive focus over posterior electrodes in the left hemisphere, weak negative focus over occipital electrodes in the right hemisphere.
- Phase range 320°-360°: negative focus over posterior electrodes mainly in the right hemisphere, weak positive focus over posterior electrodes in the left hemisphere.

In conclusion, these results for the upper hemifield indicated that during one phase of pattern reversal the main activation was located in the hemisphere **contralateral to the side of visual stimulation.** The first and the last phase range showed a similar activation as expected, given that they represent the beginning

and the end of the phase. The 5th map showed a similar topography compared to the first and the last one but with an opposite amplitude (from negative to positive) representing the peak in the middle of the phase with similar amplitude but with opposite potential.

For stimulus presentation to the lower visual quadrants, both left and right, the response started with a positive peak (Fig. 62).

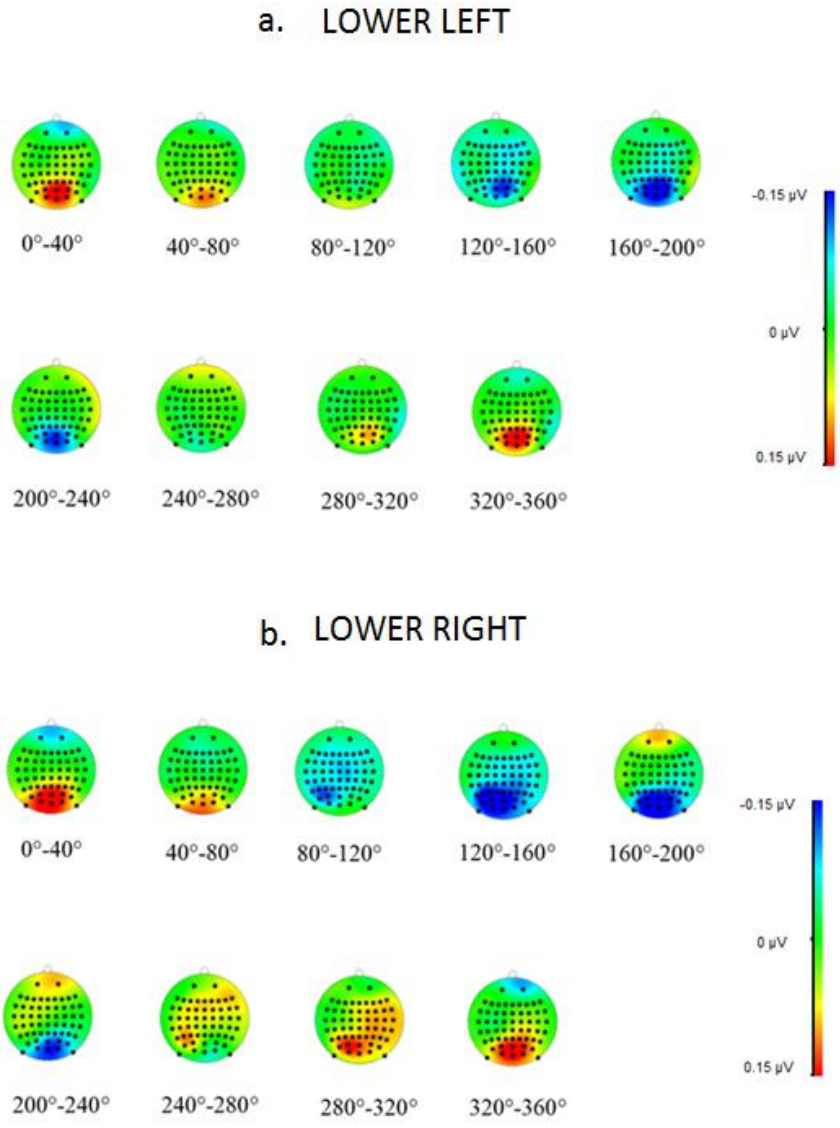

Fig.62. Topography of the phase range. Blue = negative amplitude; red = positive amplitude. a). Lower left visual quadrant; b). Lower right visual quadrant.

Lower left visual quadrant:

- Phase range 0°-120°: unitary positive focus over occipital-parietal electrodes bilaterally distributed, decreasing in the time;
- Phase range 120°-280°: unitary negative focus over occipital-parietal electrodes bilaterally distributed;
- Phase range 280°-360°: unitary positive focus over occipital-parietal electrodes bilaterally distributed.

Lower right visual quadrant:

- Phase range 0°-80°: unitary positive focus over occipital-parietal electrodes, decreasing in the time;
- Phase range 80°-120°: unitary negative focus over posterior electrodes in the left contralateral hemisphere;
- Phase range 120°-240°: strong unitary negative focus over posterior electrodes bilaterally distributed;
- Phase range 240°-280°: positive focus mainly over occipital-parietal electrodes mainly in the left hemisphere;
- Phase range 280°-360°: strong positive focus over posterior electrodes bilaterally distributed.

These results indicated that the presentation of one phase of the pattern reversal in the lower hemifield determined an activation bilaterally distributed, regardless of the side of the visual stimulus shown. The first and the last phase range represented a similar activation, as expected, representing the beginning and the end of the phase. The 5^{th} map indicated a similar topography compared to the first and the last one but with an opposite polarity (from negative to positive) representing the peak in the middle of the phase.
The topography for the second phase to complete a whole cycle (not shown) was identical to those presented.

Looking at results collected, we could argue that the activation stimulating the upper hemifield involved mainly contralateral frontal, central and posterior electrodes; instead the activation stimulating the lower visual hemifield involved

mainly bilateral posterior electrodes. Considering those results, we could make some hypothesis concerning neural mechanisms involved in the activation observed during the phase range. The scalp topography of the SSVEP varied systematically in time and it indicated that the passive stimulation was a dynamic process involving a communication between different cortical areas that projected on the scalp. This perceptual process could involve posterior and anterior structures depending on the position of the stimulus as a response to the resonance of the specific frequency of SSVEP.

It should be mentioned that these results are consistent with results obtained by Di Russo et al. (2007).

FREQUENCY DOMAIN:

1. Topographic distribution of Absolute Power, at the second harmonic of 12Hz (Fig. 63)

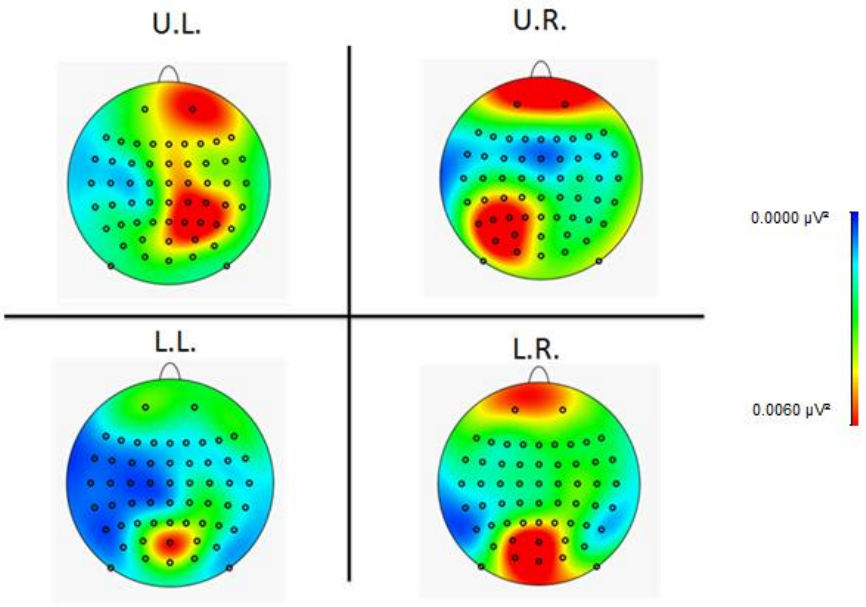

Fig.63. Topographic maps of absolute power. Blue = low; Red =high absolute power.

Upper right quadrant (UR): increased activation over left occipital-parietal electrodes.

Upper left quadrant (UL): increased activation over right central-parietal electrodes.

Lower right quadrant (LR): increased activation over occipital-parietal electrodes, medial and contralateral to the visual stimulation.
Lower left quadrant (LL): increased activation over the medial occipital-parietal scalp.

CONCLUSION:

In conclusion, in the upper visual quadrants there was a more lateralized activation over posterior electrodes within the contralateral hemisphere with respect to lower quadrants where the activation was mainly bilaterally distributed.

RESULTS WITH HEMIANOPIC PATIENTS:

A.G.:
Lesion involving basal ganglia
and the dorsal portion of the left visual primary cortex.

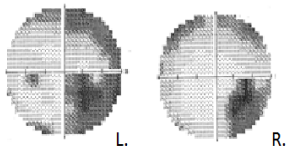

In patient A.G. we located stimuli 7° from the center of the screen on the x axis and 3° from the center considering the y axis.

TIME DOMAIN:

1. **Amplitude of Waveforms**

The amplitude of SSVEP waveforms to pattern reversal stimuli elicited at selected electrode sites by visual stimuli are shown in Fig. 64.

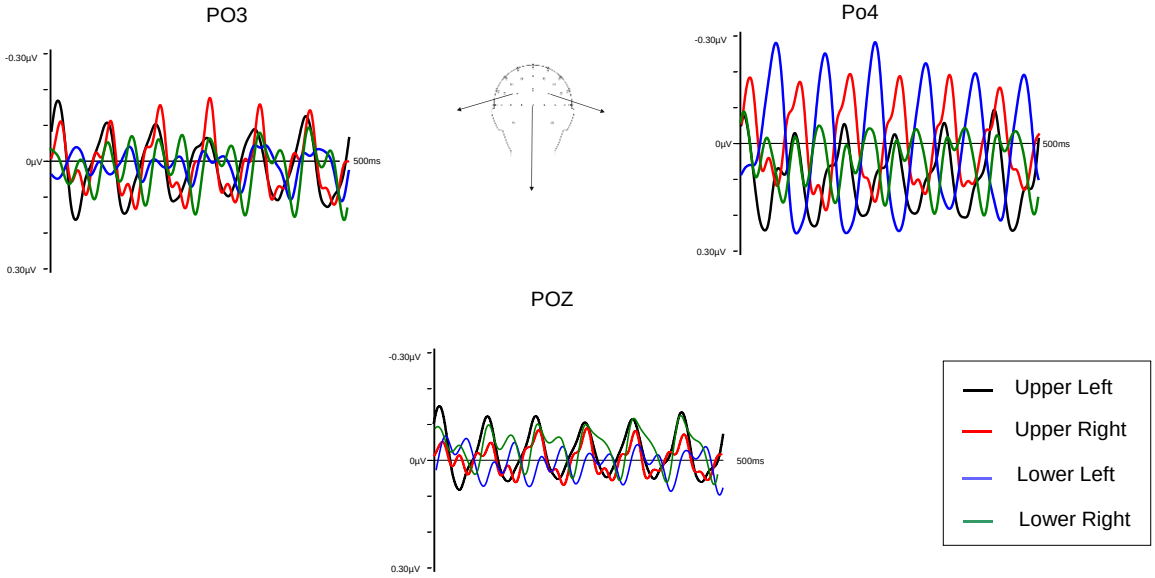

Fig.64. SSVEP waveforms elicited at electrodes PO3, POz and PO4.

In all electrodes the signal was noisy for lower visual quadrants, mainly in the lower right quadrant in which each phase was composed by two waveforms rather than one. In all electrodes, we observed a difference in phase between upper and lower visual quadrants.

Upper right vs. upper left: the amplitude was greater for upper right, at lateral sites; instead, at the midline site (POz) the amplitude was greater for the upper left stimulation.

Lower right vs. lower left: at lateral sites (PO3 and PO4) the amplitude was greater for the contralateral quadrant while at the midline site the amplitude was greater for the lower right quadrant.

Those results suggested that the stimulation in the blind quadrant could determine a synchronization of cortical activity to the specific frequency even in the damaged hemisphere, similar compared with the synchronization produced by stimulating the sighted quadrants. Interesting, stimulating the blind quadrant, the amplitude was greater in the contralateral damaged hemisphere, even if the stimulus could not be consciously perceived.

2. Topography of phase range

The scalp topography of SSVEP varied systematically as a function of response phase, which indicated that more than a generator was contributing to the waveform. Fig. 65. shows the sequential changes in time in the topography of the response to visual stimulation.

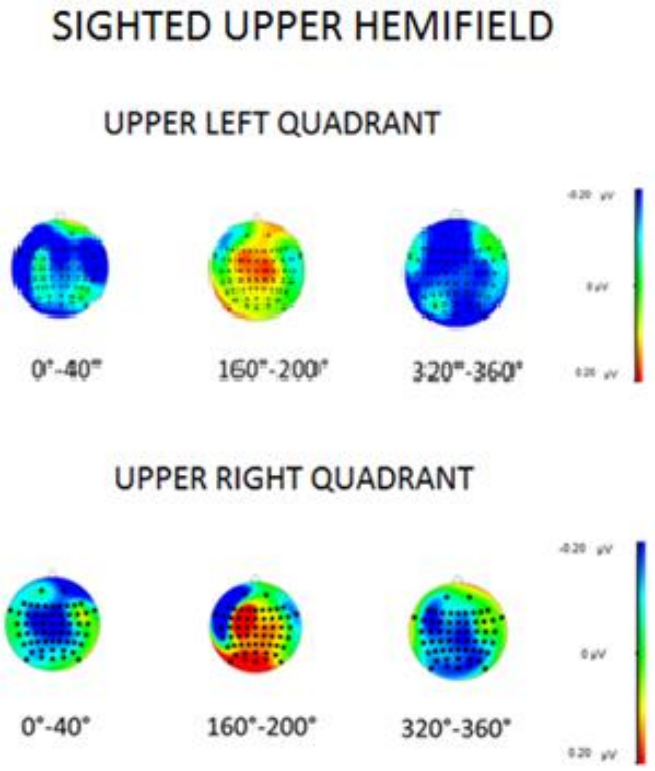

Fig.65. Topographic maps of a phase range.
Blue = negative amplitude; red = positive amplitude.

Upper left visual quadrant:

- First phase range: negative widespread focus mainly over lateral frontal, temporal and occipital electrodes in both hemispheres;
- Second phase range: unitary positive focus over central-parietal and frontal electrodes, bilaterally distributed;
- Last phase range: widespread negative focus involving mostly the entire scalp.

Upper right visual quadrant:

- First phase range: unitary negative focus over parietal-central electrodes bilaterally distributed;
- Second phase range: positive focus over frontal, central and posterior electrodes bilaterally distributed; negative focus over frontal and temporal electrodes in the damaged left hemisphere;
- Last phase range: negative focus over occipital-parietal and central electrodes bilaterally distributed; weak positive focus over frontal right electrodes.

In conclusion the activation in the time domain confirmed that more than one generator was contributing to the waveform when stimulating the upper hemifield; those generators appeared to be bilaterally distributed involving frontal, central and posterior electrodes.

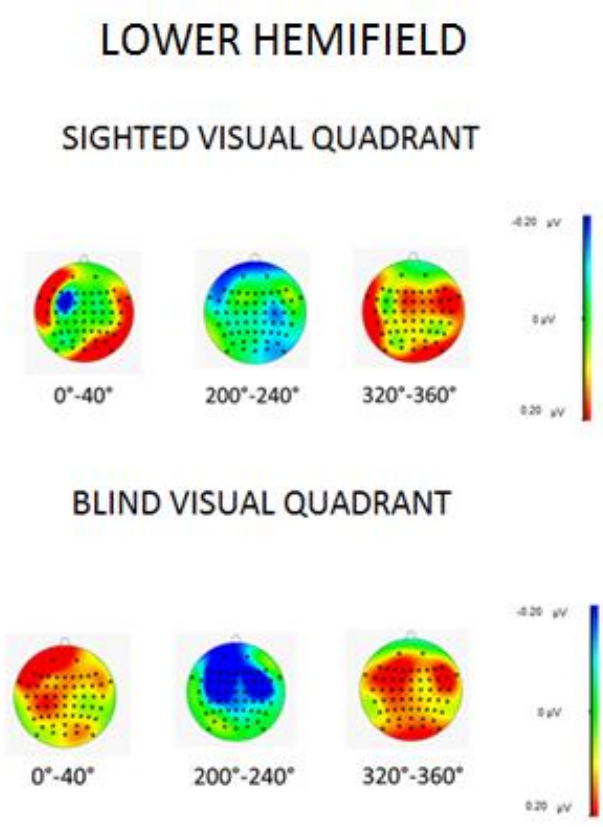

Fig. 66. Topographic maps of a phase range.
Blue = negative amplitude; red = positive amplitude.

Sighted visual quadrant:

- First phase range: two positive foci of activation over occipital-parietal and temporal electrodes lateralized within the intact right hemisphere and over frontal and temporal electrodes within the damaged left hemisphere;
- Second phase range: two negative foci of activation over occipital-parietal and central electrodes lateralized within the intact right hemisphere and over frontal electrodes in the damaged left hemisphere;
- Last phase range: positive focus of activation almost in the whole peripheral brain being more widespread over frontal and central electrodes in the right hemisphere.

Blind visual quadrant:

- First phase range: positive focus practically over the whole brain being stronger over frontal-temporal and central electrodes within the damaged left hemisphere;
- Second phase range: negative focus over frontal and central electrodes bilaterally distributed; weak positive focus over occipital-parietal electrodes in the damaged left hemisphere;
- Last phase range: positive focus over the whole brain being stronger over frontal-central-temporal and posterior electrodes bilaterally distributed but mainly in the damaged left hemisphere.

In conclusion the activation in the time domain confirmed that more than one generator was contributing to the waveform when stimulating the lower visual hemifield; those generators appeared to be mostly located in the hemisphere contralateral to the visual stimulation. Concerning the blind visual quadrant the activation was mainly located over frontal and parietal electrodes in the left hemisphere and started involving bilateral posterior electrodes only during the last phase ranges (320°-360°) determining the involvement of a bilateral dynamic mechanism composed by anterior and posterior structures during the perceptual process. Concerning the sighted visual quadrant the activation was mainly located over frontal, central and posterior electrodes in the contralateral hemisphere and over frontal and temporal electrodes in the ipsilateral, determining the

involvement of a bilateral dynamic mechanism composed by anterior and posterior structures during the perceptual process.

FREQUENCY DOMAIN:

1. Bootstrap Analysis to compare real and simulated stimulation frequency (graph. 15).

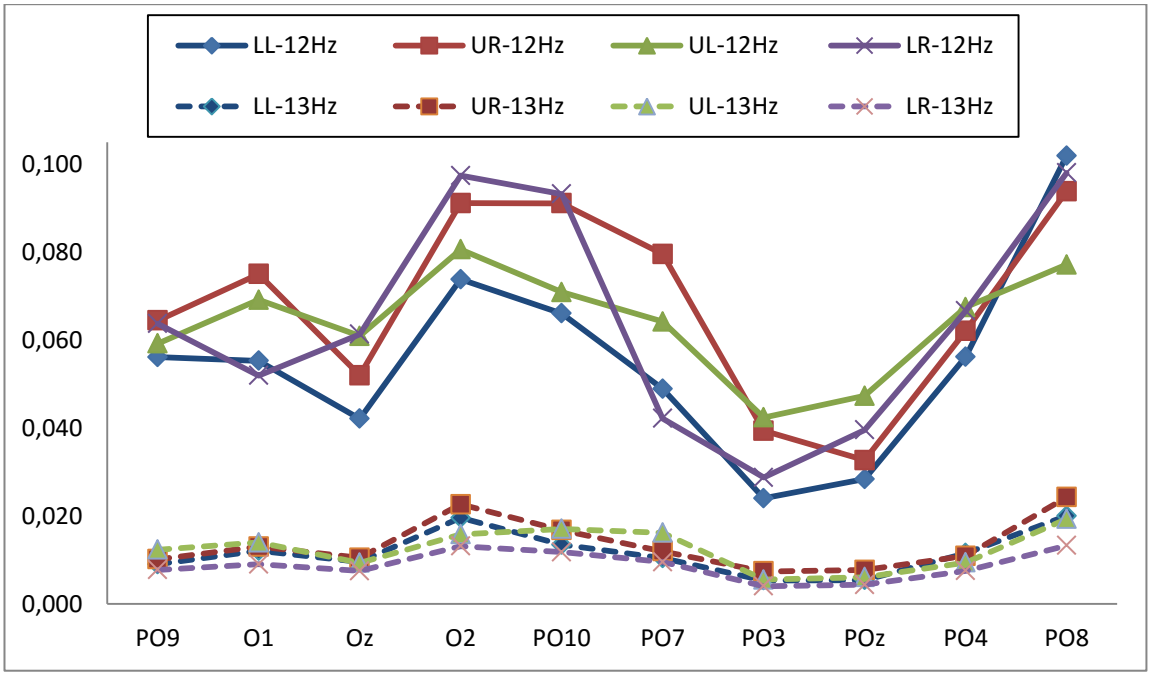

Graph.15. Absolute power of activation at posterior electrodes comparing 12Hz (real frequency of visual stimulation; continuous line) and 13 Hz (simulated frequency; dotted line).

With the Bootstrap analysis we found a significant difference in absolute power between the two frequencies, see graph. 15, for posterior electrodes. This demonstrates that the SSVEP response was related to the specific frequency of visual stimulation.

2. Topographic distribution of Absolute Power, at the second harmonic of 12Hz (fig. 67)

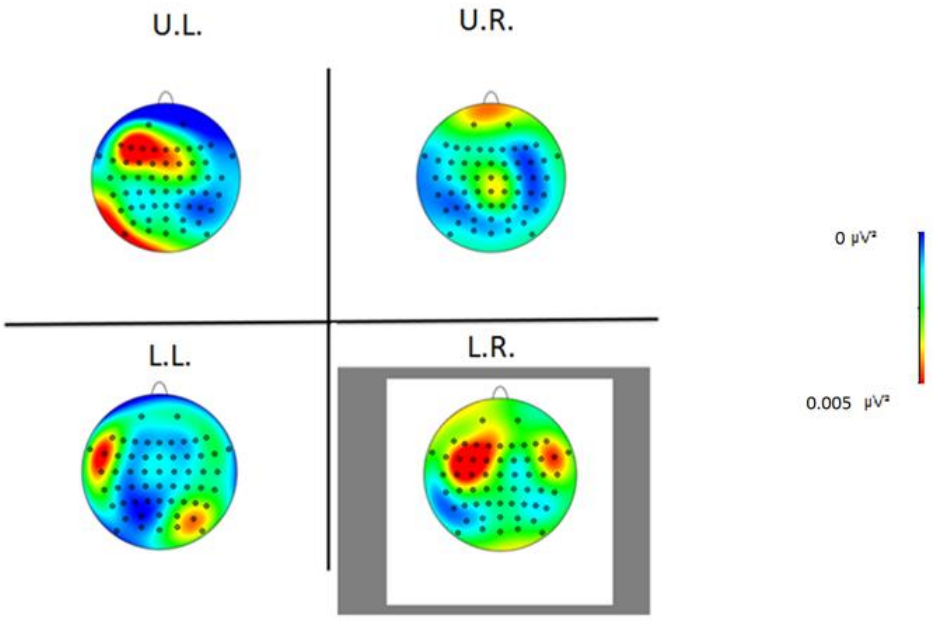

Fig.67. Topographic maps of absolute power. Blue = low absolute; red =high absolute power. Grey background = blind quadrant

SIGHTED VISUAL QUADRANTS:

Upper right quadrant (UR): weak activation over central electrodes bilaterally distributed.

Upper left quadrant (UL): strong activation mainly over frontal electrodes, ipsilateral to the visual stimulation and weak activation bilaterally distributed.

Lower left quadrant (LR): higher activation over occipital-parietal electrodes within the intact right hemisphere, contralateral to visual stimulation and over frontal-temporal electrodes in the damaged left hemisphere, ipsilateral to visual stimulation.

BLIND VISUAL QUADRANT:

Lower right quadrant (LR): strong activation over frontal-central electrodes within the damaged left hemisphere; weaker activation over frontal-temporal electrodes in the intact right hemisphere.

In conclusion these results broadly confirm those found in the time domain: the activation was mainly located within the contralateral hemisphere stimulating the blind right quadrant involving mainly frontal and central electrodes; instead it was mainly located over posterior contralateral and frontal-temporal bilateral electrodes stimulating the lower left visual quadrant.

3. DIFFERENCE OVER POSTERIOR ELECTRODES comparing ABSOLUTE POWER of the BLIND LOWER RIGHT QUADRANT in healthy participants and patient (Fig. 68).

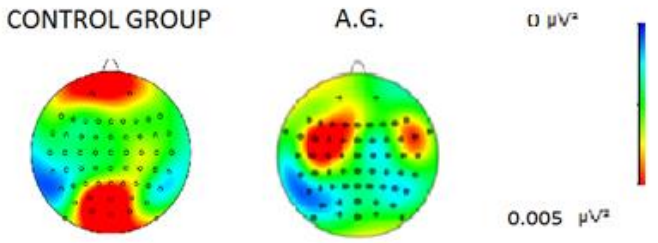

Fig.68. Topographic maps of control group and A.G. while stimulating the blind visual quadrant. Blue =low absolute power of activation; red = high absolute power of activation.

Absolute power of activation at 12z at posterior electrodes (graph. 16)

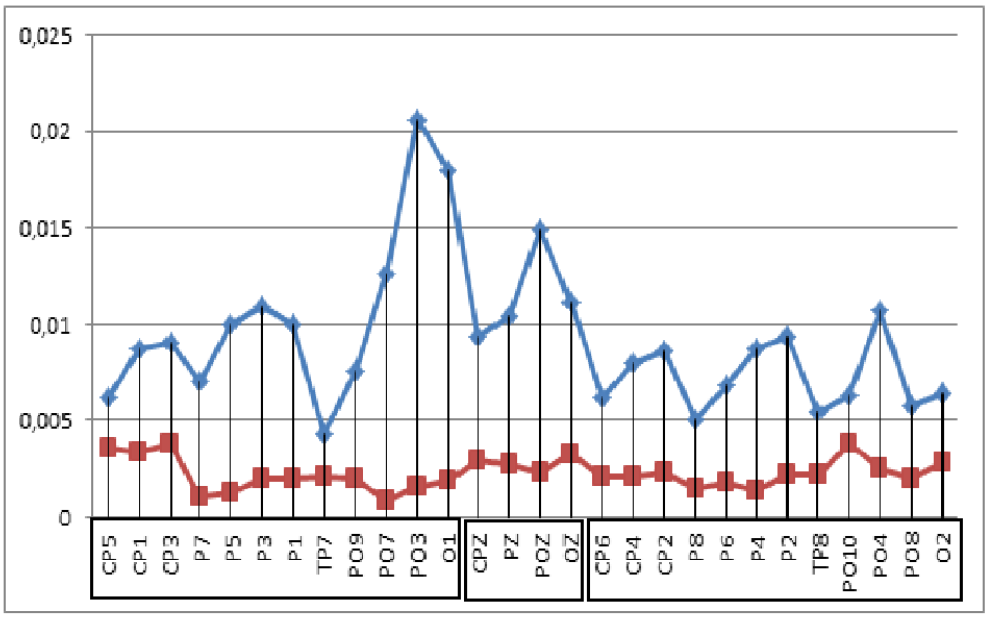

Graph. 16. Absolute power of activation at 12Hz. Blue line = healthy participants; red line = A.G.

A.G. absolute power was below the group mean over occipital-parietal electrodes in the damaged **left hemisphere** and along the vertical midline. Interesting we could still find a modulation in absolute power produced by a visual stimulus shown in the blind quadrant, even if it was lower than healthy participants.

CONCLUSION:

In summary, in patient A.G. with a lesion involving basal ganglia and the dorsal portion of the left primary visual cortex, causing a lower right quadrantanopia, we found a modulation of response in both time and frequency domain in the damaged hemisphere following stimulus presentation to the blind lower right quadrant. This modulation was mainly located over frontal and central electrodes.
As far as the intact hemifield is concerned we found that in the frequency domain the absolute power was lower than in healthy participants stimulating all sighted quadrants except for some posterior electrodes in the damaged left hemisphere.

S.L.

Lesion involving the medial part of the left occipital lobe

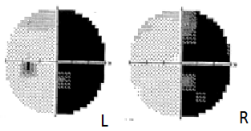

With S.L. we located stimuli 5° from the center of the screen considering both x and y axes.

TIME DOMAIN:

1. Amplitude of Waveforms

,

The amplitude of SSVEP waveforms to pattern reversal stimuli elicited at selected electrode sites by visual stimuli are shown in Fig. 69.

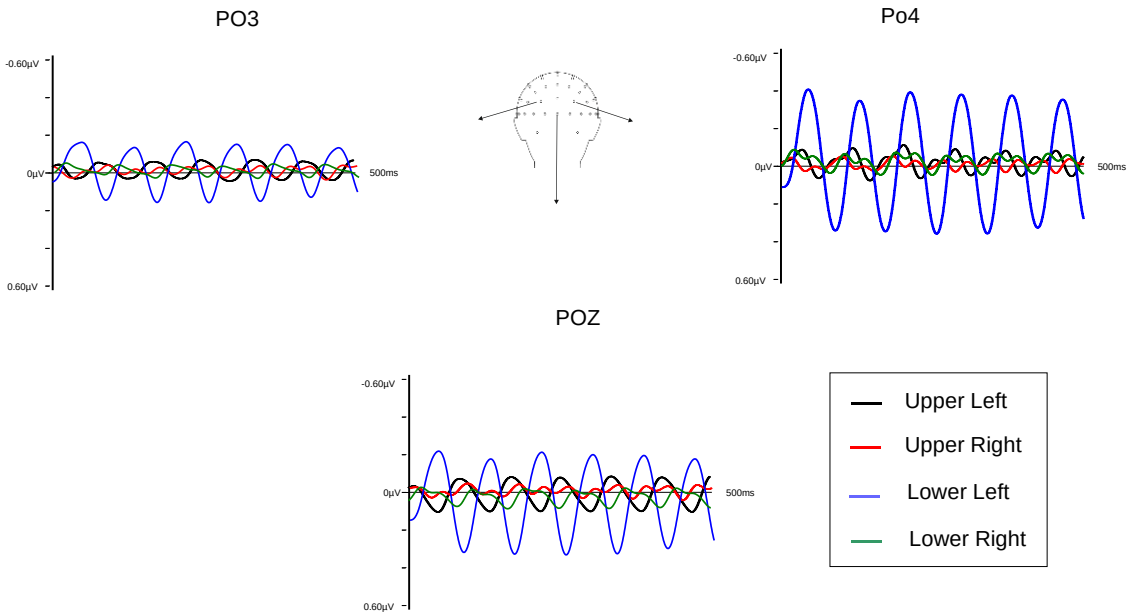

Fig.69. SSVEP waveforms elicited at electrodes PO3, POz and PO4.

In all electrodes the signal appeared noisy while stimulating the right visual hemifield, mainly the upper one. Thus, mainly in all electrodes considered, each phase appeared to be composed by two waves instead of one, stimulating the upper right visual quadrant.

Upper right vs. upper left: the amplitude was greater for upper left mainly at the contralateral site (PO4) and at the midline site (POz).

Lower right vs. lower left: the amplitude was always greater for lower left regardless of the side of electrode considered. Those results were in line with the fact that the right visual hemifield was the blind one.

Those results suggested that the stimulation in the blind hemifield could determine a synchronization of cortical activity to the specific frequency even in the damaged hemisphere even if this signal was lower and noisier than stimulating the sighted hemifield.

2. Topography of phase range

The scalp topography of SSVEP varied systematically as a function of response phase, which indicated that more than a generator was contributing to the

waveform. In the following Fig. 70, the sequential changes in topography in response to visual stimulation in time is shown.

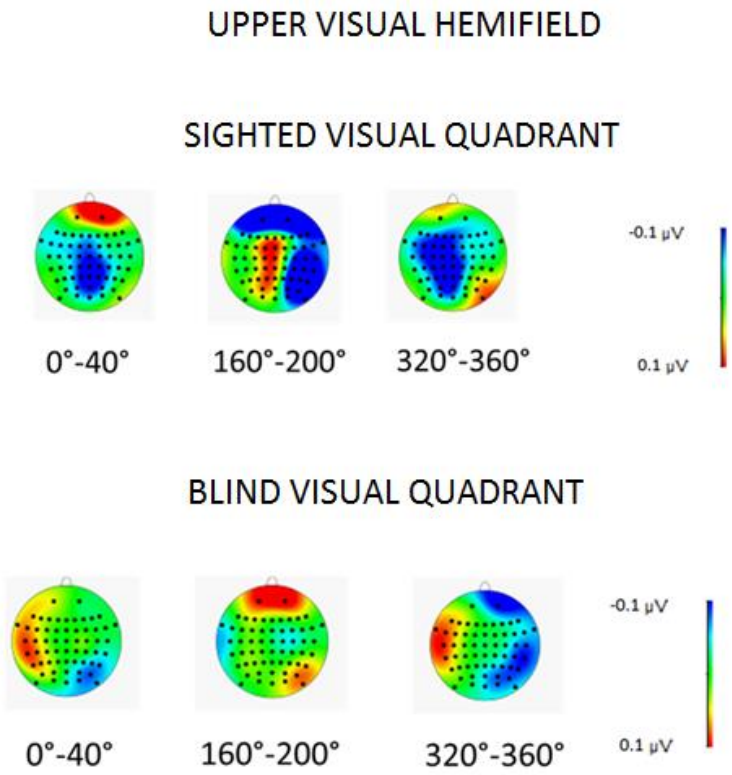

Fig.70. Topographic maps of a phase range.
Blue = negative amplitude; red = positive amplitude.

Sighted visual quadrant:

- First phase range: negative focus mainly over central-parietal electrodes bilaterally distributed;
- Second phase range: positive focus mainly over central-parietal electrodes bilaterally distributed; negative focus over occipital-parietal electrodes in the right hemisphere and over frontal electrodes bilaterally distributed;
- Last phase range: negative focus over frontal, central and posterior electrodes bilaterally distributed but mainly in the damaged left hemisphere.

Blind visual quadrant:

- First phase range: negative focus over parietal-occipital electrodes mainly in the intact **right hemisphere**, ipsilateral to visual stimulation; positive focus over frontal electrodes, in the damaged left hemisphere;
- Second phase range: positive focus over parietal-occipital electrodes in the intact right hemisphere and over frontal electrodes bilaterally distributed**;**
- Last phase range: positive focus over frontal-temporal electrodes in the damaged left hemisphere; negative focus over frontal, temporal and posterior electrodes in the intact right hemisphere.

In conclusion the activation in the time domain confirmed that more than one generator was contributing to the waveform when stimulating the upper hemifield; those generators appeared to be mostly bilaterally distributed. When considering posterior electrodes, they involved mainly the contralateral posterior electrodes stimulating the sighted quadrant and the ipsilateral posterior electrodes stimulating the blind one.

Considering the sighted quadrant, those results suggested that the visual information determined an activation over frontal, temporal and posterior electrodes in the contralateral hemisphere; the communication of visual information with different areas in the left hemisphere determined the involvement of a bilateral dynamic mechanism composed by anterior as well as posterior structures during the perceptual process.

Considering the blind quadrant, the visual information determined an activation over frontal and temporal electrodes in the contralateral hemisphere; the communication of visual information with posterior areas in the right hemisphere determined the involvement of a bilateral dynamic mechanism composed by anterior as well as posterior structures during the perceptual process.

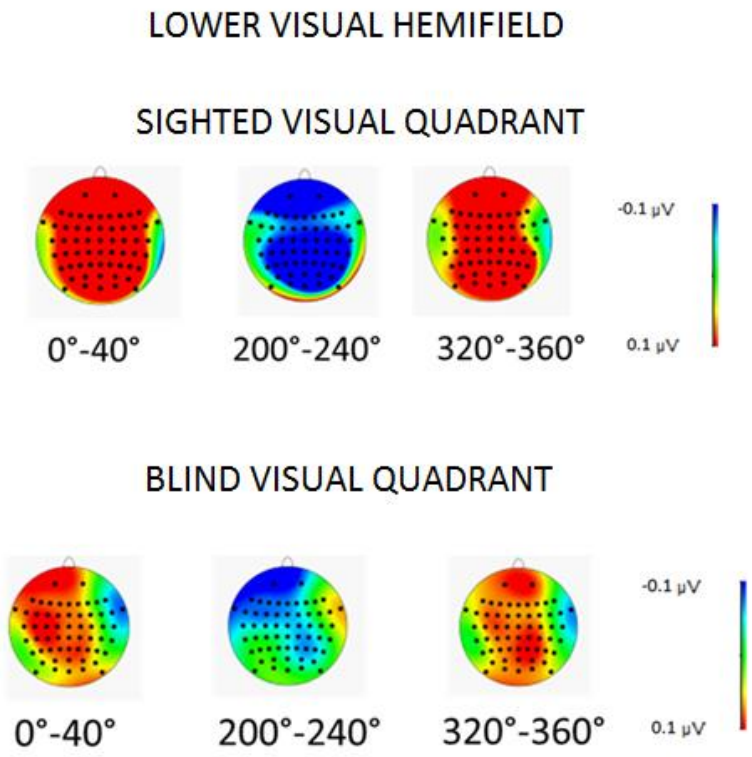

Fig.71. Topographic maps of a phase range.
Blue = negative amplitude; red = positive amplitude.

Sighted visual quadrant:

- First phase range: strong widespread positive focus of activation mainly over the whole brain, bilaterally distributed;
- Second phase range: strong widespread negative focus of activation mainly over the whole brain, bilaterally distributed;
- Last phase range: strong widespread positive focus of activation mainly over the whole brain, bilaterally distributed.

Blind visual quadrant:

- First phase range: positive focus bilaterally distributed but involving mainly over the whole damaged left hemisphere;
- Second phase range: negative focus involving mainly frontal-temporal electrodes in the left hemispehre**;**
- Last phase range: unitary positive focus over occipital-parietal, frontal and central electrodes bilaterally distributed.

In conclusion the activation in the time domain was mostly bilaterally distributed regardless the side of visual stimuli presented in the lower hemifield.

Considering the sighted quadrant, those results suggested that the visual information determined an activation over frontal, temporal and posterior electrodes in the contralateral hemisphere; the communication of visual information with different areas in the left hemisphere determined the involvement of a bilateral dynamic mechanism composed by anterior as well as posterior structures during the perceptual process.

Considering the blind quadrant, the visual information determined an activation over frontal, temporal and posterior electrodes in the contralateral hemisphere; the communication of visual information with the right hemisphere determined the involvement of a bilateral dynamic mechanism composed by anterior as well as posterior structures during the perceptual process.

Furthermore, the activation was weaker while stimulating the blind visual hemifield, mainly the upper one, than stimulating the sighted hemifield.

FREQUENCY DOMAIN:

1. Bootstrap Analysis to compare real and simulated stimulation frequency (graph. 17).

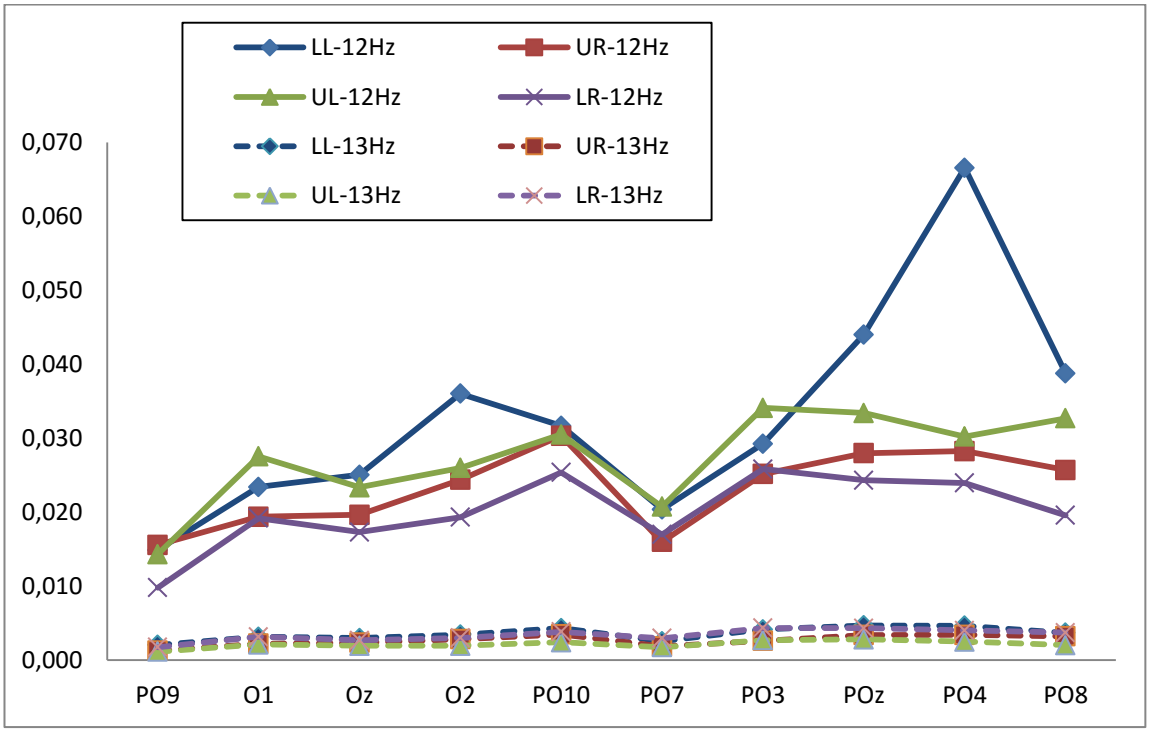

Graph.17. Absolute power of activation at posterior electrodes comparing 12Hz (real frequency of visual stimulation; linear line) and 13 Hz (simulated frequency; dotted line).

With the Bootstrap analysis we found a significant difference in absolute power between the two frequencies for posterior electrodes, see graph. 17. This demonstrates that the SSVEP response was related to the specific frequency of visual stimulation.

2. Topographic distribution of Absolute Power, at the second harmonic of 12Hz (fig. 72)

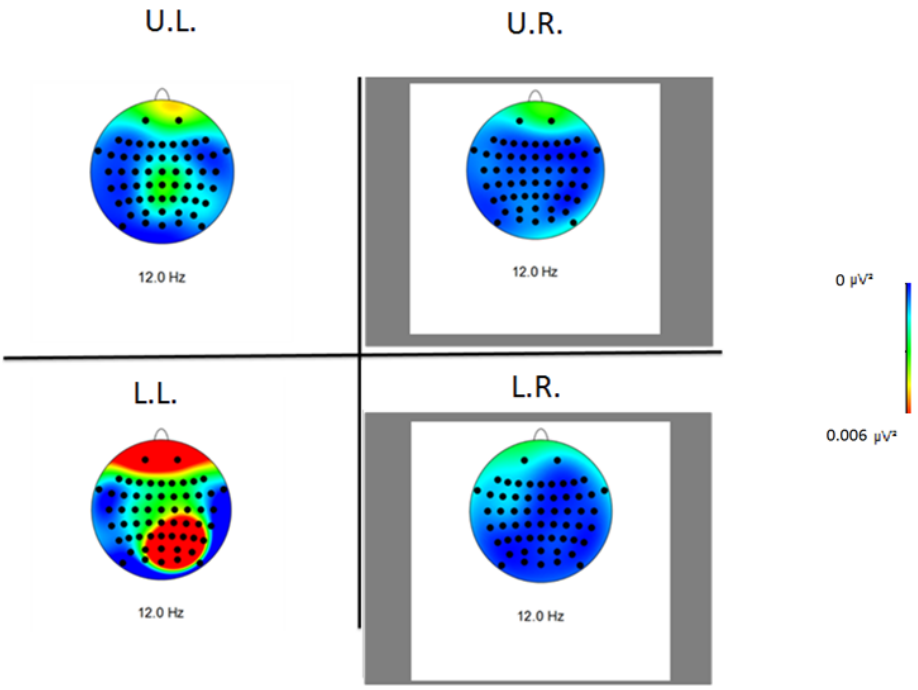

Fig.72. Topographic maps of absolute power. Blue = low absolute; red = high absolute power. Grey background = blind quadrants

SIGHTED VISUAL QUADRANTS:

Upper left quadrant (UL): weak activation over parietal and central electrodes bilaterally distributed but mainly in the intact right hemisphere, contralateral to visual stimulation.

Lower left quadrant (LL): widespread strong activation over occipital-parietal and central electrodes mainly in the intact right hemisphere, contralateral to visual stimulation.

BLIND VISUAL QUADRANT:

Upper right quadrant (UR): weak activation over frontal electrodes, bilaterally distributed and over posterior electrodes in the left hemisphere.

Lower right quadrant (LR): weak activation over left fronto-temporal electrodes mainly in the damaged left hemisphere.

Considering both quadrants, we observed a weak activation over posterior, frontal and temporal electrodes, in the left hemisphere.

In conclusion, in the frequency domain we could observe a weak activation over posterior electrodes stimulating the blind hemifield; in the time domain, we observed a posterior bilateral activation mainly stimulating the lower right quadrant, during the first and the last phase ranges (0°-40° and 320°-360°).

3. DIFFERENCE OVER POSTERIOR ELECTRODES comparing ABSOLUTE POWER of the BLIND UPPER RIGHT QUADRANT in healthy participants and patient (Fig. 73).

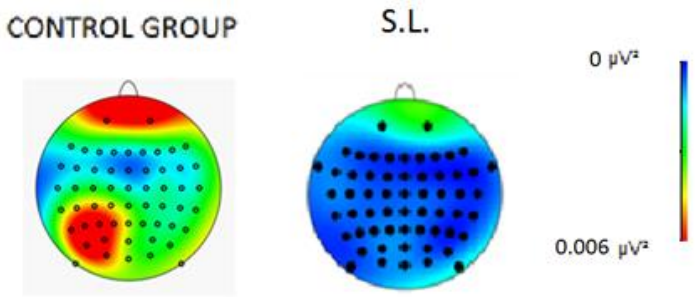

Fig.73. Topographic maps of control group and S.L. while stimulating the upper blind visual quadrant. Blue =low absolute power of activation; red = high absolute power of activation.

Absolute power of activation at 12z at posterior electrodes (Graph. 18)

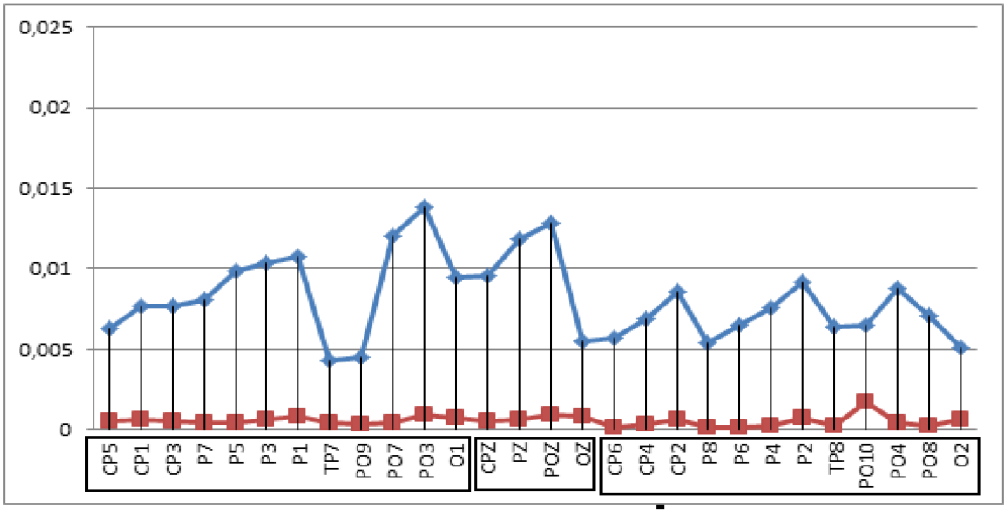

Graph. 18. Absolute power of activation at 12Hz. Blue line = healthy participants; red line = S.L.

We observed a difference mainly over parietal-occipital electrodes along the vertical midline and within the damaged left hemisphere, contralateral to visual stimulation. In this case S.L. absolute power was below the group mean mainly within the damaged hemisphere.

DIFFERENCE OVER POSTERIOR ELECTRODES comparing ABSOLUTE POWER of the BLIND LOWER RIGHT QUADRANT in healthy participants and patient (Fig. 74).

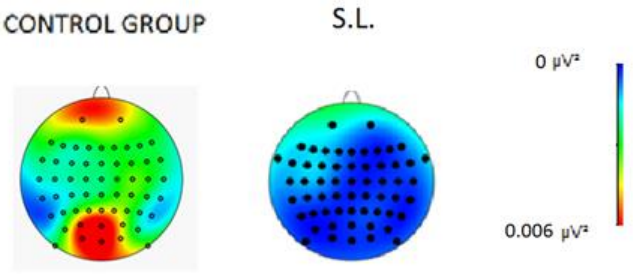

Fig.74. Topographic maps of control group and S.L. while stimulating the lower blind visual quadrant. Blue =low absolute power of activation; red = high absolute power of activation.

Absolute power of activation at 12z at posterior electrodes (Graph. 19)

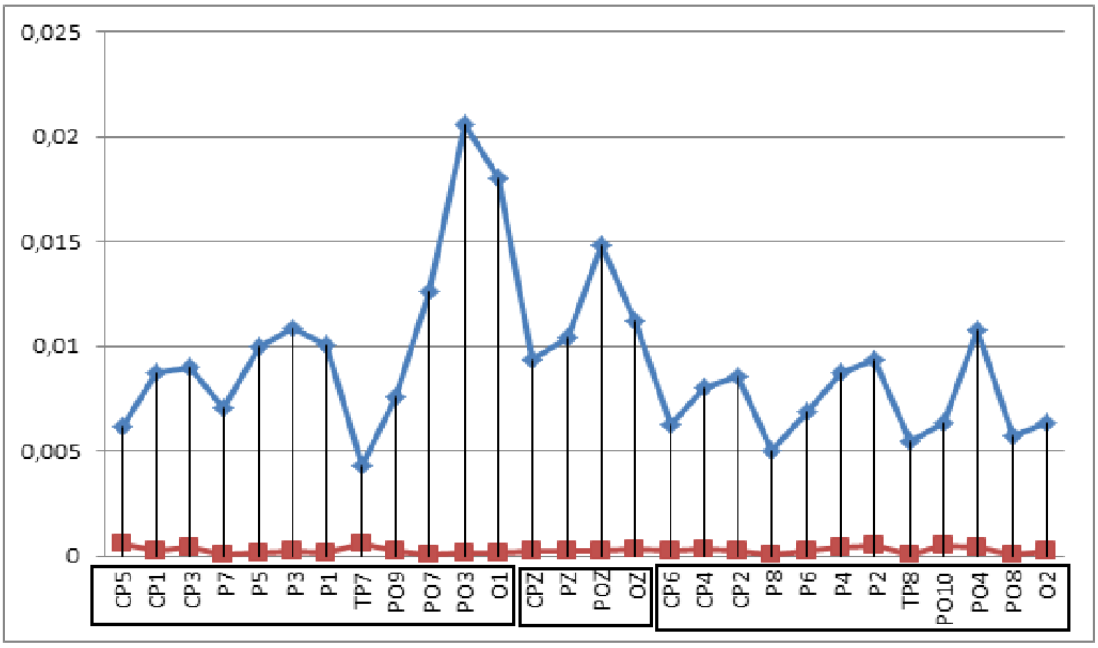

Graph. 19. Absolute power of activation at 12Hz. Blue line = healthy participants; red line = S.L.

We observed a difference mainly located over occipital parietal electrodes in the damaged left hemisphere and along the vertical midline. The difference indicated a lower absolute power in S.L.

CONCLUSION:

In summary, in patient S.L. with a lesion involving the medial part of the left occipital lobe, causing a right lateral homonymous hemianopia, we found a modulation of response mainly in the time domain in the damaged hemisphere following stimulus presentation to the blind hemifield. This modulation was mainly located over frontal and central electrodes stimulating the upper blind quadrant; instead it was involving the whole contralateral hemisphere stimulating the lower blind quadrant. Concerning the frequency domain, we observed a weak activation over frontal, temporal and posterior electrodes.

As far as the intact hemifield is concerned we found that in the frequency domain the absolute power was lower than in healthy participants stimulating the upper sighted quadrant; instead it was higher over electrodes CP4, CP2, P6, P4, P2, PO4, PO8 and 02 stimulating the lower sighted quadrant.

L.F.:
Lesion involving a small portion of the primary visual cortex, along the calcarine fissure

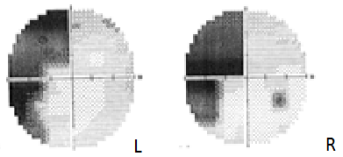

In patient LF, we located the stimuli 12° from the center of the screen on the x axis and 6° from the center on the y axis.

TIME DOMAIN:

1. Amplitude of Waveforms

The amplitude of SSVEP waveforms to pattern reversal stimuli elicited at selected electrode sites are shown in Fig.75.

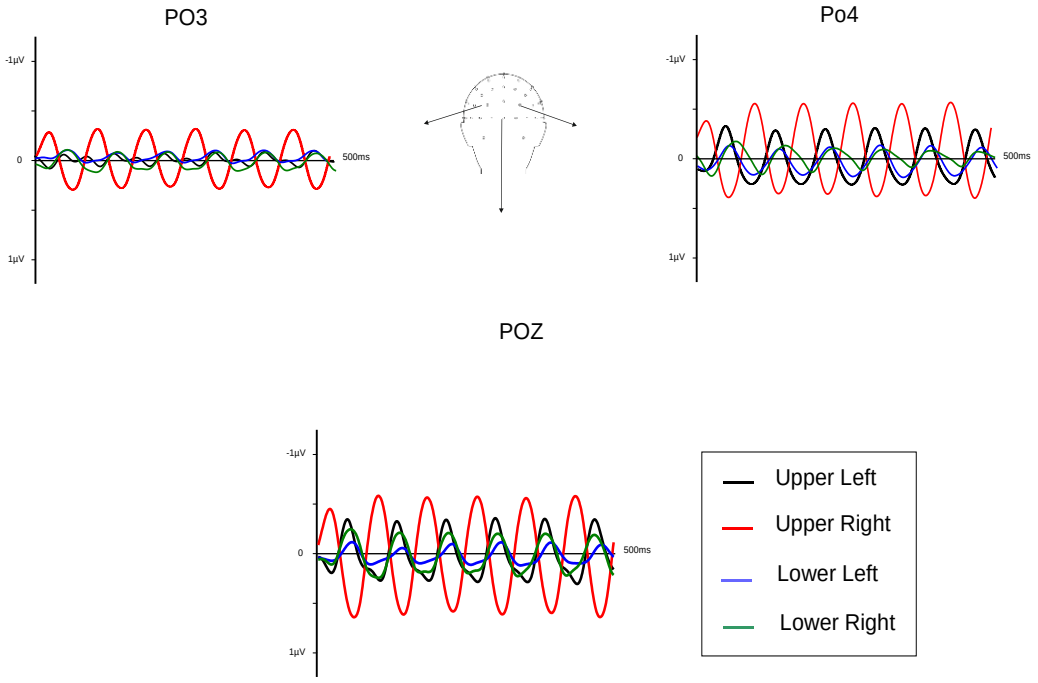

Fig. 75. SSVEP waveforms elicited at electrodes PO3, POz and PO4.

In all electrodes, there was a difference in phase between upper right and both lower visual quadrants; importantly, in contrast to healthy participants, we found a difference in phase between upper right and left (blind) visual quadrants.

Upper right vs. upper left: the amplitude was always greater stimulating the right than the left visual quadrant regardless of the location of electrodes. This result is in line with the fact that the upper left quadrant is the blind one.

Lower right vs. lower left: the amplitude was similar stimulating both quadrants at lateral sites while it was greater stimulating the lower right quadrant at the midline site.

Those results suggested that the stimulation in the blind quadrant could determine a synchronization to the specific frequency even in the damaged hemisphere

(electrode PO4) similar compared with the synchronization produced by stimulating sighted quadrants, even if lower in amplitude.

2. Topography of phase range

The scalp topography of SSVEP varied systematically as a function of response phase, which indicated that more than one generator was contributing to the response. In the following figure (76) the sequential changes in topography in response to visual stimulation in time in each single quadrant are shown.

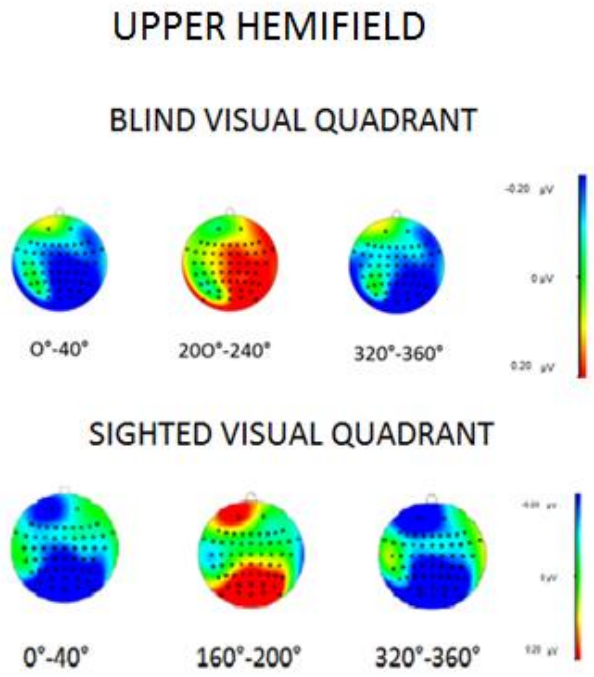

Fig.76. Topographic maps of a phase range.
Blue = negative amplitude; red = positive amplitude.

Blind visual quadrant:

- First phase range: negative widespread focus over central-parietal-occipital electrodes mainly within the damaged right contralateral hemisphere;
- Second phase range: positive widespread focus over central-parietal-occipital electrodes mainly within the damaged right contralateral hemisphere;

- Last phase range: negative widespread focus over central-parietal-occipital electrodes mainly within the damaged right contralateral hemisphere (same topography as in the first phase range).

Sighted visual quadrant:

- First phase range: unitary negative focus over parietal-central-occipital electrodes bilaterally distributed and over frontal electrodes within the intact left hemisphere;
- Second phase range: unitary positive focus over parietal-central-occipital electrodes bilaterally distributed and over frontal electrodes within the intact left hemisphere;
- Last phase range: unitary negative focus over parietal-central-occipital electrodes bilaterally distributed and over frontal electrodes within the intact left hemisphere.

In conclusion, the activation in the time domain confirmed that more than one generator was contributing to the response when stimulating the upper hemifield, letting possible to define this perceptual process as a dynamic mechanism. Considering the blind quadrant, the visual information determined a widespread activation involving a contralateral dynamic mechanism composed by anterior as well as posterior structures during the perceptual process.

Considering the sighted quadrant, those results suggested that the visual information determined an activation over frontal and posterior electrodes in the contralateral hemisphere; the communication of visual information with the posterior area in the left hemisphere determined the involvement of a bilateral dynamic mechanism composed by frontal and posterior structures during the perceptual process.

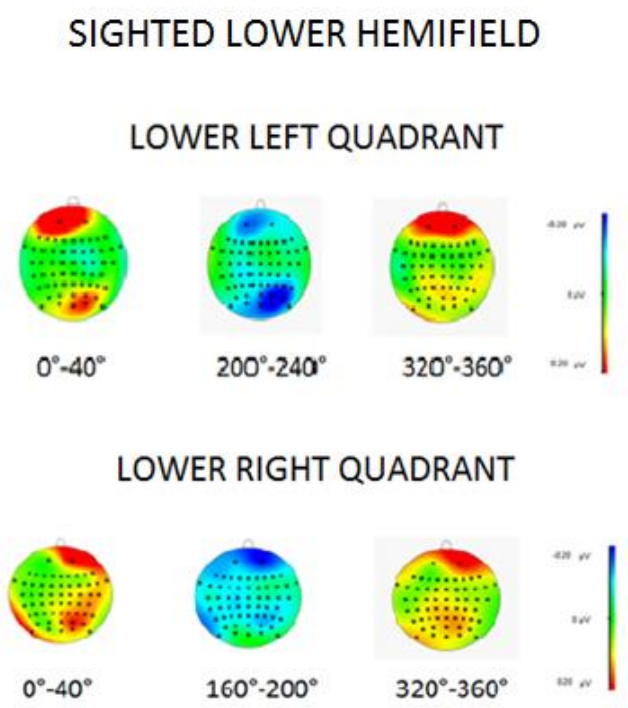

Fig.77. Topographic maps of a phase range.
Blue = negative amplitude; red = positive amplitude.

Lower left visual quadrant:

- First phase range: positive focus over occipital-parietal electrodes, mainly in the damaged right contralateral hemisphere and over frontal electrodes in the ipsilateral left hemisphere;
- Second phase range: negative focus over occipital-parietal electrodes, mainly in the damaged right contralateral hemisphere and over frontal electrodes in the ipsilateral left hemisphere;
- Last phase range: weak positive focus over occipital-parietal electrodes mostly in the right hemisphere and a strong positive focus bilaterally distributed over frontal electrodes.

Sighted visual quadrant:

- First phase range: unitary positive focus over parietal, occipital, central- and frontal electrodes mainly in the damaged right hemisphere, ipsilateral to visual stimulation;

- Second phase range: negative focus over parietal-central-occipital and frontal electrodes mainly in the left hemisphere;
- Last phase range: positive focus involving mostly occipital-parietal and frontal electrodes bilaterally.

In conclusion, the activation in the time domain confirmed that more than one generator was contributing to the response when stimulating the lower hemifield; those generators appeared to be mainly bilaterally distributed involving frontal, central and posterior electrodes.

FREQUENCY DOMAIN:

1. Bootstrap Analysis to compare real and simulated stimulation frequency (graph. 20).

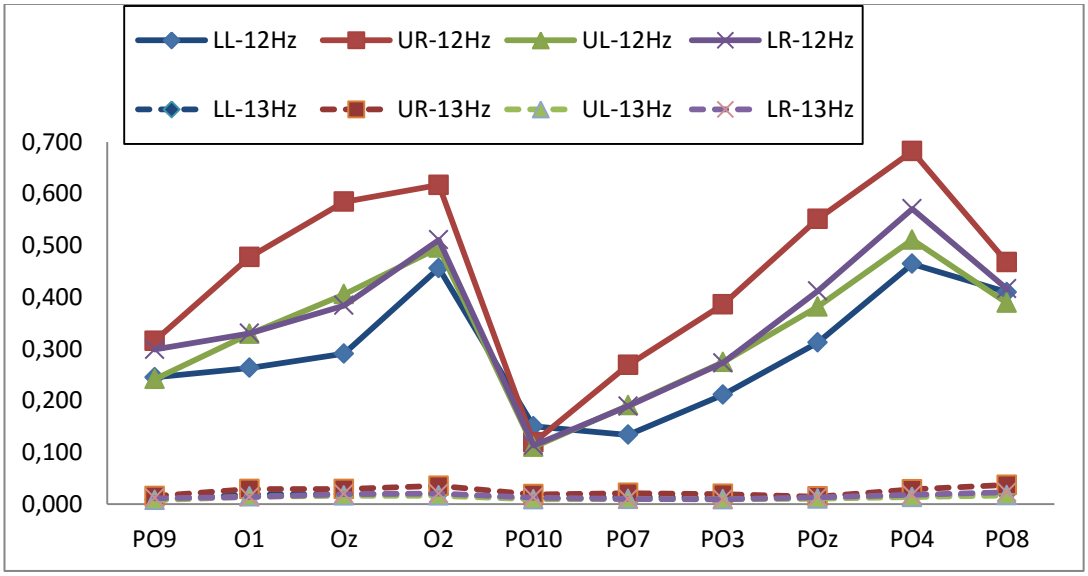

Graph. 20. Absolute power of activation at posterior electrodes comparing 12Hz (real frequency of visual stimulation; continuous line) and 13 Hz (simulated frequency; dotted line).

With the Bootstrap analysis for all electrodes we found a significant difference in absolute power between 12Hz and 13Hz thus demonstrating that the response modulation was related to the specific frequency of visual stimulation.

2. Topographic distribution of Absolute Power, at the second harmonic of 12Hz (Fig. 78)

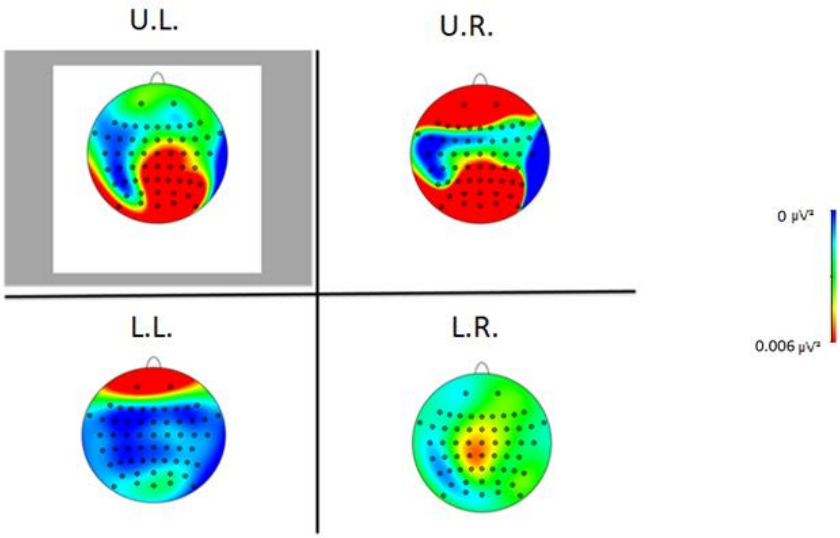

Fig.78. Topographic maps of absolute power. Blue = low absolute power; Red = high absolute power. Grey background = blind quadrant

SIGHTED VISUAL QUADRANTS:

Upper right quadrant (UR): strong activation over occipital-parietal and central electrodes bilaterally distributed.

Lower right quadrant (LR): weak activation over central electrodes bilaterally distributed.

Lower left quadrant (LR): weak activation over occipital-parietal electrodes bilaterally distributed but mostly within the damaged right hemisphere, contralateral to the visual stimulation.

BLIND VISUAL QUADRANT:

Upper left quadrant (UL): strong activation mainly over occipital-parietal right electrodes, contralateral to the visual stimulation and within the damaged hemisphere.

In conclusion these results confirmed those found in the time domain: the activation was mainly located within the contralateral hemisphere while

stimulating the blind left quadrant and was bilaterally distributed when stimulating the sighted visual hemifield.

3. DIFFERENCE OVER POSTERIOR ELECTRODES comparing ABSOLUTE POWER of the BLIND QUADRANT in healthy participants and patient (Fig. 79).

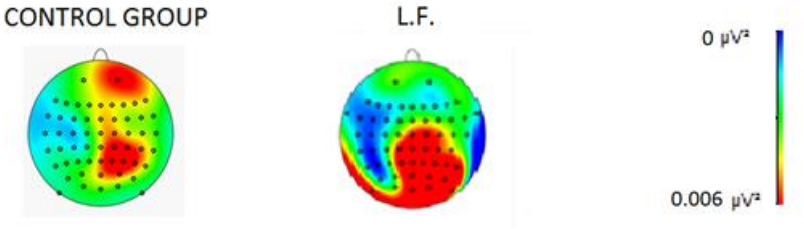

Fig.79. Topographic maps of the control group and L.F while stimulating the blind visual quadrant Blue = low absolute power of activation; red = high absolute power of activation.

Absolute power of activation at 12hz at posterior electrodes (Graph. 21)

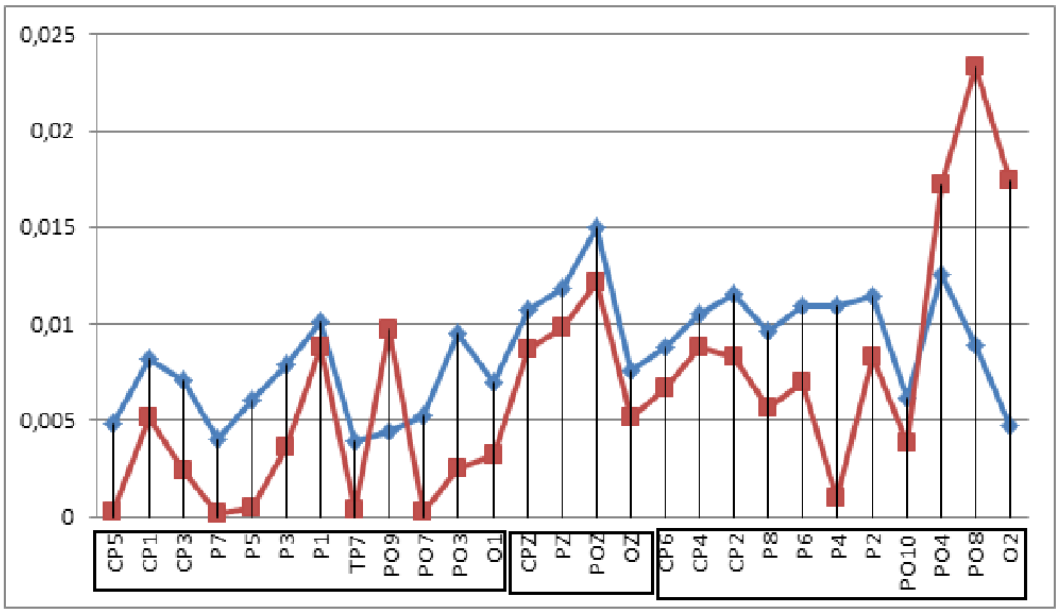

Graph. 21. Absolute power of activation at 12Hz. Blue line = healthy participants; red line = L.F.

There was a strong difference over occipital-parietal electrodes mainly in the damaged **right hemisphere**, contralateral to visual stimulation, indicating a

higher activation in L.F. than in control participants over electrodes PO4, PO8, O2 and PO9.

CONCLUSION:

In summary, in patient L.F. with a lesion involving a small portion of the right primary visual cortex, along the calcarine fissure, causing a upper left quadrantanopia, we found a modulation of response in both time and frequency domain in the damaged hemisphere following stimulus presentation to the blind upper left quadrant. Importantly, the affected left upper quadrant yielded an increased power of activation with respect to the control group.

As far as the intact hemifield is concerned we found that in the frequency domain the absolute power was lower than in healthy participants in the lower hemifield while was higher in the upper right quadrant.

F.B.

Lesion involving the right temporal-parietal-occipital cortex

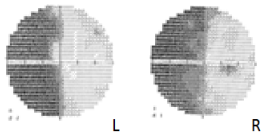

In this experiment, we located stimuli 14° from the center of the screen on the x axis and 6° from the center on the y axis.

TIME DOMAIN:

1. Amplitude of Waveforms

The amplitude of SSVEP waveforms in response to pattern reversal stimuli elicited at selected electrode sites are shown in fig. 80.

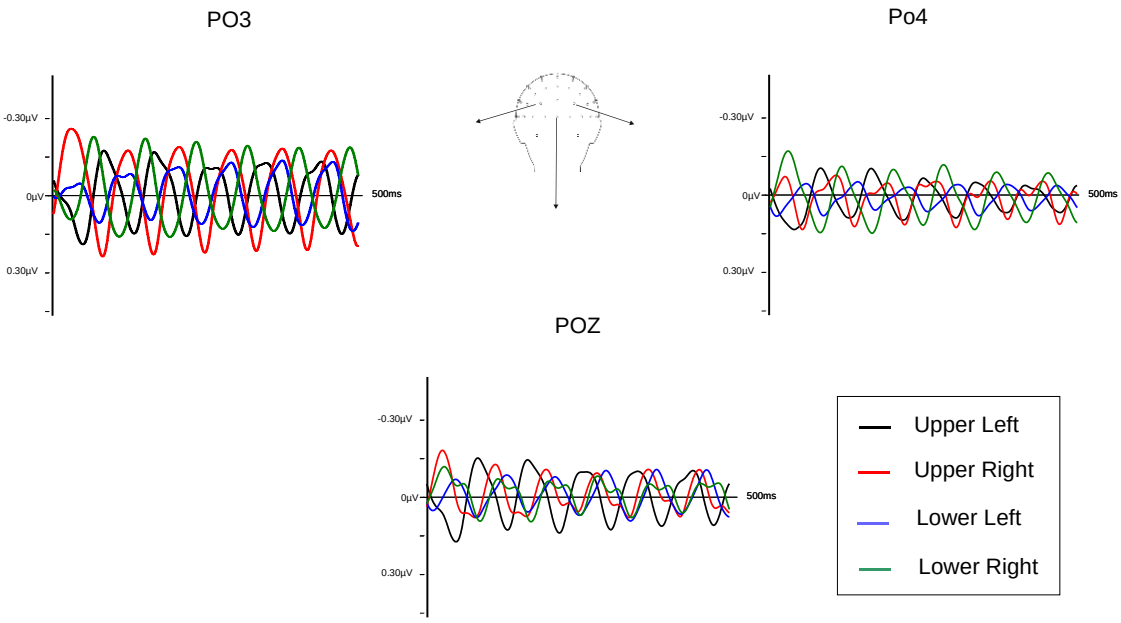

Fig. 80. SSVEP waveforms elicited at electrodes PO3, POz and PO4.

In all electrodes the signal appeared noisy while stimulating the right visual hemifield, mainly the upper one. Thus, mainly in all electrodes considered, each phase appeared to be composed by two waves instead of one, stimulating the upper right visual quadrant.

Upper right vs. upper left: amplitude was always greater over the electrode contralateral to the visual stimulation (upper right = PO3; upper left = PO4); instead it was similar over the midline site (POz).

Lower right vs. lower left: the amplitude was greater stimulating the lower right quadrant at both lateral sites; it was similar over the midline site (POz).

Those results suggested that the stimulation in the blind quadrant could determine a synchronization of cortical activity to the specific frequency even in the damaged hemisphere, similar compared with the synchronization produced by stimulating the sighted quadrants. Interesting, we observed that over right

electrode PO4 the amplitude in upper left condition was higher than in upper right demonstrating that the amplitude was greater stimulating the contralateral quadrant even if the stimulus could not be consciously perceived.

2. Topography of phase range

The scalp topography of SSVEP varied systematically as a function of response phase, which indicates that more than one generator contributed to the response. Figure 81 shows the sequential changes in topography in response to visual stimulation in time, within each quadrant.

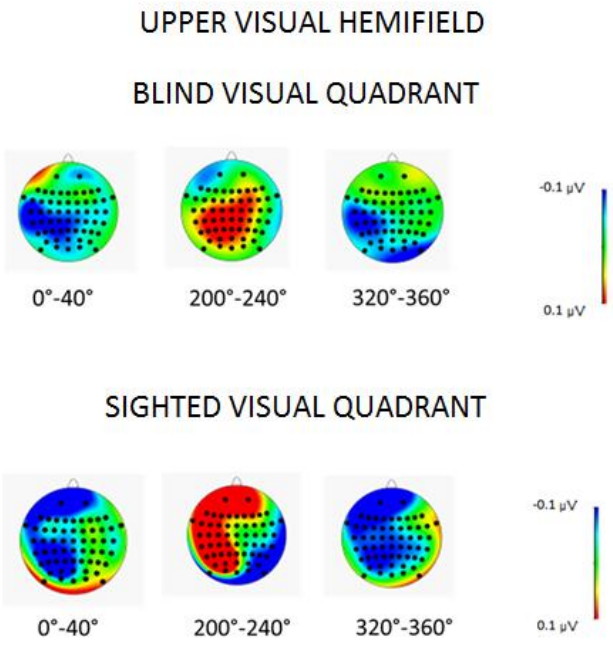

Fig.81. Topographic maps of a phase range.
Blue = negative amplitude; red = positive amplitude.

Blind visual quadrant:

- First phase range: unitary negative focus over occipital-parietal and central electrodes in the intact left hemisphere, ipsilateral to visual stimulation;
- Second phase range: unitary positive focus over occipital-parietal and central electrodes within the intact left hemisphere, ipsilateral to visual stimulation;

- Last phase range: negative focus over central-parietal electrodes within the left hemisphere and over occipital electrodes in the right.
-

Sighted visual quadrant:

- First phase range: negative focus over parietal-occipital and frontal electrodes mainly within the intact left hemisphere, contralateral to visual stimulation;
- Second phase range: positive focus over parietal-occipital and frontal electrodes mainly in the intact left hemisphere, contralateral to visual stimulation;
- Last phase range: negative widespread focus involving almost the whole left hemisphere.

In conclusion the activation in the time domain confirmed that more than one generator was contributing to the waveform when stimulating the upper hemifield; those generators appeared to be mostly located in the intact left hemisphere.

Considering the blind quadrant the activation was mainly located over frontal and central electrodes in the contralateral hemisphere; the communication of visual information with posterior areas in the left hemisphere determined the involvement of a bilateral dynamic mechanism composed by anterior as well as posterior structures during the perceptual process;

Considering the sighted quadrant the activation was located over frontal, temporal and posterior electrodes in the contralateral hemisphere; the communication of visual information with different areas in the right hemisphere determined the involvement of a bilateral dynamic mechanism composed by anterior as well as posterior structures during the perceptual process.

Considering both quadrants, the intact left hemisphere was more activated by both stimulation as a consequence of the lesion involving the right hemisphere.

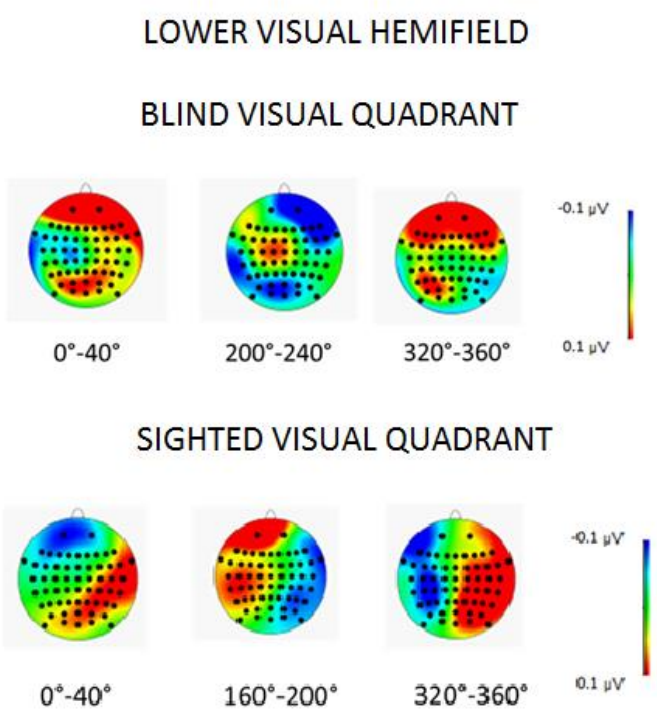

Fig. 82. Topographic maps of a phase range.
Blue = negative amplitude; red = positive amplitude.

Blind visual quadrant:

- First phase range: strong positive focus over occipital-parietal and frontal electrodes bilaterally distributed; negative focus over central electrodes in the intact left hemisphere;
- Second phase range: negative focus over posterior and temporal electrodes in the left hemisphere and over frontal electrodes in the right one; positive focus over central electrodes bilaterally distributed;
- Last phase range: strong positive focus over posterior electrodes in the intact left hemisphere and over bilateral frontal electrodes.

Sighted visual quadrant:

- First phase range: positive focus of activation over central-parietal and occipital electrodes in the damaged right hemisphere; unitary negative focus over frontal electrodes mainly in the intact left hemisphere;

- Second phase range: unitary positive focus over frontal and temporal electrodes in the left hemisphere; negative focus over posterior and temporal electrodes in the damaged right hemisphere.
- Last phase range: strong positive focus over frontal electrodes bilaterally distributed and over parietal-occipital electrodes in the left hemisphere.

In conclusion the activation in the time domain confirmed that more than one generator was contributing to the waveform when stimulating the lower hemifield; those generators appeared to be mostly bilaterally distributed considering the sighted quadrant and ipsilateral considering the blind one.

Considering the blind quadrant we observed the involvement of a bilateral dynamic mechanism composed by anterior as well as posterior structures during the perceptual process.

Considering the sighted quadrant the activation was mainly located over posterior electrodes in the contralateral hemisphere; the communication of visual information with frontal, central and posterior electrodes in the right hemisphere determined the involvement of a bilateral dynamic mechanism composed by anterior as well as posterior structures during the perceptual process.

FREQUENCY DOMAIN:

1. Bootstrap Analysis to compare real and simulated frequency (Graph. 22).

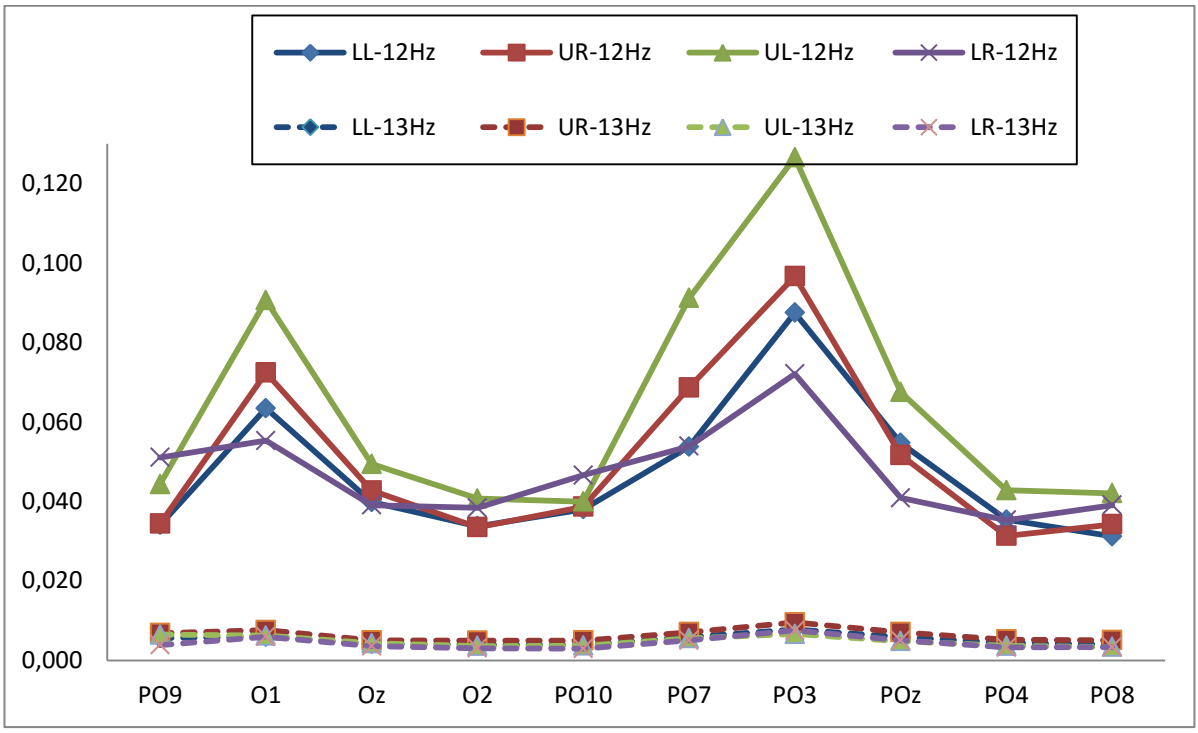

Graph. 22. Absolute power of activation at posterior electrodes comparing 12Hz (real frequency of visual stimulation; linear line) and 13 Hz (simulated frequency; dotted line).

With the Bootstrap analysis we found a significant difference in absolute power between the two frequencies at all electrodes, see graph. 22 for posterior electrodes. This demonstrates that the SSVEP response was related to the specific frequency of visual stimulation.

2. Topographic distribution of Absolute Power, at the second harmonic of 12Hz (fig. 83)

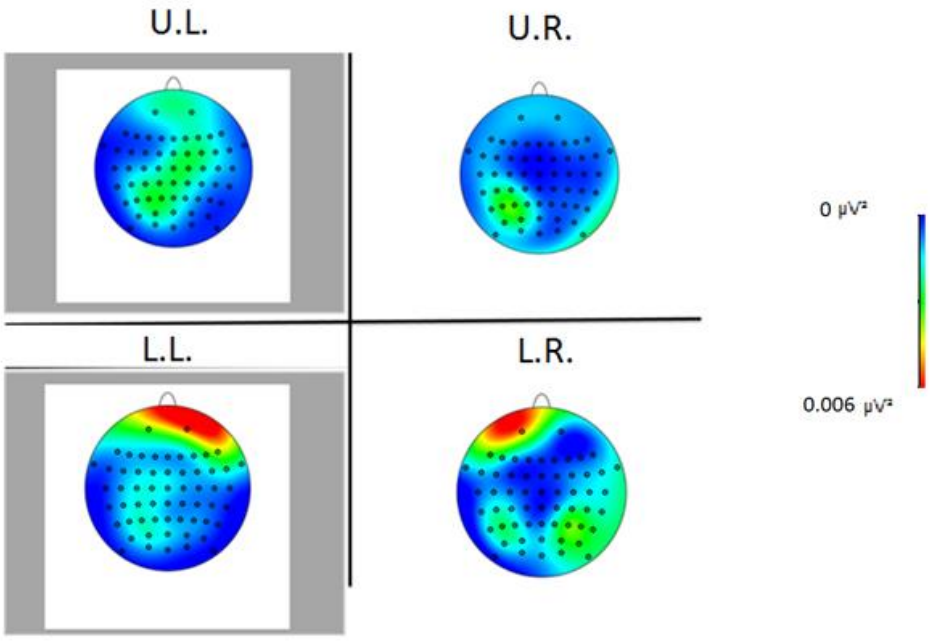

Fig. 83. Topographic maps of absolute power. Blue = low power; red= high absolute power. Grey background = blind quadrants

SIGHTED VISUAL QUADRANTS:

Upper right quadrant (UR): weak activation over occipital-parietal electrodes in the intact left hemisphere, contralateral to visual stimulation.

Lower right quadrant (LR): weak bilateral activation involving occipital-parietal electrodes within both hemispheres and strong activation over frontal electrodes in the left hemisphere.

BLIND VISUAL QUADRANTS:

Upper left quadrant (UL): weak activation over parietal and central electrodes mostly in the ipsilateral hemisphere.

Lower left quadrant (LL): weak activation over parietal and occipital electrodes in the left hemisphere and a strong activation over the frontal right scalp.

In conclusion these results broadly confirmed those found in the time domain: the activation was mainly located within the ipsilateral hemisphere stimulating the blind hemifield, involving mainly frontal, central and posterior electrodes; instead

it was mainly located over contralateral or bilateral frontal, central and posterior electrodes stimulating the sighted hemifield.

3. DIFFERENCE OVER POSTERIOR ELECTRODES comparing ABSOLUTE POWER of the BLIND UPPER QUADRANT in healthy participants and patient (Fig. 84).

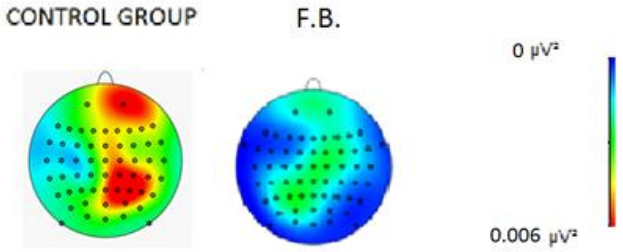

Fig.84. Topographic maps of control group and F.B. while stimulating the upper blind visual quadrant. Blue =low absolute power of activation; red = high absolute power of activation.

Absolute power of activation at 12z at posterior electrodes (Graph. 23)

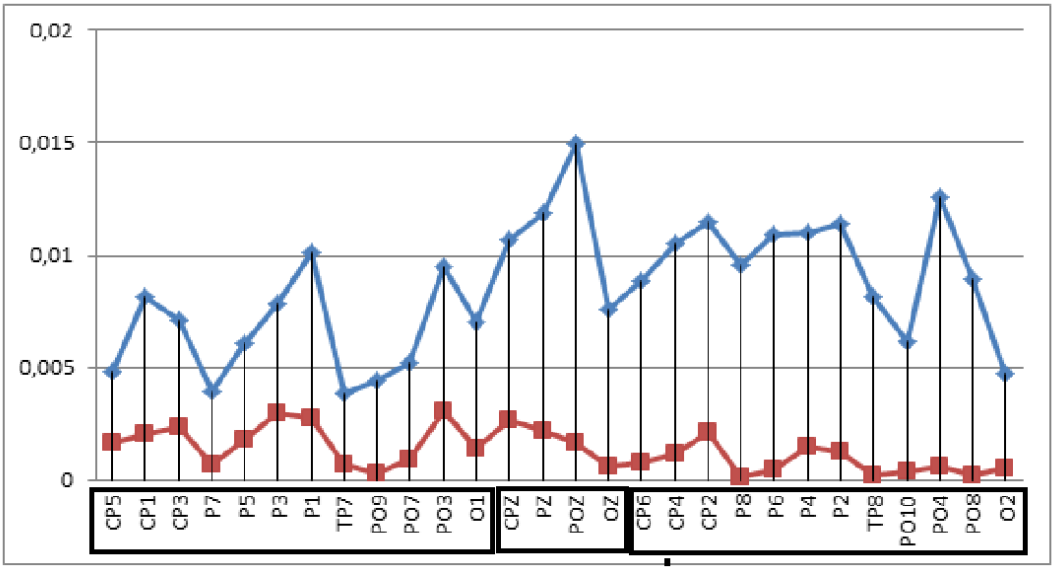

Graph. 23. Absolute power of activation at 12Hz. Blue line = healthy participants; red line = F.B.

The largest difference was located over occipital-parietal electrodes in the damaged **right hemisphere**, contralateral to visual stimulation and along the vertical midline. The difference observed indicated that the absolute power of F.B.

was below the group mean. However, one should note the presence of a modulation in the absolute power produced by a visual stimulation not consciously perceived.

DIFFERENCE OVER POSTERIOR ELECTRODES
comparing ABSOLUTE POWER of the BLIND LOWER QUADRANT
in healthy participants and patient (Fig. 85).

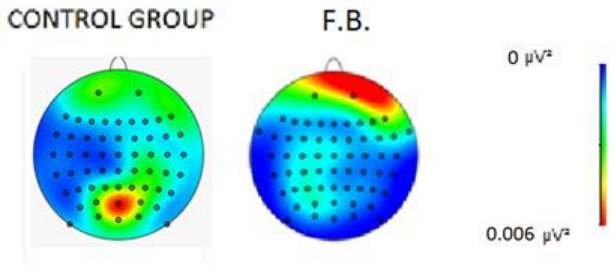

Fig.85- Topographic maps of control group and F.B. while stimulating the lower blind visual quadrant. Blue =low absolute power of activation; red = high absolute power of activation.

Absolute power of activation at 12z at posterior electrodes (Graph. 24)

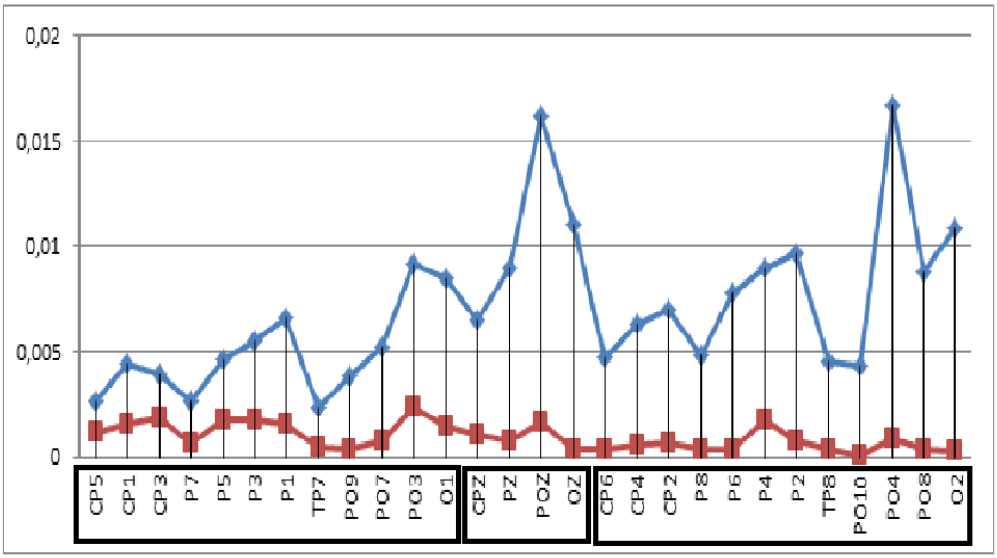

Graph. 24. Absolute power of activation at 12Hz. Blue line = healthy participants; red line = F.B.

The difference was mainly located over occipital-parietal electrodes in the damaged **right hemisphere**, contralateral to visual stimulation and along the vertical midline. Also in this case, the difference observed indicated that the

absolute power of F.B. was below the group mean but it is noteworthy the presence of a modulation produced by a visual stimulation not consciously perceived.

CONCLUSION:

In summary, in patient F.B. with a widespread lesion involving the right temporo-parietal and occipital lobe, causing a left lateral homonymous hemianopia, we found a modulation of response mainly in both time and frequency domain in both hemispheres but mainly over frontal, central and posterior electrodes in the ipsilateral intact left hemisphere, following stimulus presentation to the blind hemifield.

As far as the intact hemifield is concerned we found that in the frequency domain the absolute power was lower than in healthy participants stimulating both quadrants but it maintained the same topography.

L.C.

Lesion involving the

right parietal-temporal-occipital lobe

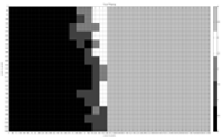

BINOCULAR

In this experiment, we located the stimuli 14° from the center of the screen on the x axis and 6° from the center considering the y axis.

TIME DOMAIN:

1. Amplitude of Waveforms

The amplitude of SSVEP waveforms to pattern reversal stimuli elicited at selected electrode sites by visual stimuli are shown in fig. 86.

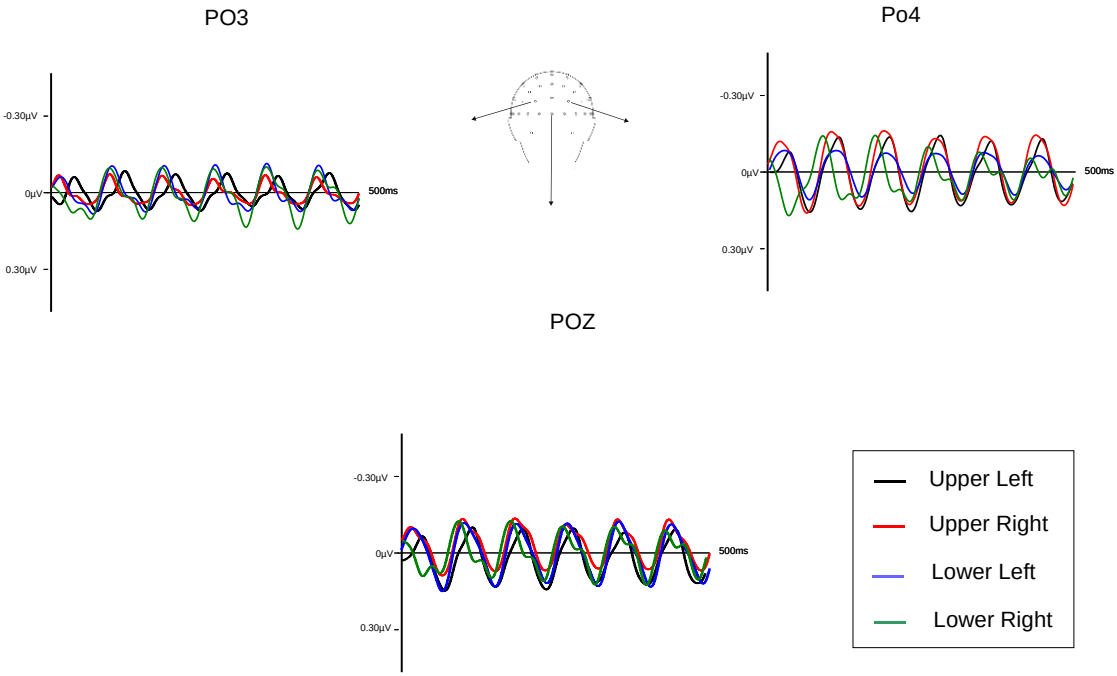

Fig. 86. SSVEP waveforms elicited at electrodes PO3, POz and PO4.

In all electrodes we could not observe the difference in phase comparing upper and lower visual quadrants, being all waveforms perfectly overlapped.

Upper right vs. upper left: over electrodes PO3 and POz the amplitude was similar; instead it was greater for upper right over the ipsilateral electrode PO4.

Lower right vs. lower left: the amplitude was similar stimulating both quadrants.

Those results suggested that the stimulation in the blind quadrant could determine a synchronization of cortical activity to the specific frequency even in the damaged hemisphere, similar compared with the synchronization produced by stimulating the sighted quadrants.

2. Topography of phase range

The scalp topography of SSVEP varied systematically as a function of response phase, which indicated that more than a generator was contributing to the waveform. In the following figure (87) the sequential changes in topography in response to visual stimulation in time are shown.

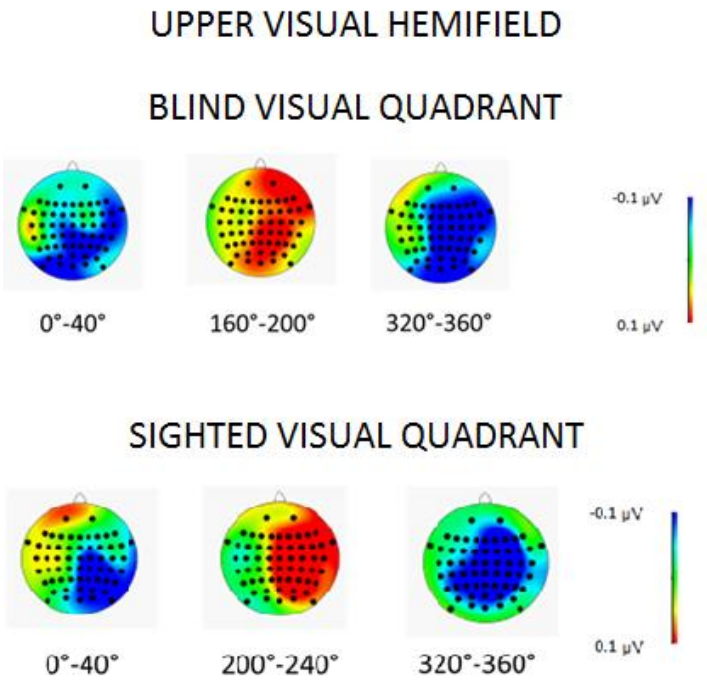

Fig.87. Topographic maps of a phase range.
Blue = negative amplitude; red = positive amplitude.

Blind visual quadrant:

- First phase range: unitary focus of negative activation over occipital-parietal electrodes bilaterally distributed and over temporo-frontal electrodes in the damaged **right hemisphere**, contralateral to visual stimulation; focus of positive activation over temporal electrodes in the intact left hemisphere;
- Second phase range: widespread positive focus of activation involving almost the whole right hemisphere;
- Last phase range: widespread negative focus of activation involving almost the whole right hemisphere.

Sighted visual quadrant:

- First phase range: negative focus over parietal-occipital electrodes within the damaged right hemisphere, ipsilateral to visual stimulation, and a weaker positive focus over frontal electrodes within the intact left hemisphere;

- Second phase range: widespread positive focus of activation involving almost the whole right hemisphere;
- Last phase range: negative widespread focus involving frontal, central and posterior electrodes bilaterally distributed.

In conclusion the activation in the time domain confirmed that more than one generator was contributing to the waveform when stimulating the upper hemifield; those generators appeared to be mostly located in the damaged right hemisphere.
Considering the blind quadrant the activation was mainly located over frontal, central and posterior electrodes in the contralateral hemisphere; the communication of visual information with frontal, central and posterior areas in the left hemisphere determined the involvement of a bilateral dynamic mechanism composed by anterior as well as posterior structures during the perceptual process;
Considering the sighted quadrant the activation was mainly located over frontal electrodes in the contralateral hemisphere; the communication of visual information with frontal, central and posterior electrodes in the right hemisphere determined the involvement of a bilateral dynamic mechanism composed by anterior as well as posterior structures during the perceptual process.

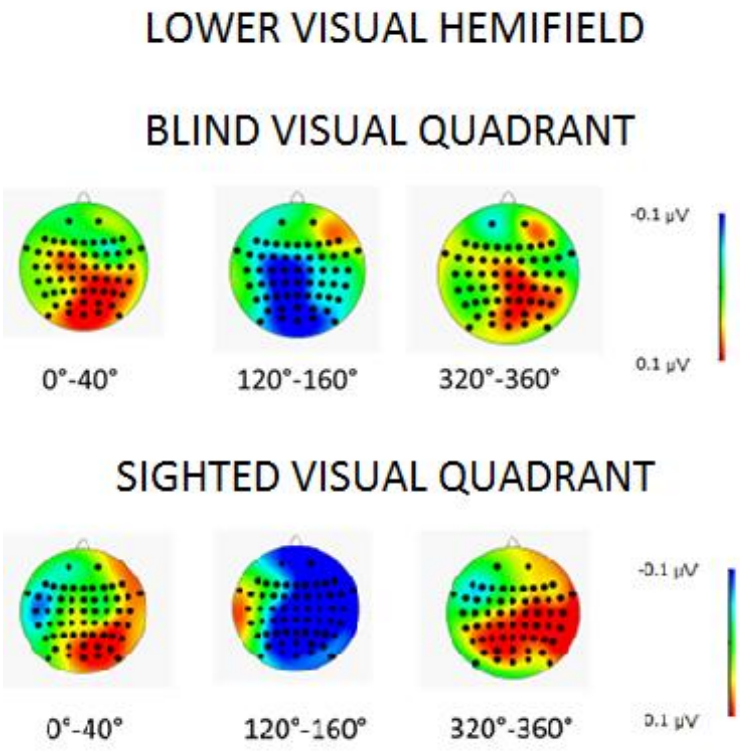

Fig.88. Topographic maps of a phase range.
Blue = negative amplitude; red = positive amplitude.

Blind visual quadrant:

- First phase range: strong positive focus over occipital-parietal electrodes mainly in the damaged right hemisphere;
- Second phase range: strong negative focus of activation over central and posterior electrodes bilaterally distributed;
- Last phase range: positive focus over central and posterior electrodes in the right damaged hemisphere.

Sighted visual quadrant:

- First phase range: positive focus of activation over occipital-parietal and fronto-temporal electrodes in the damaged **right hemisphere**; weak negative focus over fronto-temporal electrodes mainly in the intact left hemisphere;

- Second phase range: widespread negative focus of activation involving the whole right hemisphere and the portion of the left hemisphere closer to the vertical midline;
- Last phase range: strong positive focus of activation over central and posterior electrodes bilaterally distributed.

In conclusion the activation in the time domain confirmed that more than one generator was contributing to the waveform when stimulating the lower hemifield; those generators appeared to be mostly located in the damaged right hemisphere.
Considering the blind quadrant the activation was mainly located over central and posterior electrodes in the contralateral hemisphere; the communication of visual information with central and posterior areas in the left hemisphere determined the involvement of a bilateral dynamic mechanism composed by anterior as well as posterior structures during the perceptual process;
Considering the sighted quadrant the activation was mainly located over temporal electrodes in the contralateral hemisphere; the communication of visual information with frontal, central and posterior electrodes in the right hemisphere determined the involvement of a bilateral dynamic mechanism composed by anterior as well as posterior structures during the perceptual process. Surprisingly, considering all quadrants, the damaged right hemisphere was more activated by both visual stimulations.

FREQUENCY DOMAIN:

1. Bootstrap Analysis to compare real and simulated frequency (Graph. 25).

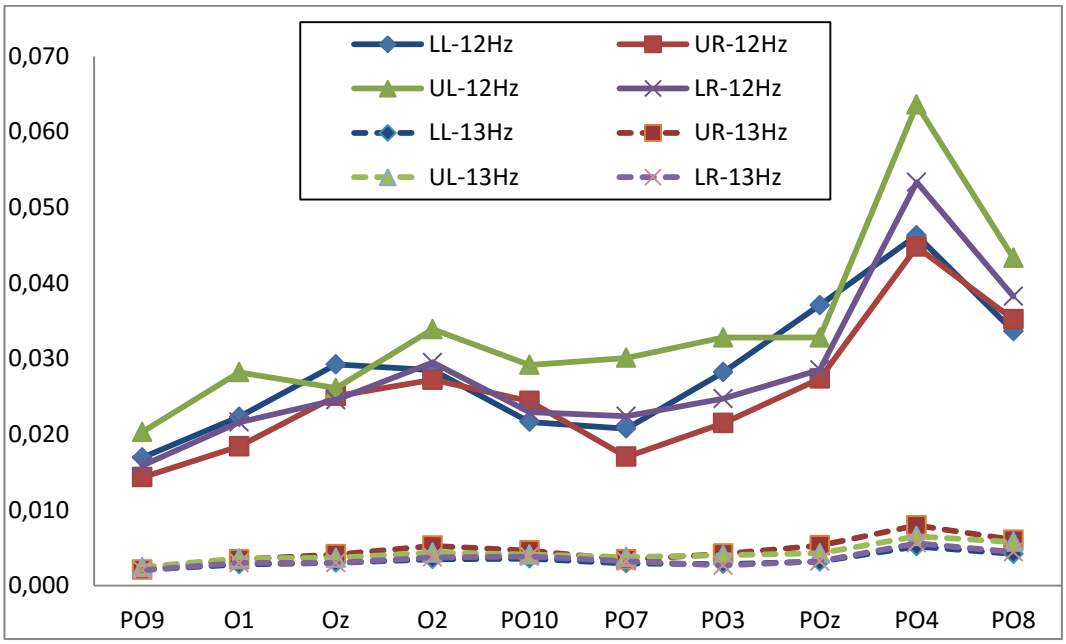

Graph.25. Absolute power of activation at posterior electrodes comparing 12Hz (real frequency of visual stimulation; linear line) and 13 Hz (fake frequency; dotted line).

With the Bootstrap analysis we found a significant difference in absolute power between the two frequencies at all electrodes, see graph. 25 for posterior electrodes. This demonstrates that the SSVEP response was related to the specific frequency of visual stimulation.

2. Topographic distribution of Absolute Power, at the second harmonic of 12Hz (Fig. 89).

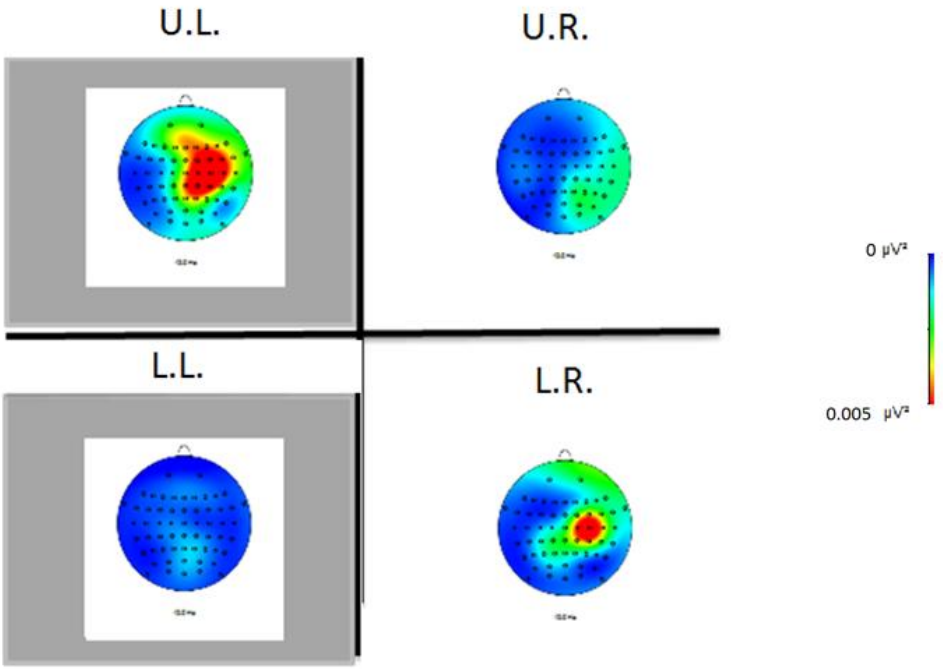

Fig. 89. Topographic maps of absolute power. Blue = low absolute; red = high absolute power. Grey background = blind quadrants

SIGHTED VISUAL QUADRANTS:

Upper right quadrant (UR): weak activation over central, occipital and parietal electrodes in the damaged right hemisphere, ipsilateral to visual stimulation.

Lower Right quadrant (LR): strong activation over frontal, central and parietal electrodes mainly in the damaged right hemisphere.

BLIND VISUAL QUADRANTS:

Upper left quadrant (UL): strong activation over parietal-central and frontal electrodes in the damaged right hemisphere.

Lower Left quadrant (LL): weak activation over occipital electrodes bilaterally distributed but mainly in the right damaged hemisphere.

In conclusion these results broadly confirmed those found in the time domain: the activation was mainly located in the damaged right hemisphere, regardless of the side of visual stimulation.

3. DIFFERENCE OVER POSTERIOR ELECTRODES comparing ABSOLUTE POWER of the BLIND UPPER QUADRANT in healthy participants and patient.

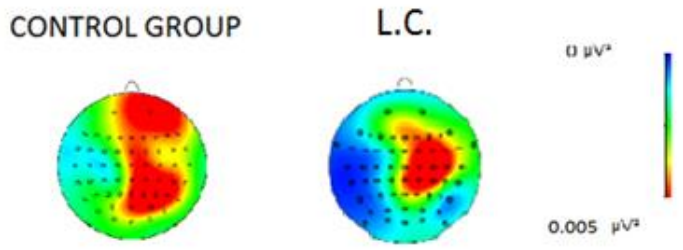

Fig.90. Topographic maps of control group and L.C. while stimulating the upper blind visual quadrant. Blue =low absolute power of activation; red = high absolute power of activation.

Absolute power of activation at 12z at posterior electrodes (Graph. 26)

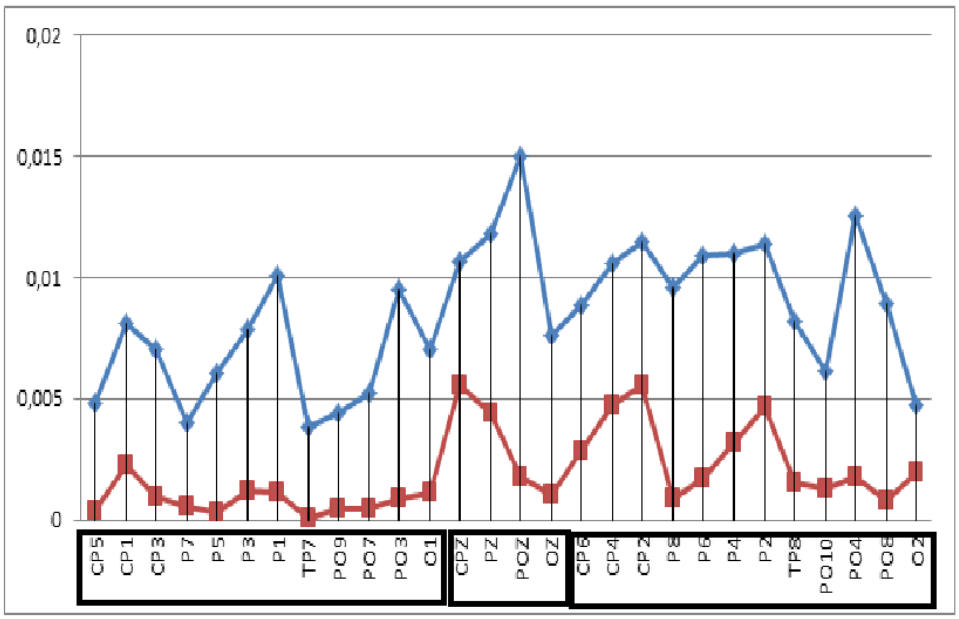

Graph. 26. Absolute power of activation at 12Hz. Blue line = healthy participants; red line = L.C.

The main difference was located over occipital-parietal electrodes along the vertical midline and within the damaged **right hemisphere**, contralateral to visual stimulation. In this case the absolute power of L.C. was lower than in healthy participants. However, it should be stressed that there was a modulation in the absolute power at all electrodes considered while stimulating the blind quadrant.

DIFFERENCE OVER POSTERIOR ELECTRODES

comparing ABSOLUTE POWER of the BLIND LOWER QUADRANT

in healthy participants and patient.

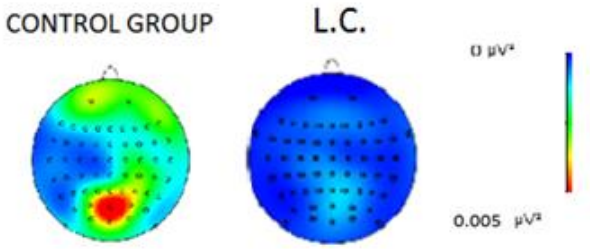

Fig.91. Topographic maps of control group and L.C. while stimulating the lower blind visual quadrant. Blue =low absolute power of activation; red = high absolute power of activation.

Absolute power of activation at 12z at posterior electrodes (Graph. 27)

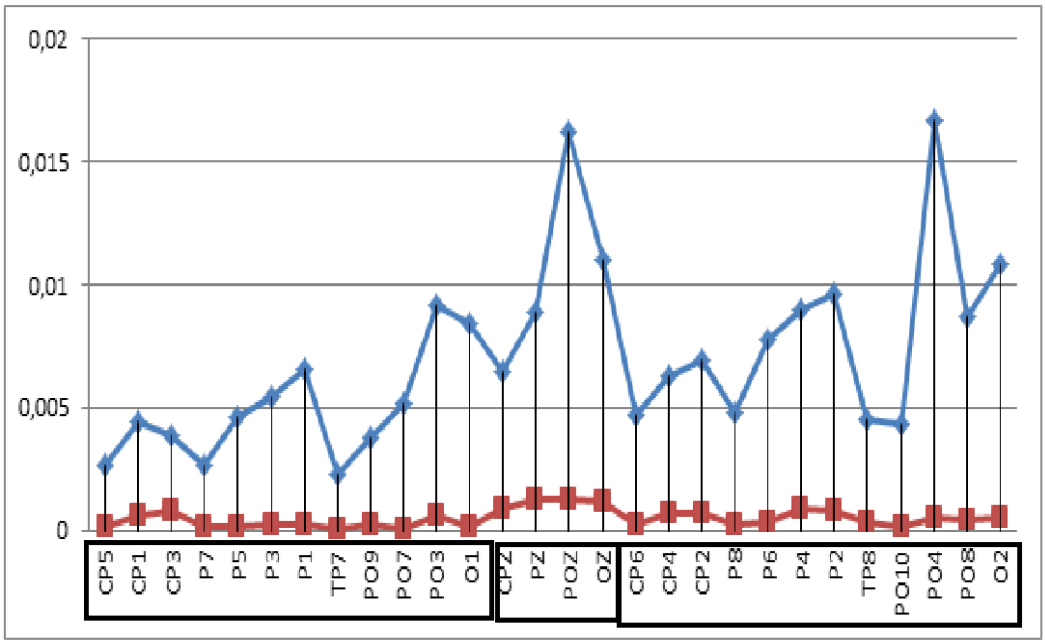

Graph. 27. Absolute power of activation at 12Hz. Blue line = healthy participants; red line = L.C.

We found a great difference over posterior electrodes mainly within the damaged **right hemisphere**, contralateral to visual stimulation, and along the vertical midline. Also in this case there was a modulation in the absolute power of activation stimulating a blind quadrant even if it was lower compared with that produced by visual stimulation in the upper left visual quadrant.

CONCLUSION:

In summary, in patient L.C. with a widespread lesion involving the right temporo-parietal and occipital lobe, causing a left lateral homonymous hemianopia, we found a strong modulation of response in both the time and frequency domain in the damaged hemisphere following stimulus presentation to the blind hemifield. This modulation involved mostly the whole right hemisphere stimulating the upper quadrant; instead it involved posterior and central right electrodes stimulating the lower quadrant.

As far as the intact hemifield is concerned we found that in the frequency domain the absolute power was lower than in healthy participants stimulating both quadrants and followed a different topography.

A.M.

Lesion involving the whole area of the Willis' Circle

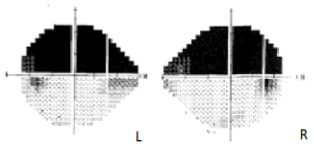

In this experiment, we located stimuli 12.5° from the center of the screen on the x axis and 9° from the center on the y axis.

TIME DOMAIN:

1. Amplitude of Waveforms

The amplitude of SSVEP waveforms to pattern reversal stimuli elicited at selected electrode sites by visual stimuli are shown in fig.92.

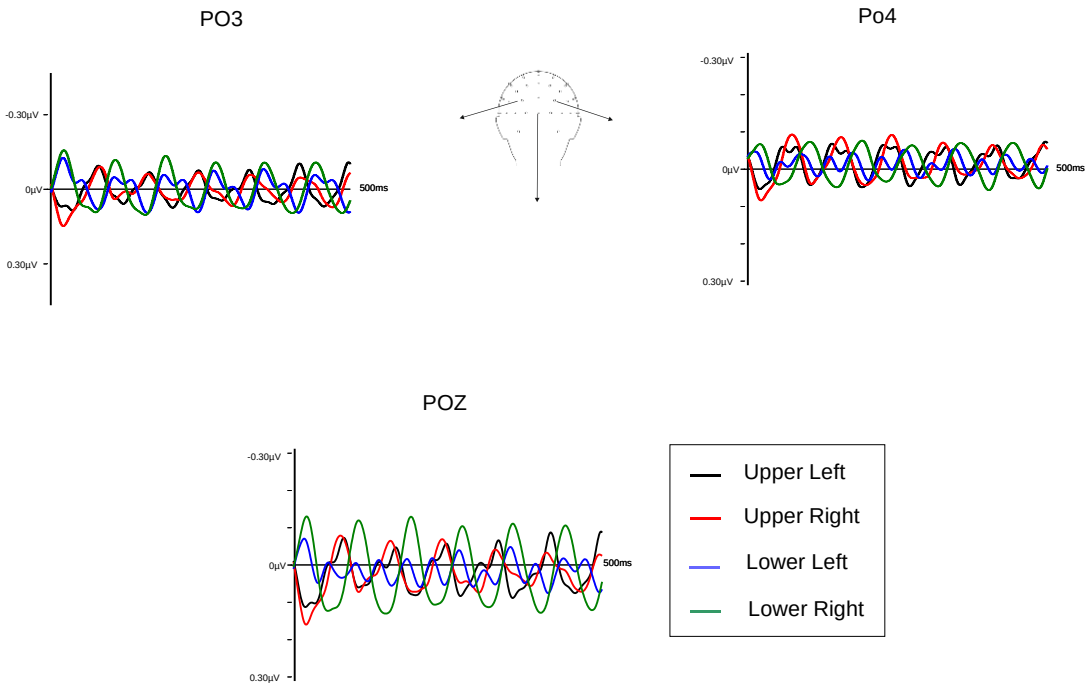

Fig. 92. SSVEP waveforms elicited at electrodes PO3, POz and PO4

In all electrodes we noticed the difference in phase comparing upper and lower visual quadrants. The signal appeared noisier while stimulating upper and lower left visual quadrants being the signal within each phase composed by two waves instead of one.

Upper right vs. upper left: the amplitude was similar considering all quadrants stimulation;

Lower right vs. lower left: the amplitude was always greater stimulating the lower right quadrant.

Those results suggested that the stimulation in the blind quadrant could determine a synchronization of cortical activity to the specific frequency even in the damaged hemisphere, similar compared with the synchronization produced by stimulating the sighted quadrants.

2. Topography of phase range

The scalp topography of SSVEP varied systematically as a function of response phase, which indicated that more than a generator was contributing to the

waveform. In the following figure (93) the sequential changes in topography in response to visual stimulation in time, within each single quadrant is shown.

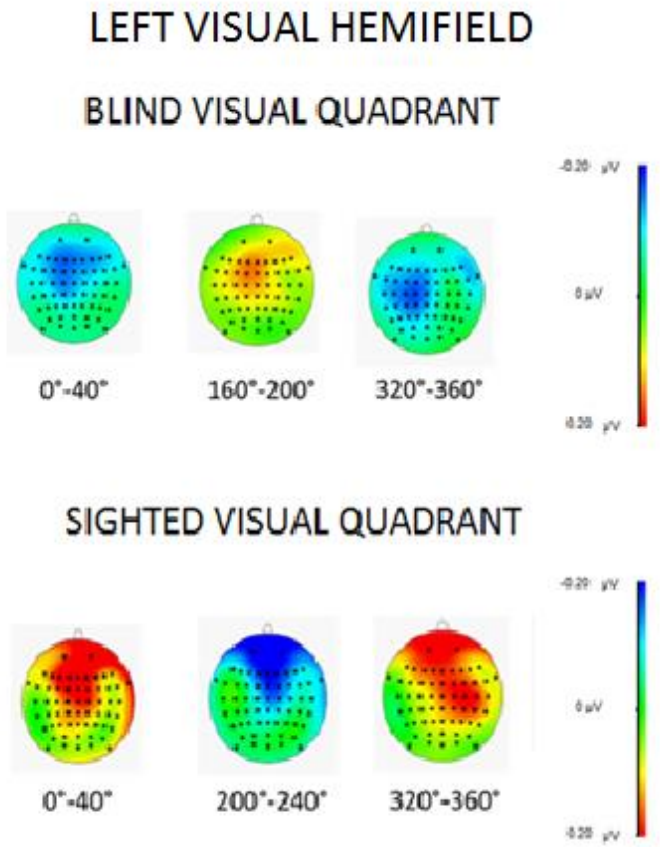

Fig.93. Topographic maps of a phase range.
Blue = negative amplitude; red = positive amplitude.

Blind visual quadrant:

- First phase range: unitary negative focus over central-frontal electrodes bilaterally distributed;
- Second phase range: unitary positive focus of activation over central-frontal electrodes bilaterally distributed;
- Last phase range: negative focus over frontal and central electrodes in the ipsilateral left hemisphere.

Sighted visual quadrant:

- First phase range: strong positive focus over frontal and central electrodes bilaterally distributed;

- Second phase range: strong negative focus over frontal and central electrodes bilaterally distributed;
- Last phase range: positive focus over frontal and central electrodes mainly in the contralateral right hemisphere.

In conclusion the activation in the time domain confirmed that more than one generator was contributing to the waveform when stimulating the left hemifield.
Considering the blind quadrant the activation was mainly located over frontal electrodes in the contralateral hemisphere; the communication of visual information with frontal and central areas in the left hemisphere determined the involvement of a bilateral dynamic mechanism composed by anterior structures during the perceptual process;
Considering the sighted quadrant the activation was located over frontal and central electrodes in the contralateral hemisphere; the communication of visual information with frontal and central electrodes in the left hemisphere determined the involvement of a bilateral dynamic mechanism composed by anterior structures during the perceptual process. Surprisingly, considering both quadrants, posterior electrodes were not activated as the main activation was located over frontal and central electrodes.

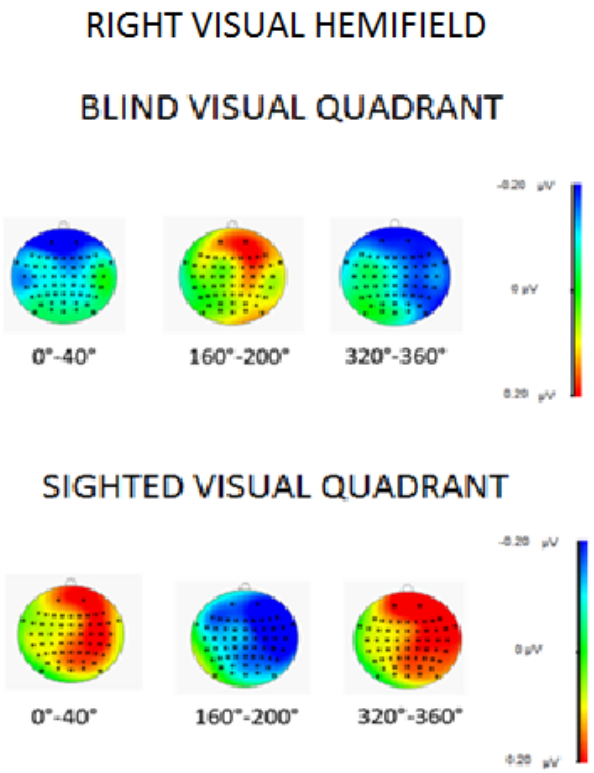

Fig. 94. Topographic maps of a phase range.
Blue = negative amplitude; red = positive amplitude.

Blind visual quadrant:

- First phase range: negative focus over frontal electrodes bilaterally distributed and over temporal and central electrodes bilaterally distributed;
- Second phase range: positive focus over frontal and central electrodes mainly in the right hemisphere, ipsilateral to visual stimulation;
- Last phase range: strong positive focus over frontal, central and posterior electrodes mainly in the right hemisphere, ipsilateral to visual stimulation.

Sighted visual quadrant:

- First phase range: strong positive focus of activation over almost the entire **right hemisphere,** ipsilateral to visual stimulation;
- Second phase range: negative widespread focus involving almost the whole right hemisphere;
- Last phase range: positive widespread focus involving almost the whole right hemisphere.

In conclusion the activation in the time domain confirmed that more than one generator was contributing to the waveform when stimulating the right hemifield; those generators were mainly located in the ipsilateral hemisphere.
Considering the blind quadrant a weak activation over frontal electrodes in the contralateral hemisphere was observed; the communication of visual information with frontal, central and posterior electrodes in the right hemisphere determined the involvement of a ipsilateral dynamic mechanism composed by anterior and posterior structures during the perceptual process;
Considering the sighted quadrant a weak activation over frontal electrodes in the contralateral hemisphere was observed; the communication of visual information with frontal, central and posterior electrodes in the right hemisphere determined the involvement of a bilateral dynamic mechanism composed by anterior structures during the perceptual process.

To summarize, the activation in the time domain appeared to be located mainly in the hemisphere ipsilateral to the visual stimulation except for the lower left quadrant where we observed a activation mainly located in the hemisphere contralateral to the visual stimulation.

FREQUENCY DOMAIN:

1. Bootstrap Analysis to compare real and simulated frequency (Graph. 28).

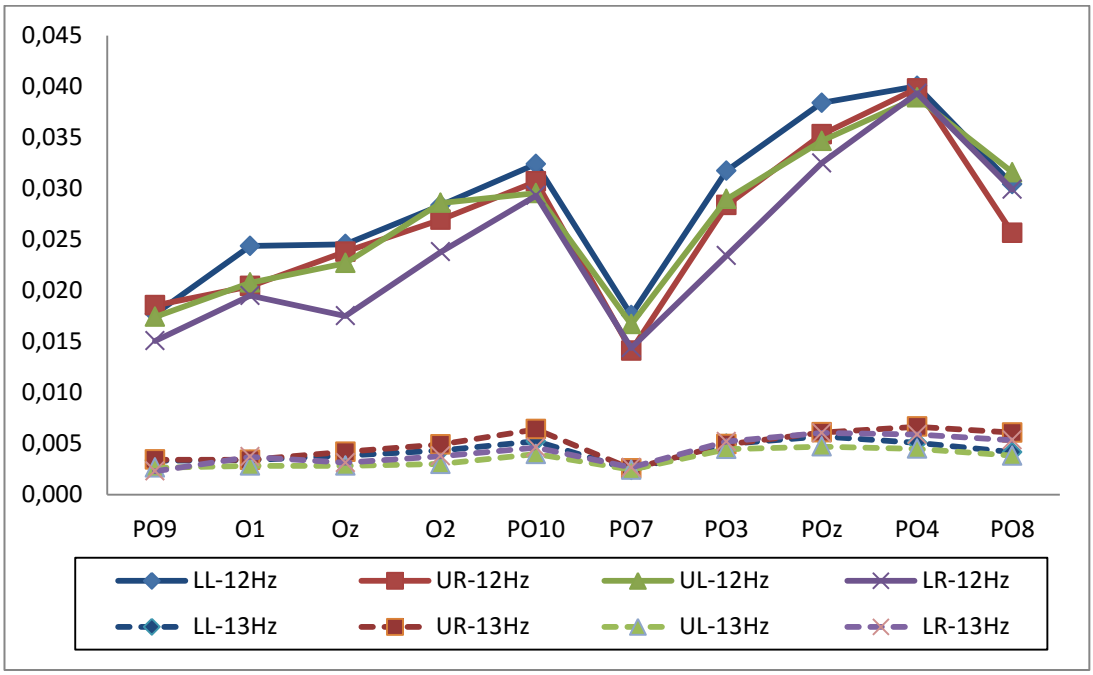

Graph. 28. Absolute power of activation at posterior electrodes comparing 12Hz (real frequency of visual stimulation; linear line) and 13 Hz (simulated frequency; dotted line).

With the Bootstrap analysis we found a significant difference in absolute power between the two frequencies at all electrodes, see Graph. 28 for posterior electrodes. This demonstrates that the SSVEP response was related to the specific frequency of visual stimulation.

2. Topographic distribution of Absolute Power, at the second harmonic of 12Hz (fig. 95)

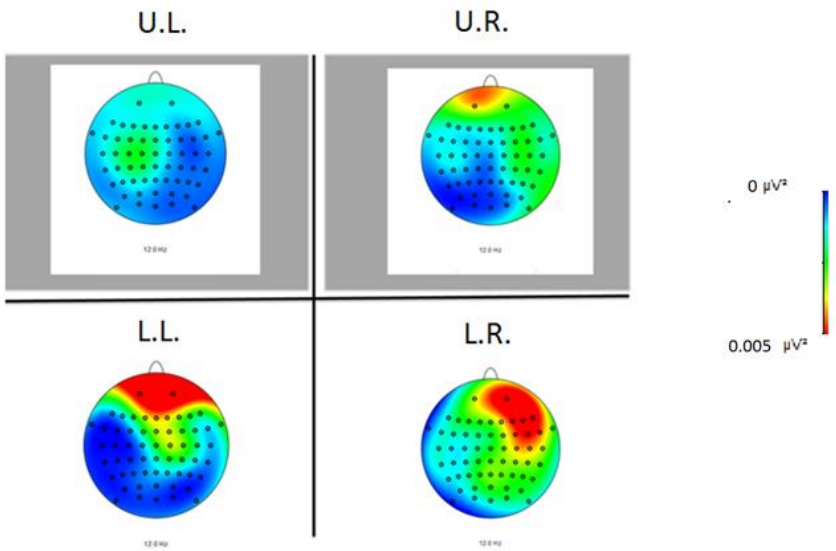

Fig. 95. Topographic maps of absolute power. Blue = low absolute; red = high absolute power. Grey background = blind quadrant

SIGHTED VISUAL QUADRANTS:

Lower right quadrant (LR): strong activation over frontal electrodes in the right hemisphere, ipsilateral to visual stimulation, and weak activation over central-parietal and occipital electrodes in the same hemisphere;

Lower left quadrant (LL): strong activation over frontal electrodes bilaterally distributed and central-temporal electrodes mainly in the right contralateral hemisphere.

BLIND VISUAL QUADRANTS:

Upper right quadrant (UR): weak activation over parietal-temporal and frontal electrodes in the right hemisphere, ipsilateral to visual stimulation.

Upper left quadrant (UL): weak activation over parietal-central electrodes in the left hemisphere, ipsilateral to the visual stimulation.

In conclusion these results broadly confirmed those found in the time domain: the activation was mainly located in the hemisphere ipsilateral to visual stimulation except for the visual stimulation in the lower left quadrant where we observed a activation in the contralateral hemisphere.

3. DIFFERENCE OVER POSTERIOR ELECTRODES comparing ABSOLUTE POWER of the BLIND LEFT QUADRANT in healthy participants and patient.

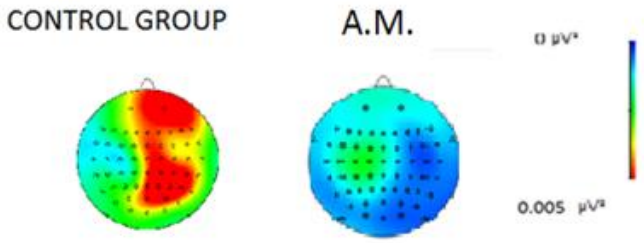

Fig.96. Topographic maps of control group and A.M. while stimulating the blind left visual quadrant. Blue =low absolute power of activation; red = high absolute power of activation.

Absolute power of activation at 12z at posterior electrodes (Graph. 29):

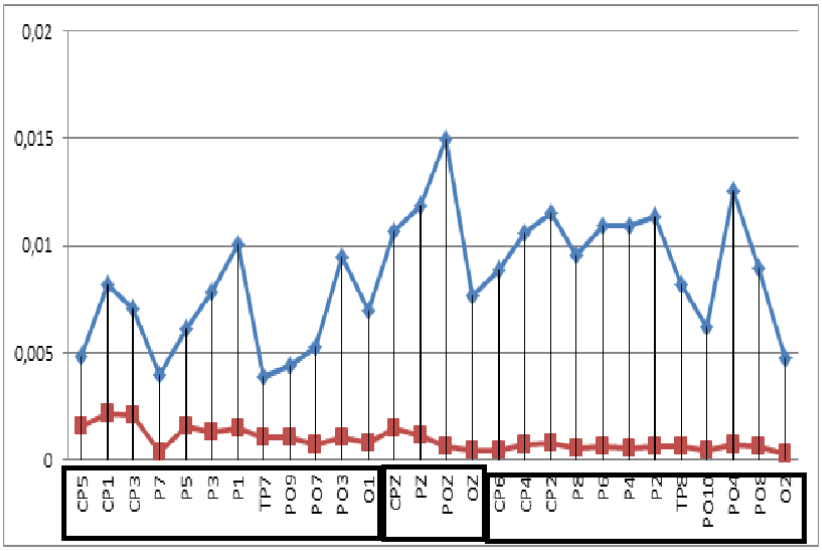

Graph. 29. Absolute power of activation at 12Hz. Blue line = healthy participants; red line = A.M.

We found a difference mainly over parietal-occipital electrodes along the vertical midline and in the **right hemisphere**, contralateral to visual stimulation. This

difference indicated that absolute power in A.M. was lower than in healthy participants but it is important to notice the modulation in the absolute power of activation mainly over electrodes in the left hemisphere, ipsilateral to visual stimulus, while stimulating a blind quadrant.

DIFFERENCE OVER POSTERIOR ELECTRODES
comparing ABSOLUTE POWER of the BLIND RIGHT QUADRANT
in healthy participants and patient

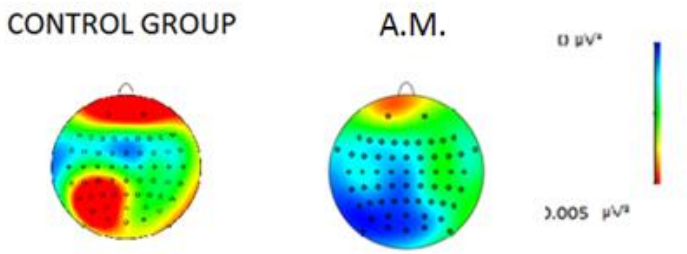

Fig.97. Topographic maps of control group and A.M. while stimulating the blind right visual quadrant. Blue =low absolute power of activation; red = high absolute power of activation.

Absolute power of activation at 12z at posterior electrodes (Graph. 30)

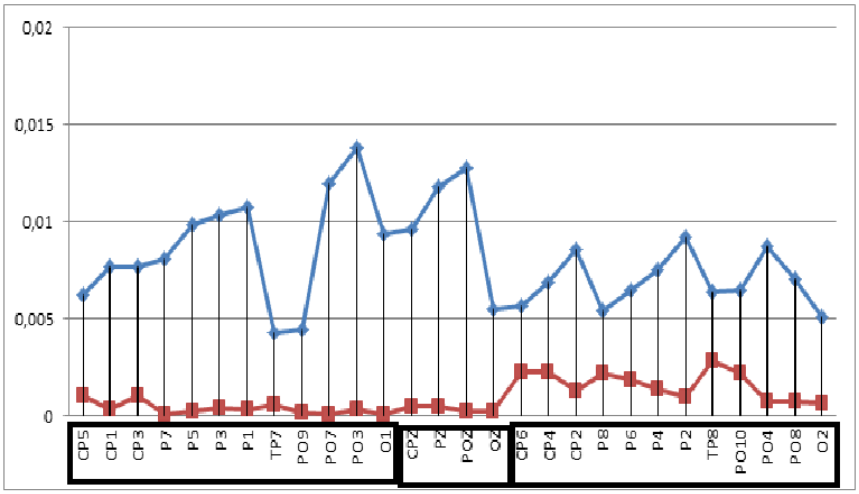

Graph. 30. Absolute power of activation at 12Hz. Blue line = healthy participants; red line = A.M.

The main difference was over parietal-occipital electrodes in the **left hemisphere**, contralateral to visual stimulation. Also in this case the difference indicated that the absolute power in A.M. was lower than in healthy participants but it is

important to notice that there was a modulation in the absolute power of activation mainly over electrodes in the right hemisphere, ipsilateral to visual stimulus, while stimulating the blind quadrant.

CONCLUSION:

In summary, in patient A.M. with a bilateral lesion involving the whole area of the Willi's' Cycle, causing a altitudinal bilateral hemianopia, we found a modulation of response in both the time and frequency domain in both damaged hemispheres following stimulus presentation to the blind hemifield. This modulation involved mainly frontal and central electrodes in the hemisphere ipsilateral to visual stimulation.

As far as the intact hemifield is concerned we found that in the frequency domain the absolute power was lower than in healthy participants stimulating both quadrants and followed a different topography. In the time domain we observed that the activation during a phase range was located in the ipsilateral hemisphere stimulating the lower right quadrant while we found a contralateral activation while stimulating the lower left quadrant.

SUMMARY OF RESULTS:

Patient A.G. with a lesion in the left hemisphere showed responses in the blind hemifield in both time and frequency domain mainly over frontal and temporal electrodes in the damaged left contralateral hemisphere.

Patient S.L. with a lesion in the left hemisphere showed a bilateral activation over frontal, temporal and posterior electrodes stimulating both the upper and lower visual quadrants in the time domain; in the frequency domain we observed a weak activation mainly over frontal, temporal and posterior electrodes in the left damaged hemisphere, contralateral to visual stimulation.

Patient L.F. with a small lesion in the right hemisphere showed responses in the blind hemifield in both time and frequency domain mainly over frontal, temporal and posterior electrodes in the right damaged hemisphere.

Patient F.B. with a widespread lesion in the right hemisphere showed responses in the upper blind quadrant in both time and frequency domain mainly over posterior and central electrodes of the intact left ipsilateral hemisphere. She showed responses in the blind lower visual quadrant in both the time and frequency domain mainly over frontal, central and posterior electrodes in the intact left ipsilateral hemisphere.

Patient L.C. with a lesion in the right hemisphere showed responses in the blind hemifield in both time and frequency domain mainly over frontal, central and posterior electrodes in the damaged right contralateral hemisphere.

Patient A.M. with a bilateral lesion showed responses in the blind upper right quadrant in both time and frequency domain mainly over frontal, central and parietal electrodes in the right ipsilateral hemisphere. He showed responses in the blind upper left visual quadrant in both time and frequency domain mainly over frontal and central electrodes in the left ipsilateral hemisphere.

In conclusion the neural activity triggered by visual stimulation in the blind hemifield was present in all patients and its source was more often over frontal, temporal and central electrodes in the contralateral damaged hemisphere. Patients with left lesion (A.G. and S.L.) showed mainly a frontal and temporal activation in the contralateral hemisphere, in the frequency domain. Instead, in the time domain, S.L. shows mainly a bilateral activation. Patients with right lesion (F.B., L.F. and L.C.) showed more differences among them: in L.F. and L.C. we found a contralateral activation over frontal, central and posterior electrodes; instead in F.B. we observed an ipsilateral activation mainly over frontal, central and posterior electrodes. In A.M., with a bilateral lesion, we observed an ipsilateral activation mostly over frontal and central electrodes (Table 32).

NAME	HEMISPHERE DAMAGED	RESPONSE IN THE BLIND FIELD	SITE OF RESPONSE
A.G.	LEFT	YES	FRONTAL, TEMPORAL DAMAGED HEMISPHERE
S.L.	LEFT	YES	TIME DOMAIN: FRONTAL, TEMPORAL, POSTERIOR BILATERAL; FREQUENCY DOMAIN: WEAK ACTIVATION OVER FRONTAL, TEMPORAL, POSTERIOR DAMAGED HEMISPHERE
L.F.	RIGHT	YES	FRONTAL, TEMPORAL, POSTERIOR DAMAGED HEMISPHERE
F.B.	RIGHT	YES	FRONTAL, CENTRAL, POSTERIOR INTACT HEMISPHERE
L.C.	RIGHT	YES	FRONTAL, CENTRAL, POSTERIOR DAMAGED HEMISPHERE
A.M.	BILATERAL	YES	FRONTAL AND CENTRAL IPSILATERAL HEMISPHERE

Table 32. Summary of results collected in the SSVEP passive stimulation

DISCUSSION:

The main important conclusion of this Passive Stimulation is represented by the modulation produced in all hemianopic patients in both the time and frequency domain by the visual stimulation flickering within the blind area. In the **time domain**, we found that more than one generator located both in the intact or in the lesioned hemisphere determined the activity observed on the scalp during one phase range both on the blind field of hemianopics and in healthy controls even if with a different topography. In the **frequency domain** we found a modulation in absolute power of activation produced by visual stimuli presented to the blind quadrant and involving the damaged or the intact hemisphere.

Thus, SSVEP confirmed to be a useful means to assess neural responses modulation triggered by stimuli in the blind area of hemianopic patients

Attentional Task

Aim:

In the literature many theories can be found which posit the existence of two separate networks in the human brain for the deployment of attention and the reorientation to unexpected events. One of the most influential theories is that by Corbetta and Shulman who proposed the concept of two anatomically and functionally distinct visual attentional systems in the human brain (Corbetta and Shulman 2002), see Fig. 98.

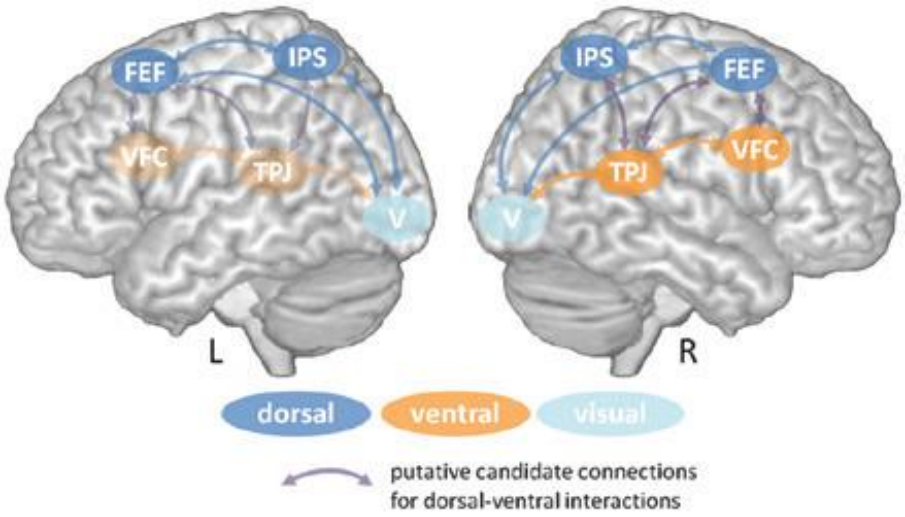

Fig. 98. Schematic illustration of the components of the dorsal (blue) and ventral (orange) attention system (Vossel et al., 2014)

The dorsal bilateral fronto-parietal system (intraparietal sulcus and frontal eye fields) mediates the top-down guided voluntary allocation of attention to locations or features, while right ventral fronto-parietal system (ventral frontal cortex and temporo-parietal junction) is involved in detecting unattended or unexpected stimuli and triggering shifts of attention (Vossel et al., 2014). These networks are bidirectionally connected with the visual cortex. The neural bases of visual attention can be profitably studied by means of the SSVEP technique (Morgan et al., 1996) as amplitude and phase of SSVEP can be modulated by a cognitive process as attention (Wu et al., 2014) and as visual evoked responses can be enhanced if the flickering visual stimulus falls within the area of spatial attention (Keil et al., 2005, Keil and Heim, 2009; Di Russo, 2002). In the light of this evidence we decided to carry out a SSVEP attentional task by asking participants to allocate attention toward a specific hemifield to detect a target. The aim of this experiment was to verify in hemianopic patients if focusing of spatial attention onto the blind portion of the visual field would lead to detection of otherwise invisible stimuli and to a corresponding neural response presumably in spared portions of the visual cortex or extrastriate areas or in frontal, parietal or temporal areas of the ipsi- or contra-lesional hemisphere. In this kind of task a top-down attention mechanism was activated as it was driven by conscious orientation of attention toward a specific direction and portion of the visual field.

Method:

Apparatus, Stimuli, Procedure

Two pairs of black and white Gabor gratings were presented simultaneously in the upper or lower visual fields. The grating on the left hemifield pattern-reversed every 90.9ms (fundamental frequency 5.5 Hz; reversal rate 11Hz) while the one on the right was flickered every 76.9ms (fundamental frequency 6.5Hz; reversal rate 13Hz). Participants were asked to attend to the left or right hemifield in a trial blocked sequence. With patients we started always with attention to the sighted visual hemifield. With healthy participants we counterbalanced the left-right order. We asked healthy participants to press the keyboard when the stimulus in the attended hemifield rotated from horizontal to oblique 45°. To make the task easier patients were to press the keyboard when the stimulus in the attended hemifield changed from horizontal to vertical orientation (90°). We counterbalanced the hand used to respond to the target.

Healthy participants were asked to perform the task twice, one with stimuli presented in the upper visual field and the other with stimuli in the lower visual field. This was done to compare healthy participants and brain damaged patients in corresponding positions of the visual field with patients with upper or lower quadrantanopia.

Participants

In this experiment we tested the same healthy control group and hemianopic patients tested in the previous passive stimulation. For the upper visual hemifield, we could keep all 20 healthy participants while for the lower visual hemifield we could test only 16 participants since four of them did not come back to perform the second task with stimuli presented in the lower visual hemifield. All patients tested in the previous passive stimulation experiment completed the whole attention experiment.

Electrophysiological recordings

The Electroencephalogram (EEG) was recorded by means of acti-CAP with 64 electrodes mounted on an elastic cap (fig. 58) as in the previous passive session.

All recording procedures were similar to those of the previous passive stimulation experiment.

Behavioural data statistical analysis

Behavioural responses in healthy participants were filtered by considering only RTs between 140ms and 750ms. Responses were classified as hits if participants responded to the correct target (change in orientation) in the attended hemifield or as false alarms if they pressed the space bar for responding to a target presented in the unattended hemifield. Finally, responses were classified as omissions if the target occurred in the attended visual hemifield but they did not press the space bar. With healthy participants we performed ANOVAs to assess the presence of significant difference for the effects of orienting attention toward the left or right visual hemifield in either upper or lower visual quadrants.

In addition, we evaluated the sensitivity index (d') to assess the ability in detecting the target in the attended field; a high d' indicates that the signal was more readily detected.

SSVEP Data Analysis

We analyzed the signal in both the time and the frequency domain.

Time Domain:

We carried out a visual inspection of the **amplitude of waveforms** elicited at posterior electrodes Oz, O1 (left hemisphere) and O2 (right hemisphere) in the attended and unattended condition. The hypothesis was to obtain greater waveforms amplitude in the attended compared with the unattended condition. (Di Russo et al., 1999).

Statistical Analysis in the Frequency Domain:

The 11Hz and 13Hz waveform were extracted at each recording site by performing the Fast Fourier Transformation of the SSVEP over the 2,000-ms epoch. The aim of this experiment was to study the difference in absolute power of activation between attended and unattended condition at the second harmonic of visual stimulation on the basis of the hypothesis that the absolute power in the attended would be higher than in the unattended condition. Therefore, we

performed a non-parametric one-tailed **Monte Carlo Percentile Bootstrap Simulation** (Efron and Tibshirani, 1993; Oruc et al., 2011; Bagattini et al., 2015). This procedure creates a simulated data set by re-sampling the raw data with replacement. We used this non parametric method as we wanted to evaluate the difference between conditions in each patient, making a comparison within subject. To avoid inhomogeneity in the statistical analysis performed we used the same non parametric technique with healthy participants as well. With the healthy control group we created 50000 re-samples of healthy subjects for attended minus unattended condition power values. With hemianopic patients we performed a single-case analysis creating a 50000 re-samples of 20 blocks each one including 185 trials for left attended, 188 for left unattended, 222 for right attended and 225 for right unattended power values. The lower 5^{th} percentile of the re-sampled data distribution served as the critical values for the one-tailed 0.05 significant level starting from the strong hypothesis that the power in attended condition should be higher than in the unattended one. If the 5^{th} percentile results to be above the zero level (attended > unattended), it follows that the attended condition yields a significantly larger power than the unattended one.

Behavioural Results in Healthy Participants:
UPPER VISUAL HEMIFIELD

ACCURACY Percentage	**MEAN**	**STANDARD DEVIATION**	**d' (sensitivity index)**
HITS LEFT	**76.25**	15.30	**3.09**
FALSE ALARMS LEFT	1.40	1.47	
HITS RIGHT	**75.65**	15.27	**3.15**
FALSE ALARMS RIGHT	1.15	2.52	

Table 33. Accuracy in the attentional task; stimuli in the upper visual hemifield

REACTION TIMES Milliseconds	MEAN	STANDARD DEVIATION
HITS LEFT	**486.13**	41.90
FALSE ALARMS LEFT	312.17	258.72
HITS RIGHT	**475.63**	43.35
FALSE ALARMS RIGTH	147.77	209.02

Table 34. Reaction Times in the attentional task; stimuli in the upper visual hemifield

Accuracy was higher in the left visual field but the difference was far from significance as assessed with a t- test (p=0.774) while reaction times were faster in the right visual hemifield and this difference was significant (p =0.030).

LOWER VISUAL HEMIFIELD:

ACCURACY Percentage	MEAN	STANDARD DEVIATION	d' (sensitivity index)
HITS LEFT	**83.69**	12.98	**3.53**
FALSE ALARMS LEFT	0.88	1.45	
HITS RIGHT	**79.13**	14.15	**3.32**
FALSE ALARMS RIGHT	0.75	1.18	

Table 35. Accuracy in the attentional task; stimuli in the lower visual hemifield

REACTION TIMES Milliseconds	**MEAN**	**STANDARD DEVIATION**
HITS LEFT	**463.68**	49.93
FALSE ALARMS LEFT	162.87	232,45
HITS RIGHT	**476.01**	62.01
FALSE ALARMS RIGTH	182.83	254.17

Table 36.Reaction Times in the attentional task; stimuli in the lower visual hemifield

As for the upper hemifield accuracy was higher in the left visual field but the difference was not significant (p=0.065). Reaction times were faster in the left visual field and the difference was significant (p =0.048).

SSVEP Results: WAVEFORMS

UPPER VISUAL HEMIFIELD:

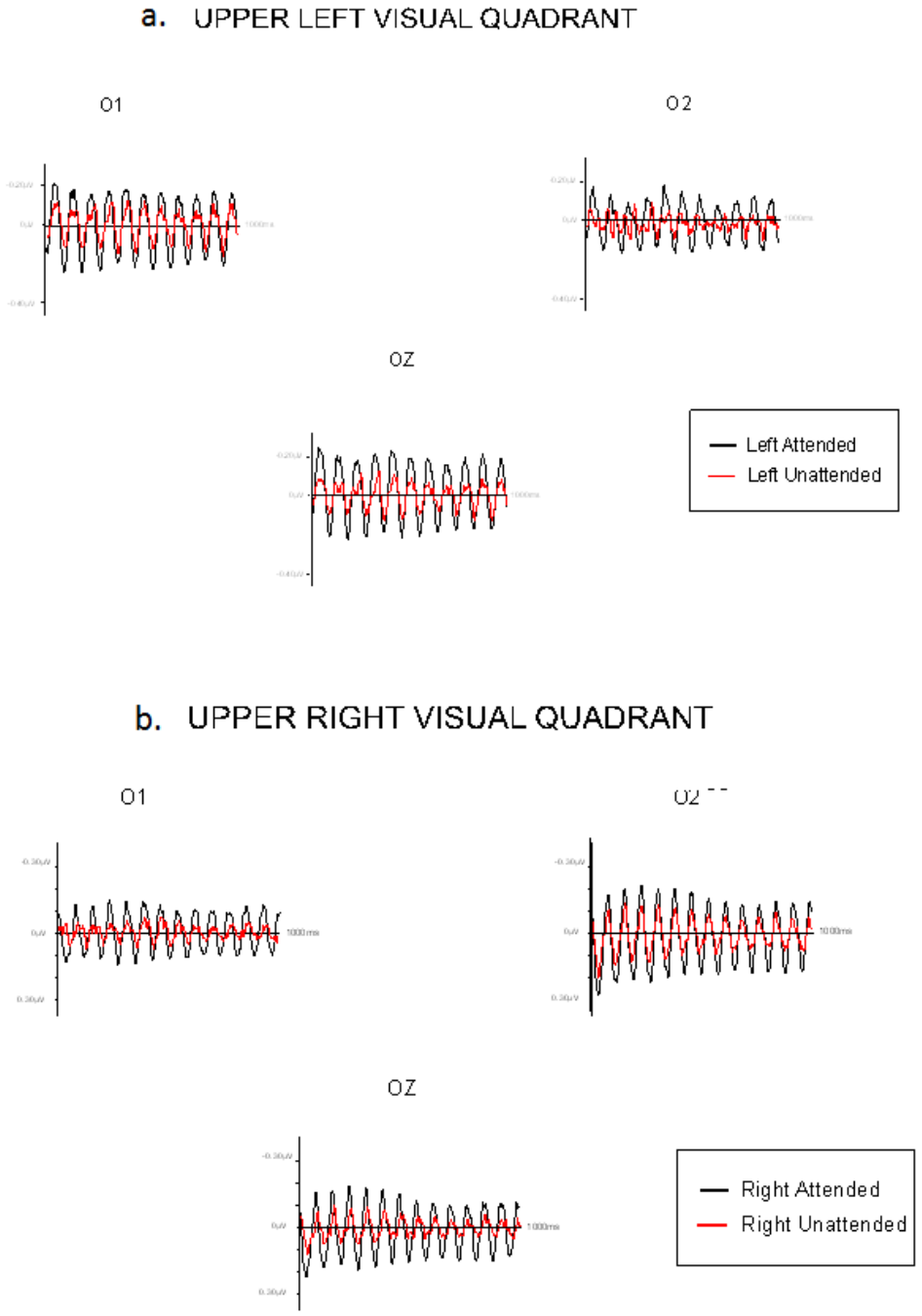

Fig- 99. a). Comparison of SSVEP amplitude between upper left attended and upper left unattended condition. b). Comparison of SSVEP amplitude between upper right attended and upper right unattended condition.

In the upper left visual quadrant we found that the amplitude of waveforms in the attended condition was higher than in the unattended one, as expected, see fig. 99. As for the upper left visual quadrant also for the upper right quadrant we found that the amplitude of waveforms in the attended condition was higher than in the unattended one, as expected.

LOWER VISUAL HEMIFIELD:

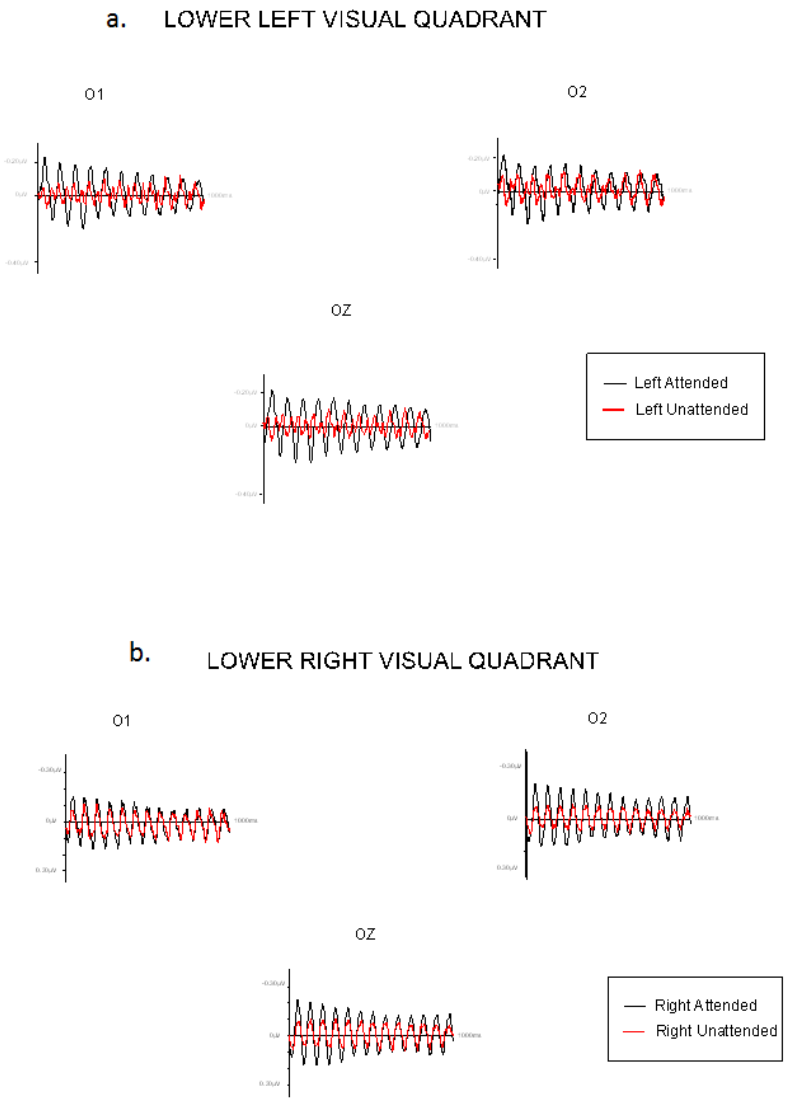

Fig. 100. a). Comparison of SSVEP amplitude between lower left attended and lower left unattended condition. b). Comparison of SSVEP amplitude between lower right attended and lower right unattended condition.

As for the upper quadrants in the lower left visual quadrant we found that the amplitude of waveforms in the attended condition was higher than in the unattended one, see fig. 100. For the lower right visual quadrant we found that the amplitude of waveforms in the attended was higher than in the unattended condition, as expected.

FREQUENCY DOMAIN: Bootstrap Analysis

ATTENTION TO THE UPPER LEFT VISUAL QUADRANT (Fig. 101)

In the upper left condition we found a **significant difference** in absolute power comparing **left attended vs. left unattended** over electrodes **Cz and C2.** ($p<0.05$) indicating that for these sites the absolute power of activation in the attended condition was significantly higher than in the unattended one. Fig. 101a shows the location of these electrodes surrounded by a red square and Fig. 101b shows the results for a given electrode as example.

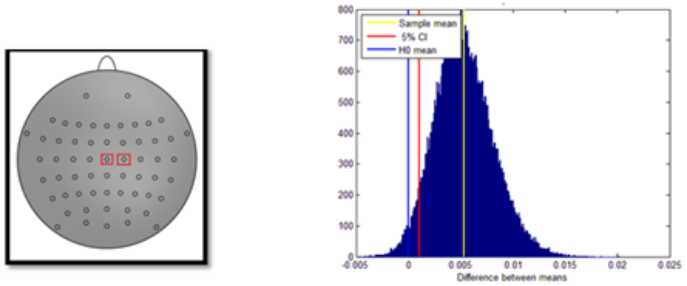

a. b.

Fig.101 . a). Significant higher absolute power in the attended compared with the unattended condition. **b).** Results of Bootstrap analysis performed on electrode Cz, as an example, evaluating the difference between attended and unattended conditions. On y axes the number of samples is represented while on the x axes the sample mean is shown. Solid yellow line represents the mean power of the difference between attended and unattended condition. The solid red line represents the 5^{th} percentile while the blue line corresponds to zero. If the red line is above zero indicates the presence of a statistically significant difference.

ATTENTION TO THE UPPER RIGHT VISUAL QUADRANT (Fig. 102)

In the upper right condition we found a significant difference comparing right attended vs. right unattended condition over posterior, central, temporal and frontal electrodes with a bilateral distribution, indicating that absolute power of activation in attended condition was higher than in the unattended one. In Figure 102a is shown the location of electrodes where the difference between attended and unattended condition was significant (electrodes surrounded by a red square) at $p<0.05$ and Fig.102b shows the results for a given electrode as example.

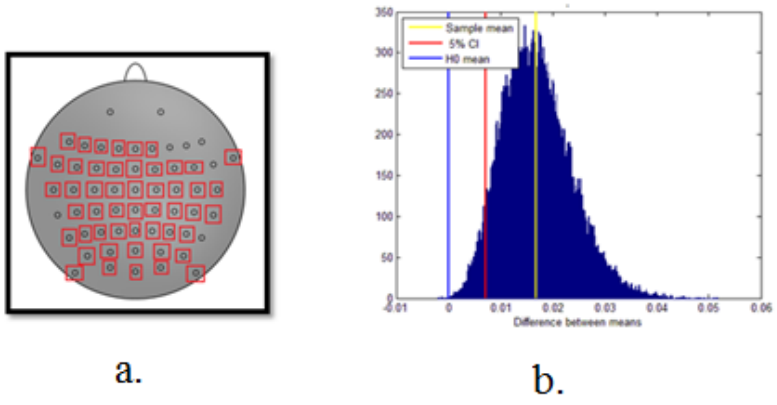

Fig.102 . a). Electrodes where we observed significant higher levels of power in the attended compared with the unattended condition. **b).** Results of Bootstrap analysis performed on electrode POz, as an example, considering the upper right visual hemifield, evaluating the difference between attended and unattended conditions.

ATTENTION TO THE LOWER LEFT VISUAL QUADRANT (Fig. 103)

In the lower left condition we found a significant difference comparing left attended vs. left unattended condition over frontal, central and posterior electrodes in the right hemisphere, contralateral to the location of attention, indicating that absolute power of activation in attended condition was higher than in the unattended one. In Figure 103a the location of these electrodes is shown (electrodes surrounded by a red square showed a significant difference; $p<0.05$) and Figure 103b shows the results for a given electrode as example.

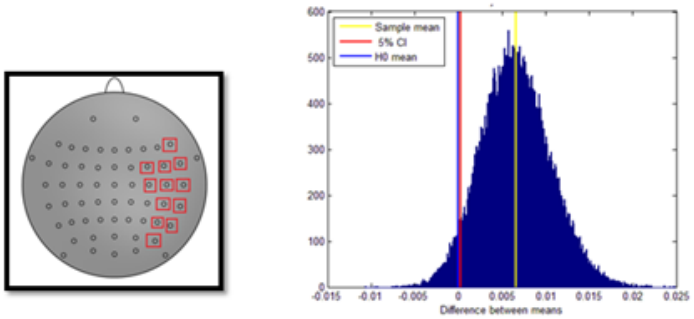

Fig.103. a). Electrodes where we observed significant higher levels of power in the attended compared with the unattended condition. **b).** Results of Bootstrap analysis performed on electrode PO8, as an example, considering the upper right visual hemifield, evaluating the difference between attended and unattended conditions.

ATTENTION TO THE LOWER RIGHT VISUAL QUADRANT (Fig. 104)

In the lower right condition we found a significant difference comparing right attended vs. right unattended condition over posterior, central and frontal electrodes bilaterally distributed, indicating that absolute power of activation in the attended condition was higher than in the unattended one, see Figure 104a and b.

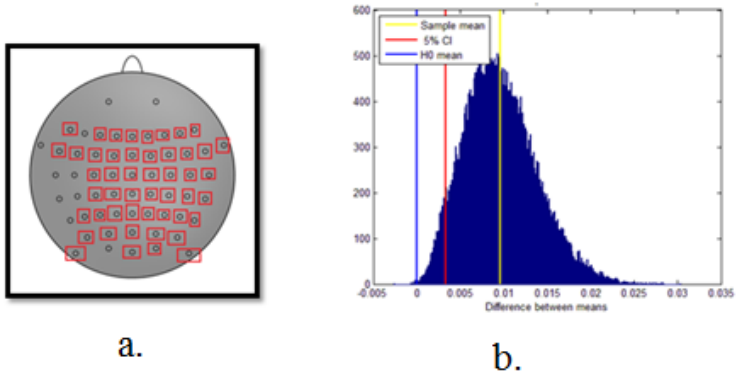

Fig.104 . a). Electrodes where we observed significant higher levels of power in the attended compared with the unattended condition. **b).** Results of Bootstrap analysis performed on electrode POz, as an example, considering the upper right visual hemifield, evaluating the difference between attended and unattended conditions.

By performing the Bootstrap Analysis, we found a higher activation in the attended compared with the unattended condition as a result of orienting the attention toward the required quadrant.

A.G.:
Lesion involving basal ganglia
and the dorsal portion of the left visual primary cortex.

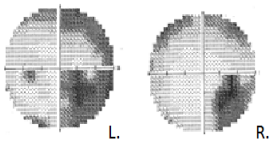

In this experiment stimuli where located in the lower visual hemifield.

Behavioural Results:

ACCURACY:

HEMIFIELD	HITS	FALSE ALARMS	d' (sensitivity index)
SIGHTED	**40%**	4%	**1.497**
BLIND	**2%**	0	

Table 37.Accuracy in the attentional task.

REACTION TIMES:

HEMIFIELD	HITS	FALSE ALARMS
SIGHTED	**506.65 ms**	350.25 ms
BLIND	**438.5 ms**	

Table 38. Reaction Times in the attentional task.

In the blind visual field A.G. responded only to 2% of stimuli and was unaware of the stimuli. In the intact the performance was reasonably accurate with a d' of 1.5.

SSVEP Results: AMPLITUDE

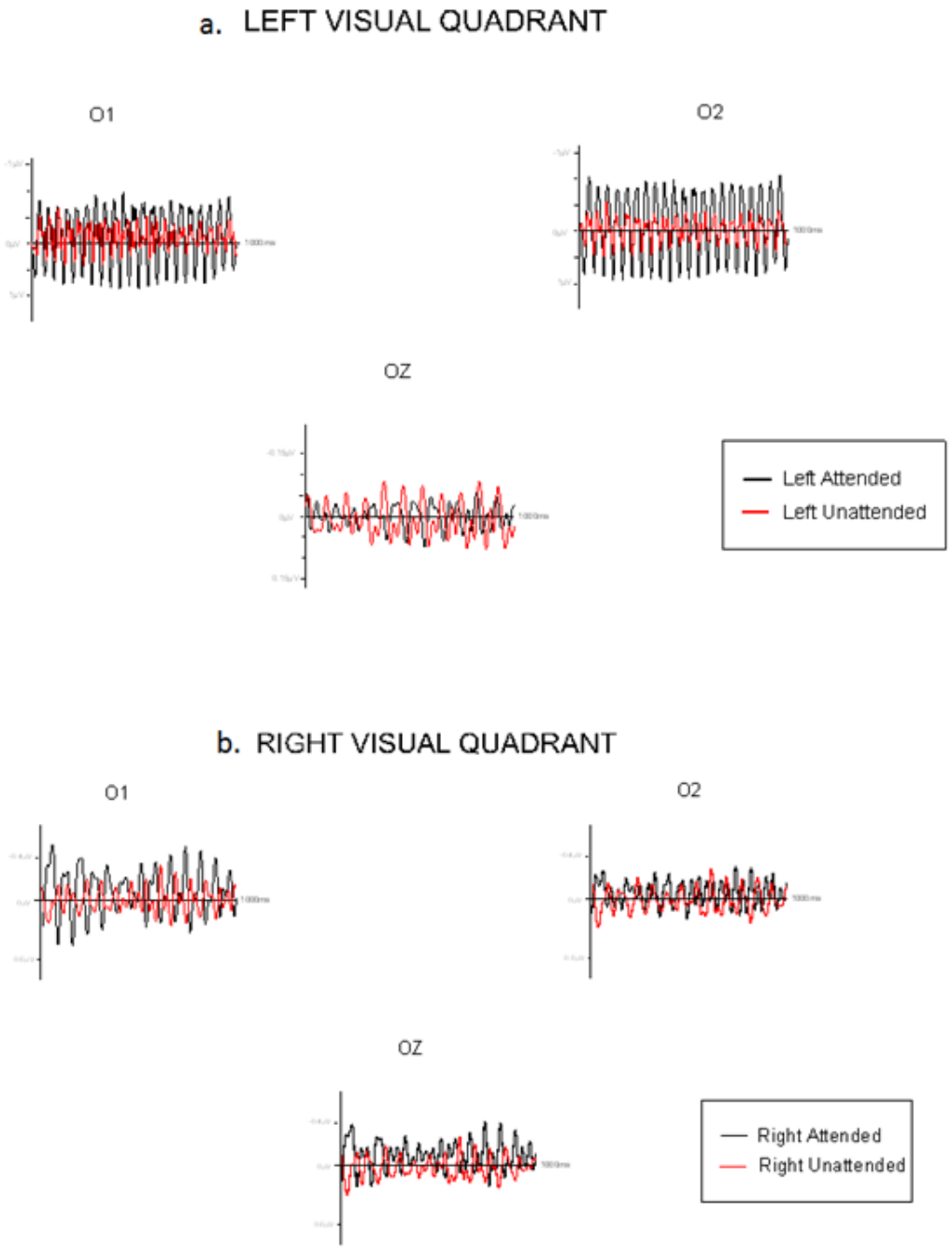

Fig.105. a). Comparison of SSVEP amplitude between sighted attended and unattended condition. b). Comparison of SSVEP amplitude between blind attended and unattended condition.

In keeping with the behavioural results, in the sighted visual quadrant the amplitude of waveforms in the attended condition was higher than in the

unattended one over lateral sites O1 and O2 while it was similar over electrode Oz, see fig. 105. Thus, the attentional effort could modulate the amplitude of the waveforms at lateral sites. In the blind visual quadrant the amplitude of waveforms in the attended condition was higher than in the unattended one over electrodes O1 and Oz while was similar in both conditions over electrode O2. Thus, the attentional effort could modulate the amplitude of the waveforms in the left hemisphere and at central sites.

FREQUENCY DOMAIN: Bootstrap Analysis

ATTENTION TO THE SIGHTED VISUAL QUADRANT (Fig. 106)

We found a **significant difference** over some electrodes, see Figure 106 with the absolute power of activation in the attended condition significantly higher than in the unattended condition.

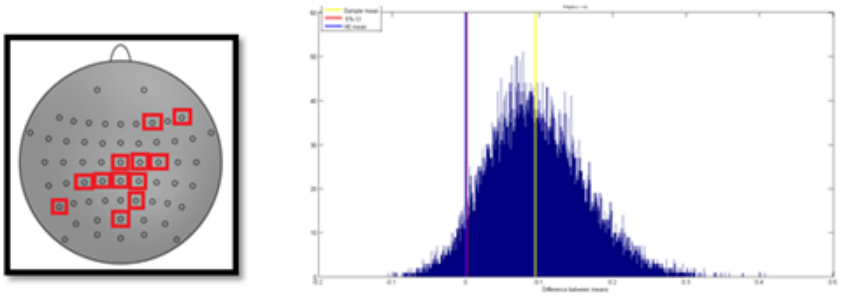

Fig.106 . a). Electrodes where we observed significant higher levels of power in the attended compared with the unattended condition. **b).** Results of Bootstrap analysis performed on electrode POz considering the upper right visual hemifield, evaluating the difference between attended and unattended conditions.

Higher absolute power of activation was assessed over frontal, central and posterior electrodes, in both hemispheres but mainly located within the intact right hemisphere, contralateral to the location of the attention.

ATTENTION TO THE BLIND VISUAL QUADRANT (Fig. 107)

We found a **significant difference** bilaterally distributed mainly over posterior electrodes (see Figure 107) with the absolute power of activation in the attended condition significantly higher than in the unattended condition.

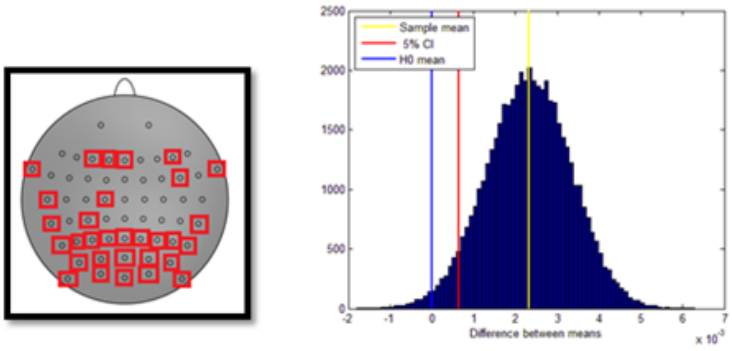

a. b.

Fig.107. a). Electrodes where we observed significant higher levels of power in the attended compared with the unattended condition. **b).** Results of Bootstrap analysis performed on electrode POz considering the upper right visual hemifield, evaluating the difference between attended and unattended conditions.

In conclusion, in patient A.G. the amplitude of waveforms was higher in the attended than in the unattended condition over the electrodes in the contralateral hemisphere regardless of the hemifield. Concerning the Bootstrap Analysis, the modulation produced by the attentional effort toward either sighted or blind visual quadrants was represented by a significant increase in absolute power of activation over bilateral frontal, central and posterior electrodes, even if the stimulus in the right quadrant was not consciously perceived. In reference to the aim of the study, these results indicated that similar cortical areas could be activated by attentional orienting despite the lesion in the visual cortex.

S.L.

Lesion involving the medial part of the left occipital lobe

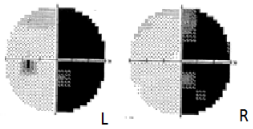

In this experiment stimuli were located in the upper visual hemifield.

Behavioural Results:

ACCURACY:

HEMIFIELD	HITS	FALSE ALARMS	d' (sensitivity index)
SIGHTED	**88%**	7%	**2.65**

Table 39..Accuracy in the attentional task.

REACTION TIMES:

HEMIFIELD	HITS	FALSE ALARMS
SIGHTED	**501.63 ms**	530.89 ms

Table 40. Reaction Times in the attentional task.

In the blind visual field S.L. did not respond to any targets and reported no conscious perception. In the sighted field performance was high and at the level of healthy controls with a high d'.

SSVEP Results: AMPLITUDE

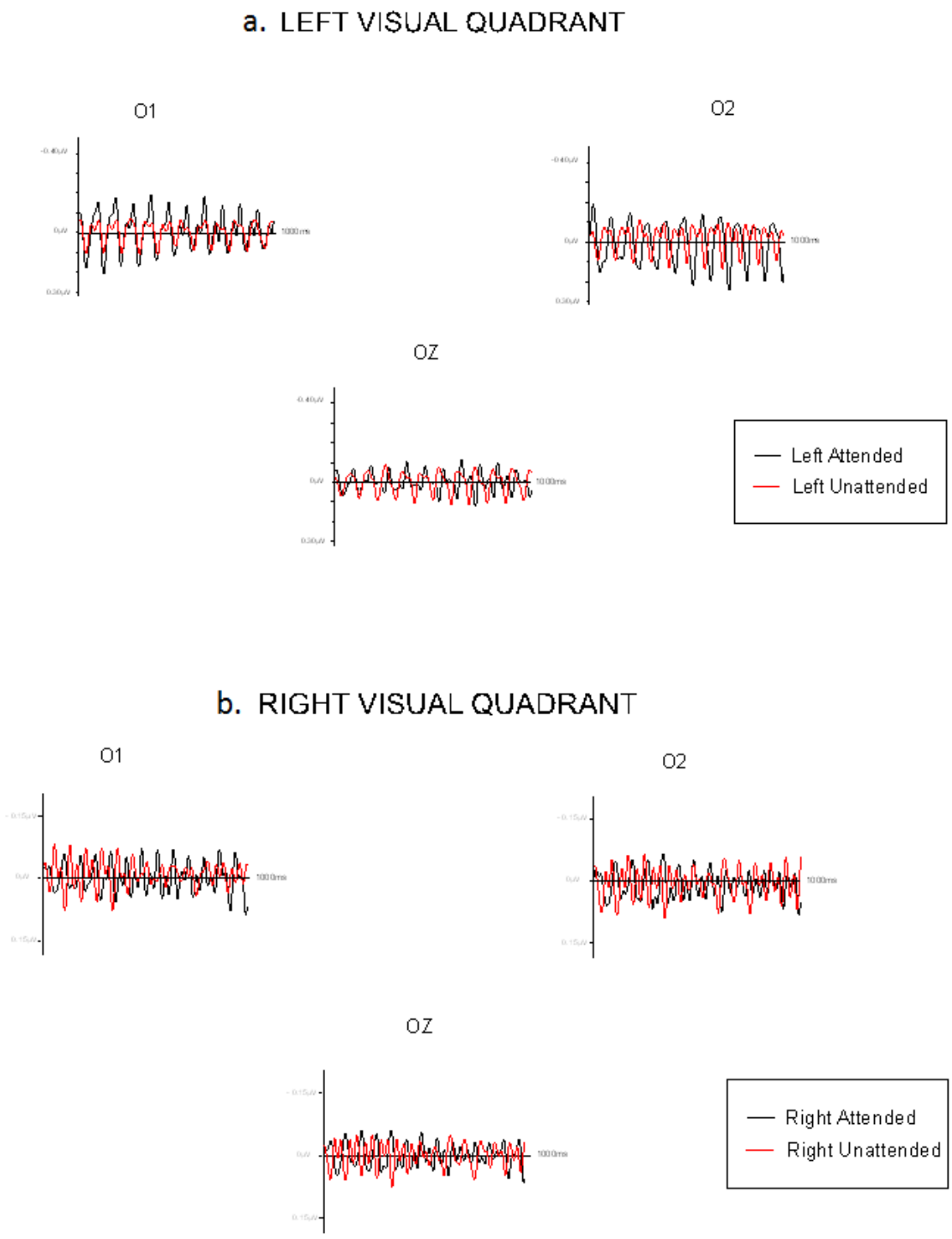

Fig.108. a). Comparison of SSVEP amplitude between sighted attended and unattended condition.
b). Comparison of SSVEP amplitude between blind attended and unattended condition.

For the sighted left visual quadrant, the amplitude of waveforms was higher in the attended than unattended condition at all electrodes considered, as expected given the behavioural results, see fig. 108. In contrast, in the blind right visual quadrant, the amplitude of waveforms was similar in both the attended and the unattended condition.

FREQUENCY DOMAIN: Bootstrap Analysis

ATTENTION TO THE SIGHTED VISUAL QUADRANT (Fig. 109)

We found a **significant difference** with the absolute power of activation in the attended condition higher than in the unattended condition over posterior electrodes in both hemispheres, see Figure 109.

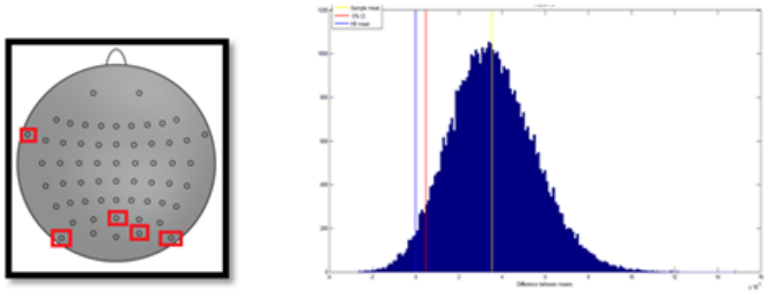

a. b.

Fig.109 . a). Electrodes where we observed significant higher levels of power in the attended compared with the unattended condition. **b).** Results of Bootstrap analysis performed on electrode POz considering the upper right visual hemifield, evaluating the difference between attended and unattended conditions.

ATTENTION TO THE BLIND VISUAL QUADRANT (Fig. 110)

We found a significantly higher activation in the attended vs the unattended condition, in the damaged left hemisphere over anterior-lateral electrodes shown in Figure 110.

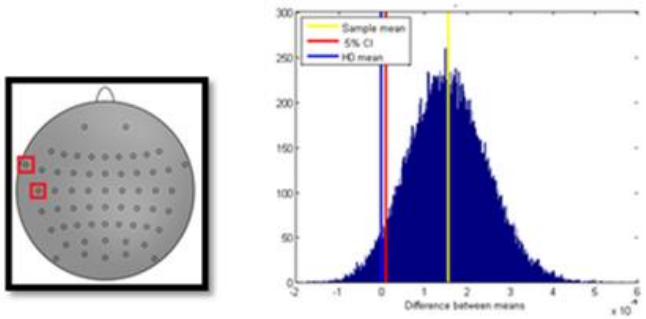

a. b.

Fig.110 . a). Electrodes where we observed significant higher levels of power in the attended compared with the unattended condition. **b).** Results of Bootstrap analysis performed on electrode T7 considering the upper right visual hemifield, evaluating the difference between attended and unattended conditions.

In conclusion, in patient S.L. the amplitude of waveforms was greater in the attended compared with the unattended condition only when allocating the attention toward the sighted visual quadrant while it was similar in both conditions while moving the attention toward the blind quadrant. Concerning the Bootstrap Analysis, the modulation produced by the attentional effort toward the sighted visual quadrant was represented by a significant increase in absolute power over bilateral posterior electrodes. Instead, that toward the blind visual quadrant indicated a significant increase in absolute power over frontal and temporal electrodes in the left contralateral hemisphere.

In reference to the principal aims of this experiment we found that the topography observed while moving the attention toward the blind quadrant involved ipsilesional fronto-temporal electrodes while moving the attention toward the sighted quadrant involved bilateral posterior electrodes.

L.F.:
Lesion involving a small portion of the primary visual cortex, along the calcarine fissure

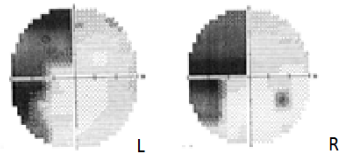

In this experiment, we located the stimuli in the upper visual hemifield.

Behavioural Results:

ACCURACY:

HEMIFIELD	HITS	FALSE ALARMS	d' (sensitivity index)
SIGHTED	**62%**	47%	**0.38**

Table 41. Accuracy in the attentional task.

REACTION TIMES:

HEMIFIELD	HITS	FALSE ALARMS
SIGHTED	**501.63 ms**	530.89 ms

Table 42. Reaction Times in the attentional task.

In the blind visual field L.F. did not respond to any target reporting that she could not perceive any stimulus. Moreover, accuracy of response was low with a low d'.

SSVEP Results: AMPLITUDE

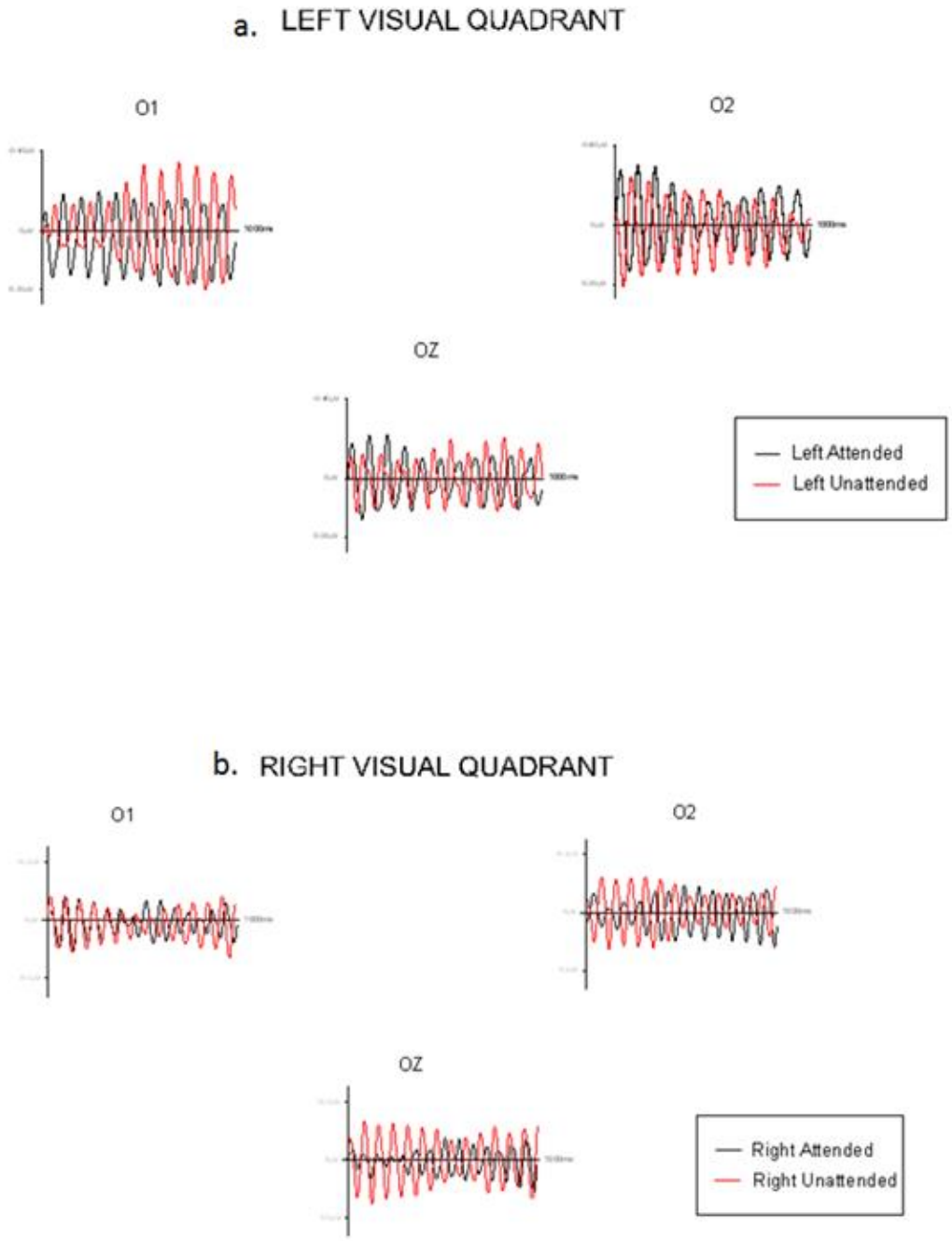

Fig.111. a). Comparison of SSVEP amplitude between blind attended and unattended condition.
b). Comparison of SSVEP amplitude between sighted attended and unattended condition.

In the blind quadrant, the waveform amplitude was similar in both conditions over electrodes O2 and Oz while it was unexpectedly greater in the unattended than in the attended condition over electrode O1, see fig. 111.

In the sighted quadrant, the waveforms amplitude in the attended and unattended condition was similar over electrode O1 and greater in the unattended condition over electrode O2 and Oz.

FREQUENCY DOMAIN: Bootstrap Analysis

ATTENTION TO THE BLIND VISUAL QUADRANT

We did **not** find **any significant difference** in absolute power of activation between attended and unattended condition.

ATTENTION TO THE SIGHTED VISUAL QUADRANT

We found a **significant difference** between the attended and the unattended condition over electrodes shown in Figure 112.

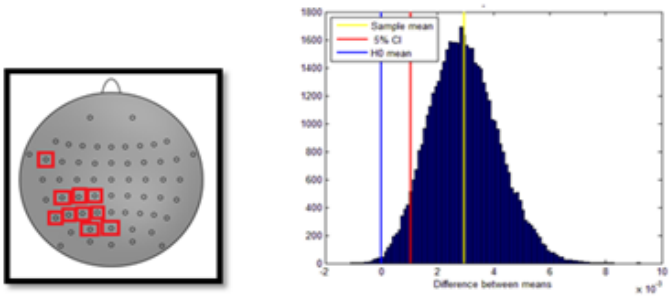

a. b.

Fig.112 . a). Electrodes where we observed significant higher levels of power in the attended compared with the unattended condition. **b).** Results of Bootstrap analysis performed on electrode POz considering the upper right visual hemifield, evaluating the difference between attended and unattended conditions.

A higher absolute power of activation was found over central and posterior electrodes in the intact left hemisphere contralateral to the location of the attention.

In conclusion, in patient L.F. the amplitude of waveforms was similar or even greater in the unattended than attended condition suggesting that there was no neural (or behavioural) effect of focusing of attention. Concerning the Bootstrap Analysis, the modulation produced by attentional orienting toward the sighted visual quadrant was represented by a significant increase in absolute power over posterior electrodes within the contralateral hemisphere. In contrast, orientation of attention toward the blind visual quadrant showed a non-significant increase in absolute power over bilateral frontal electrodes.

In this patient there was no behavioural or electrophysiological evidence of an effect of orienting attention to the blind field. As to the intact field the lack of behavioural effect of attention makes the electrophysiological effect found difficult to interpret.

F.B.
Lesion involving the right temporal-parietal-occipital cortex

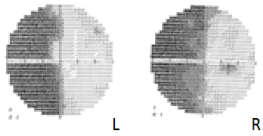

In this experiment stimuli were located in the lower visual hemifield.

Behavioural Results:

ACCURACY:

HEMIFIELD	HITS	FALSE ALARMS	d' (sensitivity index)
SIGHTED	**6%**	1%	**0.77**

Table 43. Accuracy in the attentional task.

REACTION TIMES:

HEMIFIELD	HITS	FALSE ALARMS
SIGHTED	**763.85**	239

Table 44. Reaction Times in the attentional task.

In the blind visual field F.B. did not respond to any targets and could not perceive any stimulus feature. The performance was very low in the intact field with a low d'.

SSVEP Results: AMPLITUDE

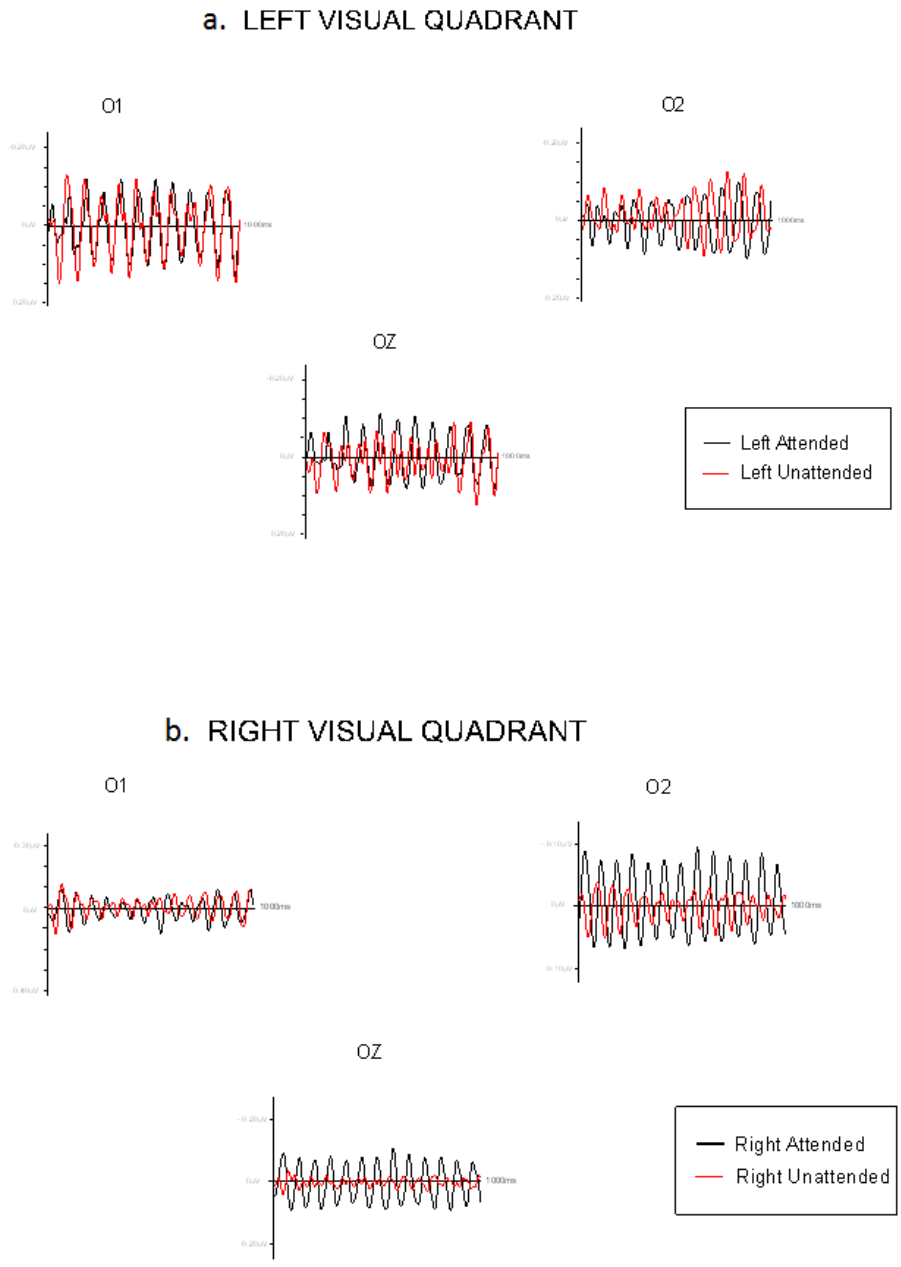

Fig.113. a). Comparison of SSVEP amplitude between blind attended and unattended condition. b). Comparison of SSVEP amplitude between sighted attended and unattended condition

In the blind visual quadrant, the amplitude of waveforms was similar in both the attended and unattended conditions, see fig. 113. For the sighted visual quadrant, the amplitude of waveforms was higher in the attended than unattended condition

over electrodes O2 and Oz while it was similar over electrode O1, in the intact left hemisphere. It means that the attentional effort could modulate the amplitude of the waveforms.

FREQUENCY DOMAIN: Bootstrap Analysis

ATTENTION TO THE BLIND VISUAL QUADRANT

We did **not** find **significant difference** considering the attended versus the unattended condition.

ATTENTION TO THE SIGHTED VISUAL QUADRANT

We found a **significant difference** in the attended versus unattended comparison over frontal, temporal and posterior electrodes mainly in the intact left hemisphere, contralateral to the allocation of attention. In figure 114 those electrodes are shown.

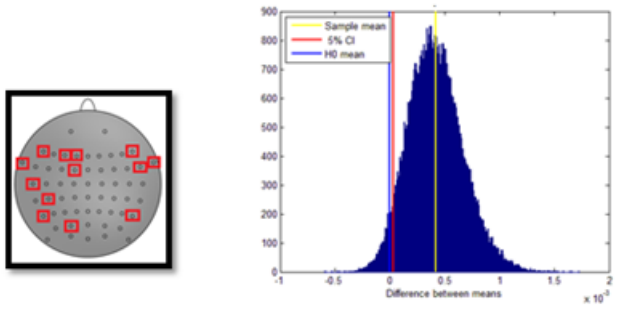

Fig.114 . a). Electrodes where we observed significant higher levels of power in the attended compared with the unattended condition. **b).** Results of Bootstrap analysis performed on electrode PO3 considering the upper right visual hemifield, evaluating the difference between attended and unattended conditions.

In conclusion, in patient F.B. the amplitude of waveforms was higher in the attended than unattended condition when allocating attention toward the sighted visual quadrant while it was similar for the blind quadrant. In the Bootstrap Analysis, the modulation produced by the attentional effort toward the sighted quadrant was represented mostly by an increase in absolute power of activation over frontal, central and posterior electrodes mainly in the contralateral

hemisphere. In contrast, orientation of attention toward the blind visual quadrant showed a non-significant increase in absolute power over frontal, central and posterior electrodes in the damaged right hemisphere, contralateral to the allocation of attention.

L.C.

Lesion involving the

right parietal-temporal-occipital lobe

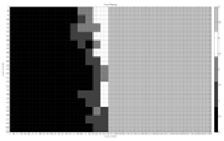

BINOCULAR

In this experiment stimuli were located in the lower visual hemifield.

Behavioural Results:

ACCURACY:

HEMIFIELD	HITS	FALSE ALARMS	d' (sensitivity index)
SIGHTED	**33%**	27%	**0.77**

Table 45. Accuracy in the attentional task.

REACTION TIMES:

HEMIFIELD	HITS	FALSE ALARMS
SIGHTED	**475.73 ms**	426.11

Table 46. Reaction Times in the attentional task.

In the blind visual field L.C. did not respond to any stimulus as he could not perceive any stimulus feature. Accuracy was low in the intact field with a low sensitivity index.

SSVEP Results: AMPLITUDE

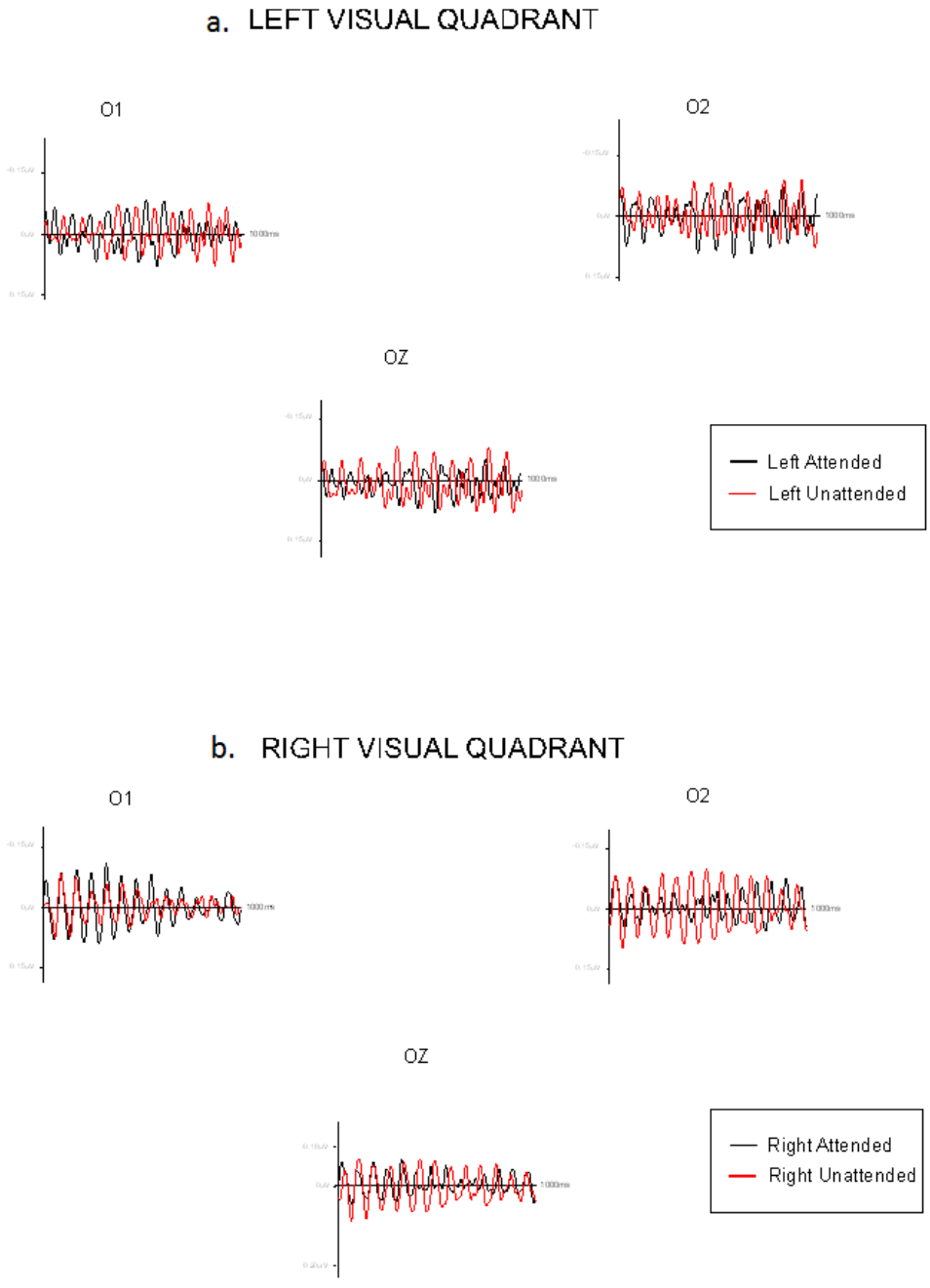

Fig.115. a). Comparison of SSVEP amplitude between blind attended and unattended condition. b). Comparison of SSVEP amplitude between sighted attended and unattended condition

In the blind visual quadrant, the amplitude of waveforms in the attended and unattended condition was similar over all electrodes considered, see fig. 115. In the sighted visual quadrant, the amplitude of waveforms was higher in the attended than unattended condition only over electrode O1, in the intact left hemisphere while it was lower over central electrode Oz and lateral electrode O2, in the damaged right hemisphere.

FREQUENCY DOMAIN: Bootstrap Analysis

ATTENTION TO THE BLIND VISUAL QUADRANT (Fig. 116):

We found a **significant difference** in the attended versus unattended condition over electrodes shown in the following Figure 116.

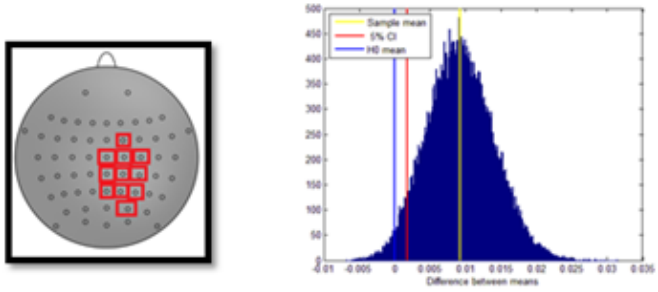

Fig.116. a). Electrodes where we observed significant higher levels of power in the attended compared with the unattended condition. **b).** Results of Bootstrap analysis performed on electrode PZ considering the upper right visual hemifield, evaluating the difference between attended and unattended conditions.

A significantly higher absolute power of activation was found over central and posterior electrodes, mainly within the damaged right hemisphere, contralateral to visual stimulation, even if the stimulus could not be consciously perceived.

ATTENTION TO THE SIGHTED VISUAL QUADRANT (Fig. 117):

We found a **significant difference** over frontal electrodes mainly in the intact left hemisphere considering the attended versus the unattended condition, see figure 117.

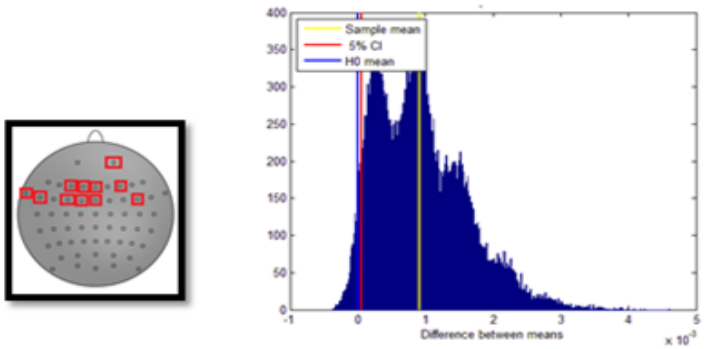

Fig.117. a). Electrodes where we observed significant higher levels of power in the attended compared with the unattended condition. **b).** Results of Bootstrap analysis performed on electrode FC6 considering the upper right visual hemifield, evaluating the difference between attended and unattended conditions.

In conclusion, in patient L.C. visual inspection performed over occipital electrodes indicated that the amplitude of waveforms was higher in the attended than in the unattended condition in the contralateral hemisphere while allocating the attention toward the sighted quadrant. Instead a similar amplitude was observed in both conditions while allocating the attention toward the blind visual quadrant. Concerning the Bootstrap Analysis, the modulation produced by the attentional effort toward the sighted visual quadrant was represented by a significant increase in absolute power over bilateral frontal electrodes and a similar non-significant trend in almost all other electrodes. Instead, the modulation produced by the attentional effort toward the blind visual quadrant indicated a significant increase in absolute power over central and parietal electrodes contralateral to the visual stimulation. In reference to the principal aims of this experiment we found that the topography observed when moving the attention toward the blind quadrant involved contralateral central and parietal electrodes while when moving the attention toward the sighted quadrant involved bilateral frontal electrodes.

A.M.

Lesion involving the whole area of the Willis' Circle

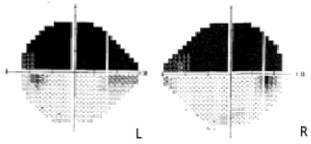

With patient A.M. who has an altitudinal hemianopia the experiment was divided in two parts in which we tested the left and right hemifield in two separate sessions by comparing upper (blind) vs lower (intact) quadrants

Behavioural Results:

ACCURACY:

HEMIFIELD	HITS	FALSE ALARMS	d' (sensitivity index)
SIGHTED LEFT	**14%**	5%	**0.56**
BLIND LEFT	**7%**	4%	**0.27**
SIGHTED RIGHT	**28%**	9%	**0.76**
BLIND RIGHT	**6%**	11%	**-0.33**

Table 47. Accuracy in the attentional task.

REACTION TIMES ms

HEMIFIELD	HITS	FALSE ALARMS
SIGHTED LEFT	**469.93**	566.4
BLIND LEFT	**575**	739.25
SIGHTED RIGHT	**586.64**	819.89
BLIND RIGHT	**462.50**	687.18

Table 48. Reaction Times in the attentional task.

Accuracy was low in both the intact and the blind quadrants with a low sensitivity index.

SSVEP Results: AMPLITUDE

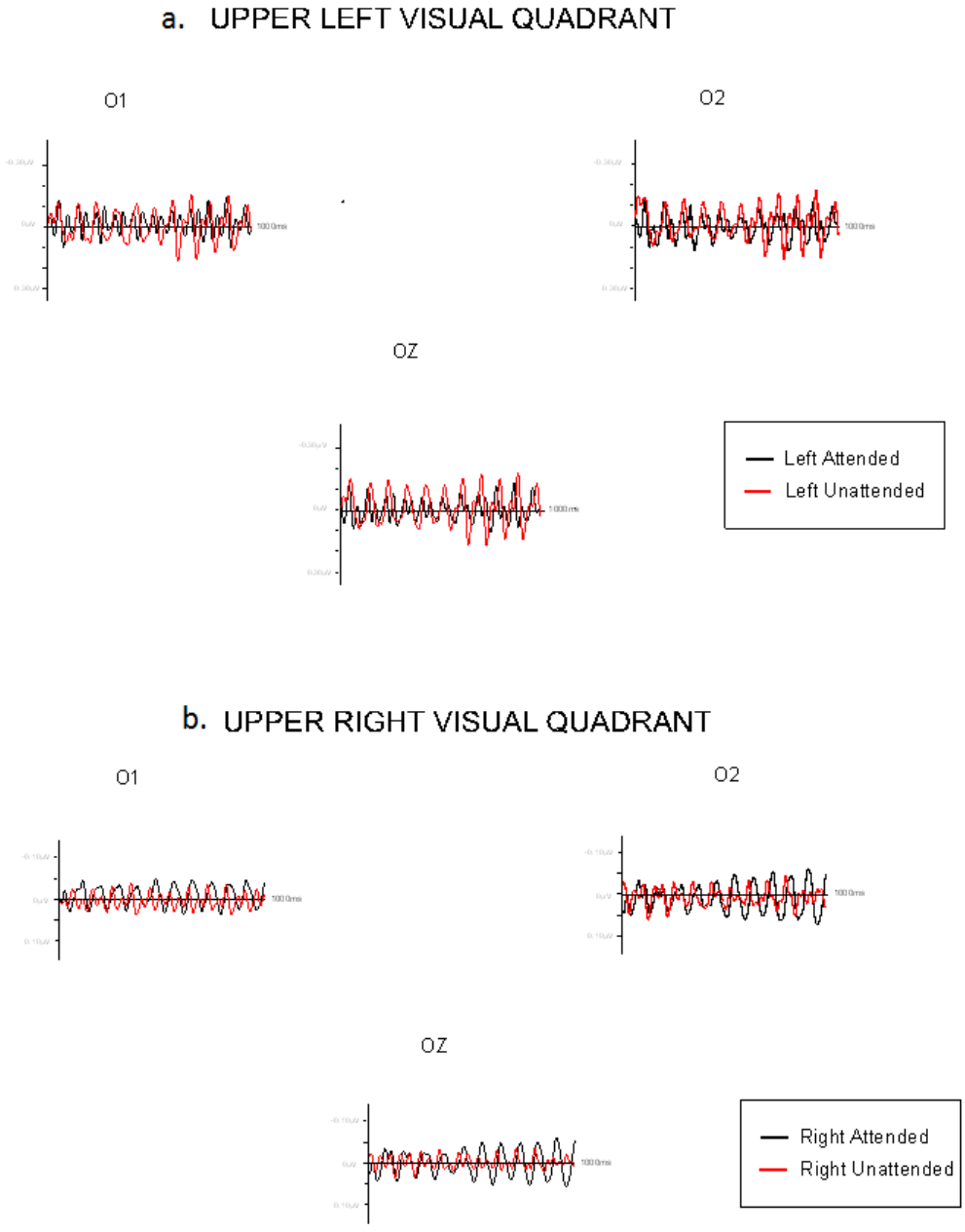

Fig.118. a). Comparison of SSVEP amplitude between blind attended and unattended condition. b). Comparison of SSVEP amplitude between blind attended and unattended condition

Considering both upper quadrants, the amplitude of waveforms was similar in either attended and unattended condition.

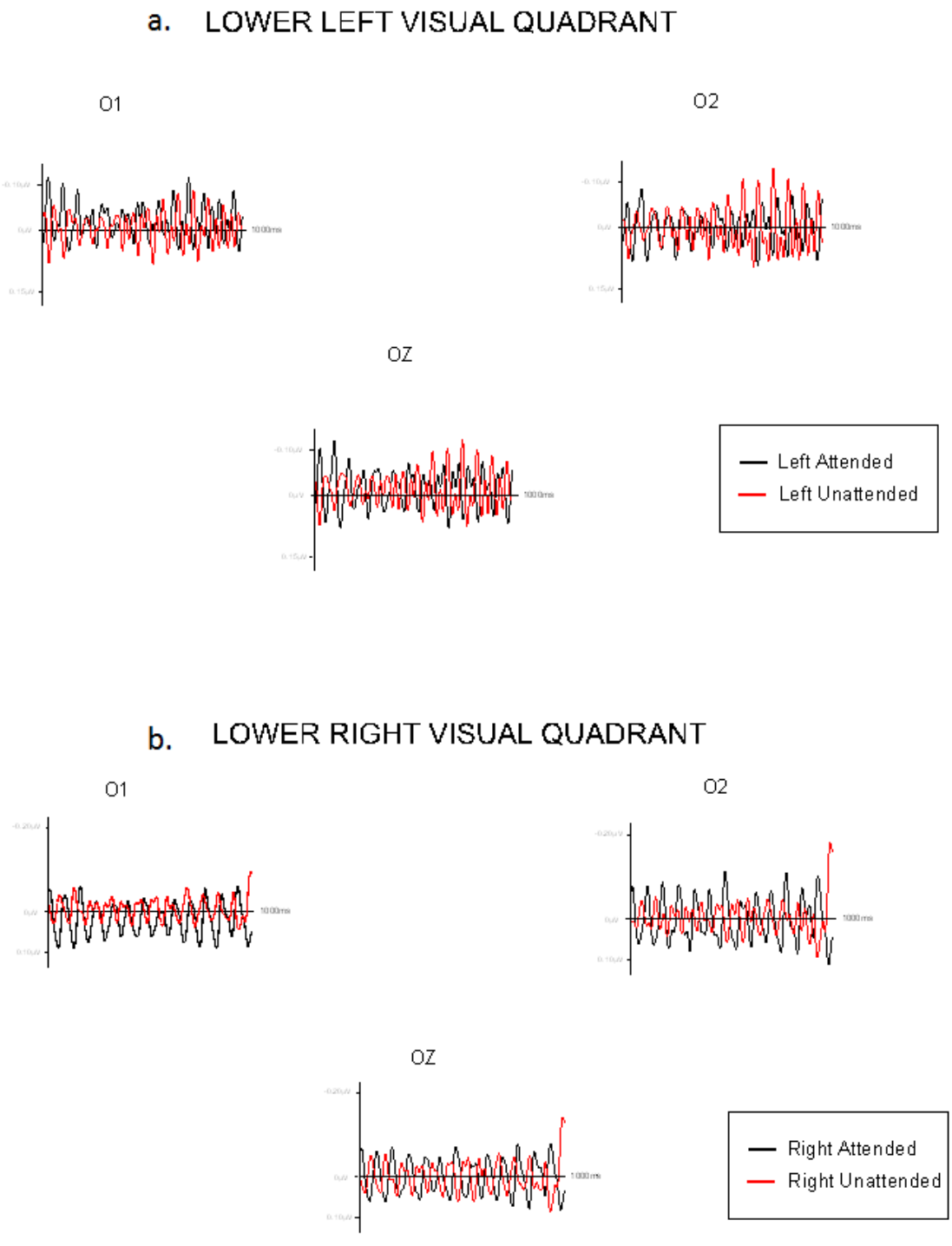

Fig.119. a). Comparison of SSVEP amplitude between sighted attended and unattended condition.
b). Comparison of SSVEP amplitude between sighted attended and unattended condition

In the sighted left quadrant, the amplitude of waveforms was similar in both attended and unattended conditions. Considering the sighted right visual quadrant we found that the amplitude of waveforms in the attended condition was higher over central (Oz) as well as lateral sites (O1 and O2).

FREQUENCY DOMAIN: Bootstrap Analysis

ATTENTION TO THE BLIND LEFT VISUAL QUADRANT

We found **significantly higher absolute power in attended than unattended condition** over some frontal and temporal electrodes in the left ipsilateral hemisphere, see Figure 120.

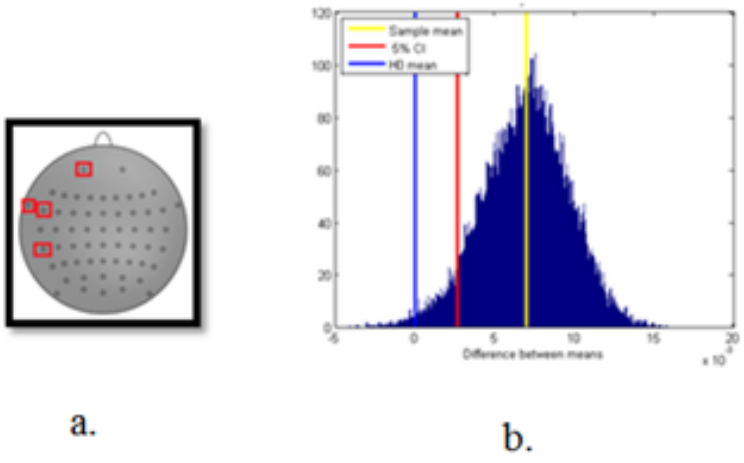

Fig.120. a). Electrodes where we observed significant higher levels of power in the attended compared with the unattended condition. **b).** Results of Bootstrap analysis performed on electrode FT7 considering the upper right visual hemifield, evaluating the difference between attended and unattended conditions.

ATTENTION TO THE BLIND RIGHT VISUAL QUADRANT

We found **significantly higher absolute power in attended than unattended condition** over some frontal, central and posterior electrodes mainly in the left contralateral hemisphere, see Figure 121.

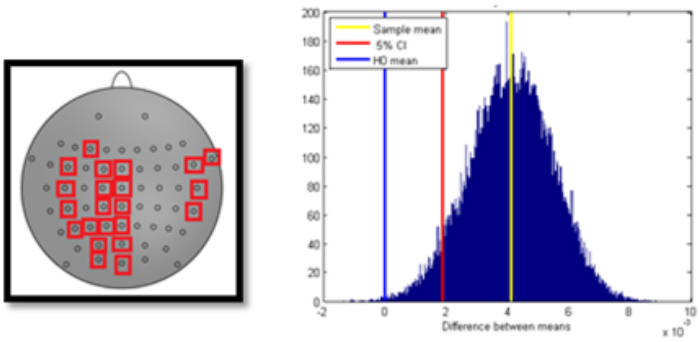

a. b.

Fig.121. a). Electrodes where we observed significant higher levels of power in the attended compared with the unattended condition. **b).** Results of Bootstrap analysis performed on electrode POz considering the upper right visual hemifield, evaluating the difference between attended and unattended conditions.

.

ATTENTION TO THE SIGHTED LEFT VISUAL QUADRANT

We found **significant difference** considering the attended versus the unattended condition only over a parietal electrode P7 in the ipsilateral left hemisphere, see Figure 122.

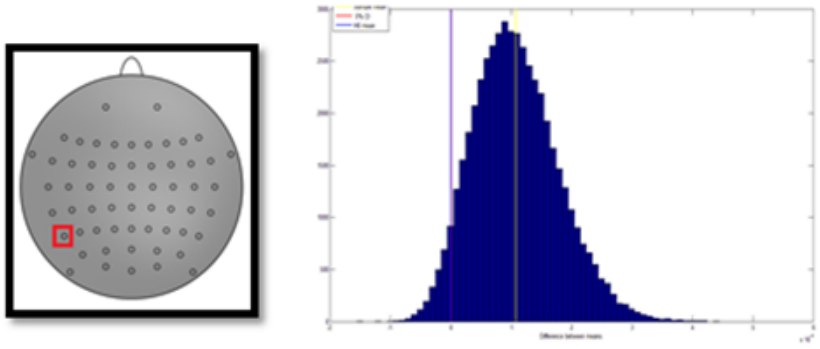

a. b.

Fig.122. a). Electrodes where we observed significant higher levels of power in the attended compared with the unattended condition. **b).** Results of Bootstrap analysis performed on electrode P7 considering the upper right visual hemifield, evaluating the difference between attended and unattended conditions.

ATTENTION TO THE SIGHTED RIGHT VISUAL QUADRANT

We found a **significant difference** considering the attended versus the unattended condition only over a parietal electrode TP7 in the contralateral left hemisphere, see Figure 123.

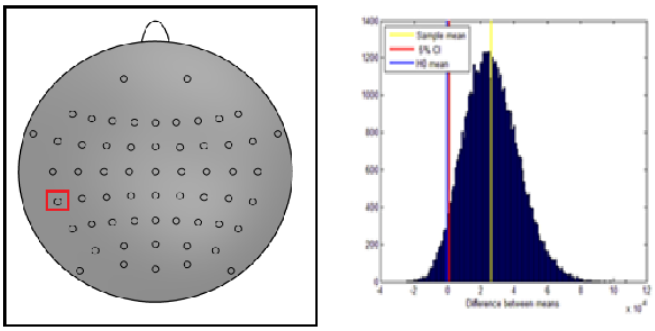

a. b.

Fig.123 . a). Electrodes where we observed significant higher levels of power in the attended compared with the unattended condition. **b).** Results of Bootstrap analysis performed on electrode TP7 considering the upper right visual hemifield, evaluating the difference between attended and unattended conditions.

In conclusion, in patient A.M. the amplitude of waveforms was basically similar in the attended than unattended condition. Concerning the Bootstrap Analysis, the modulation produced by the attentional effort toward the blind left visual quadrant was represented mostly by a significant increase in absolute power of activation over ipsilateral frontal and temporal electrodes; instead, the modulation produced by the attentional effort toward the blind right visual quadrant was represented mostly by a significant increase in absolute power of activation over frontal, central and posterior electrodes mainly in the contralateral hemisphere.

The modulation produced by the attentional effort toward the sighted left visual quadrant was represented by a significant increase of power only over the parietal electrode P7 in the left hemisphere; instead the modulation produced by the attentional effort toward the sighted right visual quadrant was represented by a significant increase of power only over the temporo-parietal electrode TP7 in the left hemisphere.

In reference to the aim of this experiment we found that the topography observed when moving the attention toward the blind hemifield involved left frontal, temporal, central and posteriors electrodes; instead, when moving the attention toward the sighted quadrant, it involved few temporo-parietal electrodes in the left hemisphere. As in L.C., the results suggest the presence of a higher difference between attended and unattended condition moving the attention toward the blind quadrant, over posterior electrode, than toward the sighted one.

SUMMARY OF RESULTS:

Left hemisphere lesioned patients:

A.G.	INTACT FIELD	BLIND FIELD
EFFECT OF ATTENTION ON BEHAVIOUR	YES	NO
EFFECT OF ATTENTION ON SSVEP	YES	YES
S.L.		
EFFECT OF ATTENTION ON BEHAVIOUR	YES	NO
EFFECT OF ATTENTION ON SSVEP	YES	YES

Table 49

Right Hemisphere lesioned patients:

L.F.	INTACT FIELD	BLIND FIELD
EFFECT OF ATTENTION ON BEHAVIOUR	NO	NO
EFFECT OF ATTENTION ON SSVEP	YES	NO

F.B.		
EFFECT OF ATTENTION ON BEHAVIOUR	NO	NO
EFFECT OF ATTENTION ON SSVEP	YES	NO
L.C.		
EFFECT OF ATTENTION ON BEHAVIOUR	NO	NO
EFFECT OF ATTENTION ON SSVEP	YES	YES

Table 50.

Bilateral lesioned patients:

A.M.	INTACT FIELD	BLIND FIELD
EFFECT OF ATTENTION ON BEHAVIOUR	NO	NO
EFFECT OF ATTENTION ON SSVEP	YES	YES

Table 51.

DISCUSSION:

In all these patients we found a modulation in the neural activity produced by the attentional effort when moving the attention toward the blind quadrant where they could not consciously perceive the stimulus. This modulation reached the significant threshold in patients A.G., S.L., L.C. and A.M.; instead it could not reach the significant threshold in patients L.F. and F.B. This modulation was not directly related to the behavioural performance as they could not detect the target stimulus in the blind hemifield.

We found different sites of activation: in some patients (A.G., F.B., L.C. and A.M. for the blind right quadrant) modulation was mainly located mainly over posterior electrodes confirming the initial hypothesis represented by the possibility of increasing the absolute power over posterior electrodes even in hemianopic patients by means of attentional effort. In other patients (L.F., S.L. and A.M. for the blind left quadrant) we observed a modulation located mainly over frontal and temporal electrodes indicating that the same cognitive process could determine an increase in absolute power over different cortical areas. This is probably related to the site and extent of the lesion and to find a reliable correlation between effect of attention on the blind field and lesion we need to study a more numerous cohort of patients.

As far as behavioural results are concerned, we found that, in general, patients could not perform the attentional task as good as healthy participants even in the sighted hemifield. In the literature it is possible to find different papers that demonstrated a significant impairment even in the sighted hemifield of hemianopic patients, in different kind of cognitive tasks as detection, discrimination and categorization (so called *sightblindness* phenomenon; Paramei et al., 2008; Bola et al. 2013, Cavezian et al., 2010). In this experiment we confirmed this finding. However, we found that the performance in the sighted hemifield was better in patients A.G. and S.L. with a lesion involving the left hemisphere. This result can be explained making reference to previous studies demonstrating that patients with a lesion in the right hemisphere performed worse than patients with a damage in the left hemisphere (Cavezian et al., 2015) and to the fact that the attentional cognitive task could be more affected by a lesion in the right hemisphere being attentional function mainly located there. Furthermore, patients L.C. and F.B., had a widespread lesion involving also the parietal lobe and this kind of lesion could involve the attentional skill more than what a left lesion does.

GENERAL CONCLUSION

Taking together the results of these experiments carried out with various techniques (behavioural, electrophysiological and neural imaging) have enabled to provide further evidence on unconscious behavioural and physiological responses to stimuli presented in the blind field of hemianopic patients. This endeavour has a double value: first, to cast light on the neural mechanisms that may allow a shift from unconscious to conscious vision, second to provide a rational approach for rehabilitation of cortical blindness.

ACKNOWLEDGEMENTS:

This research was partially supported by ERC Grant 339939 Perceptual Awareness.

References

- Ajina S., Kennard C., Rees G. & Bridge H. (2014). Motion area V5/MT + response to global motion in the absence of V1 resembles early visual cortex. *Brain, a Journal of Neurology*, 1:15;

- Alexander I & Cowey A. (2010). Edges, colour and awareness in blindsight. *Consciousness and Cognition*, 19; 520-533;

- Alexander, A.I., Lee, J.E., Lazar, M. & Field, A.S. (2007). Diffusion Tensor imaging of the brain. *Neurotherapeutics* 4(3): 316–329;

- Antonini, A., Berlucchi, G., Di Stefano, M. & Marzi, C.A, (1981). Differences in binocular interactions between cortical areas 17 and 18 and superior colliculus of Siamese cats. *J Comp Neurol* 200(4): 597-611;

- Azzopardi P & Cowey A. (2001). Motion discrimination in cortically blind patients. *Brain* 124, 30-46.

- Azzopardi P. & Hock H.S. (2011). Illusory motion perception in blindsight. *PNAS*, 108: 876-881;

- Bagattini, C., Mazzi, C. & Savazzi, S. (2015). Waves of awareness for occipital and parietal phosphenes perception. *Neuropsychologia* 70: 114-125;

- Barbur, J.L., Harlow, A.J. & Weiskrantz, L. (1994). Spatial and temporal response response properties of residual vision in a case of hemianopia. *Philos Trans R Soc Lond B Biol Sci.* 343(1304): 157-66;

- Barleben, M., Stoppel, C.M., Kaufmann, J., Merkel, C., Wecke, T., Goertler, M., Heinze, H.J., Hopf, J.M. & Schonefeld, M.A. (2014). Neural Correlates of Visual Motion Processing Without Awareness in Patients With Striate Cortex and Pulvinar Lesions. *Human Brain Mapping*.

- Bola M., Gall G. & Sabel B.A. (2013). "Sightblind": perceptual deficits in the "intact" visual field. *Frontiers in Neurology*, 4 (80);

- Bordier C., Hupè J.M. & Dojat M. (2015). Quantitative evaluation of fMRI retinotopic maps, from V1 to V4, for cognitive experiments. *Frontiers in human neuroscience*, 9 (277).

- Bridge, H., Thomas, O., Jbabdi, S. & Cowey, A. (2008). Changes in connectivity after visual cortical brain damage underlie altered visual function. *Brain* 131: 1433-1444;

- Bullier, J. (2001). Integrated model of visual processing. *Behavioural Brain Science,* 36, 96-107.

- Cavèzian, C., Gaudry, I., Perez, C., Coubard, O., Doucet, G., Peyrin, C., Marendaz, C., Obadia, M., Gout, O. & Chokron, S. (2010). Specific impairments in visual processing following lesion side in hemianopic patients. *Cortex* 46: 1123-1131;

- Cavezian, C., Perez, C., Peyrin, C., Gaudry, I., Obadia, M., Gout, O. & Chokron, S. (2015). Hemisphere-dependent ipsilesional deficits in hemianopia: sightblindness in the "intact" visual field. *Cortex* 69: 166-174;

- Chelazzi, L., Marzi, C. A., Panozzo, G., Pasqualini, N., Tassinari, G., & Tomazzoli, L. (1988). Hemiretinal differences in speed of light detection in esotropic amblyopes. *Vision Research* 28, 95–104;

- Corbetta, M. & Shukman, G.L: (2002). Control of goal directed and stimulus driven attention in the brain. *Nat. Rev. Neuroscience* 3:201-15;

- Cowey, A. & Stoering, P. (1991). The neurobiology of blindsight. *Trends of Neuroscience* 14(4): 140-5;

- Cowey, A., & Stoerig, P. (1989). Projection patterns of surviving neurons in the dorsal lateral geniculate nucleus following discrete lesions of striate cortex: implications for residual vision. *Experimental Brain Research*, 75, 3,631-638.

- Crick, F., & Koch, C. (1995). Are we aware of neural activity in primary visual cortex? *Nature*, 375, 121-123.

- Cynader, M., & Berman, N. (1972). Receptive-field organization of monkey superior colliculus. *Journal of Neurophysiology*, 35, 187-201.

- Das, A., Tadin, D. & Huxlin, K.R. (2014). Beyond blindsight: properties of visual relearning in cortically blind fields. *The journal of neuroscience*, 34(35): 11652-11664;

- Deyoe, E.A., Carman, G.J., Bandettini, P., Glickman, S., Wieser, J., Cox, R., et al., (1996). Mapping striate and exstrastriate visual areas in human cerebral cortex. *Proc. Natl. Acad. Sci. U.S.A.* 93, 2382-2386;

- Di Russo F., Pitzalis S., Aprile T., Spitoni G., Patria F., Stella A., Spinelli D. & Hylliard S.A. (2007). Spatiotemporal analysis of the cortical sources of the Steady-State Visual Evoked Potential. *Human Brain Mapping*, 28: 323-334;

- Di Russo F., Stella A., Spitoni G., Strappini F., Sdoia S., Falati G., Hillyard S.A., Spinelli D. & Pitzalis S. (2012). Spatiotemporal brain mapping of spatial attention effects on pattern-reversal ERPs. *Human Brain Mapping*, 33: 1334-1351;

- Di Russo F., Teder-Salejaravi W.A. & Hillyard S.A (2002). The cognitive lectrophysiology of Mind and Brain. Chapter 11: *Steady-state VEP and Attentional Visual Processing*.

- Di Russo, F. & Spinelli, D. (1999). Electrophysiological evidence for an early attentional mechanism in visual processing in humans. *Vision Research* 39: 2975-2985.

- Di Russo, F. & Spinelli, D. (2002). Effects of sustained voluntary attention on amplitude and latency of steady-state visual evoked potential: a costs and benefits analysis. *Clinical Neurophysiology* 113(11): 1771-7;

- Di Russo, F., Spinelli, D. & Morrone, M.C. (2001). Automatic gain control contrast mechanisms are modulated by attention in humans: evidence from visual evoked ptentials. *Vision Research* 41(19): 2435-47;

- Diller, L., and Weinberg, J. (1977). Hemi-inattention in rehabilitation: the evolution of a rational remediation program. *Adv. Neurol*. 18, 63–82;

- Dumoulin S.O, Bittar R.G., Kabani N.J., Baker jr C.I., Le Goualher G., Pike G.B. & Evans A.C. (2000). A new anatomical landmark for reliable identification of human area V5/MT: a quantitative analysis of sulci patterning. *Cerebral Cortex*, 10, 454-463.

- Dumoulin, S.O., Hoge, R.D., Baker, C.L:, Hess, R.F., Achtman, R.L. & Evans, A.C. (2003). Automatic volumetric segmentation of human visual retinotopic cortex. *Neuroimage* 18, 57-587;

- Efron, B.& Tibshirani, R.J. (1993). An introduction to the Bootstrap. Chapman Hall, New Yoirk, NY;

- Engel, S., Rimelhart, D.E., Wandell, B.A., Lee, A.T., Glover, G.H., Chichilnisky, E.J. et al. (1994). fMRI ofhuman visual cortex. *Nature* 369:525;

- Engel, S.A., Glover, G.H. & Wandell, B.A. (1997). Retinotopic organization in human cortex and the spatial precision of functional MRI. *Cerebral Cortex* 7(2): 181-92;

- Felleman, D. J., & Van Essen, D. C. (1991). Distributed hierarchical processing in the primate cerebral cortex. *Cerebral Cortex,* 1, 1-47.

- Fendrich, R., Wessinger, C. M., & Gazzaniga, M. S. (1992). Residual vision in a scotoma: Implications for blindsight. *Science,* 258, 1489-1491.

- Fries, W. (1984). Cortical projections to the superior colliculus in the macaque monkey: a retrograde study using horseradish peroxidase. *Journal Comp Neurol* 230 (1): 55-76;

- Gaglianese A., Costagli M., Bernardi G., Ricciardi E. & Pietrini P. (2012). Evidence of a direct influence between the thalamus and hMT+ independent of V1 in the human brain as measured by fMRI. *Neuroimage* 60(2):1440-7;

- Gauthier, L., Dehaut, F. & Joanette, Y. (1989). The Bells Test: a quantitative and qualitative test for visual neglect. *International Journal of Clinical Neuropsychology*, 11(2): 49-54;

- Goebel, R., Khorram-Sefat, D., Muckli, L., Hacker, H., & Singer, W. (1998). The constructive nature of vision: direct evidence from functional magnetic resonance imaging studies of apparent motion and motion imagery. *European Journal of Neuroscience*, 10, 1563-1573.

- Goebel, R., Mucki, L., Zanella, F.E., Singer, W. & Stoerig, P. (2001). Sustained exstrastriate cortical activation without visual awareness revealed by studies of hemianopic patients. *Vision Research*, 41: 1459-1474;

- Goldberg, M. E., & Wurtz, R. H. (1972). Activity of superior colliculus in behaving monkey. I. Visual receptive fields of single neurons. *Journal of Neurophysiology,* 35, 542-559.

- Harting, J. K., Huerta, M. F., Hashikawa,T., & van Lieshout D. P. (1991). Projection of the mammalian superior colliculus upon the dorsal lateral geniculate nucleus: Organization of tectogeniculate pathways in nineteen species. *The Journal of Comparative Neurology*, 304, 2, 275-306.

- Henriksson L., Karvonen J., Salminen-Vaparanta N., Railo H. & Vanni S. (2012). Retinotopic maps, spatial tuning and locations of human visual areas in surface coordinates characterized with multifocal and blocked fMRI designs. *PLOS One* 7(5);

- Huettel, S.A., Song, A.W. & McCarthy G. (2009). Functional Magnetic Resonance Imaging, second edition;

- Kandel, E.R., Schwartz, J.H., Jessell, T.M. (2000). *Principles of Neural Science, 4th ed.* McGrawHill, NewYork;

- Keil, A. & Heim, S. (2009). Prolonged reduction of electrocortical activity predicts correct performance during rapid serial visual processing. *Psychophysiology* 46(4): 718-725;

- Keil, A., Moratti, S., Sabatinelli, D., Bradley, M.M. & Lang, P.J. (2005). Additive effects of emotional content and spatial selective attention on electrocortical facilitation. *Cerebral Cortex* 15(8): 1187-1197;

- Kentridge R.W., Heywood C.A. & Weiskrantz L. (2004). Spatial attention speeds discrimination without awareness in blindsight. *Neuropsychologia,* 42: 831-835;

- Kentrige R.W. (2014). What is it like to have type-2 blindsight? Drawing inferences from residual function in type-1 blindsight. *Consciousness and Cognition*;

- Kraft, A., Schira, M.M., Hagendorf, H., Schmidt, S., Olma, M. & Brandt, S.A. (2005). fMRI localizer technique: efficient acquisition and functional properties of single retinotopic positions in the human visual cortex. *Neuroimage* 28, 453-463;

- Lamme, V. A., & Roelfsema, P. R. (2000). The distinct modes of vision offered by feedforward and recurrent processing. *Trends in Neuroscience*, 23, 571-579.

- Le Bihan, D., Mangin, J.F., Puopon, C., Clark, C.A., Pappata, S., Molko, N. & Chabriat, H. (2001). Diffusion Tensor Imaging: concepts and applications. *Journal of magnetic resonance imaging* 13:534–546;

- Leh, S. E., Ptito, A., Schönwiesner, M., Chakravarty, M. M., & Mullen, K. T. (2010). Blindsight mediated by an S- cone-independent collicular pathway: an fMRI study in hemispherectomized subjects. *Journal of Cognitive Neuroscience*, 22, 4 ,670-682;

- Leh, S.E., Mullen, K.T. & Ptito, A. (2006). Absence of S-cones input in human blindsight following hemispherectomy. *Eur Journal of Neuroscience* 24(19): 2954-60;

- Mangione, C. M., Lee, P. P., Gutierrez, P. R., Spritzer, K., Berry, S., & Hays, R. D. (2001). Development of the 25-Item National Eye Institute Visual Function Questionnaire. *Archives of Ophthalmology*, 119, 1050-1058.

- Marrocco, R. T., & Li, R. H. (1977). Monkey superior colliculus: properties of single cells and their afferent inputs. *Journal of Neurophysiology*, 40, 844-860.

- Marzi, C. A., Tassinari, G., Aglioti, S., & Lutzemberger, L. (1986). Spatial summation across the vertical meridian in hemianopics: a test for blindsight. *Neuropsychologia*, 34, 9-22;

- Miller, J. (1982). Divided attention: Evidence for coactivation with redundant signals. *Cognitive Psychology* 14:247-279;

- Milner, A. D., & Goodale, M. A. (1995). The visual brain in action. New York, Oxford University Press.

- Mohler, C. W., & Wurtz, R. H. (1977). Role of striate cortex and superior colliculus in visual guidance of saccadic eye movements in monkeys. *Journal of Neurophysiology*, 40, 74- 94.

- Morgan, S.T., Hansen, J.C., Hillyard, S.A. (1996). Selective attention to stimulus location modulated the steady state evoked potential. *Proc. Natl. Acad. Sci. U.S.A.* 93: 470-4774;

- Morland, A.B., Jones, S.R., Finlay, A.L:, Deyzac, E., Le, S. & Kemp, S. (1999). Visual perception of motion, luminance and colour in a human hemianope. *Brain* 122(Pt6): 1183-1198;

- Morris, J.S., De Gelder, B., Weiskrantz, L., Dolan, R.J. (2001). Differential extrageniculostriate and amygdala responses to presentation of emotional faces in a cortically blind field. *Brain 1*24:1241–1252. 5;

- Morris, J.S., Ohman, A., Dolan, R.J. (1999). A subcortical pathway to the right amygdala mediating ‘‘unseen’’ fear. *Proc Natl Acad Sci USA* 96:1680 –1685. 6.

- Mukheriìjee, P., Berman, J.L., Chung, S.W., Hess, C.P. & Henry, R.G. (2008). Diffusion tensor MT imaging and fiber tractography: theoretic underpinning. AJNR An Journal of Neuroradiology 29(4): 632-41;

- Oruç, I., Krigolson, O., Dalrymple, K., Nagamatsu, L.S., Handy, T.C. & Barton, J.J.S. (2015). Bootstrap analysis of the single subject with event related potentials. *Cognitive Neuropsychology* 28:5, 322-337;

- Paramei, G-V. & Sabel, B.A. (2008). Contour-integration deficits on the intact side of the visual field in hemianopia patients. *Behavioural Brain Research* 188: 109-124;

- Pavan A., Alexander I., Campana G. & Cowey A. (2011). Detection of first- and second-order coherent motion in blindsight. *Experimental Brain Research*, 214: 261-271;

- Poeppel, E., Frost, D., Held (1973). Residual visual function after brain wounds involving the central visual pathways in man. *Nature, 243:295-296*;

- Pollen, D. A. (1999). On the neural correlates of visual perception. *Cerebral Cortex,* 9, 4-19.

- Ptito, M., Johannses P., Faubert J & Gjedde A. (1999). Activation of human extrageniculostriate pathways after damage to area V1. *Neuroimage* 9, 97-107.

- Raab, D. (1962). Statistical facilitation of simple reaction times. Transactions of the New York Science 24: 574-590;

- Rafal, R., Smith, J., Krantz, J., Cohen, A. & Brennan, C. (1990). Extrageniculate vision in hemianopic humans. Saccade inhibition by signals in the blind field. *Science*, 250, 4977, 118-21;

- Ramsoy, T.Z. & Overgaard, M. (2004). Introspection and subliminal perception. *Phenomenology and the cognitive Sciences*, 3: 1-23;

- Regan, D. (1989). Human Brain Electrophysiology evoked potentials and evoked magnetic field. In science and medicine. Elsevier, New York;

- Salin, P. A., & Bullier, J. (1995). Corticocortical connections in the visual system: structure and function. *Physiological Review,* 75, 107-154.

- Schenkenberg, T., Bradford , D.C. & Ajax, E.T. (1980). Line bisection and unilateral visual neglect in patients with neurologic impairment. *Neurology* 30(5): 509-17;

- Schiller, P.H. & Malpeli, J.G. (1977). Properties and tectal projections of monkey retinal ganglion cells. *Journal of Neurophysiology* 40(2): 428-45;

- Schneider, K. A., & Kastner, S. (2005). Visual responses of the human superior colliculus: a high-resolution functional magnetic resonance imaging study. *Journal of Neurophysiology*, 94, 2491-2503.

- Sereno, M., Dle, A.M., Reppas, J.B. & Kwong, K.K: (1995). Borders of multiple visual areas in humans revealed by functional magnetic resonance imaging. *Science* 268, 889-893;

- Silvanto J. (2014). Why is "blindsight" blind? A new perspective on primary visual cortex, recurrent activity and visual awareness. *Consciousness and Cognition;*

- Slotnick S.D., Klein S.A., Carney T. & Sutter E.E. (2001). Electrophysiological estimate of human cortical magnification. *Clin Neurophysiol.* 112(7): 1349-1356;

- Slotnick, S. & Yantis, S. (2003). Efficient acquisition of human retinotopic maps. *Human Brain Mapping* 18, 22-29;

- Tamietto M., Catselli, L., Vighetti, S., Perozzo, P., Geminiani, G., Weiskrants, L. & De Gelder, B. (2009). Unseen facial and bodily expressions trigger fast emotional reactions. *Proc Natl Acad Sci U.S.A.* 106(42): 17661-6;

- Tamietto, M., Cauda, F., Corazzini, L. L., Savazzi, S., Marzi, C. A., Goebel, R., Weiskrantz, L., & de Gelder, B. (2010). Collicular vision guides nonconscious behaviour. *Journal of Cognitive Neuroscience*, 22, 5, 888-902;

- Tomaiuolo, F., Ptito, M. Marzi, C.A., Paus, T. & Ptito, A. (1997). Blindsight in hemispherectomized patients as revealed by spatial summation across the vertical merdian. *Brain* 120: 795-803;

- Tong, F. (2003). Primary visual cortex and visual awareness, *Nature Reviews, Neuroscience*, 4, 219-229.

- Tootell, R.B. et al. (1998). Functional analysis of primary visual cortex (V1) in humans. *Proc. Natl. Acad. Sci.* 95, 811-817;

- Tootell, R. B. H., Reppas, J. B., Kwong, K. K., Malach, R., Born, R.T., Brady, T. J., Rosen, B. R., & Belliveau, J. W. (1995). Functional analysis of human MT and related

visual cortical areas using magnetic resonance imaging. *Journal of Neuroscience*, 15, 3215-3230.

- Ungerleider, L.G., Galkin, T.W. & Mishkin, M. (1983). Visuotopic organization of projections from striate cortex to inferior and lateral pulvinar in rhesus monkey. *J Comp Neurol*. 217(2): 137-57;

- Van Buren, J. M. (1963). The Retinal Ganglion Cell Layer. Springfield, IL: Charles C. Thomas.

- Vanni, S., Henriksson, L. & James (2005). Multifocal fMRI mapping of visual cortical areas. *Neuroimage* 27, 95-105;

- Vialatte F.B., Maurice M., Dauwels J. & Cichocki A. (2010). Steady-state visually evoked potentials: Focus on essential paradigms and future perspective. *Progress in Neurobiology*, 90: 418-438;

- Vossel, S., Geng, J.J. & Fink, G.R. (2014). Dorsal and ventral attention system: distinct neural circuits but collaborative roles. *The Neuroscientist* 20(2): 150-159;

- Wandell B.A. & Winawer J. (2011). Imagining retinotopic maps in the human brain. *Vision Research* 51; 718-737;

- Warnking J., Dojat M., Guérin-Dugué A., Delon-Martin C., Olympieff S., Richard N., Chehikian A. & Segebarth C. (2002). fMRI Retinotopic mapping – Step by Step. *NeuroImage* 17, 1665-1683;

- Watson, J. D. G., Myers, R., Frackowiak, R. S. J., Hajnal, J. V., Woods, R. P., Mazziotta, J. C., Shipp, S., & Zeki, S. (1993). Area V5 of the human brain: evidence from a combined study using positron emission tomography and magnetic resonance imaging. *Cerebral Cortex*, 3, 79-94.

- Weiskrantz L, Warrington EK, Sanders MD, Marshall J.(1974). Visual capacity in the hemianopic field following a restricted occipital ablation. *Brain*, 97(4):709-28;

- Weiskrantz, L. (1996). Blindsight Revisited. *Current Opinion in Neurobiology, 6:215-220*;

- Weiskrantz, L. (1998). Consciousness and commentaries. *International journal of psychology*, 33(3):227-233;

- Wessinger, C.M., Fendrich, R. & Gazzaniga, M.S. (1997). Islands of residual vision in hemianopic patients. *Journal of Cognitive Neuroscience* 9(2): 203-21;

- Wessinger, C.M., Fendrich, R. & Gazzaniga, M.S. (1999). Variability of residual vision in hemianopic subjects. *Restor Neurol Neuroscience* 15(2-3): 243-53;

- Wilson, M.E. & Toyne, M.J. (1970). Retino-tectal and cortico-tectal projections in Macaca mulatta. *Brain Research* 24(3): 395-406;

- Wu, Z. (2014). Studying modulation on simultaneously activated SSVEP neural networks by a cognitive task. *J Biol Phys* 40 : 55-70.